Role of TDP-43 and hnRNP Proteins in the Regulation of Different RNA Targets

Thesis

Role of TDP-43 and hnRNP proteins in the regulation of different RNA targets

Sara Cappelli

A thesis submitted in fulfilment for the requirements of the Open University (UK) for the degree of Doctor of Philosophy

Life Sciences

International Centre for Genetic Engineering and Biotechnology
(ICGEB)
Trieste, Italy

Director of studies: Dr. Emanuele Buratti
External supervisor: Prof. David Elliott

February 2019

TABLE OF CONTENTS

PUBLICATIONS

Appocher, C., Mohagheghi, F., **Cappelli, S.**, Stuani, C., Romano, M., Feiguin, F., Buratti, E. (2017) 'Major hnRNP proteins act as general TDP-43 functional modifiers both in *Drosophila* and human neuronal cells', *Nucleic Acids Res.,* vol. 45, pp. 8026–8045. [Online]. DOI: 10.1093/nar/gkx477

Cappelli, S., Romano, M., Buratti, E. (2018) 'Systematic analysis of gene expression profiles controlled by hnRNP Q and hnRNP R, two closely related human RNA Binding Proteins implicated in mRNA processing mechanisms', *Front Mol Biosci.,* vol. 5, pp. 79. [Online]. DOI: 10.3389/fmolb.2018.00079.

LIST OF FIGURES

LIST OF TABLES

ABBREVIATIONS

12XQ/N	TDP-43 Q/N rich amino acid sequence 331–369 repeated 12 times
ABAT	4-aminobutyrate Aminotransferase
ABCC9	ATP Binding Cassette Subfamily C Member 9
AcD	Acidic Domain
ACHE	Acetylcholinesterase
ACP5	ACP5, Acid phosphatase 5, Tartrate Resistant
AD	Alzheimer's disease
ADCY1	Adenylate Cyclase 1
ADD3	Adducin 3
AGO2	Argonaute 2
AGP	α1-Acid Glycoprotein
ALL	Acute Lymphoblastic Leukemia
ALS	Amyotrophic Lateral Sclerosis
AP-1	Active Activator Protein-1
apoB	Apolipoprotein B
ApoII	Apolipoprotein AII
ARE	AU-rich elements
ARHGAP36	ARHGAP36, Rho GTPase activating Protein 36
ATG7	Autophagy Related 7
ATM	Ataxia Teleangectasia Mutated
BDNF	Brain Derived Neurotrophic Factor
BRCA1	Breast Cancer 1
BRD8	Bromodomain Containing 8
Brunol	Bruno-like

c-Fos	Cellular Oncogene Fos
C25	C-terminal region of 25 amino acids involved in DAZAP1's nuclear localization
CACNA1C	Voltage-dependent L-type Calcium Channel Subunit α1C
CAMs	Cell Adhesion Molecules
CAPN5	Calpain 5
CARTPT	CARTPT, CART Prepropeptide
CASP3	Caspase 3
CDK5R1	Cyclin Dependent Kinase 5 Regulatory Subunit 1
CDK6	Cyclin-Dependent Kinase 6
cDNA	complementary DNA
CELF	CUGBP, Elav-like family
CELF5	CELF5, CUGBP, Elav-like Family Member 5
CFTR	Cystic Fibrosis Transmembrane Conductance Regulator
CLIP-seq	Cross-Linking Immunoprecipitation Sequencing
CNS	Central Nervous System
Co-IP	Co-Immunoprecipitation
CPSF	Polyadenylation Specificity Factor
Cry	Cytochrome 1
CT	Pyrimidine-Rich Elements
CT55	CT55, Cancer/testis Antigen 55
CTFs	C-terminal fragments
CTSS	Cathepsin S
CUG-BP	CUG binding protein
DAB1	Disabled Homologue 1

DAZ	Deleted in Azoospermia
DAZAP1	DAZ Associated Protein 1
DAZL	DAZ-like
DDX20	DEAD-Box Helicase 20
DDX58	DExD/H-Box Helicase 58
DEG(s)	Differential Expressed Gene(s)
DGE	Differential Gene Expression
DM1	Myotonic Dystrophy of Type 1
DNA	DeoxyriboNucleic Acid
DSB	Double Strand Breaks
dsRBD	Double-stranded RNA Binding Domain
DUOXA1	DUOXA1, Dual Oxidase Maturation Factor 1
ECM	Extracellular Matrix
EFEMP1	EFEMP1, EGF containing Fibulin-like Extracellular Matrix Protein 1
EGF	Epidermal Growth Factor
ELAV	Embryonic Lethal Abnormal Division
ELAVL3	ELAV like Neuron-specific RNA Binding Protein 3
Elk-1	ETS Domain-containing Protein Elk-1
EMSA	Electromobility Shift Assay
ERG	Early-Response Genes
ERK2	Extracellular Signal Regulated Kinase 2
ESCs	Self-renewal of Embryonic Stem Cells
ETF1	Eukaryotic Translation Termination Factor 1
ETR-3	Elav-type RNA Binding Protein 3
FGF2	Fibroblastic Growth Factor 2

FOSB	FOSB, FBJ Murine Osteosarcoma Viral Oncogene Homolog B
FTLD	Frontotemporal Lobar Degeneration
FUS/TLS	Fused in Sarcoma/translocated in Liposarcoma
FXTAS	Fragile X-associated Tremor/Ataxia Syndrome
GABA	Gamma-aminobutyric Acid
GAPDH	Glyceraldehyde-3-phosphate Dehydrogenase
GO	Gene Onthology
GOF	Gain-of-Function
HDAC6	Histone Deacetylase 6
HEK293	Human Embryonic Kidney 293 Cell Line
HeLa	Human Epithelial Cell Line
HIV-1	Human Immunodeficiency Type 1
HMOX1	HMOX1, Heme Oxygenase (Decycling) 1
hnRNA	Heterogeneous Nuclear RNA (pre-mRNA)
hnRNP A/B	Heterogeneous Ribonucleoprotein A/B
hnRNP A1	Heterogeneous Ribonucleoprotein A1
hnRNP A2/B1	Heterogeneous Ribonucleoprotein A2
hnRNP C	Heterogeneous Ribonucleoprotein C
hnRNP D	Heterogeneous Ribonucleoprotein D
hnRNP H	Heterogeneous Ribonucleoprotein H
hnRNP I	Heterogeneous Ribonucleoprotein I
hnRNP K	Heterogeneous Ribonucleoprotein K
hnRNP L	Heterogeneous Ribonucleoprotein L
hnRNP M	Heterogeneous Ribonucleoprotein M
hnRNP Q	Heterogeneous Ribonucleoprotein Q

hnRNP R	Heterogeneous Ribonucleoprotein R
hnRNP U	Heterogeneous Ribonucleoprotein U
hnRNP(s)	Heterogeneous Ribonucleoprotein(s)
HPRT1	Hypoxanthine Posphoribosyltransferase 1
HS3ST2	Heparan Sulfate-Glucosamine 3-Sulfotransferase 2
hTDP-43	human TDP-43
HTS	High-Throughput Screening
IBMPFD	Inclusion Body Myopathy associated with Paget's Disease of Bone and Frontotemporal Dementia
ICAM1	Intercellular Adhesion Molecule 1
ICAM5	ICAM5, Intercellular Adhesion Molecule 5, Telencephalin
IF	Immunofluorescence
IGF2	Insuline-like Growth Gactor 2
IGF2BP1	Insulin-like Growth Factor-II mRNA-binding Proteins 1
iPSC	Induced Pluripotent Stem Cells
ISE	Intronic Splicing Enhancer
JAG1	JAG1, Jagged 1
K/R	Lysine and Arginine
KCNAB1	KCNAB1, Potassium Voltage-gated Channel, Shaker-related Subfamily, Beta Member 1
KH	K-homology
KLF4	KLF4, Kruppel-like Factor 4 (gut)
KLHL4	KLHL4, Kelch-like Family Member 4
LOF	Loss-of-Function
MADD	MAP Kinase-activating Death Domain Protein

MEF2D	Myocyte Enhancer Factor 2D
MEK/Erk	Extracellular Signal-regulated Protein Kinase
mRNA	messenger RNA
N42	42 amino acid residues located at the N-terminal
ncRNA	non-coding RNA
NE	Neurotransmitter Norepinephrine
NEFL	Low Molecular Weight Neurofilament
NES	Nuclear Export Signal
NGS	Next-Generation Sequencing
NLS	Nuclear Localization Signal
NMJ	Neuromuscular Junction
NOVA2	Neuro-oncological Ventral Antigen 2
NRG3	NRG3, Neuregulin 3
NSC-34	Mouse Motor Neuron-like NSC-34 Cell Line
P-bodies	Processing Bodies
PABP	Polyadenylate Binding Protein
PABPN1	Nuclear Poly(A) Binding Protein
PCR	Polimerase Chain Reaction
PD	Parkinson’s Disease
PDZ	Postsynaptic density protein, Discs-large, Zona occludens
PENK	PENK, Proenkephalin
PIWI	P-element Induced Wimpy Testis
PND	Paraneoplastic Neurologic Syndrome
PNS	Paraneoplastic Neurologic Syndrome
POLDIP3	Polymerase Delta-interacting Protein 3

POLDIP3/SKAR	Polymerase Delta Interacting Protein/S6 Kinase 1 Aly/REF-like Target
POLR2A	RNA Polymerase II Subunit A
polyA	Polyadeylation
POMA	Opsoclonus Myoclonus Ataxia
PPP1R15A	Protein Phosphatase 1 Regulatory Subunit 15A
pre-mRNA	precursor mRNA
pre-rRNA	pre-ribosomal RNA
Pro-Rich	Proline rich region
Prrp	Proline-rich RNA Binding Protein
PTBP1	Polypyrimidine Tract-binding Protein 1
PTBP2	Polypyrimidine Tract-binding Protein 2
PUFAs	Polyunsaturated Fatty Acids
Q/N	Glutamine/Asparagine
qPCR	quantitative PCR
R/G	Arginine and Glycine
RA	Retinoic Acid
RAB26	RAB26, RAB26, Member RAS Oncogene Family
RAB31	RAB31, Member RAS Oncogene Family
RBD(s)	RNA-binding domain(s)
RBFOX1	RNA-binding Protein FOX1 Homologue 1
RBP(s)	RNA-binding protein(s)
RELN	Reelin
RGG	Arginine-Glycine-Glycine box
RIP-seq	RNA Immunoprecipitation Sequencing
RISC	RNA-induced Silencing Complex

RNA-IP	RNA Immunoprecipitation
RNA-seq	RNA Sequencing
RNA(s)	Ribonucleic Acid(s)
RNAi	RNA Interference
RNP	Riboucleoprotein
RNP1	Ribonucleoprotein Motif-1
RNP2	Ribonucleoprotein Motif-1
ROS	Reactive Oxygen Species
RPL13A	Ribosomal Protein L13a
RRM	RNA-Recognition Motif
RXRG	Retinoid X Receptor Gamma
S/R	Serine and Arginine
SDCBP2	SDCBP2, Syndecan Binding Protein (Syntenin) 2
SDHA	Succinate Dehydrogenase Complex Flavoprotein Subunit A
SG(s)	Stress Granule(s)
SH-SY5Y	Human Neuroblastoma Cell Line
SHANK3	SH3 and Multiple Ankyrin Repeat Domains Protein 3
SLIRP	Steroid Receptor RNA Activator Stem-loop Interacting RNA Binding Protein
SMA	Spinal Muscular Atrophy
SMN	Survival of Motor Neurons
SNAP25	Synaptosomal-associated Protein of 25 kDa
SNARE	Soluble *N*-ethylmaleimide Sensitive Factor Attachment Protein Receptor
snoRNA	small nucleolar RNA

SNPs	Single-Nucleotide Polymorphisms
snRNA	small nuclear RNA
SORT1	Sortilin 1
SR protein	Serine Arginine Rich Splicing Factors
SRRM4	Ser/Arg Repetitive Matrix Protein 4
SRSFs	Serine and Arginine Rich Splicing Factors
ssDNA	single strand DNA
STAG2	Stromal Antigen 2
STX3	Syntaxin 3
Syp	Syncrip/hnRNP Q
SYT14	Synaptotagmin 14
TAF15	TATA-Box Binding Protein Associated Factor 15
TBPH	TDP-43 homolog protein in Drosophila
TDP-43	Trans-activating response region (TAR)-DNA Binding Protein 43 kDa
TDPBR	Extended Binding Region for TDP-43
TERRA	Telomeric Repeat- containing RNA
TGF-β	Transforming Growth Factor Beta
TLR	Toll-like Receptor
TLR7	Toll Like Receptor 7
TNF	Tumor Necrosis Factor
TNFR	Tumor Necrosis Factor Receptor
TNFRSF9	Tumor Necrosis Factor Receptor Superfamily, Member 9
TNIK	TRAF2 And NCK Interacting Kinase
Tra2β	Transformer-2 Protein Homolog β
tRNA	transfer RNA

TSC2	Tuberous Sclerosis 2 Protein
UPS	Ubiquitin Proteasome System
V1C	Primary Visual Cortex
WB	Western Blotting
YPEL	Yippe-like
YPEL4	PEL4, Yippee-like 4 (Drosophila)
ZBP1	Zipcode-binding Protein
ZNC	Nucleocytoplasmic Shuttling Signal
ZnF	Zinc-finger

ABSTRACT

Heteregeneous ribonucleoproteins (hnRNPs) are a family of RNA-binding proteins (RBPs) implicated in several steps of RNA metabolism, including transcription, pre-mRNA splicing, mRNA transport and turnover. Therefore, alteration of their physiological levels may lead to many pathological disorders, such as neurodegeneration and cancer.

In this thesis, we focused the attention on three hnRNP proteins, namely DAZAP1, hnRNP Q and hnRNP R, that we previously identified in *Drosophila melanogaster* as strong modulators of TAR DNA-binding Protein 43 kDa (TDP-43) activity, an RBP involved in Amyotrophyc Lateral Sclerosis (ALS) and Frontotemporal Lobar Degeneration (FTLD).

First of all, we evaluated the effects of their depletion on TDP-43-controlled mRNAs within human neuroblastoma SH-SY5Y cells and in a cellular model of TDP-43 loss-of-function. We found that DAZAP1 and, to a lesser extent, hnRNP Q were the most consistent modifiers of TDP-43 activity. Therefore, to examine the connection between DAZAP1 and TDP-43, we initially characterized the interaction between these two proteins by immunoprecipitation analysis, demonstrating that DAZAP1 does not bind TDP-43 but can bind TDP-43 controlled mRNAs. Next, we decided to identify all the potentially targets regulated by TDP-43 and DAZAP1, by looking at the transcriptome status of cells silenced for these two hnRNPs and we found differently expressed genes associated with neurodegeneration (*ELAVL3 NOVA2, CELF5*) and inflammation (*TNF, TNFRSF9, ICAM1*).

Finaly, we extended our analysis to the characterization of hnRNP Q and hnRNPR, since the functional rescue of TDP-43 alterations was described only for hnRNP Q, but not for hnRNPR. We investigated the subcellular distribution and profiled differentially expressed genes analysis from RNA-seq after their knockdown. Interestingly, despite their high sequence similarity, these two proteins show different cellular distribution and affect

different cellular pathways, tipically associated with neurodegeneration (*PENK, NGR3, RAB26, JAG1*) and inflammatory response (*TNF, ICAM1, TNFRSF9, ICAM5*). In conclusion, our work provides insights on the involvement of the hnRNP family in controlling neuronal and inflammatory pathways, and suggests that the differential expression of these proteins could play an essential role in modulating the onset as well as the progression of neurodegenerative disorders, in particular when related to the TDP-43 proteinopathies.

1. INTRODUCTION

1.1 RNA-Binding Proteins and post-transcriptional gene regulation in brain

1.1.1 A general overview of RNA-Binding Proteins

Post-transcriptional gene regulation is an essential process involved in the cellular metabolism of coding and non-coding RNAs, that is regulated by the cooperative interaction of different ribonucleoprotein (RNP) complexes, consisting of RNA-binding proteins (RBPs) transiently or stably associated with RNAs (Dreyfuss et al., 1993).

Although some RBPs were initially identified through the biochemical method, including members of the heterogeneous ribonucleoprotein (hnRNP) family (Pinol-roma et al., 1988; Dreyfuss et al., 1984), the growing amount of data generated by whole genome sequencing of all kingdoms of life have expanded the list of known RBP proteins. In an effort to validate RBPs across human genome, in 2014 Gerstberger and collaborators analysed 800 domains from the protein family (Pfam) database known to bind RNA or to be found in RNA-related proteins, identifying 1542 RBPs (about 7.5% of all protein-coding genes in humans) (Gerstberger et al., 2014).

In this census, RBPs were mainly divided into different groups based on literature reports (Figure 1A):

- messenger RNA (mRNA)-binding;
- pre-ribosomal RNA (pre-rRNA)-binding;
- transfer RNA (tRNA)-binding;
- small nuclear RNA (snRNA)-binding;

- small nucleolar RNA (snoRNA)-binding;
- non-coding RNA (ncRNA)-binding;
- ribosomal proteins;
- diverse targets;
- unknown targets.

Moreover, phylogenetic analysis revealed the creation of gene families in which most of RBP paralogues share 20-70% sequence identity (Gerstberger et al., 2014), probably to increase protein synthesis or their regulation across different cell types (Figure 1B).

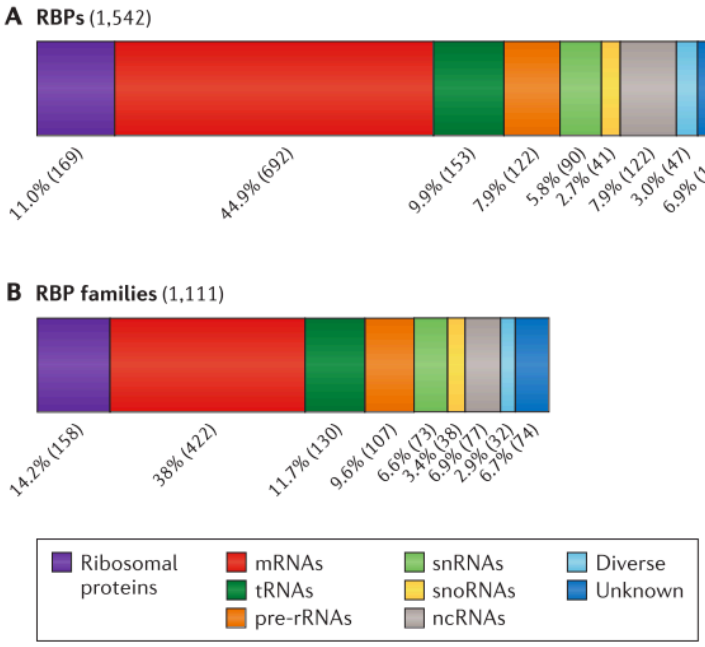

Figure 1. Classification of RNA-binding proteins. RNA-binding proteins (RBPs) **(A)** and RBP families **(B)** are divided in groups based on RNA targets. The percentage of RBPs in each category is shown. (Source: Gerstberger et al., 2014)

The importance of RBPs in the RNA metabolism became clear from their evolutionary conservation and abundance analysis. Bioinformatics analysis of yeast and *Drosophila*

genome have highlighted that 5-8% and 2-3% of genes are predicted to act as RBPs, respectively (Keene, 2001). Furthermore, a considerable number of orthologs of human RBPs have been found in lower organisms, such as archaea and bacteria (Anantharaman et al., 2002).

Despite the fact that the majority of human RBPs are ubiquitously expressed, sometimes at higher levels than average cellular proteins (Vaquerizas et al. 2009; Kechavarzi & Janga 2014), 82 specialized RBPs were found in brain, germ line, bone marrow, muscle, and liver. Overall, specialised RBPs represent 2% of all RBP families (Gerstberger et al., 2014). Examples of tissue specific RBPs are proteins involved in the germ line development and maintenance, such as the Deleted in Azoospermia (DAZ) (Reynolds and Cooke, 2005), the Insulin-like Growth Factor-II mRNA-binding Proteins 1 (IGF2BP1) and 3 (IGF2BP3) (Hammer et al., 2005) and P-element Induced Wimpy Testis (PIWI) (Siomi et al., 2011). Moreover, it is interesting to note that alterations in the cellular levels of RBPs are frequently recognized following their association with accessory binding partners (Han et al., 2010), during cellular senescence (Masuda et al., 2009) or in the presence of diseases (Pino et al., 2003).

1.1.2 Structure of RNA-Binding Proteins

As a structural point of view, RBPs have a modular architecture comprising multiple RNA binding domains that create a larger binding interface to recognize much longer stretches of nucleic acids (Figure 2) (Lunde et al., 2007). Specific regions called RNA-binding domains (RBDs) are responsible for the recognition of RNA sequences or RNA structural motifs belonging to different transcripts. In eukaryotes, the RNA-recognition motif (RRM) is by far the most common and characterized RBD. This highly conserved domain was first identified in the late 1980s by biochemical analysis which revealed the association between

heterogeneous nuclear RNAs (hnRNAs) with proteins (Dreyfuss et al., 1993). RRMs are composed of 80-90 amino acids disposed in a four-stranded anti-parallel β-sheet flanked on one side by two α-helices (α1 and α2) giving the $\beta_1\alpha_1\beta_2\beta_3\alpha_2\beta_4$ topology (Figure 2) (Oubridge et al., 1994). In this structure the RNA binding surface is represented by an arginine or lysine residue together with two conserved aromatic residues, located on the surface of the two central β-strands, β3 and β1, in the ribonucleoprotein (RNP) motif-1 (RNP1) and ribonoucleoprotein (RNP) motif-2 (RNP2), respectively (Oubridge et al., 1994). Analysis of conserved residues in the RRM-nucleic acid interface led to the definition of a common architecture of RRM-nucleic acid complex. In particular, the binding platform of RRM is based on a dinucleotide recognition by four conserved protein side chains in the centre of the β-sheet (Maris et al., 2005). Beyond these general features, the loop between secondary structure elements and the secondary structure elements themselves can be modified, in order to increase the RNA-binding affinity. For instance, the C-terminus of RRM2 and RRM3 in hnRNP I (also known as PTB) forms an extra β-strand antiparallel to β 2 (Simpson et al. 2004), and the α-helix 1 in U2AF RRM is three fold longer than the canonical one (Kielkopf et al., 2004). Higher affinity can also be achieved by the combination of two or more RRM domains, as demonstrated for Polyadenylate Binding Protein (PABP) (Maris et al., 2005). Another particular feature of some RRM domains is the ability to mediate protein-protein interactions. This contact can occur between two RRMs, between an RRM associated to RNA and a non-RRM protein that acts as a cofactor, and between RRMs that do not bind RNAs and another protein. An example of the first type of protein-protein interaction is the case of hnRNP A1, in which the two RRMs contained in the N-terminal region make contacts by using their α-helix 2 (Xu et al., 1997). Examples of the second and third types are the CBP20-CBP80-RNA complex and the Y14-Magoh complex, in which Y14 binds Magoh through the β-sheet of

the RRM domain, respectively (Maris et al., 2005).

Despite the abundance of RRMs, other well-established domains can be involved in the RNA recognition, including the K-homology (KH) domain, the zinc-finger (ZnF) domain and the double-stranded RNA binding domain (dsRBD) (Lunde et al., 2007). The characteristics of these domains and other RBDs are summarized in Figure 2.

Domain	Topology	RNA-recognition surface	Protein–RNA interactions	Representative structures (PDB ID)
RRM	αβ	Surface of β-sheet	Interacts with about four nucleotides of ssRNA through stacking, electrostatics and hydrogen bonding	U1A N-terminal RRM[18] (1URN)
KH (type I and type II)	αβ	Hydrophobic cleft formed by variable loop between β2, β3 and GXXG loop. Type II: same as type I, except variable loop is between α2 and β2	Recognizes about four nucleotides of ssRNA through hydrophobic interactions between non-aromatic residues and the bases; sugar-phosphate backbone contacts from the GXXG loop, and hydrogen bonding to bases	Nova-1 KH3 (type I)[41] (1EC6), NusA (type II)[37] (2ASB)
dsRBD	αβ	Helix α1, N-terminal portion of helix α2, and loop between β1 and β2	Shape-specific recognition of the minor–major–minor groove pattern of dsRNA through contacts to the sugar-phosphate backbone; specific contacts from the N-terminal α-helix to RNA in some proteins	dsRBD3 from Staufen[51] (1EKZ)
ZnF-CCHH	αβ	Primarily residues in α-helices	Protein side chain contacts to bulged bases in loops and through electrostatic interactions between side chains and the RNA backbone	Fingers 4–6 of TFIIIA[56] (1UN6)
ZnF-CCCH	Little regular secondary structure	Aromatic side chains form hydrophobic binding pockets for bases that make direct hydrogen bonds to protein backbone	Stacking interactions between aromatic residues and bases create a kink in RNA that allows for the direct recognition of Watson–Crick edges of the bases by the protein backbone	Fingers 1 and 2 of TIS11d[57] (1RGO)
S1	β	Core formed by two β-strands with contributions from surrounding loops	Stacking interactions between bases and aromatic residues and hydrogen bonding to the bases	Ribonuclease II[121] (2IX1), exosome[99] (2NN6)
PAZ	αβ	Hydrophobic pocket formed by OB-like β-barrel and small αβ motif	Recognizes single-stranded 3′ overhangs of siRNA through stacking interactions and hydrogen bonds	PAZ[73] (1SI3), Argonaute[76] (1U04), Dicer[72] (2FFL)
PIWI	αβ	Highly conserved pocket, including a metal ion that is bound to the exposed C-terminal carboxylate	Recognizes the defining 5′ phosphate group in the siRNA guide strand with a highly conserved binding pocket that includes a metal ion	PIWI[75] (1YTU), Argonaute (1U04)[76]
TRAP	β	Edges of β-sheets between each of the 11 subunits that form the entire protein structure	Recognizes the GAG triplet through stacking interactions and hydrogen bonding to bases; limited contacts to the backbone	TRAP[122] (1C9S)
Pumilio	α	Two repeats combine to form binding pocket for individual bases; helix α2 provides specificity-determining residues	Binding pockets for bases provided by stacking interactions; specificity dictated by hydrogen bonds to the Watson–Crick face of a base by two amino acids in helix α2	Pumilio[84] (1M8Y)
SAM	α	Hydrophobic cavity between three helices surrounded by an electropositive region	Shape-dependent recognition of RNA stem–loop, mainly through interactions with the sugar-phosphate backbone and a single base in the loop	Vts1[123] (2ESE)

dsRBD, double-stranded RNA-binding domain; KH, K-homology; OB-like, oligonucleotide/oligosaccharide binding-like; PDB ID, Protein Data Bank identification; RRM, RNA-recognition motif; siRNA, small interfering RNA; ssRNA, single-stranded RNA; ZnF, zinc finger.

Figure 2. Common RNA-binding domains. For each domain is reported a short description of the structure and properties. (Source: Lunde et al., 2007)

Together with these latter, auxiliary modules, such as regions rich in serine and arginine (S/R), arginine and glycine (R/G) or lysine and arginine (K/R)-rich basic patches (Biamonti and Riva, 1994) help increase the functional diversity of RBPs and their ability to bind multiple targets. Amongst these different auxiliary domains, the glycine-rich type is

the most frequent. This is found in most basic heterogeneous riboproteins (hnRNPs), in Nucleolin, in Fibrillarin and in several yeast RBPs (Biamonti and Riva, 1994). Basically, it contains repeats of RGG and/or RG sequence, collectively referred as RGG/RG motifs or RGG boxes, that are able to mediate RNA-binding, protein-protein interaction and cellular localization in normal and stress conditions (Thandapani et al., 2013). Moreover, the functional properties of the RGG/RG motifs can be affected by their interaction with proteins containing Tudor domains that are able to recognize arginine methylated RGG/RG motifs (Thandapani et al., 2013).

Additional layers of complexity in the structure of RBPs are achieved by post-translational modifications, including phosphorylation, arginine methylation and small ubiquitin-like (SUMO) modification (Glisovic et al., 2008). For example, hnRNP A/B, hnRNP C and hnRNP U are phosphorylated in vivo, and hnRNP A1/A2 are also methylated on arginine residues in the RGG box domain (Dreyfuss et al., 1993). The functions of these modifications seem to modulate the interactions between these proteins and RNAs or other proteins. SUMO modifications were found in hnRNP C and hnRNP M where they could contribute to the subcellular localization of these two proteins and the nucleocytoplasmic transport of associated mRNA targets (Vassileva and Matunis, 2004).

1.1.3 Different functions of RNA-binding proteins

As mentioned before, RBPs are involved in all the aspects of RNA biology, from transcription, pre-mRNA splicing and polyadenylation to modification, transport, stability and degradation of all RNAs (Figure 3) (Glisovic et al., 2008). Most importantly, RBPs can assemble in distinct multimeric complexes in order to control RNA life cycles (Romano and Buratti, 2013).

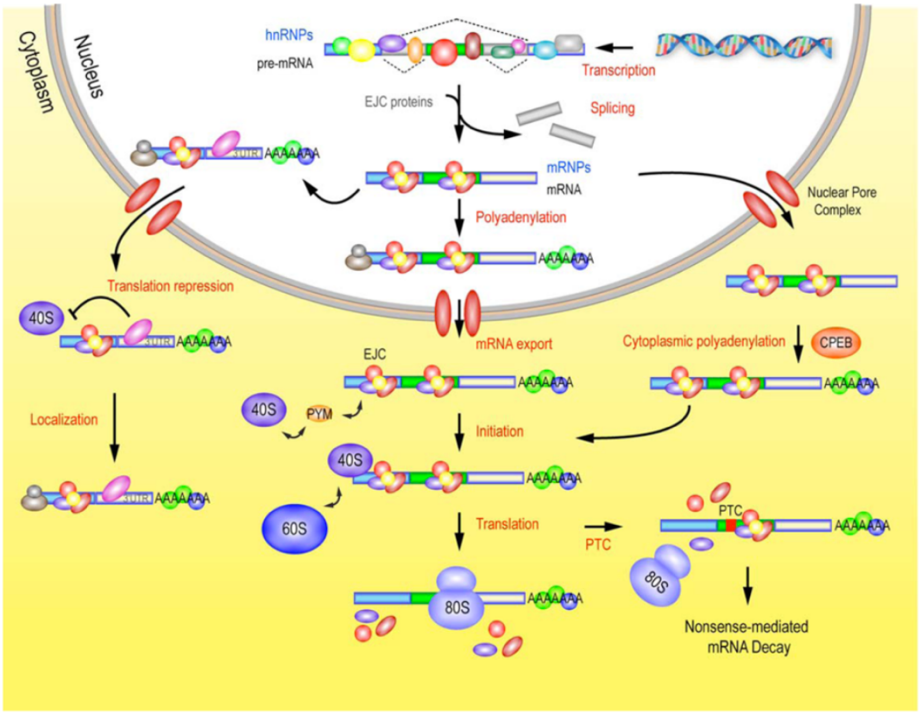

Figure 3. Function of RBPs in RNA metabolism. In eukaryotes, pre-mRNAs are transcribed by RNA polymerase II in the nucleus and further processed in different steps including splicing, polyadenylation and RNA editing. Once these modifications are concluded mRNAs are transported in cytoplasm, where they are translated in proteins and successively degraded. Each of these complex phases are controlled and organized by a network of proteins able to establish RNA-protein and protein-protein interactions. (Source: Glisovic et al., 2008)

In eukaryotes, the maturation of RNAs is a process that involves RNA cleavage and ligation reactions, in which nucleotide sequences called introns and exons are removed and joined together respectively. In protein-coding mRNAs (and long non-coding RNAs) this important step of RNA metabolism occurs in a large ribonucleoprotein (RNP) machinery, called the spliceosome (Lee and Rio, 2015). Pre-mRNA splicing takes place for > 95 to 100% of human genes, and at least 74% of human genes transcribe multiple mRNAs through alternative splicing (Lee and Rio, 2015; Glisovic et al., 2008). Extrinsic nonspliceosomal RNA-binding proteins play a role in controlling alternative splicing, basically promoting or inhibiting the recognition of alternative regions by the spliceosome machinery. Among these splicing regulator proteins are Serine Arginine Rich Splicing

Factors (SR proteins), hnRNPs and tissue-specific RBPs (Baralle and Giudice, 2017). An example of the participation of RBPs in alternative splicing events is the regulation of *β-tropomyosin* pre-mRNA, in which two SR proteins called SF2/ASF and SC35 act in an opposite way on the intronic enhancer-dependent splicing of exon 6A (Van Der Houven Van Oordt et al., 2000).

Other two important steps in post-transcriptional gene regulation are the polyadenylation of the 3'-end of pre-mRNAs and the RNA editing. Polyadenylation involves an RBP, called Nuclear Poly(A) Binding Protein (PABPN1) that is responsible for the addition of the poly(A) tail on the extremity of each transcript after cleavage of 3'-end (Glisovic et al., 2008). The Polyadenylation Specificity Factor (CPSF) complex stimulates the poly(A) polymerase activity of PABPN1. RNA editing prevalently involves the deamination of adenosine (A) to inosine (I). This conversion requires the presence of enzymes belonging to the ADAR family, which are RNA-binding proteins. Indeed, ADAR2 combines its dsRBD with an auxiliary deaminase domain that is responsible for this conversion (Valente and Nishikura, 2005).

Once pre-mRNA processing is completed, the transcripts are exported from nucleus to the cytoplasm and this further level of RNA metabolism is promoted by a network of RBPs. These include the Zipcode-binding Protein (ZBP1), which is an RBP involved in the trafficking and translation of *β-actin* mRNA (Hüttelmaier et al., 2005).

Finally, RBPs are also key factors of mRNA turnover and stability, as described by the regulation of neuronal specific transcripts by RNA-binding proteins belonging to the ELAV/Hu family (Keene, 1999).

1.1.4 Implication of RNA-Binding proteins in brain development, maintenance and disease

RNA-binding proteins are key factors of neuronal development. Several studies have demonstrated that neurons have a unique system for regulating RNA metabolism, consisting of tissue-specific RBPs (De Conti et al., 2016).

In mammals, the ELAV/Hu family is involved in the stability and trafficking of specific transcripts containing AU-rich elements (ARE) predominantly in neurons. These transcripts are particularly interesting because they encode functional subsets of Early-Response Genes (ERG) or immediate gene products, including proto-oncoproteins and cytokines (Keene, 2001). The ELAV/Hu family is composed of four members: HuR, that is widely expressed and HuB, HuC and HuD which are specifics of neurons. HuR (also called HuA) has a high level of homology with a *Drosophila* nuclear protein namely Embryonic Lethal Abnormal Division (ELAV). *Elav* deletion is lethal due to abnormal development of neurons (Robinow and White, 1991). The importance of ELAV/Hu proteins is also relevant in pathology. Indeed, it is interesting to note that tumours outside the nervous system can express these proteins leading to Paraneoplastic Neurologic Syndrome (PNS) (Albert and Darnell, 2004).

The crosstalk of different RPBs controls RNA splicing patterns essential for neuronal development and maintenance. In neuronal progenitors, Polypyrimidine Tract-binding Protein 1 (PTBP1) induces the exon skipping of *Polypyrimidine Tract-binding Protein 2* (*PTBP2*) exon 10 to form a transcript with a premature stop codon subject to non-sense mediated mRNA decay (NMD). Nevertheless, when the progenitors start to differentiate into neurons, the negative effect of *PTB1* on *PTBP2* exon 10 is lost by PTBP1 downregulation and at the same time upregulation of the splicing enhancer Ser/Arg Repetitive Matrix Protein 4 (SRRM4) (Quesnel-Vallières et al. 2015; Makeyev et al.

2007).

Another important RBP implicated in brain development and differentiation is the Neuro-Oncological Ventral Antigen 2 (NOVA2). This protein inhibits *Disabled Homologue 1 (DAB1)* exon 7bc splicing inclusion in late-generated cortical and Purkinje neurons. In turn, DAB1 regulates the Reelin signalling, an important pathway involved in neuronal development. Neuronal migration defects found in neurons with the *DAB1* longer isoform, corresponding to the inclusion of exon 7b and 7c, are similar to those observed in *Nova2*$^{-/-}$ mice (Yano et al. 2010). Similarly to ELAV/Hu proteins, the abnormal expression of NOVA1/NOVA2 in breast cancer determines the enstablisment of a PND form called Opsoclonus Myoclonus Ataxia (POMA). In fact, the alteration of NOVA proteins leads to immune system activaction and consequent formation of autoantibodies responsible for neuronal cell death in the regions of the nervous system where NOVA proteins are expressed (Lukong et al., 2008).

RNA regulation during neuronal differentiation can also involve alternative splicing of the RBP mRNAs themselves. During synaptic development, exon 19 of *RNA-binding Protein FOX1 Homologue 1* (*RBFOX1*) is alternatively spliced by RBFOX proteins, giving rise to nuclear or cytoplasmic protein isoforms. Moreover, mutations in RBFOX proteins have been found in people suffering from autism and are related to alterations of transcripts, such as *SH3 and Multiple Ankyrin Repeat Domains Protein 3 (SHANK3)*, *Voltage-dependent L-type Calcium Channel Subunit α1C (CACNA1C)* and *Tuberous Sclerosis 2 Protein (TSC2)* (Baralle and Giudice, 2017).

Finally, the spatial and temporal organization of gene expression is a particular feature adopted by the nervous system to control the synaptic plasticity (Zukin, Richter and Bagni 2009). In order to avoid the premature translation and degradation of specific mRNAs, silent mRNAs, RBPs and miRNAs are associated in macromolecular assemblies, including

synaptic mRNA-silencing foci, processing bodies (P-bodies) and stress granules (SGs). Silent mRNAs wait inside the granules to reach the exact localization in which translation can start (De Conti et al., 2016). Examples of RBPs that participate to the formation of SG granules are hnRNPA2, TATA-Box Binding Protein Associated Factor 15 (TAF15), fused in Sarcoma/Translocated in Liposarcoma (FUS/TLS) and TAR DNA-binding Protein 43 (TDP-43). Stress conditions, mutations in RBPs, aging and other pathological disorders can alter the equilibrium between soluble, disperse and aggregated states leading to increased SG formation, and progressively the formation of stable and long-lived aggregates that resemble the characteristics of pathological inclusions. Indeed, several studies have identified the presence of SGs in Alzheimer's diseases (AD), amyotrophic lateral sclerosis (ALS) and frontotemporal lobar degeneration (FTLD) (Wolozin & Apicco 2015; De Conti et al. 2016).

1.2 Transcriptome analysis using RNA sequencing and its applications in the characterization of RNA binding proteins

1.2.1 From hypothesis-driven approaches to high-throughput screening (HTS) approaches

The analysis of the complete set of all RNA molecules transcribed in a cell at a specific developmental stage or physiological condition, called its transcriptome, has given insights into how the genome is packaged and expressed, and has been useful to clarify important aspects related to genome evolution (Wang, 2001; Elliott, 2014).

In the last decade, several efforts have been made to clarify the role of RBPs in transcriptome regulation, and their involvement in neurodegeneration. Initially, the characterization of novel regulatory factors in the field of RNA metabolism was based on

traditional hypothesis-driven approaches, in which the investigation of biological effects was initiated by a prediction (Buratti, Romano and Baralle, 2013). For example, preliminary studies correlating splicing inclusion of *Cystic Fibrosis Transmembrane Conductance Regulator* (*CFTR*) exon 9, and the number of UG(m)/U(n) repeats close to the 3' splice site of exon 9 (Cuppens et al., 1998; Larriba et al., 1998), identified TDP-43 as the major hnRNP involved in this splicing recognition (Buratti et al., 2001). The advantages of using this approach are the capability to set up a precise series of experiments aimed at confirm or reject the original hypothesis. However, the process that is necessary to reach an in-depth characterization is laborious and could lead to the loss of some information important for the comprehension of the initial question (Buratti, Romano and Baralle, 2013). Thanks to the advancement of system-wide approaches and bioinformatics, the analysis of gene expression changes and the identification of RNA/protein targets at a global cellular level have became more popular and have allowed more open-ended approaches that are not strictly hypothesis-driven (Buratti et al., 2013).

The term high-throughput screening (HTS) is referred to the way of rapidly assessing a large number of biological factors and chemical compounds in order to identify those which can modulate a specific cellular pathway (Buratti, Romano and Baralle, 2013). Examples of these new techniques aimed to analyse transcriptomes are microarrays (GeneChip), RNA sequencing (RNA-seq) and cross-linking immunoprecipitation sequencing (CLIP-seq) (Figure 4).

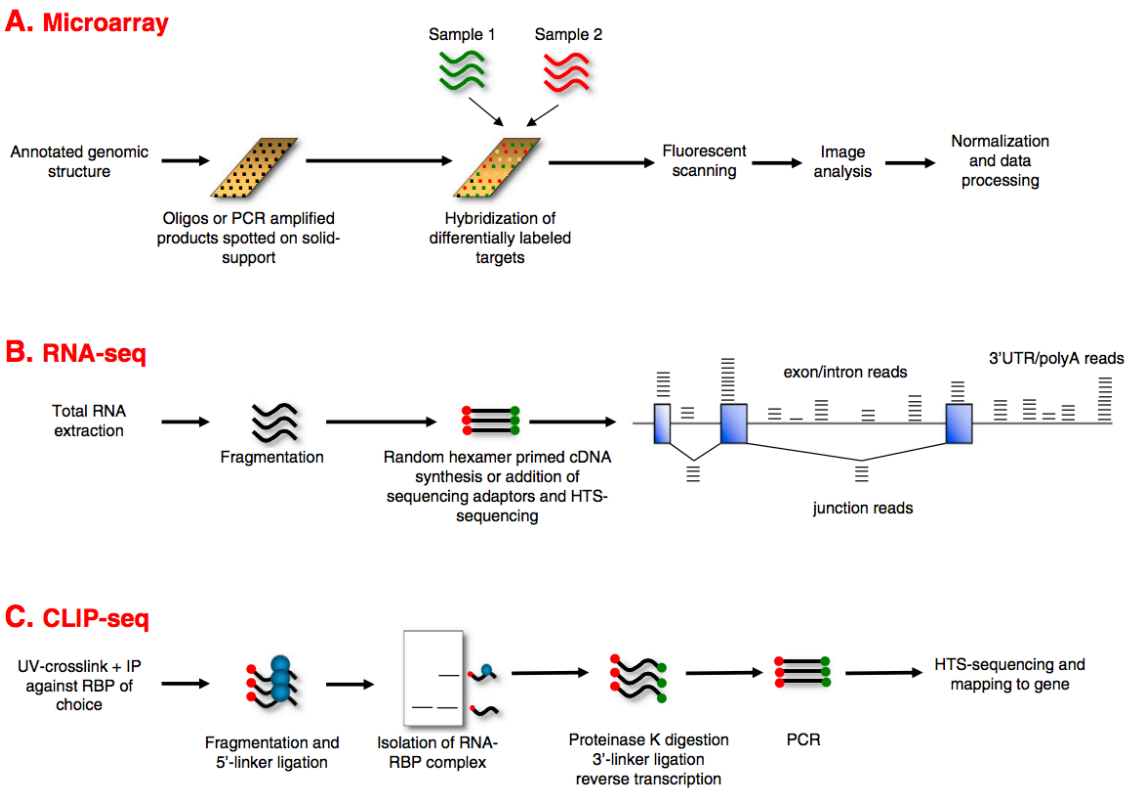

Figure 4. High-throughput screening (HTS) approaches. Flowchart of microarray **(A)**, RNA-seq **(B)** and CLIP-seq **(C)** experiments. (Source: Buratti et al., 2013)

Briefly, microarray screening consists of a pool of DNA sequences spotted on a solid surface that are hybridized with RNAs extracted from cells or tissues, labelled with fluorescent probes, washed and then finally analysed based on the fluorescence emitted (Dalma-Weiszhausz et al., 2006). These arrays can be designed in order to detect predicted splicing junctions, and therefore to analyse possible changes in splicing events.

Despite microarrays being extensively used for the characterization of RNA binding factors, including TDP-43 (Colombrita et al., 2012; Narayanan et al., 2013), hnRNP K (Liu and Szaro, 2011), hnRNP L (Hung et al., 2008) and hnRNP A1 (Liu et al., 2017), this approach has some limitations, such as the necessity to design/synthesize the probes that have to be attached on the solid surface. Hence, knowledge of the sequence to make the probe set is mandatory, making it impossible to detect mRNAs absent from databases or

with incomplete/incorrect genome annotations (Hurd and Nelson, 2009). Furthermore, the phenomenon of cross-hybridization makes it problematic to analyse and obtain reproducible results for highly related sequences. This restricts microarray analysis to non-repetitive genome sequences, therefore making arduous the analysis of splicing isoforms, allelic gene variants, and single-nucleotide polymorphisms (SNPs) (Shendure, 2008; Hurd and Nelson, 2009; Buratti, Romano and Baralle, 2013). Other limitations regard signal-to-noise ratio and the problems related to detect low-abundance sequences, the necessity to obtain DNA from PCR amplification with the possibility to introduce bias into samples, and finally, the wide amount of preparative methodologies, microarray formats and analytical approaches currently available (Hurd and Nelson, 2009; Ioannidis et al., 2009).

Some drawbacks have been solved by the sequencing of transcriptome. Therefore, in the next paragraphs, the attention will be focalised on the RNA-seq analysis and its applications in the characterization of RNA binding proteins.

1.2.2 Next-generation sequencing (NGS): RNA sequencing

The concept of sequencing was developed in the late 70s by the pioneering works of Sanger and Coulson (Sanger, Nicklen and Coulson, 1977) and Maxam and Gilbert (Maxam and Gilbert, 1977). However, the effective power of this approach applied in the research field, has been possible later with the support of industries and the development of instruments able to produce hundreds of gigabases of nucleotide sequence output in a single run (Metzker, 2010). Nowadays, we talk about next-generation sequencing (NGS) technology to describe seq-based methods, such as RNA-seq. NGS analysis has allowed us to overcome the limitations of other HTS approached not seq-based (e.g. microarray). Indeed, the gene expression analysis carried out using RNA-seq does not require the prior knowledge of genome sequences, making possible the detection of RNA editing events and

the quantification of splicing isoforms (Hurd and Nelson, 2009; Sánchez-Pla et al., 2012; Buratti, Romano and Baralle, 2013). Moreover, the fact that the sample of interest is directly sequenced results in the removal of experimental bias from the analysis, such as cross-hybridation issue and mapping of repetitive sequences, as well as problems in the quantification of signal, because it is based on counting sequence tags rather than the relative measurement between samples. Finally, nanograms of materials are necessary and sufficient for sequencing, reducing the reliance of extensive PCR amplification of the material (Hurd and Nelson, 2009).

However, there are some shortcoming in the RNA-seq approach, including the necessity to analyse biological replicates to avoid problems related to the sample assignment to lanes or runs, and the normalization of the counts after the alignment to a reference genome. This normalization resolves issue related to the libray size, the gene length and the distribution of counts among samples (Sánchez-Pla et al., 2012).

Differential gene expression (DGE) analysis (Costa-Silva, Domingues and Lopes, 2017), characterization of alternative splicing events (Park et al., 2018) and detection of gene fusion events (Kumar et al., 2016), as well as specific RNA species (Andrés-León, Núñez-Torres and Rojas, 2016) are examples of RNA-seq applications. The type of RNA-seq application affects the choice of the sequencing platform and the relative bioinformatics analysis.

Nowadays, there are different available platforms, which were initially developed for DNA, but they can easily be applied to RNA sequencing after the conversion from RNA into more stable cDNA molecules by reverse transcriptase (Sánchez-Pla et al., 2012). Moreover, each platform uses different methodologies for template preparation, sequencing-imaging and gene alignment, determining a wide range of data output in terms of cost and quality (Metzker, 2010). Examples of platforms are Illumina (Miseq, NextSeq

500, HiSeq 2500, HiSeq X Ten), Life Technologies Ion Torrent (PGN and Proton systems), Pacific Biosciences PacBio RSII and Oxford Nanopore Tecnologies MinION (Reuter et al., 2015). For instance, Illumina's and Ion Torrent's technologies provide the possibility to generate short read length (for HiSeq 2500 and Ion PGN: reads length up to 125 bp and 200 or 400 bp, respectively) making them less suitable for particular studies, including gene isoform detection (Reuter et al., 2015). On the other hand, PacBio RII and MinION systems features to obtain long-read sequence data (> 14 kb and ~ 6-65 kb, respectively) suitabled for the identification of gene splicing events, althought they are limitated by the lower coverage comparing to Illumina and Ion Torrent platforms (Reuter et al., 2015).

1.2.3. RNA sequencing applied to the characterization of RNA binding proteins

An increasing number of works described the application of sequencing analysis to explore all the possible RNA targets of a specific RBP (Buratti, Romano and Baralle, 2013), as well as to profile the transcriptomes of brain tissue affected from neurodegenerative disorders (Twine et al., 2011). In this regard, RNA-seq has been used to analyse the effect of TDP-43 knockout in the central nervous system of *Drosophila* (Hazelett et al., 2012) and in mouse embryonic stem cells (Chiang et al., 2010).

Nowadays, improvements in sequencing technology also provide the possibility to map the sites at which proteins are bound to the RNA, by coupling this technique with RNA immunoprecipitation (RIP) (Marchese et al., 2016) or cross-linking immunoprecipitation (CLIP) (Licatalosi et al., 2008). In RIP-seq analysis the RNA-complexes formed between the protein of interest and its interacting RNAs are co-immunoprecipitated and the bound RNAs are subsequently sequenced, while in the CLIP-seq analysis the target protein is

previously cross-linked *in vitro* with its RNA targets and successively these RNAs are immunoprecipitated and sequenced.

For instance, in order to describe TDP-43 targets in TDP-43-containing protein complexes within rat cortical neurons, deep sequencing analysis was performed following RNA-immunoprecipitation (Sephton et al., 2011). RIP-seq was also used to characterize mRNA targets of hnRNP L in prostate cancer LNCaP cells (Fei et al., 2017) and to identify spliceosome-associated genes in hnRNP H1 targets (Uren et al., 2016). Interestingly, most of the hnRNP H1 targets enriched in the analysis encoded other RBPs, including TDP-43, FUS, several hnRNPs and Serine and Arginine Rich Splicing Factors (SRSFs) (Uren et al., 2016). One the other hand, CLIP-seq analysis has been used for mapping *in vivo* binding positions of other RNA-binding proteins, including NOVA (Licatalosi et al., 2008), CELF1 (Le Tonquèze et al., 2016) and Transformer-2 Protein Homolog β (Tra2β) (Grellscheid et al., 2011).

1.3 The Heterogeneous Ribonucleoprotein (hnRNP) family

1.3.1 General characteristics of the hnRNP family

The most abundant RBPs belong to the heterogeneous ribonucleoprotein (hnRNP) family (Glisovic et al., 2008). hnRNPs were originally described as RBPs transiently bound to the heterogeneous nuclear RNA (hnRNA, also known as pre-mRNAs) produced by RNA polymerase II in the nucleus of eukaryotic cells (Dreyfuss et al., 1993). The 40S core particle was the first mRNA-protein complex, isolated by sucrose density gradients, and contained hnRNP A/B and C (Beyer et al., 1977). Later on, several other hnRNPs were characterized by immunoprecipitation with monoclonal antibodies and UV-cross-linking experiments leading to the identification of 20 major types of hnRNPs. These were

alphabetically named from hnRNP A1 to hnRNP U (Figure 5) (Geuens et al., 2016; Han et al., 2010). Although, the hnRNPs have many features in common with other RBPs, such as the SR proteins and ELAV-like proteins, they are generally described as a separated family. The basis for this classification arises from historical motivations, rather than phylogenetic, structural or functional evidence (Han et al., 2010).

Besides these canonical hnRNPs, several studies have classified other proteins as hnRNP-like RNA binding factors, such as CELF proteins, FOX proteins, NOVA, or TDP-43 (Busch and Hertel, 2012).

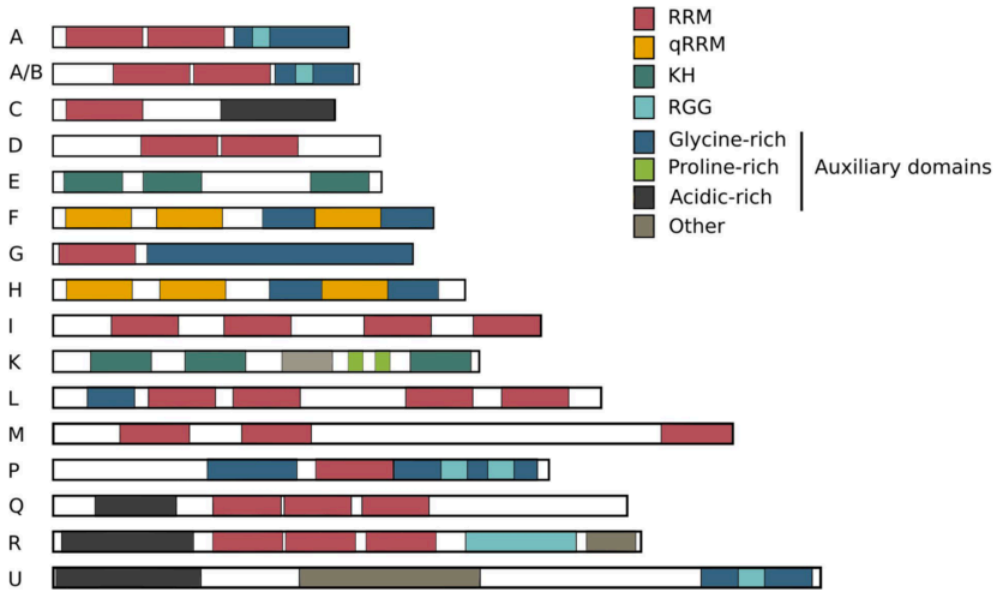

Figure 5. Structure of the canonical hnRNP family members. hnRNP proteins have different molecular weight ranging from 34 kDa to 120 kDa. Several structural features are shared among the hnRNP family, including RNA-binding domains (RRM, RNA-recognition motif; qRRM, quasi-RNA recognition motif and KH, K-homology domain), Arginine-glycine-glycine box (RGG-box) and auxiliary domains. (Source: Geuens et al., 2016)

Structurally, hnRNP proteins share common features, including RBDs (with the exception of hnRNP U). The majority of hnRNPs also have RGG-boxes and auxiliary domains. In addition, hnRNPs can have different splicing variants and undergo post-translation

modifications and nucleocytoplsmic shuttling (Han et al., 2010). However, regarding the latter, there are difference between the mechanisms that different hnRNPs adopt to translocate from nucleus and cytoplasm and *vice-versa*. For instance, hnRNP A1 and hnRNP I do not contain canonical nuclear localization signals (NLSs) and their translocation is coupled with transcription (Gama-Carvalho and Carmo-Fonseca, 2001). Interestingly, it has also been demonstrated that stress-dependent phosphorylation of hnRNP A1 is responsible for its cytoplasmic accumulation within SGs (Guil et al., 2006). On the contrary hnRNP K contains NLS and its movement is uncoupled with transcription (Gama-Carvalho and Carmo-Fonseca, 2001).

Although hnRNPs are prevalently abundant in the nucleus, it has been ascertained that hnRNP U and C are also found in cytoplasmic RNA granules (Kanai et al., 2004; Piñol-Roma and Dreyfuss, 1992), one of the hnRNP M isoforms is a membrane-bound receptor (Bajenova et al., 2003) and hnRNP Q is predominantly cytoplasmic and it is localized in mRNA granules (A Mizutani et al., 2000). hnRNP P (FUS) is also localized in cytoplasm inside stress granules (Andersson et al., 2008).

1.3.2 Multiple functions of hnRNPs

Several of the biological functions of hnRNPs involve cooperative and dynamic interactions with different proteins. Indeed, across all the steps required for mRNA biogenesis, there is a continuous remodelling of the hnRNP complex, represented by the association of particular hnRNPs with pre-mRNAs, in which the loss or acquisition of hnRNP proteins as well as other RBPs create what has been classically defined as an ‘‘mRNP code’’. This “mRNP code” is unique for each transcript and the protein composition of the complex reveals its cytoplasmic fate (Singh and Valcárcel, 2005).

Many of the functions of RBPs previously described in this thesis take place thanks to

hnRNP proteins and their interplay. For example, a role in transcriptional regulation was first described in 1996, when hnRNP K was found to bind *in vitro* to pyrimidine-rich (CT) elements in single strand DNA (ssDNA) (Michelotti et al., 1996). Successively, it has been demonstrated that hnRNP K can act as a transcriptional repressor of the *Osteocalcin* gene by inhibiting the formation of a transcriptional complex on the CT element of the *Osteocalcin* promoter (Stains et al., 2005). The transcriptional repressor activity can also take place without direct contact with DNA, as it occurs during the inhibition of *α1-Acid Glycoprotein (AGP)* gene (Miau et al., 1998).

Among all the process that influence transcriptome complexity, alternative splicing is the most important event in which hnRNPs are involved. Recently, it has been demonstrated that multiple hnRNPs, among which TDP-43, hnRNP L, PTB/nPTB and hnRNPA1/A2 are able to modulate with disparate strength the inclusion of *Sortilin 1 (SORT1)* exon 17b (Mohagheghi et al., 2016).

Interestingly, there is also substantial evidence supporting the role of RBPs in the maintenance of genome integrity and in the regulation of telomeres (Nishida et al., 2017). Indeed, hnRNP L and hnRNP C have been identified in complexes that work as DNA double strand breaks (DSB) sensors (Nishida et al., 2017). FUS/TLS is another transcriptional regulatory sensor of DNA damage, and is recruited to the *Cyclin D1* promoter after ionizing radiation exposure where it functions as a transcriptional repressor (Lagier-Tourenne et al., 2010).

Furthermore, FUS/TLS interacts through its RGG domains with a G-quadruplex consisting of telomere DNA and the functional non-coding RNAs called Telomeric Repeat-containing RNA (TERRA) to regulate histone modifications of telomeres (Takahama et al., 2015). In addition, hnRNP A/B together with other hnRNPs and telomere-binding factors, regulates the structure of telomeres, protecting them from degradation (Han et al., 2010).

1.3.3 Role of hnRNPs in neurodegenerative disorders

Albeit the equilibrium of hnRNP proteins is finely regulated and neurons are characterized by a very adaptive and dynamic architecture, perturbation of their neuronal homeostasis can lead to neurodegenerative disorders, such as ALS, FTLD, spinal muscular atrophy (SMA) and Alzheimer's disease. In particular, these pathologies are characterized by the presence of protein aggregates, also including RBPs/hnRNP proteins (Neumann et al., 2006). The formation of these aggregates is a result of several steps consisting of protein misfolding, oligomerization and eventually formation of protofribrils or amyloid fibrils (Stefani and Dobson, 2003). A clear example of the involvement of hnRNPs in neurodegeneration is the finding of TDP-43 and FUS/TLS in ALS and FTLD inclusions. These inclusions can act as a "sink" influencing the clearance of these proteins from nucleus and it can, in turn, explain the aberrant RNA processes (e.g. alternative splicing) observed in aggregation-bearing cells. Both TDP-43 and FUS contain a prion-like domain that confers them an intrinsic propensity to aggregate (Gitler and Shorter, 2011). Together with this consideration, variations in the protein sequence can trigger the establishment of diseases. In both TDP-43 and FUS coding genes the presence of ALS-linked mutations have been described, and in the case of TDP-43 it has been demonstrated that TDP-43 ALS-linked mutations accelerate aggregation *in vitro* (Ugras and Shorter, 2012). More recently, the presence of ALS/FTLD-associated mutations have also been described in the prion-like domain of hnRNP A1, A2/B1 and putative mutations have also been hypothesized by a yeast functional screening in *TAF15* encoding gene (Couthouis et al., 2011).

Most importantly, these hnRNPs seem to not act alone in mediating neurodegeneration. Indeed, it is thought that GGGGCC repeat expansion in the *C9orf72* gene are the causative agents of associate ALS/FTLD pathologies, due to the fact that these repetitions can cause

the subtraction of a significant amount of RBPs from the protein milieu (De Conti et al., 2016).

A plethora of intracellular systems are designed to maintain this intracellular homeostasis, including the ubiquitin proteasome system (UPS) (Kriegenburg et al., 2012) and the autophagy system (Feng et al., 2014). In the UPS, proteins are primarily targeted for degradation through the covalent attachment of a small protein, called ubiquitin, and then directed to the proteasome complex for degradation (Glickman and Ciechanover, 2002). Disruption of proteasome activity is sufficient to induce cytoplasmic accumulation and aggregation of TDP-43 in primary hippocampal and cortical neurons, as well as in the immortalized motor neuron cell line NSC-34 (van Eersel et al., 2011).

In the autophagy system, harmful substances contained in the cytoplasm are degraded within lysosomes/vacuoles, and the resulting macromolecular constituents are recycled (Feng et al., 2014). Recently, it has been demonstrated that the induction of autophagy system triggered the neuronal clearance of TDP-43 with consequent enhancement of survival in human Induced Pluripotent Stem Cell (iPSC)-derived neurons and astrocytes obtained from patients with familial ALS (Barmada et al., 2014).

1.4 Trans-activating Response Region (TAR) DNA-Binding protein of 43 kDa (TDP-43)

1.4.1 Brief introduction on TDP-43

Trans-activating response region (TAR) DNA-binding protein of 43 kDa (TDP-43) is a ubiquitously expressed and highly conserved protein of 414 amino acid residues belonging to the heterogeneous nuclear ribonucleoprotein (hnRNP) family. Originally described as a transcription factor bound to the regulatory element in the Human Immunodeficiency

Virus Type 1 (HIV-1) long terminal repeat known as TAR (Ou et al., 1995), in 2001 TDP-43 was rediscovered as a splicing factor involved in the regulation of *CFTR* exon 9 and successively linked to different aspects of RNA metabolism, such as mRNA stability (including its own), mRNA transport, translation, and non-coding RNAs (miRNA, lncRNAs, etc.) processing (Buratti and Baralle, 2012).

Furthermore, although mostly nuclear, TDP-43 continuously shuttles from the nucleus to the cytoplasm where it forms high molecular mass complexes that include proteins and RNAs (Sephton et al., 2011; Ayala, Zago, et al., 2008).

In 2006, TDP-43 was identified as a major component of the ubiquitin-positive, α-Synuclein and Tau-negative cytoplasmic inclusions recognized in the brain and spinal cord tissues of Frontotemporal Dementia with Ubiquitin-positive Inclusions (FTLD-U) and ALS patients (Arai et al., 2006; Neumann et al., 2006). Successively TDP-43 inclusions were also reported at lower frequencies in other neurodegenerative diseases, including Alzheimer's, and Parkinson's (PD) disease and Lewy body (LB) disorders (Nakashima-Yasuda et al., 2007). Following the growing amount of data regarding the involvement of TDP43 protein in neurodegeneration, several other studies have focused their attention on understanding the biochemistry mechanisms behind cellular functions of TDP-43 in physiology and pathology. Some of these findings are summarized in the paragraphs below.

1.4.2 Characteristics of TDP-43

TDP-43 is encoded by the *TARDBP* gene located on the short arm (p) of human chromosome 1 at position 36.22 (1p36.22) (Figure 6), and is highly conserved among *Drosophila melanogaster*, *Caenorhabditis elegans*, mouse and human (Wang et al., 2004). The *TARDBP* gene consists of 6 exons. Exons 2-6 encode the functional TDP-43 protein.

However, the genomic analysis of *TARDBP* gene performed by Wang and colleagues and successively by Alton et al., have also highlighted the presence of different splicing isoforms of TDP-43 (D'Alton et al., 2015; Wang et al., 2004). Furthermore, more than 38 nonsynonymous *TARDBP* mutations have been identified in both familiar and sporadic ALS (Scotter et al., 2015).

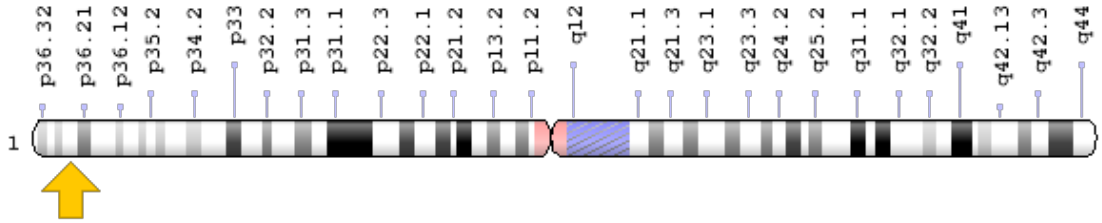

Figure 6. Localization of *TARDBP* gene on human chromosome 1. The Genomic locus encoding TDP-43 is identified by a yellow arrow. (Source: Genetic home resource)

TDP-43 expression is developmentally regulated. High levels of TDP-43 expression were found during early embryogenesis, but progressively and markedly decrease with age in post-natal brains (Sephton et al., 2010). In agreement with this finding, Huang and colleagues demonstrated the expression of TDP-43 in all post-natal tissues, such as cerebellum, forebrain, brainstem, spinal cord, skeleton muscle, heart, liver, lung, spleen and kidney, with a global decrease of TDP-43 levels with the advancement of age (Huang et al., 2010). Furthermore, TDP-43 knockout mice were also lethal during embryonic stages (Sephton et al., 2010). This observation has also been confirmed in *Drosophila* where the disruption of TDP-43 was lethal at the second larval stage (Fiesel et al., 2010), although in other *Drosophila* models, TDP-43 null flies were able to survive through adulthood (Feiguin, Vinay K. Godena, et al., 2009), suggesting the influence of modifier genes affecting TDP-43 in developmental regulation.

From a structural point of view, TDP-43 architecture reassembles the general hnRNP structural organization (Figure 7).

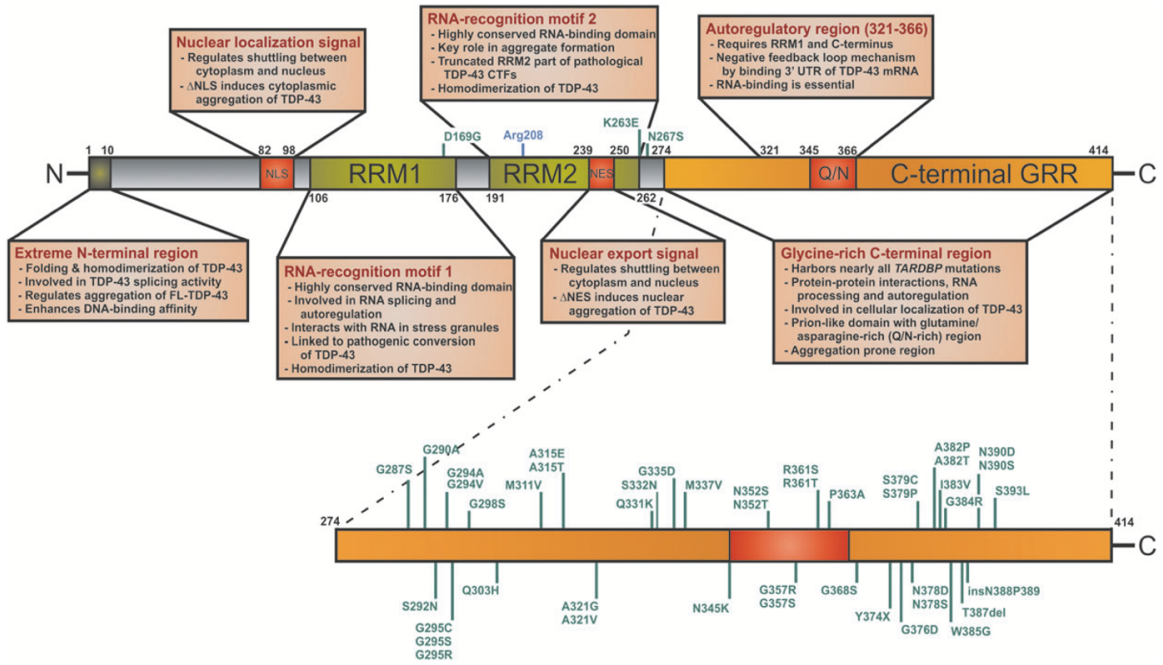

Figure 7. Schematic representation of TDP-43 protein domains and their associated functions. TDP-43 is composed of an N-terminal domain containing NLS, two RNA-recognition motifs (RMM1 and RRM2 in which NES is present) and a C-terminal domain containing a glycine-rich region (GRR). ALS-linked mutations are also reported in the figure. (Source: Janssens and Van Broeckhoven, 2013)

TDP43 protein is composed of:

- The **N-terminal domain**: contains the nuclear localization sequence (NLS) that is composed of NLS1 (K82RK84) and NLS2 (K95VKR98). Mutations in these two positions reduce the nuclear localization of TDP-43 (Buratti and Baralle, 2001).
- Two **RRMs**: highly evolutionary conserved 60 residue-long motifs. *D. melanogaster* and *C. elegans* homologs can functionally substitute for the human protein and *vice-versa* (Feiguin, Vinay K. Godena, et al., 2009; Ayala et al., 2005).
    1. **RRM1**: is responsible for binding to single-stranded RNA containing UG-repeated motifs (Ayala, Zago, et al., 2008; Buratti and Baralle, 2001). These repeats are found more often in long introns and 3′ untranslated regions (3′-UTRs) rather than exons inside the human genome. Through RRM1, TDP-

43 also binds single-stranded DNA with TG repeats, as demonstrated by the electromobility shift assay (EMSA) technique (Buratti and Baralle, 2001), and double-stranded TG repeats DNA as described in the nitrocellulose filter-binding assay (Kuo et al., 2009). In particular, these interactions are mediated by two residues (Phe 147 and Phe 149) and their substitution was found to be sufficient to abolish RNA-binding properties and splicing regulatory activities of TDP-43 (Buratti & Baralle 2001; D'Ambrogio et al. 2009).

2. **RRM2**: Together with the N-terminal sequence from residues 3 to 183, RRM2 is supposed to be involved in the TDP-43 self-interaction (ability to form homo-dimers and -multimers) (Shiina et al., 2010; Kuo et al., 2009). A role in chromatin organization has also been suggested, since it may co-crystallize with TG-rich single stranded DNA in order to form highly thermal-stable dimeric assemblies (Ayala, Zago, et al., 2008). Furthermore, this region of TDP43 protein is predicted to contain a strong nuclear export signal (NES) (Strong et al., 2007).

– The **C-terminal domain**: represents almost half of the protein, spanning residues 261- 414. It contains a glycine-rich region, corresponding to residues 345 to 366, that is essential for the interaction with other proteins, including hnRNP A2/B1 and hnRNP A1 (Buratti et al. 2005; D'Ambrogio et al. 2009). Furthermore, the region comprising amino acids 216–315 together with the RNA-recognition motif 1 domain are implicated in the assembly of TDP-43 into SGs (Colombrita et al., 2009). This region is also the "hot-spot" position in which the majority of TARDBP mutations have been identified in ALS and FTLD patients (Lagier-Tourenne et al., 2010). Moreover, the C-terminal domain includes a

Glutamine/Asparagine (Q/N) spanning residues 321-369 (D'Ambrogio et al. 2009; Fuentealba et al. 2010) that is considered the putative "prion-like domain" of TDP-43, since it has a strong tendency to aggregate (Budini et al. 2012). Deletions and mutations in the TDP-43 C-terminal domain significantly reduce the solubility of the protein and results in formation of large nuclear and cytoplasmic aggregates, thought to be a result of the lack of interaction between TDP-43 and other protein factors that promote TDP-43 solubility (Ayala, Zago, et al., 2008). Finally, the integrity of this region is extremely important for many of TDP-43's functional properties. Indeed, TDP-43 protein lacking the C-terminal domain is no longer able to regulate the skipping of exon 9 in the *CFTR* gene (Wang et al., 2004).

- **TDPBR** (extended binding region for TDP-43): is present in the 3''-UTR of *TDP-43* mRNA and contains several non-UG sequences that are essential for the auto-regulation of *TDP-43* mRNA (Igaz et al., 2011; Polymenidou, Lagier-tourenne, et al., 2011).

1.4.3 Functions of TDP-43

As previously mentioned, TDP-43 has many functional properties that are summarised in Figure 8.

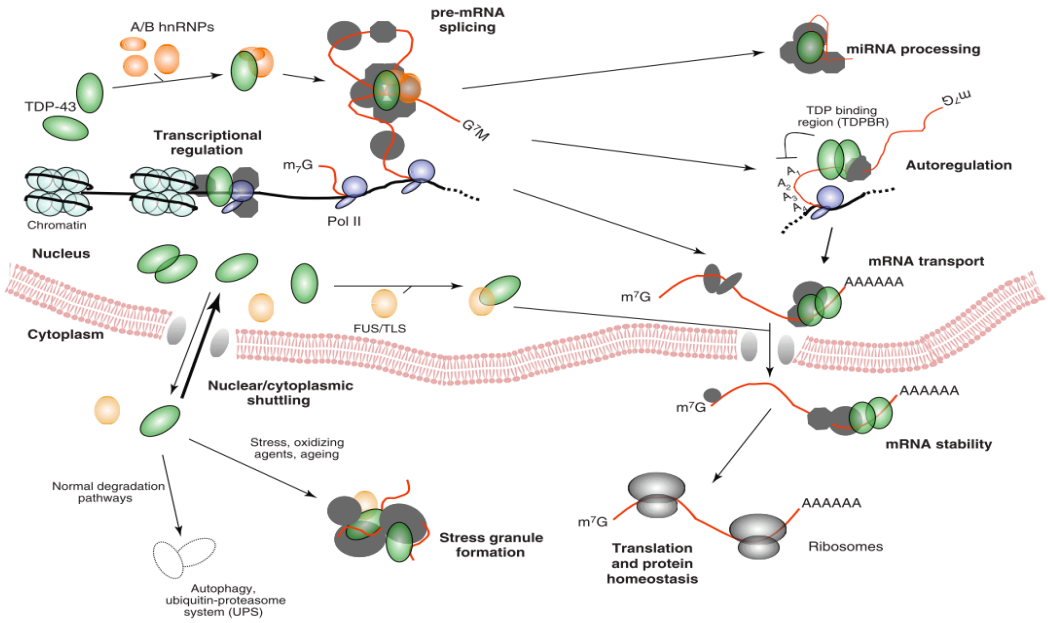

Figure 8. Schematic representation of TDP-43 functions. TDP-43 covers many functions in cells including starting from transcription to translation and degradation. TDP-43 is also involved in miRNA processing and auto-regulation. (Source: Buratti & Baralle, 2012)

TDP-43 functions include:

- **<u>Transcriptional regulation</u>**: TDP-43 was initially discovered as having a role in HIV-1 transcriptional repression, from which its name derives (Ou et al., 1995). However, the involvement of TDP-43 in HIV-1 regulation has not been confirmed by other studies, suggesting a restrictive role during HIV-1 replication in immune cells (Nehls et al., 2014). TDP-43 was also implicated in the regulation of spermatogenesis, because of its binding to the promoter of the mouse *Spermatid-specific SP-10* (*ACRV1*) gene and promoting its transcriptional repression (Lagier-Tourenne et al., 2010). Moreover, consisting with is involvement in transcription,

TDP-43 was found in the human brain and in cell cultures to be associated with euchromatin (containing actively transcribed genes) through its RMM2 (Lagier-Tourenne et al., 2010).

- **Pre-mRNA splicing**: is the best-characterized function of TDP-43. An example of an alternative splicing event regulated by TDP-43 is the skipping of exon 9 of *CFTR* gene, which is promoted by the TDP-43 recognition of an UG-tract near the 3′ splice-site of this exon (Buratti and Baralle, 2001; Buratti et al., 2001). As in the case of *CFTR* gene, TDP-43 is considered to be a splicing silencer of other genes, like *Apolipoprotein AII (ApoII)* exon 3 (Mercado et al., 2005), *Eukaryotic Translation Termination Factor 1 (ETF1)* and *Retinoid X receptor gamma (RXRG)* exon 7 (Passoni et al., 2012). However, TDP43 can also promote exon splicing, as in the case of *breast cancer 1* (*BRCA1*) -mutated substrate exon 12 (Passoni et al., 2012) and *polymerase delta interacting protein/S6 kinase 1 Aly/REF-like* target (*POLDIP3/SKAR*) exon 3 (Fiesel et al., 2012).
- **micro-RNA (miRNA) biogenesis**: mass spectrometry analysis has shown an interaction between TDP-43 and the Nuclear RNase III-type Protein (Drosha) that is involved in the first step of miRNA maturation (Gregory et al., 2004). A further confirmation of the involvement of TDP-43 in the miRNA biogenesis has arisen from the demonstration of TDP-43's association with Argonaute 2 (AGO2) and DDX17 (Freibaum et al., 2010). Indeed, DDX17 directly interacts with Drosha (Shen and Hung, 2015) and AGO2 is a catalytic component of the RNA-induced Silencing Complex (RISC) (Sen and Blau, 2005).
- **RNA subcellular localization and translation**: although TDP-43 is predominantly nuclear, it has been visualized in cytoplasmic puncta strongly stained for PABPC1, a marker for cytoplasmic RNA SGs (Freibaum et al., 2010). It is thought that

cytoplasmic RNA granules may represent physiological accumulations of mRNAs and ribonucleoproteins that regulate gene expression by affecting translation, trafficking and stability (Anderson and Kedersha, 2009). This function is particularly important for neuroplasticity in which the mRNA translation is dependent on its subcellular localization. In the motoneuron-like cell line NSC-34, TDP-43 moved into SGs as a response to oxidative stress and to environmental insults (Colombrita et al., 2009). Although the link between TDP-43 and its presence into SGs is still not completely clear, it is thought that it can mediate the stabilization and localization of *Low Molecular Weight Neurofilament (NEFL)* mRNA during axonal repair (Lagier-Tourenne et al., 2010) by binding its 3'UTR region from 135 to 185 residues after the stop codon (Buratti and Baralle, 2008). Furthermore, in 2008 Wang and colleagues have observed the presence of TDP-43 in dendritic processing body and demonstrated that it could act as a translational repressor *in vitro* (Wang et al., 2008).

- **mRNA turnover**: TDP-43 is associated with the mRNA turnover from different genes, including *Cyclin-Dependent Kinase 6* (*CDK6*) (Ayala, Misteli, et al., 2008) and *Histone Deacetylase 6* (*HDAC6*) (Fiesel et al., 2010) through the binding to their 3'UTR within the mRNA sequences. Furthermore, TDP-43 can physically interact with the mRNA of the *Drosophila melanogaster* homologue of *Microtubule-associated Protein 1B*, called *Futsc*, preventing synaptic defects related to *Futsc* downregulation (Godena et al., 2011) and that the depletion of TDP-43 could destabilized the mRNA of *Autophagy Related 7 (ATG7)* with the consequent impairment of autophagy and accumulation of polyubiquitinated proteins (Bose, Huang and Shen, 2011).

- **Auto-regulation**: TDP-43 is able to regulate own expression by promoting RNA instability through the binding to different polyadeylation (polyA) sites localized in the TDPBR at its 3'UTR (Ayala et al., 2011). Under normal conditions, two main splicing isoforms and one isoform expressed at low levels arise from the usage of either the proximal polyA1 site or the distal polyA4 and polyA2 sites, respectively, with the efficient production of TDP-43 (Ayala et al., 2011; Eréndira Avendaño-Vázquez et al., 2012). When the nuclear levels of TDP-43 are abundant there is an increase in the binding of TDP-43 to its TDPBR. This event promotes a dual effect: the activation of a normally silent intron (intron 7) which in turn eliminates utilisation of polyA1, resulting in the preferentially usage of polyA2. At the same time, this determines the direct competition of TDP-43 with the cleavage polyA factor Cstf-64 over polyA1 with the consequence usage of polyA4 (Eréndira Avendaño-Vázquez et al., 2012). Both polyA2 and polyA4 are significantly retained in the nucleus and rapidly degraded thus reducing TDP-43 levels (Eréndira Avendaño-Vázquez et al., 2012). On the contrary, low levels of TDP-43 causes the preferentially usage of polyA1 site instead of the other possible choices (polyA2 and polyA4), resulting in an efficient TDP-43 production (Eréndira Avendaño-Vázquez et al., 2012).

1.4.4 TDP-43 interacting proteins

Given the importance to understand the RNA-processing functions, nuclear–cytoplasmic shuttling and aggregation properties of TDP-43, many recent studies have focused their attention on identifying TDP-43 interacting proteins. Nowadays, the most important binding partners of TDP-43 are members of the hnRNP family, such as hnRNP A2/B1, hnRNP A1, and hnRNP C1/C2 (Buratti et al., 2005). These protein interactions are

probably essential for the modulation of the functional properties of TDP-43. For example, in the case of hnRNPA1 the alteration of mRNA processing following the loss of this RNA–binding protein correlates well with the formation of TDP-43-positive inclusions in sporadic ALS motor neurons (Honda et al., 2015). Further evidence that hnRNP proteins can play a modulatory role on TDP-43 function has been provided using cell and animal models. In particular, functional experiments of the fruit fly orthologs of the human hnRNP A1/A2 (Hrp38) overexpression in HEK293 cells have demonstrated that TDP-43 is required for the spicing inhibitor activity of this protein (Romano et al., 2014). Additionally, experiments show that the interaction between TDP-43 and fly hnRNP A2/B1 homologues Hrb87F and Hrb98DE is important to suppress CGG repeat-induced neurotoxicity in a *Drosophila* model of Fragile X-associated Tremor/Ataxia Syndrome (FXTAS) (He et al., 2014).

Notwithstanding all this evidence, the relationship between pathological mislocalization of TDP-43 and general levels of hnRNP proteins, with regards to altered RNA processing events occurring in neurodegenerative diseases, still remains unclear. In an effort to answer this question, Molecular Pathology Laboratory has been recently demonstrated that the interaction of TDP-43 with hnRNP L, PTB/nPTB and hnRNP A1/A2 affects the inclusion of the exon 17b in the neurotrophic receptor *SORT*1 mRNA, a pathologically-relevant splicing event known to be regulated by TDP-43 (Mohagheghi et al., 2016). Interestingly in this work, Mohagheghi and colleagues also looked at the expression levels of these hnRNPs in the temporal cortex of FTLD-TDP patients, in which a significant increase in exon 17b inclusion was previously observed. A significant increase in the splicing repressors hnRNP A1/A2 and PTB in FTLD-TDP-43 was observed in patients relative to controls. This may suggest that different hnRNP expression levels, which may depend on individual or age-related differences, on top of similar TDP-43 pathologies could

potentially account for different disease courses, with regards to both onset and progression.

Given these results, our group decided to further characterize the linkage between TDP-43 and hnRNP proteins, with the aim of finding other potential TDP-43 modulators belonging to this family. Taking advantage of *Drosophila melanogaster* and its available models of TDP-43 proteinopathies (see paragraph below), it was then possible to identify three promising hnRNPs, namely DAZAP1, hnRNP Q and hnRNP R (Appocher et al., 2017) that have subsequently become the object of my PhD thesis. Therefore, what is currently known about these factors will be reviewed in the next paragraphs.

1.4.5 TDP-43 proteinopathies

Abnormal cellular distribution and post-translational modifications of TDP-43 are present in many neurodegenerative disorders, which are now generally referred to as TDP-43 proteinopathies (Scotter et al., 2015). In pathology, TDP-43 was described as the major component of the ubiquitin-positive, α-Synuclein and Tau-negative cytoplasmatic inclusions recognized in the brain and spinal cord tissues of FTLD-U and ALS patients (Arai et al., 2006; Neumann et al., 2006). These intracellular aggregates are characterized by ubiquitination, S409/410 phosphorylation, and proteolytic cleavage forming C-terminal fragments (CTFs) of 20-25 kDa (Neumann et al., 2006). TDP-43 inclusions have also been reported to occur in other neurodegenerative disorders, including 30% of Alzheimer patients and various forms of Parkinson's disease, although TDP-43 inclusions exist side-by-side but only partially co-localize with tau or α-Synuclein aggregates (Lagier-Tourenne et al., 2010). Two hypotheses have been suggested to explain the pathogenic role of TDP-43 inclusions: gain-of-function (GOF) and loss-of-function (LOF). It is important to note that neither hypothesis excludes the other one, and they can act at the same time to

determine the onset and progression of the disease (Lee et al., 2011). Briefly, the "gain-of-function" mechanism is based on the cytotoxicity induced by the formation of aggregates or toxic C-terminal fragments localized in the cytoplasm (Lee et al., 2011). According to this model, stress conditions can lead to redistribution of TDP-43 into the cytoplasm resulting in aggregation. Due to the fact that the auto-regulation of *TDP-43* mRNA is a cytoplasmic event, it is possible that TDP-43 aggregates can still bind RNA and therefore auto-regulate themselves. This consequently may result in the decrease of newly synthesized TDP-43 proteins in affected cells and hence, nuclear clearance. The loss of normal nuclear TDP-43 may further increases cellular stress, again resulting in a vicious circle leading to cell death (Figure 9).

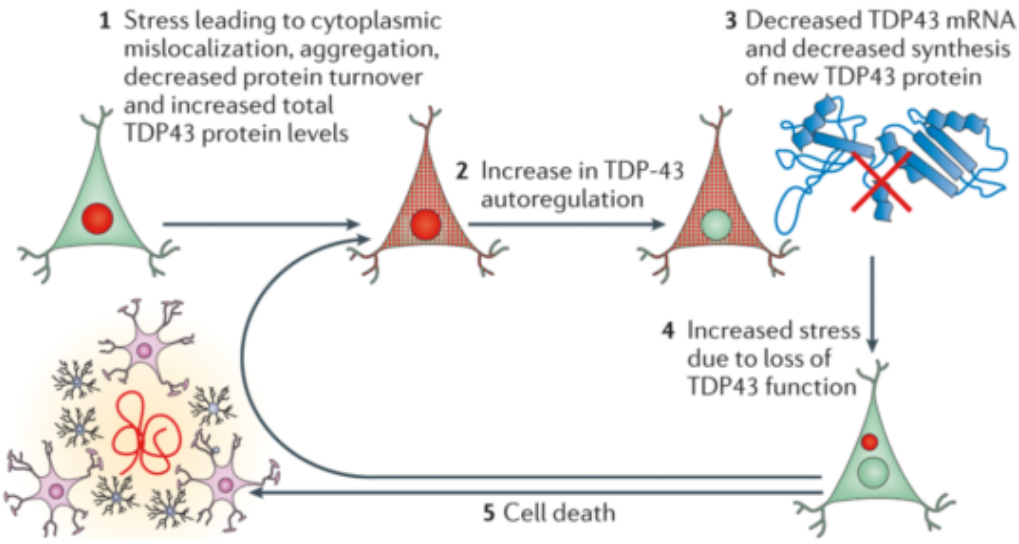

Figure 9. Schematic representation of the TDP-43 gain-of-function model. Stress conditions lead to the formation of cellular aggregates (1). These aggregates promote TDP-43 auto-regulation (2), determining a decrease of TDP-43 synthesis (3) and loss of TDP-43 nuclear functions (4), with consequent cell death (5). (Source: Lee et al., 2011)

On the other hand, the "loss-of-function" model is based on the hypothesis that cellular stress may lead to the formation of pathological stress granules or mislocalization of RNA

transport granules that are usually localized within peripheral neuritis, determining the formation of cytoplasmic inclusions that act as a "TDP-43 sink" with the clearance of this protein from the nucleus and the consequent dysregulation of many TDP-43-controlled events in RNA processing (Figure 10) (Igaz et al., 2011).

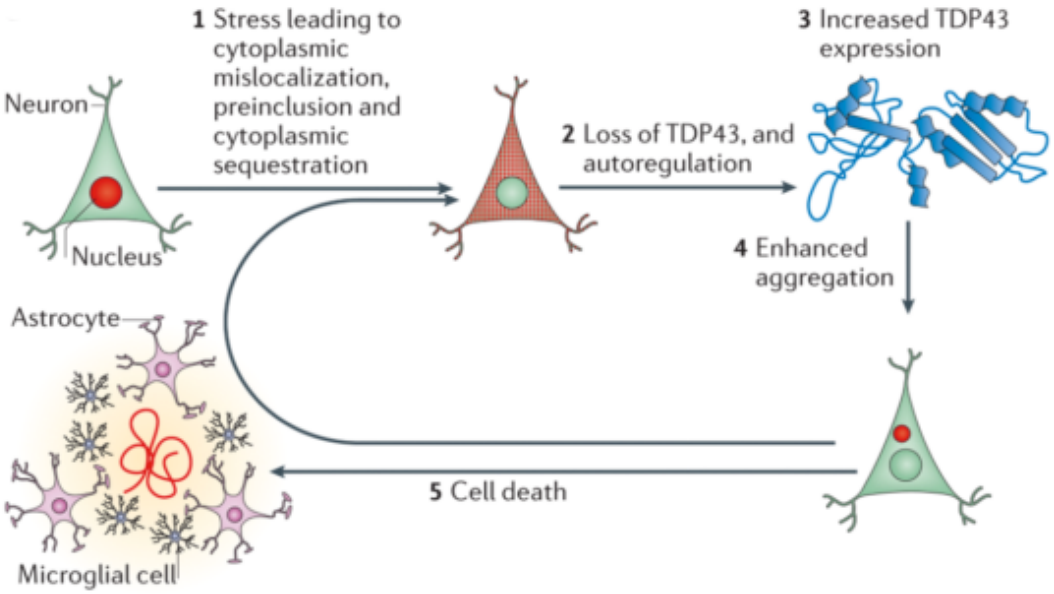

Figure 10. Schematic representation of TDP-43 loss-of-function model. Stress conditions lead to cytoplasmic mislocalization and formation of cellular aggregates (1). These aggregates promote loss of TDP-43 from nucleus (2), determining an increase of TDP-43 synthesis (3) and aggregation (4), with consequent cell death (5). (Source: Lee et al., 2011)

1.4.6 *Drosophila* as a model for understanding TDP-43 proteinopathies

The interest in *Drosophila melanogaster* as a powerful organism for studying cell biology became evident in the early twentieth century. Initially, *Drosophila* was introduced as an experimental model for investigating the Mendelian theory of heredity (Muqit and Feany, 2002), but successively it has been widely used in the neurodegeneration field. Indeed, *Drosophila* presents many advantages, including a short life cycle (from 40 to 120 days), a compact genome, the possibility to screen substances/drugs very quickly and a high

neuronal complexity due to receptors, ion channels and neurotransmitters also found in humans (Romano et al., 2012).

There are different species of *Drosophila* with differences in morphology, genetic background and habitat. Interestingly, *Drosophila melanogaster* has approximately 75% of genes whose the equivalent human homologue is associated with disease (Romano et al., 2012).

Regarding neurodegenerative disorders, various fly models have been used to understand the pathological mechanisms behind Parkinson's, Alzheimer's and Huntington's disease, well as spinocerebellar ataxia, tauopathies and TDP-43 proteinopathies (Muqit and Feany, 2002).

Here, I am going to present some of the characteristics of the main homologue of human TDP-43 in *Drosophila*, called TBPH, and some of the findings obtained using this organism as an experimental model.

Briefly, TDP-43 and TBPH have a strong homology at the level of the region containing RRM1 and RRM2 (Figure 11A) (Wang et al., 2004). Another characteristic in common with TDP-43 is the presence of different splicing isoforms (Figure 11B) (Wang et al., 2004), as well as, the preferential binding to UG-rich sequences (Ayala et al. 2005).

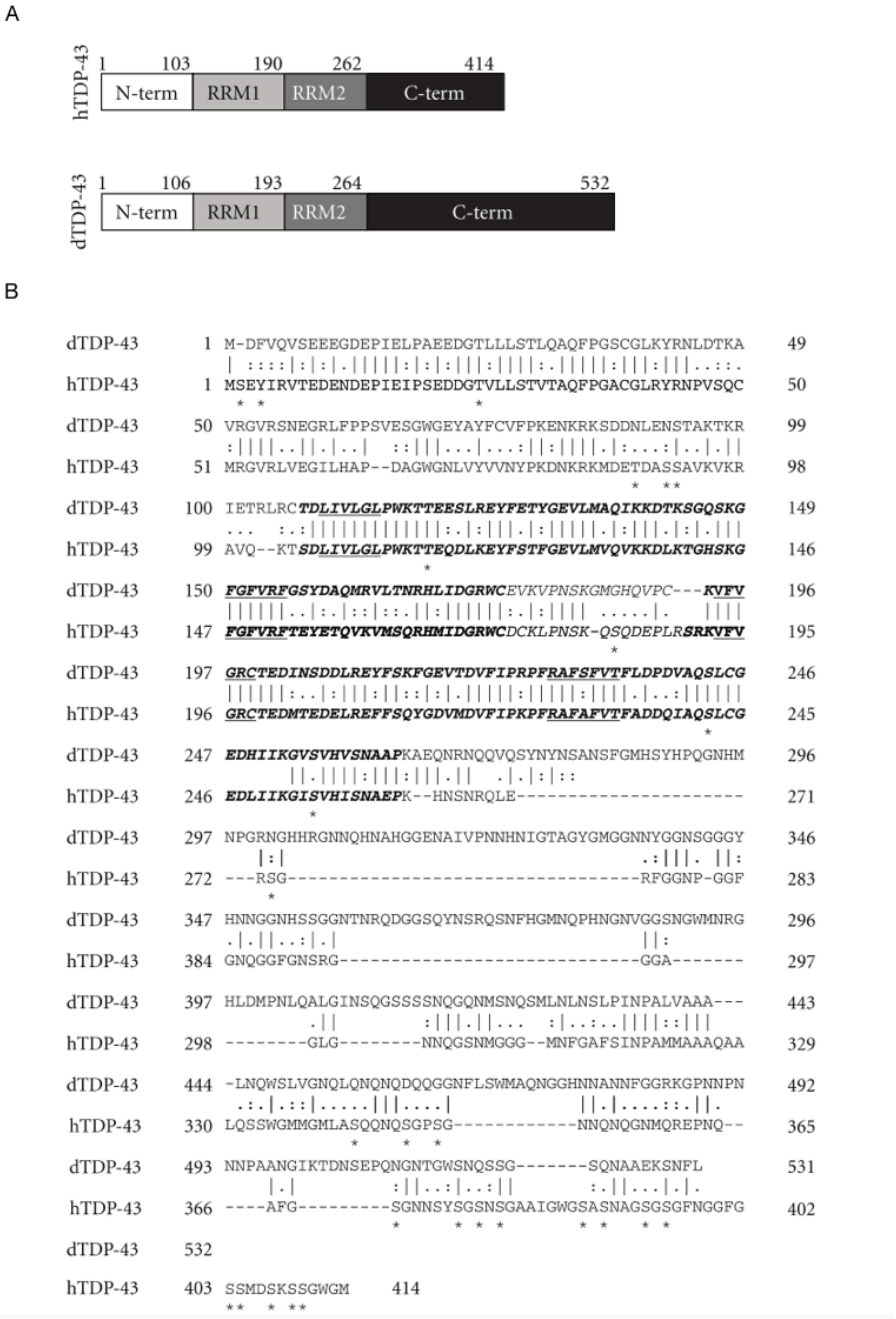

Figure 11. Comparison of human TDP-43 and *Drosophila* TBPH proteins. Schematic representation of the protein structure in both **(A)** and alignment of the human (TDP-43) and fly (TBPH) proteins **(B)** are reported. (Source: Modified from Romano et al., 2012)

Functionally, TBPH shows same splicing inhibitory effects both *in vitro* and in *vivo* (Ayala et al., 2005), and although the C-terminal tail of TBPH represents the region with less

homology with TDP-43 it can still bind to the same nuclear protein interactors as TDP-43 (D'Ambrogio et al. 2009).

Most importantly, it is possible to achieve different fly phenotypes, including null allele flies (loss-of-function model), transgenic flies overexpressing wild-type TDP-43 or ALS-related mutations (gain-of-function model), and transgenic flies silenced for this factor (RNA interference transgenic flies)

These approaches are described as follows:

- **Loss-of-function model (null allele flies)**: were created by the disruption of *TBPH* gene to test if an ALS-like phenotype could be generated. Different approaches were used to achieve this aim, including: knockout of *TBPH* through the partial removal of its coding and regulatory sequence (Feiguin et al., 2009); point mutation (G>A) in order to create a stop codon (Lu et al., 2009); deletion of 932 bp at the 5′ end of *TBPH* (Lin et al., 2011); and the generation of null allele in which the entire coding sequence was deleted (Fiesel et al., 2010). Interestingly, in this latter approach, Fiesel and collaborators observed lethality at the second larval stage. This is in contrast to the *TBPH* knockout approach of Feiguin and collaborators that has reported viability of some larvae after embryogenesis, with most of them able to reach the pupal stage and undergo metamorphosis but do not eclose, remaining trapped inside their pupal cages. However, the knockout flies able to get rid the external cuticle presented uncoordinated movements, reduction of axonal branches and synaptic boutons present inside muscles (Feiguin et al., 2009). Nevertheless, the overexpression of human TDP-43 (hTDP-43) was able to rescue the aberrant phenotype (Feiguin et al., 2009; Lu et al., 2009).
- **Transgenic flies**: were achieved by the creation of transgenic flies using the Gal4-UAS system (Figure 12) (Brand and Perrimon, 1993). This system permits the

ectopic expression of a human transgene (gain-of-function model), as well as the knockdown of an endogenous gene (RNA interference transgenic flies) in a specific tissue or cell type. For instance, it has been widely demonstrated that the overexpression of hTDP-43 or TBPH is able to cause eye degeneration associated with cell death (Hanson et al., 2010; Estes et al., 2011). In a similar way, the overexpression of wild-type TDP-43 in mushroom bodies and in motor neurons caused neuronal death and axonal loss, whereas the overexpression of TDP-43 in motor neurons lead to cytoplasmic and axonal aggregation (Li et al., 2010). Loss of motor neurons and reduction in life span were also identified after the overexpression of ALS/FTLD-linked and synthetic mutations (Voigt et al., 2010). Furthermore, it has been demonstrated that the ectopic expression of wild-type TDP-43 or its variants was associated with age- and dose-dependent toxicity (Hanson et al., 2010). TDP-43 toxicity was also found to correlate with its subcellular localization (Ritson et al., 2010; Miguel et al., 2011). Indeed, cytoplasmic and nuclear inclusions of TDP-43 were found toxic in different tissues, such as eyes, muscles and glia (Miguel et al., 2011). However, the formation of inclusions was not a prerequisite for TDP-43 toxicity, since increased levels of both nuclear and cytoplasmic TDP-43 were found toxic even in absence of inclusions (Miguel et al., 2011). In contrast, the generation of transgenic flies silenced for TBPH exclusively in neuronal tissue was found to induce similar locomotive defects observed in the null allele flies (Feiguin, et al., 2009) . Moreover, Li and collegues showed that the depletion of TBPH in the central nervous system and the mushroom bodies of *Drosophila* caused axonal loss and neuronal death (Li, et al., 2010).

Transgenic flies were not used only to assay the TDP-43 misregulation in the context of ALS-linked mutations, but also to clarify the role of TDP-43 in other degenerative disorders, as in the case of the Inclusion Body Myopathy associated with Paget's Disease of Bone and Frontotemporal Dementia (IBMPFD) (Ritson et al., 2010).

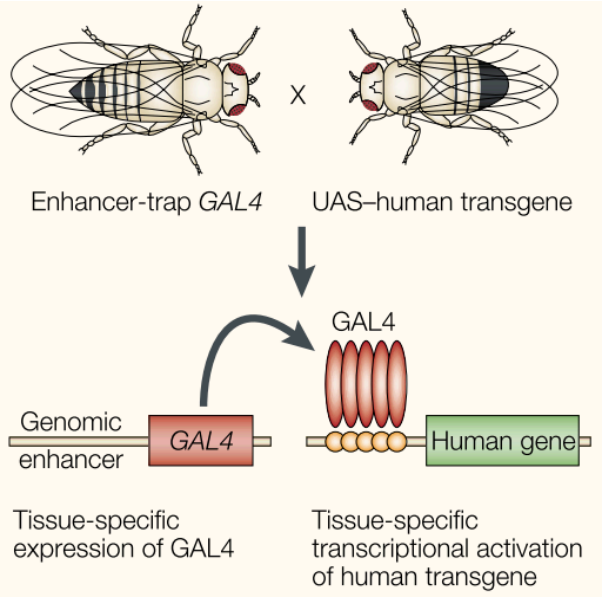

Figure 12. Gal4-UAS system. This system is based crossing two transgenic fly lines. The first fly line (UAS–human-transgene fly) harbours the transgene of interest that is placed downstream of a UAS activation domain consisting of GAL4-binding sites. The second fly line (enhancer-trap GAL4 fly) harbours a yeast transcriptional activator called GAL4 located downstream of a cell- or tissue- specific promoter. These latter flies are known as "drivers". In this system, the ectopic expression of the transgene of interest is obtained by crossing the two fly lines. There is a wide array of promoters available for the ectopic expression of a transgene, such as the pan-neural promoter *elav* (embryonic lethal, abnormal vision) or the eye-specific promoter GMR (Glass Multimer Reporter). (Source: Muqit & Feany, 2002)

1.5 DAZ Associated Protein 1 (DAZAP1)

1.5.1 Characteristics of DAZAP1

DAZ associated protein 1 (DAZAP1) was originally identified as an RBP associated with the DAZ proteins, DAZ and DAZ-Like (DAZL), using a yeast two-hybrid system (Tsui et al., 2000). DAZAP1 is encoded by the *DAZAP1* gene located on the short arm (p) of human chromosome 19 at position 13.3 (19p13.3) (Figure 13). *DAZAP1* consists of 12 exons spanning about 28 kb (Dai et al., 2001; Tsui et al., 2000).

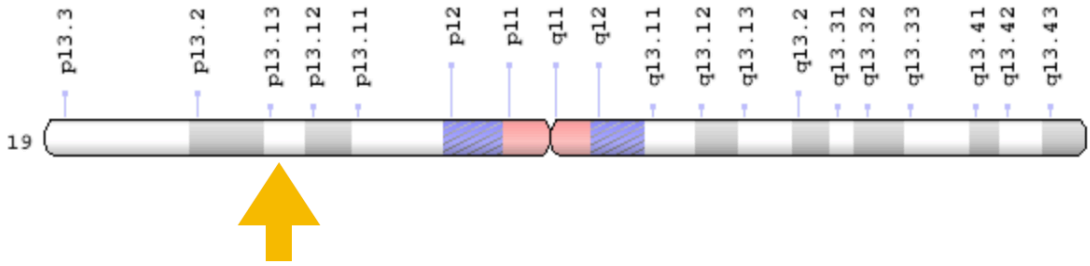

Figure 13. Localization of *DAZAP1* gene on human chromosome 19. The Genomic locus encoding DAZAP1 is identified by a yellow arrow. (Source: Modified from Genetic home resource)

Two major *DAZAP1* transcript variants of 1.75 and 2.4 kb are generated through alternative polyadenylation (Yang and Yen, 2013; Tsui et al., 2000). These transcripts are highly abundant in human testis (Dai et al., 2001; Tsui et al., 2000) and ovaries (Pan et al., 2005), with a low expression level in non reproductive organs including liver, brain, placenta, heart, skeletal muscle, kidney and pancreas (Dai et al., 2001; Tsui et al., 2000). Furthermore, DAZAP1 is extremely conserved among the evolution. Human and mouse DAZAP1 share 89% similarity in the coding sequence, although they diverge in protein sequence for 9 amino acid residues: 7 substitutions and 2 deletions/insertions. Furthermore, both of the mammalian proteins share 89% similarity and 81% identity with the Proline-rich RNA Binding Protein (Prrp) of *Xenopus* (Dai et al., 2001).

From a structural point of view, the full-length protein represents the major splicing isoform that is composed of 407 amino acid residues (≈ 45 kDa), with two RRMs in the N-terminal portion, and a proline-rich (Pro-rich) C-terminal region (Figure 14) (Dai et al., 2001; Tsui et al., 2000). The high level of similarity of these RRMs with those present in many other hnRNPs (e.g. *Drosophila* hnRNP 27C) makes DAZAP1 a member of the hnRNP protein family (Dai et al., 2001; Tsui et al., 2000).

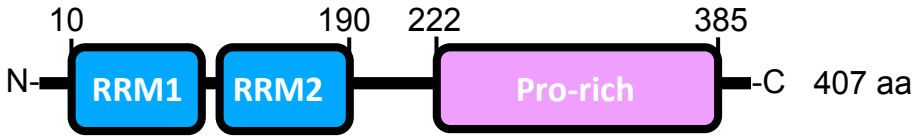

Figure 14. Schematic representation of DAZAP1 domains. The full-length DAZAP1 (407 amino acid residues) is composed of an N-terminal domain containing two RNA-recognition motifs (RMM1 and RRM2) and a C-terminal domain containing a proline-rich region (Pro-rich).

Furthermore, DAZAP1 was found to shuttle between nucleus and cytoplasm during different stage of mouse spermatid maturation, as well as in non germinal cells in response to external stimuli (Vera et al., 2002; Lin and Yen, 2006). In 2006, a study carried out in somatic cells demonstrated DAZAP1's association with nuclear structures as a component of hnRNP particles, and mapped the region comprising the last 25 amino acids at the C-terminus (C25) as important residues for the nuclear localization (Lin and Yen, 2006). This C25 region does not share sequence similarity to other NLS or shuttling signals, and it also contains the nuclear export signal for cytoplasmic localization. Therefore, it was called the nucleocytoplasmic shuttling signal (ZNC) (Lin and Yen, 2006).

The sublocalization of DAZAP1 was also found to be associated with the transcription state of its mRNA targets (Lin et al., 2012) and the acetylation of the Lysine 150 residue within its second RRM (Sasaki et al., 2012). In particular, the signal necessary and

sufficient for the transcription-dependent nuclear localization of DAZAP1 was represented by a sequence of 42 amino acid residues located at the N-terminal (N42) of DAZAP1 (Lin et al., 2012), and the mutation of Lysine 150 was correlated with its cytoplasmic retention and association with mitochondria (Sasaki et al., 2012).

1.5.2 Functions of DAZAP1

Nowadays, little information is available in literature regarding the natural RNA substrates and cellular functions of DAZAP1, albeit, as a member of hnRNP family, its cellular activity can be related to the regulation of RNA metabolism.

The first evidence supporting this hypothesis came out when DAZAP1 was found to be associated with RNA homopolymers, preferentially polyU and polyG tracts, *in vitro* (Dai et al., 2001; Tsui et al., 2000); and later when it was identified as an AU-rich element (ARE) binding protein bound to the ARE of the *Tumor Necrosis Factor-alpha (TNF-α)* (Rousseau et al., 2002) and the *Cellular Oncogene Fos (c-Fos)* (Morton et al., 2006) mRNAs. Two consensus sequences (AAAUAG and $GU_{1-3}AG$) and two secondary structures (loops L1 and L2) were further characterized in the RNA ligands of the mouse DAZAP1 orthologous and in the 3'UTR of the all known target mRNAs of *Xenopus* Prrp (Hori et al., 2005). Interestingly, the AUG sequence contained in both the DAZAP1 consensus sequences was also reported in the mRNA targets of other RBPs, including hnRNP A1 (Burd and Dreyfuss, 1994), hnRNP D (Kajita et al., 1995) and Musashi1 (Msi1) (Imai et al., 2001). In this context, it has been proposed the role of DAZAP1 in the transport/localization (Lin et al., 2012; Lin and Yen, 2006; Zhao et al., 2001) and translation of different mRNAs is through the binding to their 3'UTRs (Smith et al., 2011; Yang et al., 2009; Morton et al., 2006). In particular, DAZAP1 was found to be accumulated in the cytoplasm when transcription was inhibited, suggesting that this protein

could translocate from nucleus to cytoplasm with exported mRNAs (Lin and Yen, 2006) as described for hnRNP A1 (Piñol-Roma and Dreyfuss, 1992). Moreover, DAZAP1 was able to stimulate translational initiation of mRNAs in a manner that was sensitive to the adenylation status of those mRNAs (Smith et al., 2011).

Other interesting findings demonstrate that the nuclear fraction of DAZAP1 is able to affect the splicing of different transcripts. It was identified, together with hnRNP A1, as a splicing-inhibitor factor of the mutant T6 of *BRCA1* exon 18 (Goina et al., 2008). DAZAP1 was also implicated in the mRNA splicing of the *Ataxia Teleangectasia Mutated (ATM)* gene through the interaction with *Alu*-derived Intronic Splicing Enhancer (ISE) and the consequent inclusion of a cryptic exon (Pastor and Pagani, 2011). DAZAP1 was also found to regulate the intron inclusion of different mRNA targets in a minigene system (Chen et al., 2013), and was described as binding to an intronic splicing enhancer or silencer in human cells (Wang et al., 2012, 2013). Moreover, a recent publication has highlighted the role of DAZAP1 in cell proliferation and migration. Indeed, mRNA-seq analysis of HEK293 cell line identified several genes, most of them related to the maintenance of cell proliferation, regulated by the splicing activity of DAZAP1. This activity was also found to be affected by the Extracellular Signal-regulated Protein Kinase (MEK/Erk) signalling pathway through the phosphorylation of the DAZAP1 proline-rich domain (Choudhury et al., 2014).

1.5.3 DAZAP1 interacting proteins

Few DAZAP1 binding partners are described in the literature. The first well-characterized interactors are certainly DAZ and DAZL (Dai et al., 2001; Tsui et al., 2000), but other putative interacting proteins were established later. In most of the cases, the DAZAP1-protein contacts occurred between the RRMs of DAZAP1 and the C-terminus of its

partners, as described for hnRNP U like 1, hnRNP A/B, hnRNP A1, hnRNP D and DEAD-Box Helicase 20 (DDX20) (Yang et al., 2009). However, more recently it has been reported that the transcription-dependent nuclear localization of DAZAP1 could be involved in the association of DAZAP1 to its partners, as described for the binding to the Steroid Receptor RNA Activator Stem-loop Interacting RNA Binding Protein (SLIRP) (Lin et al., 2012).

Moreover, the phosphorylation state of DAZAP1 was demonstrated to disrupt the interaction with binding partners, affecting its cellular functions. Indeed, the phosphorylation of Thr269 and Thr315 in its Proline-rich C-terminus by the Extracellular Signal Regulated Kinase 2 (ERK2) could promote the dissociation of DAZAP1 from DAZ, allowing the interaction of DAZ with other proteins involved in mRNA translation such as PABP (Morton et al., 2006).

1.5.4 DAZAP1 and pathologies

A link between alteration of DAZAP1 homeostasis and the development of disorders is still not clear. However, two studies have described how the t(1;19)(q23;p13.3) translocation present in TS-2 Acute Lymphoblastic Leukemia (ALL) cells could lead to the expression of two in-frame fusion proteins between *DAZAP1* gene and *Myocyte Enhancer Factor 2D (MEF2D)* gene with oncogenic properties: DAZAP1/MEF2D and MEF2D/DAZAP1. Indeed, DAZAP1/MEF2D and MEF2D/DAZAP1 efficiently activated the transcription of genes important for lymphocyte growth and retained RNA-binding properties, respectively, indicating for the first time DAZAP1 as a putative factor implicated in cancer (Prima and Hunger, 2007; Prima et al., 2005).

1.6 Heterogeneous Nuclear Ribonucleoprotein Q (hnRNP Q) and Heterogeneous Nuclear Ribonucleoprotein R (hnRNP R): two closely related hnRNP proteins

1.6.1 Characteristics of hnRNP Q and hnRNP R

The RNA binding protein hnRNP Q, also known as SYNCRIP, was first described in 1997 as a nucleocytoplasmic protein interacting with the synaptotagmin isoform II (Syt-II) C2AB domain in mouse brain lysate (Mizutani et al., 1997). hnRNP Q was subsequently found in association with human Survival of Motor Neurons (SMN) (Mourelatos et al., 2001). The hnRNP Q protein is encoded by the *SYNCRIP* gene located on the long arm (q) of human chromosome 6 at position 14.3 (6q14.3) (Figure 15). *SYNCRIP* consists of 12 exons that are subjected to alternative splicing resulting in different isoforms, three of which are the most representative: hnRNP Q3, hnRNP Q2 and hnRNP Q1 (Figure 16A-C) (Mourelatos et al., 2001).

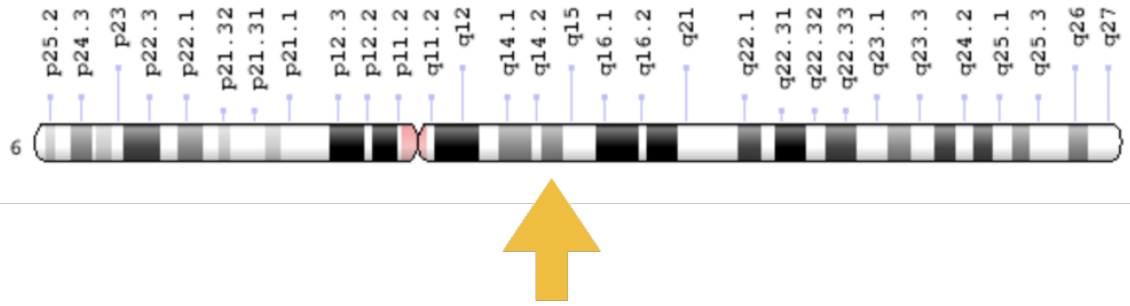

Figure 15. Localization of *SYNCRIP* gene on human chromosome 6. The Genomic locus encoding hnRNP Q is identified by a yellow arrow. (Source: Modified from Genetic home resource)

Regarding these isoforms, the nucleic acid sequence of hnRNP Q3 (also known as GRY-RBP) (Neubauer et al., 1998) encodes the longest variant with the closest protein sequence

identity (83% homology) to hnRNP R (Mourelatos et al., 2001). hnRNP Q3 is composed of 623 amino acid residues (≈ 70 kDa) containing an acidic domain (AcD), three RRMs, two NLS and a RGG-box (Figure 16B). The Q2 variant (≈ 65 kDa) lacks of 36 amino acids (302-336) between RRM2 and RRM3 comparing to the longest variant hnRNP Q3 (Figure 16A), while hnRNP Q1 (≈ 62 kDa) lacks of the second NLS and RGG-box region (549-623) with respect to hnRNP Q3 and contains a unique C-terminal domain (VKGVEAGPDLLQ) (Figure 16C) (Mourelatos et al., 2001). Furthermore, hnRNP Q is expressed in different tissues, such as spinal cord, muscle, brain, heart, kidney, liver and spleen (Rossoll et al., 2002).

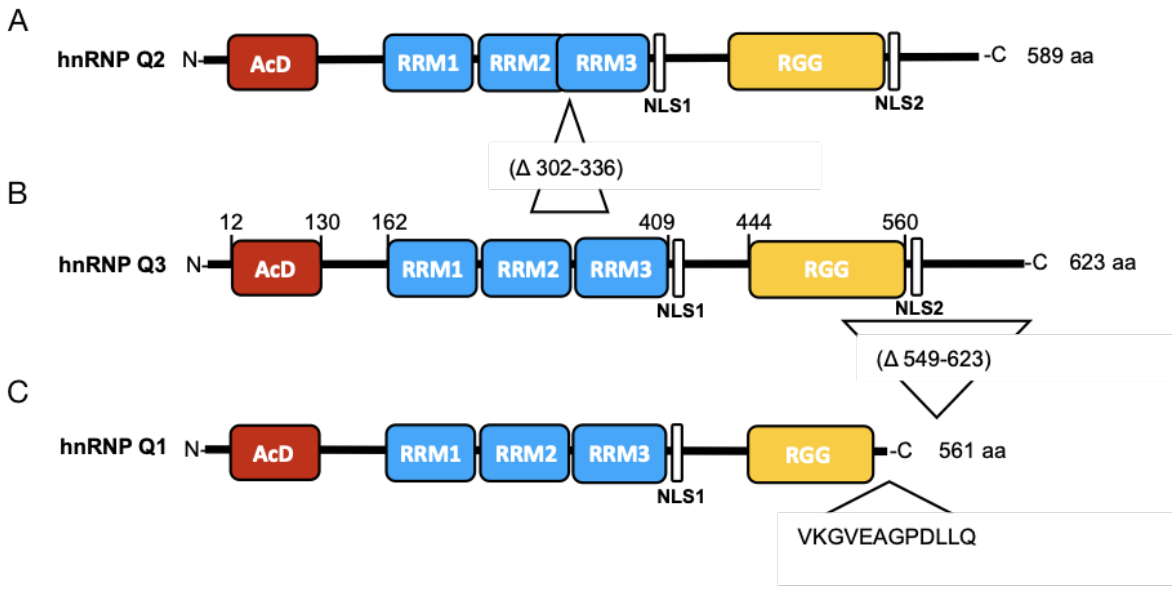

Figure 16. Schematic representation of protein domains and major isoforms of hnRNP Q. The *SYNCRIP* gene encodes three main splicing isoforms: hnRNP Q2 **(A)**, hnRNP Q3 **(B)** and hnRNP Q1 **(C)**. In this figure AcD (acidic domain), RRMs (RNA-recognition motifs), NLS (nuclear localization signal), RGG (Arg-Gly-Gly)-box and Glutamine/Asparagine (Q/N)-rich domain are highlighted in coloured boxes; relative sequence position and amino acid length of each isoform is also reported. (Source: Modified from Cappelli et al., 2018)

On the other hand, a 2.5 kb cDNA clone corresponding to hnRNP R was first described in 1998 in the serum of patients with autoimmunity symptoms (Hassfeld et al., 1998) and

subsequently identified, like hnRNP Q, as a factor bound to the SMN protein (Rossoll et al., 2002). The protein hnRNP R is encoded by the *HNRNPR* gene located on the p arm of human chromosome 1 at position 36.12 (p36.12) (Figure 17) and consists of 11 exons. Different isoforms are generated from alternative splicing events.

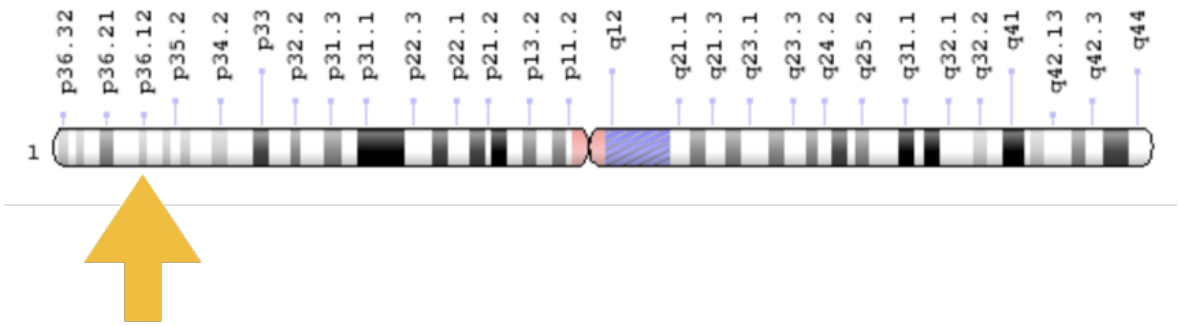

Figure 17. Localization of *HNRNPR* gene on human chromosome 1. The Genomic locus encoding hnRNP R is identified by a yellow arrow. (Source: Modified from Genetic home resource)

The isoform 1 of hnRNP R (hnRNP R1) is the most highly expressed and it is composed of 633 amino acid residues (≈ 82 kDa) containing an AcD domain, three RRMs, two NLS, a RGG-box and a Q/N-rich domain at C-teminus (Figure 18A) (Hassfeld et al., 1998). Moreover, this variant is ubiquitously expressed in all tissues (Huang et al., 2005; Rossoll et al., 2002). Recently a low level expressed and neuronal-specific isoform (hnRNP R2, ≈ 75 kDa) has been characterized. This isoform differs from the R1 because of the exclusion of exon 5 (114 bp) from the cDNA sequence, resulting in the absence of 41 amino acids (129-166) between the AcD domain and the first RRM (Figure 18B) (Huang et al., 2005).

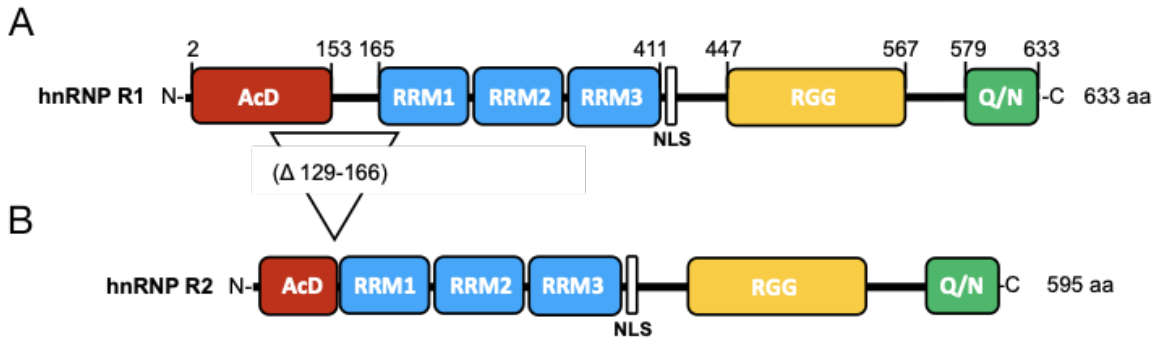

Figure 18. Schematic representation of protein domains and major isoforms of hnRNP R. The *HNRNPR* gene encodes two main splicing isoforms: hnRNP R1 **(A)** and hnRNP R2 **(B)**. In this figure AcD (acidic domain), RRMs (RNA-recognition motifs), NLS (nuclear localization signal), RGG (Arg-Gly-Gly)-box and Glutammine/Asparagine (Q/N)-rich domain are highlighted in colored boxes; relative sequence position and amino acid length of each isoform is also reported. (Source: Modified from Cappelli, Romano and Buratti, 2018)

Interestingly, hnRNP Q and hnRNP R are extremely conserved through evolution, although in lower organisms (e.g. *D. melanogaster* and *C. elegans)* they are represented by just one well-conserved orthologue (Cappelli et al., 2018; McDermott et al., 2012; Kabat et al., 2009). This suggests the occurrence of a progressive functional divergence into two distinct paralogues in higher organisms, such as mammals. In particular, the *Drosophila* homologue CG17838 (*Syp*) shares 46-47% sequence identity and ca. 57-60% of similarity to mammalian hnRNP Q and hnRNP R (Cappelli et al., 2018; McDermott et al., 2012). The human counterparts share almost 50% amino acid identity in their three RNA-binding domains with HRP-2, the nematode homologue of the mammalian hnRNP Q and R proteins (Kabat et al., 2009).

Regarding the subcellular localization of hnRNP Q and hnRNP R, the presence of a NLS motif in the protein sequence indicates the prevalent retention of these RBPs in the nucleus, even if translocation in the cytoplasm was observed in the case of hnRNP Q (McDermott et al., 2014; Quaresma et al., 2009; Akihiro Mizutani et al., 2000). Indeed, the transport of hnRNP Q within the dendrites of cultured rat hippocampal neurons has been

described as a component of mRNA granules (Bannai et al., 2004). hnRNP Q was also found re-localized to cytoplasmic granules after stress condition (Quaresma et al., 2009). Moreover, in a study performed in 2006, the methylation status of the RGG box of hnRNP Q was reported to be associated with its shuttling (Passos et al., 2006).

Contrary to hnRNP Q, Mizutani and collaborators proposed the existence of a second putative bipartite-type NLS motif (KRKADGYNPDSKRR), similar to that observed for nucleoplasmin (Robbins et al., 1991), located at the C-terminal region of hnRNP R (572–586 amino acids) to explain the prevalently nuclear localization of hnRNP R (Mizutani et al., 2000). However, the expression of hnRNP R was not only detected in the nucleus, but was also found in cytoplasm and neurites of cultured embryonic motor neurons (Dombert et al., 2014; Rossoll et al., 2002) and in the cytoplasm, dendrites and axon terminals of rat bipolar cells (Peng et al., 2009).

1.6.2 Functions of hnRNP Q and hnRNP R

Functionally, hnRNP Q and hnRNP R are known to regulate different aspects of RNA maturation. For example, the *C. elegans* orthologue of hnRNP Q and hnRNP R was found to be involved in the alternative splicing of genes containing cassette exons flanked by an intronic UCUAUC motif (Kabat et al., 2009).

More specifically to the mammal hnRNP Q counterpart, the Q3 isoform was identified as a component of the spliceosome in 1998 (Mourelatos et al., 2001; Neubauer et al., 1998). Subsequently the capability of all the other variants to bind *in vitro* pre-mRNA and intron-containing RNA intermediates has been discovered (Mourelatos et al., 2001). Recently, hnRNP Q1 was found to promote inclusion of *SMN2* exon7, whereas the other two variants (hnRNP Q2/Q3) were found to antagonize the activity of hnRNP Q1 by inducing exon 7 exclusion (Chen et al., 2008).

Controlling RNA editing was described as another hnRNP Q function, since the Q3 isoform was discovered to inhibit C-to-U RNA editing of the *Apolipoprotein B (apoB)* mRNA (Blanc et al., 2001). In addition, hnRNP Q3 can also affect mRNA transport, as demonstrated by its colocalization with ribosomal proteins and other RBPs in neuronal mRNA granules (Bannai et al., 2004; Kanai et al., 2004), and translation by competing with poly(A) binding proteins (Svitkin et al., 2013) or as in the case of mouse Cytochrome 1 (*Cry*) gene by binding its 5'UTR (Lim et al., 2016).

On the other hand, hnRNP R was identified as a splicing factor involved in the assembly of the pre-catalytic spliceosome during stress conditions (Tonevitsky et al., 2009). Depletion of hnRNP R impairs translocation of *β-actin* mRNA to the axonal growth cone in isolated embryonic mouse motor neurons (Glinka et al., 2010). Moreover, hnRNP R is involved in the transcription and degradation process of *c-Fos* mRNA in retinal cells (Huang et al. 2008) and in the expression of immunity factors (Meininger et al., 2016; Reches et al., 2016).

Finally, hnRNP Q and hnRNP R regulate the morphology and the development of neural structures (McDermott et al., 2012, 2014; Chen et al., 2012). For instance, *Drosophila Syp* is required to regulate the postsynaptic morphology of neuromuscular junction (NMJ) through the maintenance of protein levels of important transcripts associated with neuron/cell projection morphogenesis or development (McDermott et al., 2014). *Drosophila Syp* also coordinates the translation in post-synapses with retrograde signalling to pre-synapses (Halstead et al., 2014). Moreover, hnRNP Q1 is also able to modulate neuronal morphogenesis and neurite branching in a mouse neuroblastoma cell line by interacting with different mRNAs related to Cdc42 signalling (Chen et al., 2012). Depletion of hnRNP R can reduce axonal 7SK, a nuclear RNA that modulates

transcription, and in turn led to defective axon growth in NSC-34 cells (Briese et al., 2018).

1.6.3 hnRNP Q and hnRNP R interacting proteins

The interest in hnRNP Q and hnRNP R characterization was initially promoted by the identification of SMN protein as a potential binding partner (Rossoll et al., 2002; Mourelatos et al., 2001). The RGG motif in the C-terminus of both hnRNP Q and hnRNP R was proposed to mediate this association (Rossoll et al., 2002).

At the present, however, few studies have described additional interacting proteins. Among them, hnRNP Q and hnRNP R were identified as putative TDP-43-associated proteins (Ling et al., 2010), as well as it has been demonstrated their interaction with Rev protein of HIV (Hadian et al., 2009). Moreover, hnRNP Q was found to bind specifically to galectin-3, a protein that stimulates proliferation in various cell types (Yoo et al., 2009) and the Q1 isoform was found to be associated through its Gly-rich C-terminus with the multifunctional nuclear phosphoprotein NS1 required for viral replication of the minute virus of mice (Harris et al., 1999).

1.6.4 Implication of hnRNP Q and hnRNP R in pathology

Nowadays, information about the development and progression of diseases associated with aberrant levels of hnRNP Q and hnRNP R is still incomplete. One study has investigated the role of hnRNP Q1 in tumorigenesis of colorectal cancer (Lai et al., 2017). Both hnRNP Q1 protein and mRNA levels were found to be upregulated in human tumor tissues compared with adjacent normal ones. Moreover, hnRNP Q1 was identify to bind to the 5'UTR of *Aurora-A* mRNA regulating its translation and in turn increasing cell proliferation and tumor progression (Lai et al., 2017).

Replication of the minute virus of mice (Harris et al., 1999) and HIV (Hadian et al., 2009) were also affected by hnRNP Q. In the first case, hnRNP Q1 was proposed as a cofactor in the double-stranded DNA-binding activity of NS1, whereas in the second study, the overexpression of hnRNP Q in concert with other hnRNP proteins, including hnRNP R, influenced the HIV-1 production by persistently infected astrocytes.

2. AIM OF THE PROJECT

As mentioned in the previous Chapters, several evidences have suggested an interesting correlation between TDP-43 pathology and hnRNP misregulation. In order to clarify the tangled scenario underlying TDP-43 metabolism and identify physiological partners of TDP-43 among the hnRNP family, the Molecular Pathology laboratory at ICGEB has recently taken advantage of *Drosophila melanogaster* as a TDP-43 proteinopathy model.

First of all, we evaluated how many human hnRNP proteins have homologs in *Drosophila*. In total, we found 11 human hnRNPs having a counterpart conserved in *Drosophila.* Then*,* in order to determine which of these genes were able to modulate TDP-43 activity *in vivo,* we performed a systematic gene suppression screening crossing flies silenced for these hnRNPs either with TBPH/TDP-43 hypomorphic flies (loss-of-function model) or transgenic flies overexpressing TBPH/TDP-43 in the eye compartment (gain-of-function model). We found that three hnRNPs, namely Hrb27c (DAZAP1) and Syncrip/Syp (hnRNP Q and R) had an extremely negative effect when knocked out in combination with TBPH. However, at the same time, they seemed to be protective in the TBPH gain-of-function expression model. Taken together, these results suggested that alteration of the expression levels of hnRNP proteins could represent a response against TDP-43 gain and loss-of-function events and could enable an *in vitro* characterization by using cell cultures.

Therefore, the main purpose of my PhD project was to clarify the bases of the opposite results observed in both the *Drosophila* models of TDP-43 proteinopathies after DAZAP1, hnRNP Q and hnRNP R depletion. This was achieved through the investigation of their functional relationship with TDP-43 within human neuronal-like cells, in order to highligh differences and similarities in regulation of RNA metabolism.

Initially, I studied the influence of each hnRNP protein on well-known TDP-43 regulated events and subsequently analysed the overall transcriptome status of RNA samples collected from human neuroblastoma (SH-SY5Y) cells treated with siRNA against TDP-43 and each hnRNP, in order to identify commonly regulated RNA targets involved in neuron development and neurodegeneration disease.

3. MATERIALS AND METHODS

3.1 Cell cultures, gene knockdown and cell differentiation

3.1.1 Cell cultures

Human neuroblastoma SH-SY-5Y cells (ATCC), HeLa cells (ATCC) and Flp-In HEK293 cells (Invitrogen, ThermoFisher, Waltham, MA, USA) expressing inducible Flag-tagged TDP-43 12XQ/N aggregates were cultured in DMEM–Glutamax-I (Gibco-BRL, Life Technologies Inc., Frederick, MD, USA) supplemented with 10% fetal bovine serum (Gibco-BRL, Life Technologies Inc., Frederick, MD, USA) and 1% Antibiotic-Antimycotic-stabilized suspension (SigmaAldrich, St. Louis, MO, USA) at 37°C in an incubator with humidified atmosphere of 5% CO2.

The mouse motor neuron-like NSC-34 cell line (a kind gift of Antonia Ratti, University of Milan, Milan, Italy) was cultured in Dulbecco's modified Eagle's medium (DMEM)–Glutamax-I (Gibco- BRL, Life Technologies Inc., Frederick, MD, USA) supplemented with 5% fetal bovine serum (FBS) (SigmaAldrich, St Louis, MO, USA) and 1% Antibiotic-Antimycotic-stabilized suspension (Sigma-Aldrich, St Louis, MO, USA) at 37°C in an incubator with humidified atmosphere of 5% CO2.

All the cell cultures were used up to 20 passages.

3.1.2 Gene knockdown of SH-SY5Y neuroblastoma cell line

To achieve optimal knockdown efficiency, three rounds of silencing were performed on day 1, 3 and 5 using HiPerFect Transfection Reagent (Qiagen Inc, Gaithersburg, MD, USA), according to the manufacturer's instructions. Briefly, $50X10^4$ cells were seeded in 6-well plates and silenced with a mix composed of 100 µl Opti-MEM (Life-Technologies,

CA, USA), 3 µl of 40 µM siRNA and 6 µl hyperfectamine (day 1). At the third day (day 3) cells were trypsinised, plated in a p60 plate and silenced for the second time using a double volume of mix. The same procedure was repeated at the third time (day 5) plating cells in a p100 plate and using a double volume of mix with respect to the second round of silencing. The final siRNA concentration for each time of silencing was 80 nM. After 48 hours cells were analysed by western blot (WB), pre-mRNA splicing, gene expression or used for immunofluorescence (IF) analysis.

For experiments with double knockdown (siTDP-43/siDAZAP1, siTDP-43/sihnRNP Q and siTDP-43/sihnRNP R) the amount of siRNA used for depletion of each gene was the half of the single knockdown.

The siRNA sense sequences used in this study are described in Table 1.

Table 1. siRNA sequence from 5′-prime to 3′-prime are listed.

Target gene	**siRNA sense sequence**
Fire-fly luciferase (siLUC-control)	5'-uaaggcuaugaagagauac-3'
TDP-43 (siTDP-43)	5'-gcaaagccaagaugagccu-3'
DAZAP1 (siDAZAP1)	5'-gagacucugcgcagcuacu-3'
hnRNP Q (sihnRNP Q)	5'-agacagugaucucucucau-3'
hnRNP R (sihnRNP R)	5'-cauuugggaucuacgucuu-3'

3.1.3 Gene knockdown of Flp-In HEK293 cell line expressing TDP-43 aggregates

Flp-In HEK293 cells with inducible siRNA resistant FLAG-tagged TDP-43-12XQ/N aggregates ($75X10^4$) were seeded in 6-well plates in 1.5 ml of culture medium containing serum and antibiotics. A total of 4 µl of 40 µM siRNA against DAZAP1, hnRNP Q and

hnRNP R was diluted in 90 µl of Opti-MEM (Life-Technologies, CA, USA) and 6 µl of HiPerFect Transfection Reagent (Qiagen Inc, Gaithersburg, MD, USA) (day 1). Second and third siRNA treatment were performed at day 2 and day 3, respectively. For each round of silencing, cells were tripsinised, plate in a new 6-well and silenced with the same amount of siRNA mixture as described for day 1. Importantly, for all the conditions, the silencing was performed in duplicates because of one plate was used for WB analysis and the second one for IF analysis. For this latter, the third round of siRNA treatment was performed in 6-well plates containing microscope slides treated with 0.1 mg/ml Poly-L-Lysine (Sigma-Aldrich, St Louis, MO, USA).

The list of siRNA used for silencing Flip-In HEK293 is the same described in section 3.1.2 and reported in Table 1.

At day 4, culture medium was changed and the TDP-43 12XQ/N aggregation was induced by addition of 1 µg/ml tetracycline solution (Sigma-Aldrich, St Louis, MO, USA). After 48 hours, cells were prepared for WB or IF analysis.

3.1.4 NSC-34 differentiation

NSC-34 cells were seeded to reach 70% confluence the day after and the proliferation medium was exchanged 24 hours later to fresh differentiation medium containing 1:1 DMEM/F-12 Ham (Sigma-Aldrich, St Louis, MO, USA), 1% FBS (Sigma-Aldrich, St Louis, MO, USA), 1% modified Eagle's medium nonessential amino acids (NEAA) (Sigma-Aldrich, St Louis, MO, USA), 1% Antibiotic-Antimycotic-stabilized suspension (Sigma-Aldrich, St Louis, MO, USA) and 1 µM all-trans retinoic acid (RA) (Sigma-Aldrich, St Louis, MO, USA). Differentiation medium was changed every two days and cells were allowed to differentiate for up to 5 days. NSC-34 cells, maintained on proliferation medium (DMEM, 5% FBS, 1% Antibiotic-Antimycotic suspension)

represented the undifferentiated control group. Images of undifferentiated (control, CNTRL) and differentiated NSC-34 cells were acquired by light microscopy using a Leica DMIL LED mycroscope equipped with a 20X objective, a Leica DFC450 C camera (Leica Microsystems, Cambridge, UK) and LAS v.4.4.0 Software (Leica application suit). The average length of neurites in the differentiation media was compared to that in the proliferation media and quantified using Fiji NeuronJ (Meijering et al., 2004). Neurite length was analyzed by imaging a minimum of 5 cells per field. The mean of neurite length ± standard error is reported. Statistical significance was calculated using *t*-test (indicated as *** for $P \leq 0.001$).

3.2 DNA plasmids for protein overexpression

3.2.1 Generation of competent DH5α *Escherichia coli* cells

To prepare competent DH5α *E. coli* cells, the protocol of Chung and collaborators (Chung et al., 1989) was followed introducing few modifications. DH5α stored in glycerol (1:1) at -80 °C were defrosted in ice and then plate in Petri dishes containing Luria-Bertani broth (LB) without antibiotics. The day after, one colony was picked up and grown overnight at 37 °C with 10 ml of LB (pre-inoculum). The third day 1-2 ml of pre-inoculum was diluted into 50 ml of LB and grown at 37 °C until its optical density reached an OD_{590} value of 0.3-0.4. Once the OD desired was obtained, bacteria were collected by centrifugation at 1000 xg for 10 minutes at 4 °C, resuspended into 5 ml of ice-colled diluted TSS 1X pH 6.5 (Table 2) and aliquoted in 1.5 ml sterile tubes and instantly frozen in liquid NO_2 for storage at -80 °C. To evaluate the competence of cells, 0.1 ng/µl of pUC18 plasmid was used to transform 100 µl of DH5α cells (see section below). Competence was calculated as following:

$$Competence\ (10^6) = \frac{Colony\ Forming\ Units}{Concentration\ of\ pUC18}$$

Table 2. Composition of TSS 1X.

Reagent	**Amount for 50 ml**
Polyethylene glycol (PEG 400) (SERVA Electrophoresis GmbH, Heidelberg,Germany)	5 g
$MgCl_2$	35 mM
DMSO	5%
Up to 50 ml with LB	35 ml ca.

3.2.2 Trasformation of competent DH5α cells

The amplification of desired plasmid DNA was obtained through bacteria trasformation. Competent bacteria (30 µl) were transformed with 0.1 ng/µl plasmid DNA as follows:

- Incubation 30 minutes on ice
- Heat-shock 2 minutes at 42 °C
- Incubation 1 minute on ice
- Incubation 30 minutes at 37 °C (shaking) in the presence of 60- 100 µl of LB without antibiotic
- Plate in Petri dish supplemented with antibiotic and incubate over-night at 37 °C

The next day, one colony was picked up and grown overnight at 37 °C in the presence of 50 ml (inoculum for Midiprep) or 6 ml (inoculum for Miniprep) of LB with antibiotic. After that, cells were collected through centrifugation for 30 minutes at 1937 xg and the resulting pellets were stored at -20 °C.

3.2.3 Small scale preparation of plasmid DNA (Miniprep)

Small scale preparation of plasmid DNA was performed using Wizard Plus SV Minipreps DNA purification system (Promega, Fitchburg, WI, USA) following the manufacturer's instructions. Basically, bacteria pellets were resuspended with 250 µl of cell resuspension solution by vortexing. Successively, 250 µl of Cell Lysis Solution and 10 µl of Alkaline Protease Solution was added to sample, mixed by inversion 4 times and incubated for 5 minutes at room temperature. To block the reaction, the Neutralization Solution (350 µl) was added into the bacteria lysate, mixed by inversion 4 times and centrifuged at maximum speed for 10 minutes at room temperature. After that, the cleared lysate was decanted into a spin column and centrifuged at maximum speed for 1 minute at room temperature. The flow-through was discarded and the spin column was washed two times with 750 µl and 250 µl of Wash Solution, respectively. Each step of washing was spaced out by centrifugation at maximum speed for 1 and 2 minutes at room temperature. Finally, the plasmid DNA was eluted by adding 100 µl of Nuclease-Free water into the spin column and centrifuging at maximum speed for 1 minute at room temperature. The obtained DNA was stored at -20 °C.

3.2.4 Middle scale preparation of plasmidic DNA (Midiprep)

Middle scale preparation of plasmid DNA was performed using JETSTAR Plasmid Purification kit (Genomed, Brussels, Belgium) following manufacture's instructions. Before starting with the solution within the kit, 50 µl of RNAse A was added to the cell pellet. Successively, 4 ml of Cell Resuspension Buffer E1 (supplemented with RNAse A) was used for resuspending the pellet until its homogenization. After that, 4 ml of Lysis Buffer E2 was added into the cell resuspension, mixed by inverting the capped tube and incubated at room temperature for 15-20 minutes to facilitate the lysis of bacteria. To

precipitate the nucleic acids, 4 ml of Precipitation Buffer (E3) was added to the lysate, mixed by inverting the tube and centrifugated at 1937 xg for 30 minutes at 4 °C. The supernatant was then loaded onto a pre-equilibrated column with 10 ml of Equilibration Buffer (E4) and the solution was allowed to drain by gravity flow. The column was then washed twice with 10 ml Wash Buffer (E5) and the flow-through was discarded. To elute plasmid DNA, 5 ml of Elution Buffer (E6) was added to the column previously placed in a new sterile 50 ml centrifuge tube. 3.5 ml of isopropanol was then added to the eluate, mixed well and centrifuged at 1937 xg for 30 minutes at 4°C. Finally, after air-drying the pellet for 10 minutes, the DNA pellet was resuspended in 200-300 µl of Nuclease-Free water and stored at -20 °C.

3.2.5 Overexpression of Flag-tagged siRNA resistant TDP-43 and Flag-tagged DAZAP1 in HeLa cells

In this thesis, I used two plasmid DNA vectors (pFLAG-CMV4 and pFLAG-CMV2) containing a cloned sequence for the overexpression of Flag-tagged siRNA resistant TDP-43 and Flag-tagged DAZAP1, respectively (Figure 19A-B).

The expression of each cloned DNA was performed by transfection of HeLa cells with Effectene Transfection Reagent (Qiagen Inc, Gaithersburg, MD, USA) following the manufacturer's instructions. Briefly, cells were plated in a p100 tissue culture dish and grown under their normal conditions (see section 3.1.1) to reach 70% confluence on the day of transfection. The day of transfection, 3 µg of plasmid was diluted with 300 µl of DNA-condensation buffer (Buffer EC). After that, 16 µl of Enhancer was added into the solution, mixed by vortexing, spun down and incubated 5 minutes at room temperature to allow the condensation of DNA. Effectene reagent (20 µl) was then added to the condensed DNA, mixed by vortexing 10 seconds, spun down and incubated 10 minutes at

room temperature to produce condensed Effectene-DNA complexes. Cells were washed with 1X PBS and the culture medium was exchanged with new one. After 10 minutes of incubation, the Effectene-DNA complexes were mixed with medium and directly added to the cells.

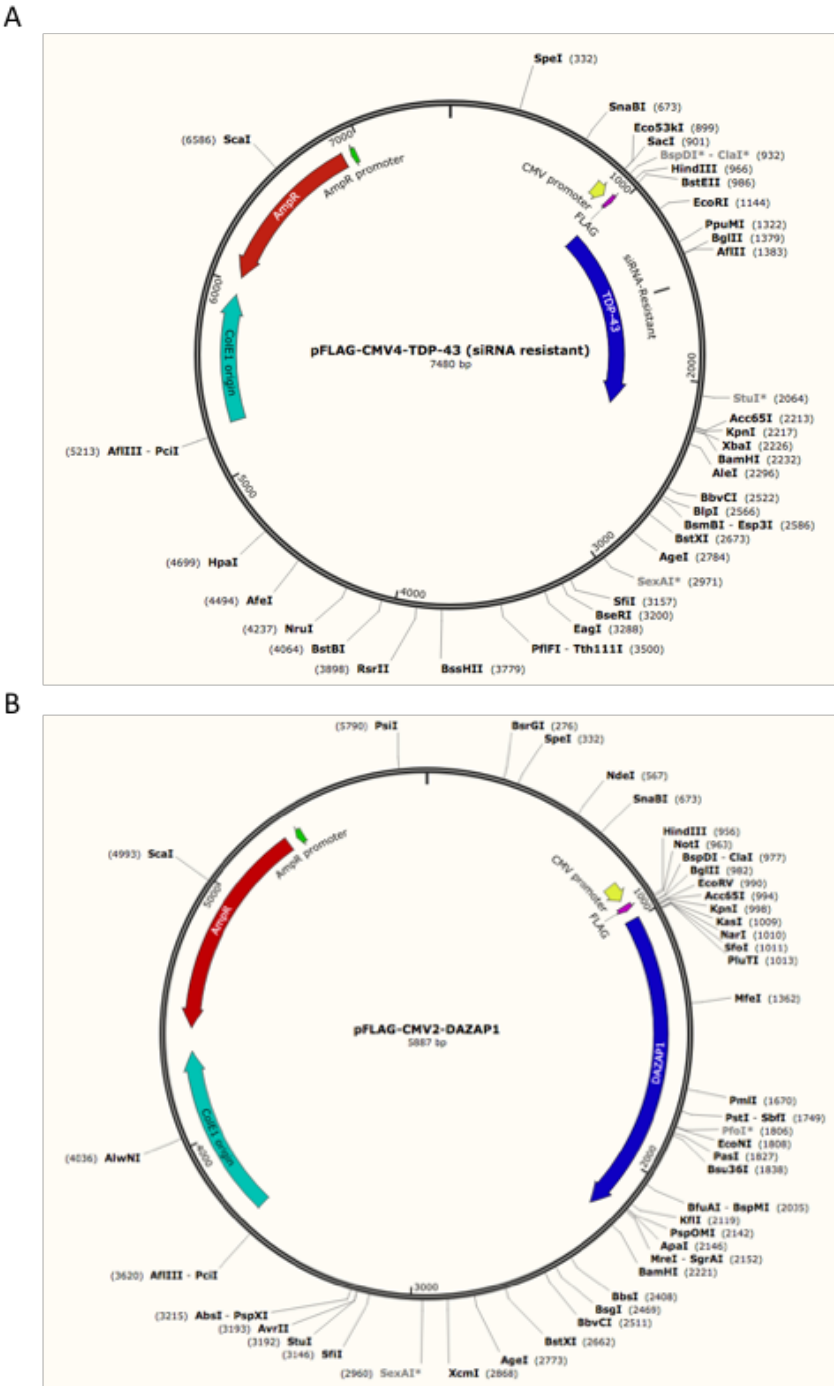

Figure 19. plasmid DNA for overexpression. (A) Map of pFLAG-CM4-TDP-43 (siRNA resistant). **(B)** Map of pFLAG-CMV2-DAZAP1.

3.3 Protein detection analysis

3.3.1 Western blot analysis for checking gene knockdown

Total protein extracts were obtained by sonicating cells two times for 5 minutes, high power with a BioRuptor UCD-200 (Diagenode, Belgium) in a mild lysis buffer composed of 1X Phosphate Saline Buffer (PBS) and 1X Complete Protease Inhibitor Cocktail (Roche Diagnostics, Mannheim, Germany). Disrupted cells were centrifuged 5 minutes at 16100 xg and the supernatant (protein extract) was collected in a new tube. Protein extract (20 µg) from each sample was resuspended in 1X sample buffer (Table 3), boiled at 95 °C for 5 minutes and loaded on a 10% Sodium Dodecyl sulfate (SDS)–polyacrylamide denaturing gel (Table 4). The gel was then electroblotted onto a PVDF blotting membrane (Immobilion-P, Millipore, Billerica, USA) pre-activated with 100% methanol by using a semi-dry protein blotter (Lighting Blotter, PerkinElmer, Massachusetts, USA) for 30 minutes keeping the voltage constant at 27 V. After blotting, the membrane was blocked with 4 % skimmed milk (Non-fat dry milk) or 4 % Bovine Serum Albumin (BSA) (Sigma-Aldrich, St Louis, MO, USA) in 1x PBS and 0.1% Tween-20 as described in the Table 5. Proteins were probed with incubation of primary (AbI) and subsequently HRP-conjugated secondary (AbII) antibodies in order to confirm the gene knockdown efficacy. The list of primary (AbI) and secondary (AbII) antibodies used for western blot are shown in Table 5. The chemiluminescence of the target proteins were detected with ECL Luminata Classico Western HRP substrate (Merck Millipore, Burlington, MA, USA) and the images were acquired using Alliance 9.7 Western Blot Imaging System (UVItec Limited, Cambridge, UK) or using X-ray film. Tubulin, available in-house, was used as total protein loading control. In order to quantify the percentage of remaining protein after siRNA knockdown, densitometric analysis of the Western Blot bands was performed using ImageJ software.

Table 3. Composition of stock 4X sample buffer.

Reagent	**Final concentration**
Tris-HCL pH 6.8	240 mM
Glycerol	40%
SDS	8%
Bromophenol blue	0.04%
2-mercaptoethanol	5%

Table 4. Composition of 10% SDS-acrylamide gel.

Running gel 10%		**Stacking gel**	
Reagent	**Volume**	**Reagent**	**Volume**
Tris-HCL 1.5 M pH 8.8	5 ml	Tris-HCL 0.5 M pH 6.8	2.50 ml
Protogel 30% (w/v) Acrylamide: 0.8 % (w/v) bis-acrylamide Stock Solution	6.66 ml	Protogel 30% (w/v) Acrylamide: 0.8 % (w/v) bis-acrylamide Stock Solution	560 µl
10% SDS	200 µl	10% SDS	50 µl
Ammonium persulfate (APS)	200 µl	Ammonium persulfate (APS)	50 µl
Tetramethylethylenediamine (TEMED)	20 µl	Tetramethylethylenediamine (TEMED)	10 µl
H_2O	8.34 ml	H_2O	2 ml

Table 5. Specifics of AbI and AbII used for checking gene knockdown.

Blocking solution	AbI	Company	Dilution	AbII	Company	Dilution
Milk	Polyclonal rabbit α-TDP-43	Proteintech	1:2000	Polyclonal goat α-rabbit	Dako Denmark A/S	1:2000
Milk	Polyclonal rabbit α-DAZAP1	Homemade	1:500	Polyclonal goat α-rabbit	Dako Denmark A/S	1:2000
BSA	Polyclonal rabbit α-hnRNP Q	Sigma-Aldrich	1:500	Polyclonal goat α-rabbit	Dako Denmark A/S	1:2000
BSA	Polyclonal rabbit α-hnRNP R	Abcam	1:500	Polyclonal goat α-rabbit	Dako Denmark A/S	1:2000
Milk	Polyclonal mouse α-Tubulin	Homemade	1:10000	Polyclonal goat α-mouse	Dako Denmark A/S	1:2000

3.3.2 TDP-43 and DAZAP1 co-immunoprecipitations (CO-IP) analysis

HeLa cells ($1.2X10^6$) were grown overnight in a p100 tissue culture dish to achieve 70% of confluence for transfection with 3 µg of pFLAG-TDP-43 wild-type using the Effectene reagent as described in section 3.2.5. After 24 hours, cell culture medium was removed and cells were washed with cold 1X PBS and harvested. Cells were lysed in 500 µL of IP buffer (Table 6) by sonication (3 min., mid power) in an ice-cooled sonicating bath (BioRuptor UCD-200, Diagenode, Belgium). The cell lysate was pre-cleared by incubation with 30 µl Protein A/G PLUS agarose beads (Santa Cruz Biotechnology Inc., Dallas, Texas, USA) in IP buffer for 1.5 hours at 4 °C. The pellet was discarded, and the supernatant was used for immunoprecipitation: the cell lysate was incubated with 2 µg of mouse monoclonal anti-FLAG M2 antibody (Sigma-Aldrich, St Louis, MO, USA) on a

rotating device for 1 hour at 4 °C. Then, 30 µl of Protein A/G PLUS agarose beads were added to each sample and incubated overnight at 4°C. The pellet was then washed three times in ice-cold IP buffer. The supernatant was discarded, and the pellet was re-suspended in 30 µl of 4X loading buffer. The samples were fractionated by SDS-PAGE (10%) and analysed by immunoblotting as described in section 3.3.1 using the antibodies reported in Table 7.

Table 6. Composition of IP buffer.

Reagent	**Final concentration**
Tris-HCL pH 7.5	20 mM
NaCl	110 mM
Triton-X	0.5%
Complete Protease Inhibitor Cocktail	1X

Table 7. List of AbI and AbII used for CO-IP experiment.

Blocking solution	**AbI**	**Company**	**Dilution**	**AbII**	**Company**	**Dilution**
Milk	Polyclonal rabbit α-TDP-43	Proteintech	1:2000	Polyclonal goat α-rabbit	Dako Denmark A/S	1:2000
Milk	Polyclonal rabbit α-DAZAP1	Homemade	1:500	Polyclonal goat α-rabbit	Dako Denmark A/S	1:2000
Milk	Polyclonal rabbit α-hnRNP H	Homemade	1:500	Polyclonal goat α-rabbit	Dako Denmark A/S	1:2000

3.3.3 Nuclear and cytoplasmic extraction using NER-PER kit

SH-SY5Y cells were seeded in p100 dishes to reach 90% confluence the day of nuclear and cytoplasm extraction. Cells from two dishes were pooled together and the resulting

pellet was treated using NER-PER Nuclear and Cytoplasmic Extraction Reagents (ThermoFischer, Waltham, MA, USA) as described in the manufacturer's instructions.

Briefly, 24 hours after seeding cell culture medium was removed and cells were washed with 1X PBS and harvested. The cell pellet was resuspended with ice-cold CER I buffer according to the packed cell volumes (Table 8) and vortexed on the highest setting for 15 seconds to fully suspend the cell pellet. The lysate was incubated on ice for 10 minutes and successively ice-cold CER II buffer according to Table 8 was added to tube. After that, the lysate was vortexed twice for 5 seconds on the highest setting with 1 minute incubation on ice between each round and then centrifuged for 5 minutes at maximum speed. The obtained supernatant (cytoplasmic fraction) was transferred to a pre-chilled tube and stored at -80°C until WB analysis. The insoluble pellet, containing nuclei, was suspended with ice-cold NE buffer according to Table 8, vortexed in the highest setting for 15 seconds every 10 minutes for a total of 40 minutes. After that, the nuclear fraction was centrifuged at maximum speed for 10 minutes and moved in a pre-chilled tube stored at -80 °C until the WB analysis.

For each sample fractionated with NER-PER kit, 15 µg of cytoplasmic and nuclear extracts were analyzed by WB as described in section 3.3.1 using the antibodies reported in Table 9.

Table 8. Reagent volumes for different packed cell volumes.

Packed cell volume (µl)	**CER I (µl)**	**CER II (µl)**	**NER (µl)**
10	100	5.5	50
20	200	11	100
50	500	27.5	250
100	1000	55	500

Table 9. List of AbI and AbII antibodies used for nuclear and cytoplasmic fractionation.

Blocking solution	AbI	Company	Dilution	AbII	Company	Dilution
BSA	Polyclonal rabbit α-hnRNP Q	Sigma-Aldrich	1:500	Polyclonal goat α-rabbit	Dako Denmark A/S	1:2000
BSA	Polyclonal rabbit α-hnRNP R	Abcam	1:500	Polyclonal goat α-rabbit	Dako Denmark A/S	1:2000
Milk	Polyclonal mouse α-Tubulin	Homemade	1:1000	Polyclonal goat α-mouse	Dako Denmark A/S	1:2000
Milk	Monoclonal mouse α-p84	Abcam	1:1000	Polyclonal goat α-mouse	Dako Denmark A/S	1:2000

3.4 pre-mRNA splicing, gene expression and RNA-seq analysis

3.4.1 RNA extraction

RNA was obtained using EuroGold Trifast (Euroclone, Milan, Italy), following the manufacturer's instructions. Briefly, cell culture medium was removed and cells were washed with cold 1X PBS and harvested. According to the volumes reported in Table 10, cell pellet was resuspended with EuroGold Trifast by pipetting and incubated for 5 minutes at room temperature. Chloroform (Table 10- chloroform I) was then added to each sample and the mixture was strongly shacked and incubated 10 minutes at room temperature.

Subsequently, samples were centrifuged at maximum speed for 20 minutes at 4 °C and the supernatant fraction (transparent upper phase) was transferred in a new sterile tube and mixed with an equal volume of chloroform for a second cleaning step (chloroform II). Samples were then centrifuged at maximum speed for 10 minutes at 4 °C and the supernatant was transferred in a new sterile tube. The RNA was precipitated adding isopropanol to this latter (Table 10), incubated for 10 minutes on ice, and then centrifuged at maximum speed for 20 minutes at 4 °C. At the end of the process, the resulting pellet (RNA) was washed with 70% ethanol, centrifuged at maximum speed for 5-10 minutes at 4 °C, resuspended in 30-60 µl of RNase-free water and quantified with Nanodrop 1000 (ThermoFisher, Waltham, MA, USA).

Table 10. Volume of reagent using for RNA extraction according to cell dish.

6-well/ p35 dish		**p100 dish**	
Reagent	**Volume**	**Reagent**	**Volume**
EuroGold Trifast	500 ml	EuroGold Trifast	1 ml
Chloroform I	100 µl	Chloroform I	200 µl
Isopropanol	250 µl	Isopropanol	500 µl
70 % Ethanol	400 µl	70 % Ethanol	800 µl
RNase-free water	30 µl	RNase-free water	60 µl

3.4.2 Reverse transcription reaction

Complementary DNA (cDNA) was retrotranscribed by using 1 µg of total RNA in the presence of random primers (Sigma-Aldrich, St Louis, MO, USA) and Moloney murine leukemia virus (M-MLV) Reverse Transcriptase (Invitrogen, ThermoFisher, Waltham, MA, USA). RNA samples prepared as described in Table 11 were denaturated at 85 °C for

5 minutes and chilled 1 minutes on-ice to avoid renaturation of RNA. After that, 20 µl of mixture containing M-MLV enzyme (Table 12) were added to RNA sample mixture (20 µl) and incubated 1-2 hours at 37 °C for reverse transcription reaction. cDNA samples were then stored at -20 °C or placed on-ice for pre-mRNA splicing analysis or gene expression analysis.

Table 11. Preparation of RNA sample mixture.

Reagent	**Final concentration (20 µl of reaction)**
RNA sample	50 ng/µl
Random primers	1 ng/µl

Table 12. Mixture for reverse transcription reaction.

Reagent	**Final concentration (20 µl of reaction)**
5X First strand buffer	2X
Dithiothreitol (DTT) 0.1 M	0.02 M
Deoxynucleotide (dNTP) Solution Mix 5mM	1 mM
M-MLV 200 U/µl	5 U/µl

3.4.3 pre-mRNA splicing analysis

To evaluate the pre-mRNA splicing, polymerase chain reaction (PCR) was performed from cDNA obtained as described in section 3.4.2, and derived from SH-SY5Y cells depleted for TDP-43, DAZAP1, hnRNP Q and hnRNP R, or co-silenced for TDP-43/DAZAP1, TDP-43/hnRNP Q and TDP-43/hnRNP R. For each sample, 3 µl of cDNA was mixed with 47 µl of PCR mix solution prepared as described in Table 13. Taq DNA polymerase (New England Biolabs, Ipswich, MA, USA) was used for reaction. Forward and reverse primer

sequences for each gene tested and the relative PCR conditions are reported in Table 14 and figure 20A-B, respectively. For each target gene, PCR amplification was performed for 35 cycles and products (10 µl of total volume of reaction) were routinely fractionated in 1.5% (w/v) agarose gels. The percentage of exon inclusion for each tested gene was evaluated by densitometric analysis using ImageJ software. For *MADD* gene was calculated the percentage of pseudoexon inclusion. The statistical significance was calculated using an unpaired *t*-test. $P<0.05$ was considered significant ($n = 3$) (* $P < 0.05$, ** $P < 0.01$, and *** $P<0.001$).

Table 13. PCR reaction mixture.

Reagent	**Final concentration (50 µl of reaction)**
10X ThermoPol reaction Buffer	1X
Deoxynucleotide (dNTP) Solution Mix 5mM	0.2 mM
Primer Forward 10 ng/µl	0.3 ng/µl
Primer Reverse 10 ng/µl	0.3 ng/µl
Taq Biolabs 5 U/µl	0.02 U/µl

Table 14. List of genes and relative primers (forward and reverse sequences) used for pre-mRNA splicing analysis.

Target gene	**Forward sequence (5'-3')**	**Reverse sequence (5'-3')**
POLDIP3	5′-gcttaatgccagaccgggagttg-3′	5′-tcatcttcatccaggtcatataaatt-3′
TNIK	5′-caaaggcgagagaaggagctg-3′	5′-ctgatgctgaagggaaactaag-3′
STAG2	5′-gtatgtttacttggaaaagttcatg-3′	5′-tgattcatccataattgaagctgga-3′
MADD	5′-gacctgaattgggtggcgagttccct-3′	5′-cattggtgtcttgtacttgtggctc-3′

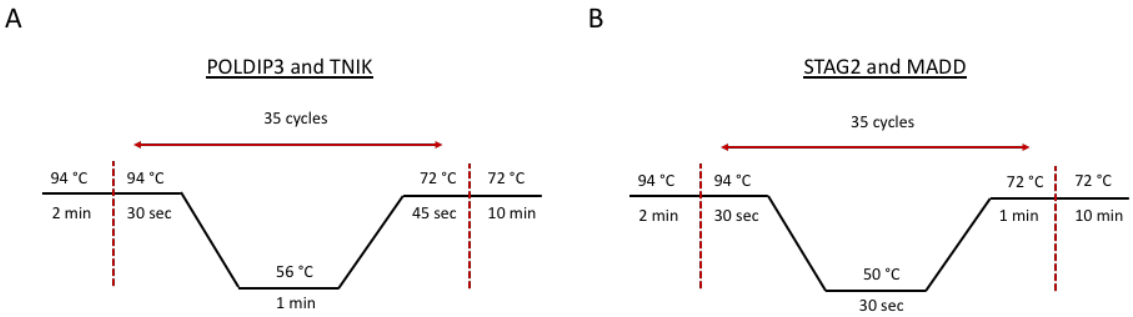

Figure 20. PCR conditions used in the pre-mRNA splicing assay. (A) Protocols for PCR amplification of *POLDIP3* and *TNIK* gene. **(B)** Protocols for PCR amplification of *STAG2* and *MADD* gene.

3.4.4 RNA immunoprecipitation (RNA-IP) analysis

HeLa cells ($1.2X10^6$) were grown overnight in a p100 tissue culture dish to achieve 70% of confluence for transfection with 3 µg flag-DAZAP1 plasmid using Effectene reagent as described in section 3.2.5. After 24 hours, the cell culture medium was removed and cells were washed with cold 1X PBS and harvested. Cells were lysated with HEGN buffer (Table 15) and sonicated (5 minutes, high power) in an ice-cooled sonicating bath (BioRuptor UCD-200, Diagenode, Belgium). HeLa lysate (40 µg) was incubated for 1 hour at 4 °C in HEGN buffer supplemented with 7.5 µg/µl heparin (Sigma-Aldrich, St Louis, MO, USA) and Protein A/G Agarose beads (Santa Cruz Biotechnology Inc., Dallas, Texas, USA), pre-coated for 1 hour, 4 °C in rotation with 5 µg of anti-Flag antibody (IP-Flag) (Sigma-Aldrich) or with uncoated beads as controls (IP-Beads). After washes with HEGN + DOC 0.2% + Urea 0.5 M (four-times separated with centrifugation of 5 minutes at 15000 xg), mRNA was extracted from immunoprecipitated RNPs using EuroGold Trifast (see section 3.4.1; volumes for p35 dish). The abundance of possible DAZAP1 target genes was measured by quantitative Real-Time PCR on three independent experiments as described below.

Table 15. Composition of HEGN buffer.

Reagent	**Final concentration**
Hepes pH 7.5	20 mM
NaCl	150 mM
EDTA	0.5 mM
Glycerol	10%
Triton-X	0.1%
DTT	1 mM
Complete protease inhibitor cocktail	1X

3.4.5 Gene expression analysis

Total RNA was extracted from SH-SY5Y cells transfected with siRNA against TDP-43, DAZAP1, hnRNP Q and hnRNP R or co-transfected with siRNA against TDP-43 in the presence of siRNA against each of the three tested hnRNPs as describe in section 3.1.2. RNA obtained from SH-SY5Y cells treated with siRNA against luciferase (siLUC) was used as a negative control. For each RNA sample, reverse transcription was performed in order to synthetize cDNA as described in section 3.4.2. The quantification of gene expression levels was carried out by quantitative Real-time PCR using iQ SYBR green supermix (Bio-Rad, Hercules, CA, USA). For each sample, 4 µl of cDNA (diluted 1:10-1:5 in sterile water) was mixed with 6 µl of iQ mix solution prepared as described in Table 16. Quantitative Real-time PCRs were performed on a MiniOpticon real-time PCR and on a CFX96 Real-time systems (Bio-Rad, Hercules, CA, USA). The expression levels were determined using the $2^{-\Delta\Delta CT}$ method (Schmittgen and Livak, 2008). For primer designer two online tools were used: PrimerBank (https://pga.mgh.harvard.edu/primerbank/) and qPrimerDepot (http://primerdepot.nci.nih.gov/). The list of primers (forward and reverse

sequence) and the qPCR conditions are reported in Table 17 and Figure 21A-C, respectively. To normalize the results, the housekeeping gene *Glyceraldehyde-3-phosphate Dehydrogenase (GAPDH)*, *Ribosomal Protein L13a (RPL13A), Hypoxanthine Posphoribosyltransferase 1 (HPRT1)* and *RNA Polymerase II Subunit A (POLR2A)* were also used (Table 18). In particular, GAPDH and RPL13A were used to normalize simultaneously the expression of *MADD, BRD8, TNIK, ELAVL3, NOVA2, RELN, STX3, CELF5, YPEL4, ACHE, TNF, TNFRSF9* and *ICAM1* gene in SH-SY5Y cells. Whereas, HPRT1 and POLR2A were used to normalize simultaneously the expression of *PENK, KLF4, KLHL4, NRG3, RAB26, ARHGAP36, CT55, CARTPT, FOSB, JAG1, ICAM5, DUOXA1, HMOX1, KCNAB1, ACP5, SDCBP2, EFEMP1, SYNCRIP (hnRNP Q)* and *HNRNPR* gene in SH-SY5Y cells. Moreover, *Succinate Dehydrogenase Complex Flavoprotein Subunit A* (*SDHA)* was used as a negative control for RNA-immunoprecipitation analysis performed in HeLa cells.

The mean of relative expression levels ± standard deviation/ standard error of three independent experiments are reported. Statistical significance was calculated using an unpaired *t*-test. P<0.05 was considered significant (n = 3) (* P < 0.05, ** P < 0.01, and *** P<0.001).

Table 16. Composition of iQ mix solution.

Reagent	**Final concentration**
iQ SYBR green supermix	Dilution 1:2
20 μM Primer forward	0.05 μM
20 μM Primer forward	0.05 μM

Table 17. List of target genes and relative primers (forward and reverse sequences) used for gene expression analysis.

Target gene	**Forward sequence (5'-3')**	**Reverse sequence (5'-3')**
MADD	5'-ttgagaccaactctgccaca-3'	5'-agactcgctggctcacatct-3'
BRD8	5'-gcagcctgttacagatgac-3'	5'-aatagttgacaaatccataggc-3'
TNIK	5'-tggaacatacgggcaagttt-3'	5'-tcctcttcatcccctgtgac-3'
POLDIP3	5'-tctcagcccattggaaggc-3'	5'-tgatggcatcgtccttttcac-3'
STAG2	5'-aaaatcaaaaccatctacagg-3'	5'-tactactactttcttcagtgag-3'
ELAVL3	5'-cctcaaattacagacgaagacca-3'	5'-gctgacgtacaggttagcatc-3'
NOVA2	5'-aaggcgaatacttcctgaaggt-3'	5'-gctgacgtacaggttagcatc-3'
RELN	5'-ttggaggttccagtgctttc-3'	5'-tcctcatcggttgtctttttgc-3'
STX3	5'- tcggcagaccttcggattc-3'	5'-tcctcatcggttgtctttttgc-3'
CELF5	5'-aaactcttcgtgggccagat-3'	5'-ggcacagtaggtg aggaagg-3'
YPEL4	5'-cggagatctctggagcagac-3'	5'-gtgtttcagggca ggagaag-3'
ACHE	5'-agaaagcgtcttccggttct-3'	5'-tacgagccctcatccttcac-3'
TNF	5'-cctctctct aatcagccctctg-3'	5'-gaggacctgggagtagatgag-3'
TNFRSF9	5'-ttggatggaaagtctgtgcttg-3'	5'-aggagatgatctgcggagagt-3'
ICAM1	5'- ggccggccagcttatacac-3'	5'-tagacacttgagctcgggca-3'
PENK	5'-gtgcagctaccgcctagtg-3'	5'-tgcaggtttcccaaattttc-3'
KLF4	5'-gcggcaaaacctacacaaag-3'	5'-ccccgtgtgtttacggtagt-3'
KLHL4	5'-ttggagatgatggctgatga-3'	5'-aagagtttgctctgcgtggt-3'
NRG3	5'-tattcaaaggtggaaaggcatcc-3'	5'-tgaaggcattcctatggagca-3'
RAB26	5'-tcatctccaccgtaggcatt-3'	5'-ccggtagtaggcatgggtaa-3'
ARHGAP36	5'-ttgaactgacagccacgatg-3'	5'-gccagactatccacagacac-3'
CT55	5'-atgttgtgactggcaacgtg-3'	5'-gccagactatccacagacac-3'
CARTPT	5'-ccgagccctggacatctact-3'	5'-atgggaacacgtttactcttgag-3'
FOSB	5'-accctctgccgagtctcaat-3'	5'-gaaggaaccgggcatttc-3'
JAG1	5'-atcgtgctgcctttcagttt-3'	5'-gatcatgcccgagtgagaa-3'
ICAM5	5'-ggctcttcggcctctcag-3'	5'-gcagttggtgctgcaattc-3'

DUOXA1	5'-ccaagccaaccttcccgat-3'	5'-cccgatgaataagctggtcac-3'
HMOX1	5'-gccagcaacaaagtgcaag-3'	5'-gagtgtaaggacccatcgga-3'
KCNAB1	5'-gcaaatcgaccggacagtaac-3'	5'-gccatgccttggtttatcacat-3'
ACP5	5'-ctacccactgcctggtcaag-3'	5'-cacgccattctcatcttgc-3'
SDCBP2	5'-ccactacgtgtgtgaggtgg-3'	5'-tgctcgtagatcacactggg-3'
EFEMP1	5'-cgagcaaagtgaacacaacg-3'	5'-gatatccaggagggcactga-3'
SYNCRIP (hnRNP Q)	5'-actgttgaatgggctgatcc-3'	5'-cctccaagtctttgccattc-3'
HNRNPR	5'-gcaaggtgcaagagtccaca-3'	5'-cacgccagagtacacactgtc-3'

Table 18. List of housekeeping genes and relative primers (forward and reverse sequences) used for normalization of gene expression analysis.

Housekeeping gene	**Forward sequence (5'-3')**	**Reverse sequence (5'-3')**
GAPDH	5'-cgctctctgctcctcctgtt-3'	5'-ccatggtgtctgagcgatgt-3'
RPL13A	5'-cctggaggagaagaggaaagaga-3'	5'-ttgaggacctctgtgtatttgtcaa-3'
SDHA	5'-tgggaacaagagggcatctg-3'	5'-ccaccactgcatcaaattcatg-3'
HPRT1	5'-tgacactggcaaaacaatgca-3'	5'-ggtccttttcaccagcaagct-3'
POLR2A	5'-gcccacgtccaatgacat-3'	5'-gtgcggctgcttccataa-3'

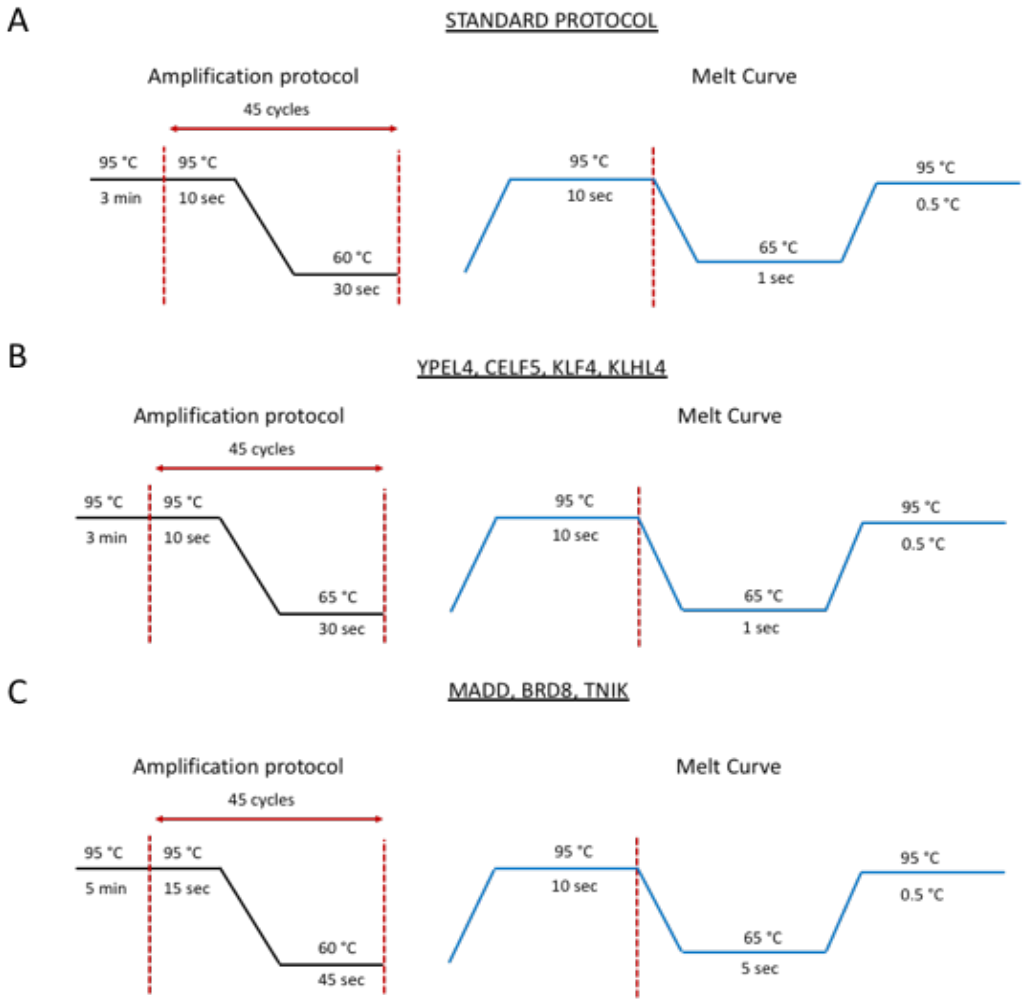

Figure 21. Real-Time PCR conditions for gene expression analysis. (A) Standard protocol for amplification of target genes. **(B)** Specific Real-Time PCR protocol for amplification of *MADD, BRD8* and *TNIK* gene. **(C)** Specific Real-Time PCR protocol for amplification of *YPEL4, CELF5, KLF4, KLHL4* gene.

3.4.6 RNA-seq and analysis of differentially expressed genes (DEGs)

Total RNA was extracted from luciferase (control), TDP-43, DAZAP1, hnRNP Q and hnRNP R depleted SH-SY5Y cells, as described previously. RNA sequencing was performed by Eurofins (www.eurofins.com) using an Illumina HiSeq 2500 instrument on three independent experiments obtained for each tested hnRNPs. Data processing was carried out with the following software: HiSeq Control Software v2.0.12.0, RTA v1.17.21.3 and bcl2fastq-1.8.4. Alignment to human reference sequence was performed by

BWA-MEM (version 0.7.12-r1039,http://bio-bwa.sourceforge.net/) and the raw read counts were created using featureCounts (http://bioinf.wehi.edu.au/featureCounts/). Only reads with unique mapping positions and a mapping quality score at least 10 were considered for read counting. Raw read counts were converted to Counts per million (CPM) values by Trimmed mean of M-values (TMM) normalization (edgeR package http://bioconductor.org/packages/release/bioc/html/edgeR.html, (Robinson and Oshlack, 2010). Features had to have a counts-per-million value of more than one in at least three samples or were removed, resulting in the removal of 47622 of the 64769 features. Differential expression analysis was performed on the remaining 17417 genes using edgeR package.

Regarding the interpretation of the differential expression genes data and pathway mapping related to TDP-43 and DAZAP1, PANTHER (Protein ANalysis THrough Evolutionary Relationships) Classification System and the Database for Annotation, Visualization and Integrated Discovery (DAVID) v6.7 tools were used. Venn diagrams were generated using the VENN diagram generator at http://bioinfogp.cnb.csic.es/tools/venny/. GOseq package from R (Young et al., 2010) was also used for Gene ontology (GO) and KEGG pathway analysis of RNA-seq data. Categories significantly enriched (P< 0.05) were considered.

3.4.7 Statistical analysis of data

Statistical analysis of gene expression and splicing analysis were carried out by an unpaired two-sample *t test* on three independent experiments. P<0.05 was considered significant (* P < 0.05, ** P < 0.01, and *** P<0.001). Regarding the RNA-seq analysis, DEGs were identified using the fold change cut-off of 30% with respect to a control sample treated with siRNA against fire-fly luciferase (siLUC) (upregulation cut-off: >1.3; downregulation cut-off: <0.7-FC) and the cut-off P< 0.05 for statistical significance.

3.5 Immunofluorescence (IF) analysis

3.5.1 Immunofluorescence analysis of Flp-In HEK293 cell line expressing TDP-43 aggregates

Flp-In HEK293 cells expressing inducible TDP-43 aggregates were plated and treated as described in section 3.1.3. For immunofluorescence analysis the cells were washed 3 times with PBS, fixed in 3.2% paraformaldehyde in PBS for 1 hour at room temperature and permeabilized by using 0.3% Triton in PBS for 5 minutes on ice. Cells were then blocked with 2% BSA/PBS for 20 minutes at room temperature and incubated overnight at 4 °C in a humidified chamber with 60 µl of primary antibody against TDP-43 and the FLAG-tag prepared as described in Table 19. The day after, cells were washed 3 times with PBS, incubated with secondary antibodies conjugated with probes (Table 19) for 1 hour at room temperature and coverslipped with Vectashield-DAPI mounting medium (Vector Laboratories, Burlingame, CA, USA). Each slide was analyzed using Nikon Ti-E confocal microscope with a 60X oil objective.

Table 19. List of AbI and AbII for IF analysis of Flp-In HEK293 expressing TDP-43 12XQ/N.

AbI	Company	Dilution	AbII	Company	Dilution
Polyclonal rabbit α-TDP-43	Proteintech	1:200	AlexaFluor 488 donkey α-rabbit	Invitrogen	1:500
Monoclonal mouse α-FLAG	Sigma-Aldrich	1:200	AlexaFluor 594 donkey α-mouse	Invitrogen	1:500

3.5.2 Immunofluorescence analysis of SH-SY5Y cells and differentiated NSC-34 cells

SH-SY5Y cells (40×10^4), SH-SY5Y treated with siRNA against DAZAP1, hnRNP Q and hnRNP R (40×10^4) and differentiated NSC-34 cells (35×10^4) were plated in 6-well plates containing coverslips. For SH-SY5Y depleted cells and differentiated NSC-34 cells coverslips were coated with poly-L-lysine solution at a final concentration of 0.01% (w/v) in H20 (SigmaAldrich, St Louis, MO, USA). After 24 hours, cells were washed three times with PBS, fixed in 3.2% paraformaldehyde in PBS for 1 hour at room temperature and permeabilized by using 0.3% Triton in PBS for 5 minutes on ice. Cells were then blocked with 2% BSA/PBS for 20 minutes at room temperature and incubated overnight at 4 °C in a humidified chamber with 60 µl of primary antibodies prepared as described in Table 20. The day after, cells were washed 3 times with PBS, incubated with secondary antibodies conjugated with a fluorescent dye (Table 20) for 1 hour at room temperature and coverslipped with Vectashield-DAPI mounting medium (Vector Laboratories, Burlingame, CA, USA). Each slide was analysed using Nikon Ti-E confocal microscope with a 60X oil objective available in ICGEB institute or at the microscopy facility of University of Trieste, using a Nikon Eclipse C1si confocal microscope system mounted on a Nikon TE-2000U inverted microscope with a 60X objective.

Table 20. List of AbI and AbII for IF analysis of SH-SY5Y cells and differentiated NSC-34 cells.

AbI	**Company**	**Dilution**	**AbII**	**Company**	**Dilution**
Polyclonal rabbit α-TDP-43	Proteintech	1:200	AlexaFluor 594 donkey α-rabbit	Invitrogen	1:500
Polyclonal rabbit α-hnRNP Q	Sigma-Aldrich	1:200	AlexaFluor 488 donkey α-rabbit	Invitrogen	1:500
Polyclonal rabbit α-hnRNP R	Abcam	1:200	AlexaFluor 488 donkey α-rabbit	Invitrogen	1:500

4. RESULTS

4.1 Effects of DAZAP1, hnRNP Q and hnRNP R suppression on TDP-43 activity in SH-SY5Y cell line

4.1.1 DAZAP1, hnRNPQ and hnRNPR can regulate and rescue TDP-43 controlled splicing events without altering the expression of TDP-43

Thanks to the results obtained from the *Drosophila melanogaster* model of TDP-43 loss- or gain-of-function, in collaboration with the Neurobiology group in ICGEB, we decided to investigate the effects of DAZAP1, hnRNP Q and hnRNP R within human neuroblastoma (SH-SY5Y) cells. First of all, we measured the efficiency of siRNA treatment against each hnRNP and subsequently, we evaluated if the silencing of DAZAP1, hnRNP Q and hnRNP R was capable to affect the expression of TDP-43 at the protein level, by using Western Blot analysis. As shown in Figure 22A-B the efficiency of siRNA treatment against TDP-43, DAZAP1, hnRNP Q and hnRNP R was sufficient to knockdown ~ 80-70% of each protein in SH-SY5Y cells. Moreover, the depletion of these hnRNP proteins was not able to modify TDP-43 expression (Figure 22B), as well as the protein expression of DAZAP1, hnRNP Q and hnRNP R did not change after siRNA depletion of TDP-43 (Figure 22C-E).

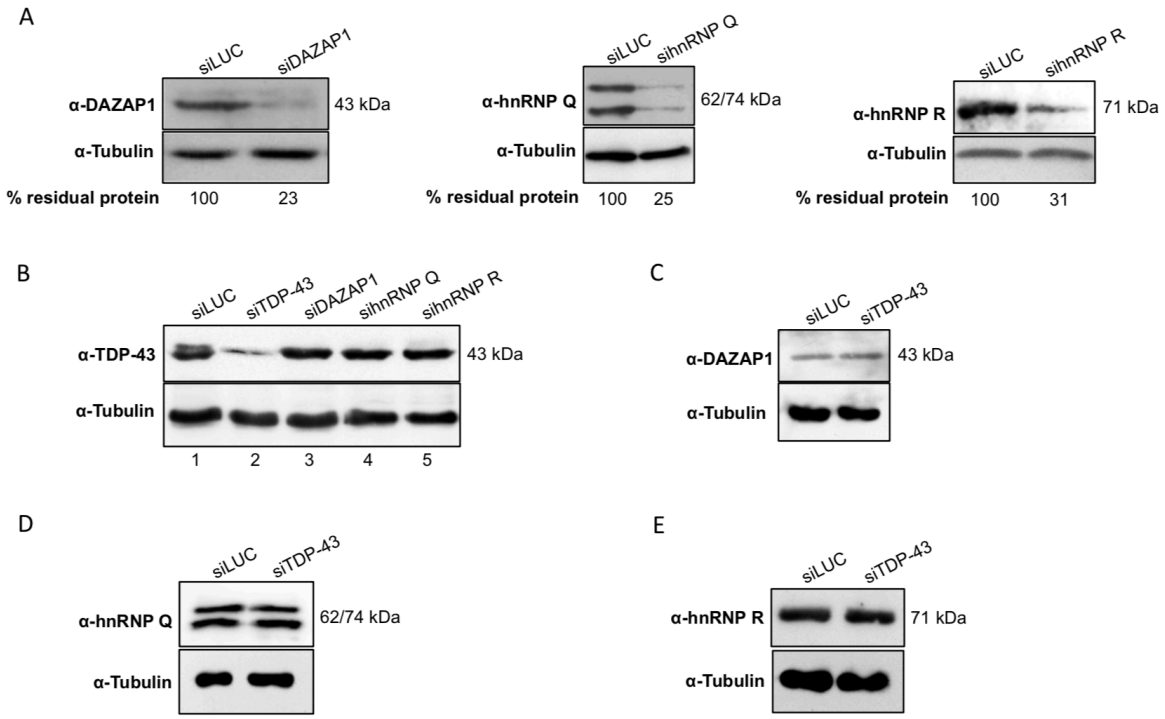

Figure 22. Western Blot analysis of siRNA treatments in SH-SY5Y cells. (A) Protein expression level of DAZAP1, hnRNP Q and hnRNP R after siRNA treatment comparing to cells treated with siRNA against fire-fly luciferase (siLUC) used as a control. The percentage of residual protein is also reported. **(B)** TDP-43 expression level following siRNA silencing of DAZAP1, hnRNP Q, and hnRNP R comparing to siLUC treated cells. Silencing of TDP-43 is also reported (the percentage of residual protein is 27%). **(C-E)** Protein expression level of DAZAP1 **(C),** hnRNP Q **(D)** and hnRNP R **(E)** were measured in SH-SY5Y cells treated with siRNA against TDP-43 comparing to siLUC treated cells. These experiments were performed in collaboration with Dr. Fatemeh Mohagheghi.

Successively, we analysed the ability of these hnRNP proteins to modulate pre-mRNA splicing events known to be controlled by TDP-43. Indeed, recent studies have demonstrated that the knockdown of TDP-43 causes exon 3 skipping of the *POLDIP3/SKAR* gene (Fiesel et al., 2012), as well as an increase in *TNIK* exon 15 (Colombrita et al., 2015) and *STAG2* exon 30b inclusion (De Conti et al., 2015) and the exclusion of exon 31, in addition to the inclusion of a pseudoexon, in the *MADD* gene (De Conti et al., 2015)

We silenced each tested hnRNP protein (including TDP-43) in SH-SY5Y cells by using siRNA, and then we evaluated the different splicing pattern of *SKAR/POLDIP3* exon3, *TNIK* exon 15, *STAG2* exon 30b and *MADD* exon 31. According to previous studies, the silencing of TDP-43 was able to reproduce the splicing profile observed for each tested gene (Figure 23). As expected, the silencing of TDP-43 was associated with an increased exclusion of *POLDIP3* exon 3 (Figure 23A), with an increased inclusion of *TNIK* exon 15 (Figure 23B), and of *STAG2* exon 30b (Figure 23C), as well as with a decrease of exon 31 inclusion and symultaneous activation of a pseudoexon in the *MADD* gene (Figure 23D). On the other hand, knocking down expression of DAZAP1 boosted *POLDIP3* exon 3 inclusion (Figure 23A), and reduced both *TNIK* exon 15 (Figure 23B) and of *STAG2* exon 30b inclusion below normal levels (Figure 23C). Likewise, removal of hnRNP Q was associated with a drop in the inclusion of both *POLDIP3* exon 3 (Figure 23A) and *TNIK* exon 15 (Figure 23B). Finally, knocking down expression of hnRNP R was able to alter only the splicing of the *TNIK* gene, by causing an enhancement of exon 15 inclusion (Figure 23B). Notably, the splicing profile of *MADD* gene was modified only by TDP-43 silencing (Figure 23D).

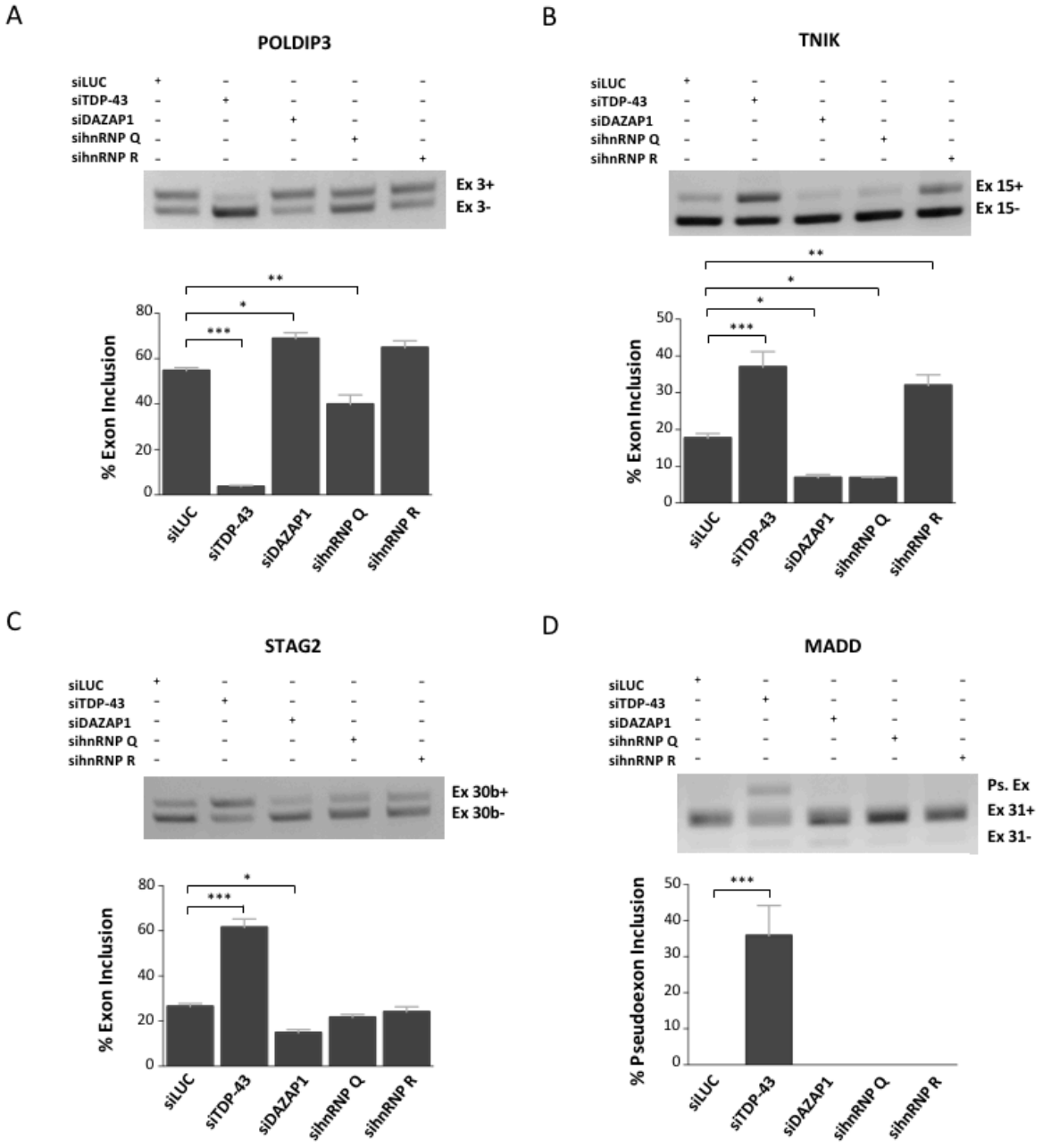

Figure 23. Effects of different siRNA treatment on TDP-43-regulated events. SH-SY5Y cells were treated with different siRNA against TDP-43, DAZAP1, hnRNP Q and hnRNP R and RT-PCR was used to evaluate the effects of this depletion on *POLDIP3* exon 3 **(A)**, *TNIK* exon 15 **(B)**, *STAG2* exon 30b **(C)** and *MADD* exon 31 **(D)**. The agarose gel was loaded with the following samples: control siRNA Luciferase transfected cells (lane 1, siLUC), depleted of TDP-43 (lane 2, siTDP-43), depleted of DAZAP1 (lane 3, siDAZAP1), depleted of hnRNP Q (lane 4, sihnRNPQ) and depleted of hnRNP R (lane 5, sihnRNPR). The identity of the various transcripts is reported on the right. For the *MADD* gene, the appearance of a pseudoexon is also reported (Ps.Ex.). *P < 0.05, **P < 0.01, ***P < 0.001 (n = 3), calculated by an unpaired *t*-test. These experiments were performed in collaboration with Dr. Fatemeh Mohagheghi.

As a result of these changes, we were also interested in investigating if the co-silencing of TDP-43 and DAZAP1, hnRNP Q or hnRNP R could rescue the splicing alteration induced by TDP-43 depletion. Therefore, we silenced SH-SY5Y cells with both siRNA against TDP-43 and each hnRNP, and we analysed the resulting splicing profile of *POLDIP*3, *TNIK, STAG2* and *MADD* gene. Co-silencing of DAZAP1 and TDP-43, on one hand, restored the splicing patterns of the *TNIK* (Figure 24B) and the *MADD* gene (Figure 24D) as observed in the control transfections. On the other hand, it was able to counteract partially the *POLDIP3* exon3 skipping (Figure 24A), and completely *STAG2* exon30b inclusion (Figure 24C), caused by TDP-43 silencing alone.

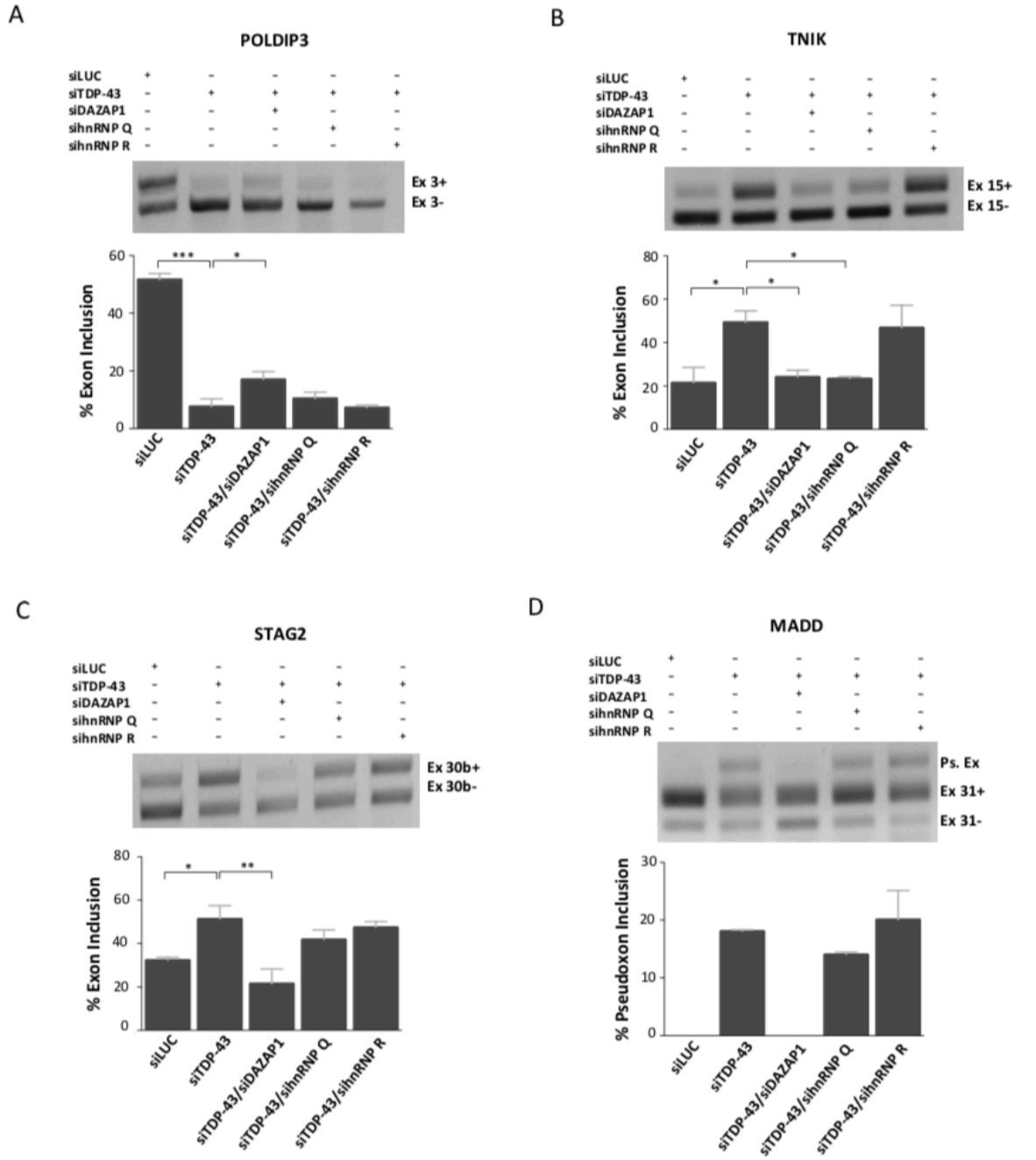

Figure 24. Rescue of TDP-43 controlled events. SH-SY5Y cells were co-silenced with siRNA against TDP-43 in the presence of siRNA against DAZAP1, hnRNP Q and hnRNP R. RT-PCR was used to evaluate the effects of this depletion on *POLDIP3* exon 3 **(A)**, *TNIK* exon 15 **(B)**, *STAG2* exon 30b **(C)** and *MADD* exon 31 **(D)**. The agarose gel was loaded with the following samples: control siRNA Luciferase transfected cells (lane 1, siLuc), depleted of TDP-43 (lane 2, siTDP-43), depleted of TDP-43 and DAZAP1 (lane 3, siTDP-43/siDAZAP1), depleted of TDP-43 and hnRNP Q (lane 4, siTDP-43/sihnRNP Q) and depleted of TDP-43 and hnRNP R (lane 5, siTDP-43/sihnRNP R). The identity of the various transcripts is reported on the right. For the *MADD* gene, the appearance of a pseudoexon is also reported (Ps.Ex.). *P < 0.05, **P < 0.01, ***P < 0.001 (n = 3), calculated by an unpaired *t*-test. These experiments were performed in collaboration with Dr. Fatemeh Mohagheghi.

Figure 25 summarizes these results:

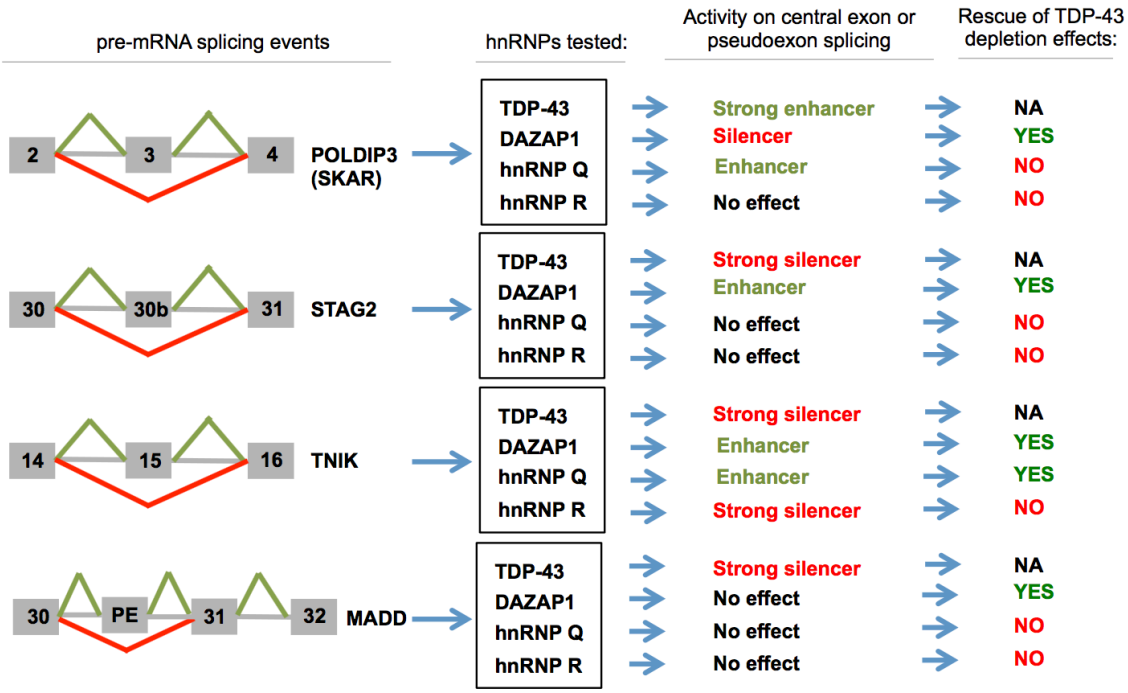

Figure 25. Schematic diagram of TDP-43, DAZAP1, hnRNPQ and hnRNPR activity on RNA splicing of *POPLDIP3, STAG2, TNIK* and *MADD* gene. Exon inclusion and exon exclusion are highlighted in green and red, respectively. The colours also indicate the relative effects (enhancer or silencer activity) of each hnRNP on the target genes. Moreover, the figure reports the rescue of TDP-43 depletion together with silencing of each hnRNP.

The second important event that we decided to test was the effect of these hnRNPs on gene expression levels of the TDP-43-controlled genes, previously published in our laboratory. Once again, we treated SH-SY5Y cells with siRNA against TDP-43 and each hnRNP of interest and then we analysed the expression of *MADD* and *BRD8* genes, since their expression was found to be altered in HEK293 cells depleted for TDP-43 (De Conti et al., 2015). We also included the evaluation of *TNIK* gene expression levels as a control. As shown in Figure 26A-C, a significant reduction of *MADD* gene expression levels was associated with siRNA depletion of TDP-43, and a slight but significant reduction of *TNIK* gene expression levels was observed after siRNA depletion of hnRNPQ, suggesting that

the other hnRNPs were not able to modify the expression of these TDP-43 targets. Afterwards, the co-silencing effects of TDP-43 and DAZAP1, hnRNP Q or hnRNP R on the gene expression were tested. Apparently, only the simultaneous depletion of TDP-43 and DAZAP1 was able to rescue the reduction of *MADD* gene expression levels and induce a significant increment of *BRD8* gene expression levels (Figure 26D). No statistically significant effect was detected for *TNIK* gene expression levels (Figure 26F).

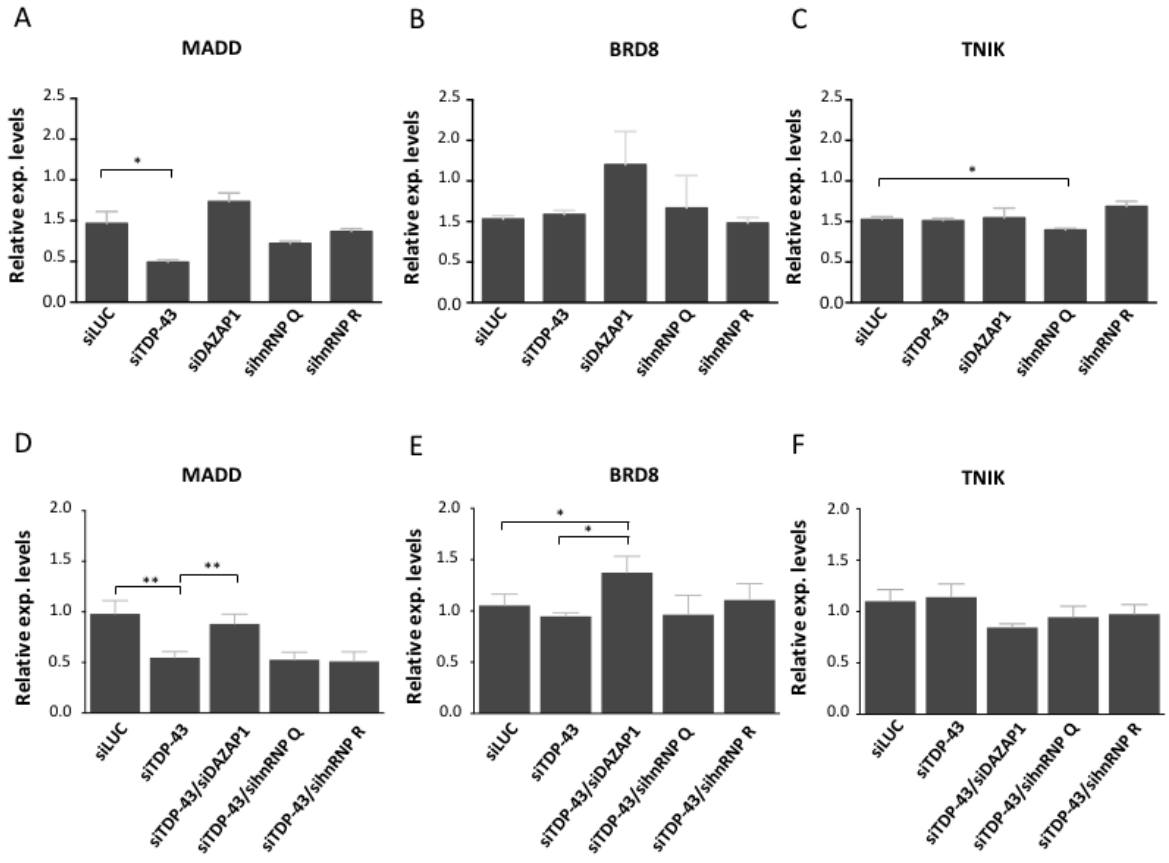

Figure 26. Effects of DAZAP1 and hnRNP Q/R depletion in the absence (A-C) or in the presence (D-F) of TDP-43 co-silencing on gene expression events controlled by TDP-43. Real-time PCR quantification analysis of *MADD* **(A, D)**, *BRD8* **(B, E)** and *TNIK* **(C, F)** endogenous transcript levels following siRNA transfection in SH-SY-5Y cells from three independent experiments. Each bar reports the mean ± standard deviation of three independent experiments. *P < 0.05, **P < 0.01 (n = 3), calculated by an unpaired t-test.

4.1.2 DAZAP1, hnRNP Q and hnRNP R do not alter TDP-43 nuclear localization

Since modifications of mRNA splicing/expression were observed in TDP-43 controlled genes after hnRNP depletion, we were also interesting in studying the localization of endogenous TDP-43, as its nucleo-cytoplasmic shuttling usually occurs after protein homeostasis alterations within the cells. For this reason, we performed immunofluorescence assays on SH-SY5Y cells treated with siRNA against each hnRNP protein of interest. As shown in Figure 27A-D, none of these treatments caused appreciable changes in TDP-43 localization, that remained mostly nuclear.

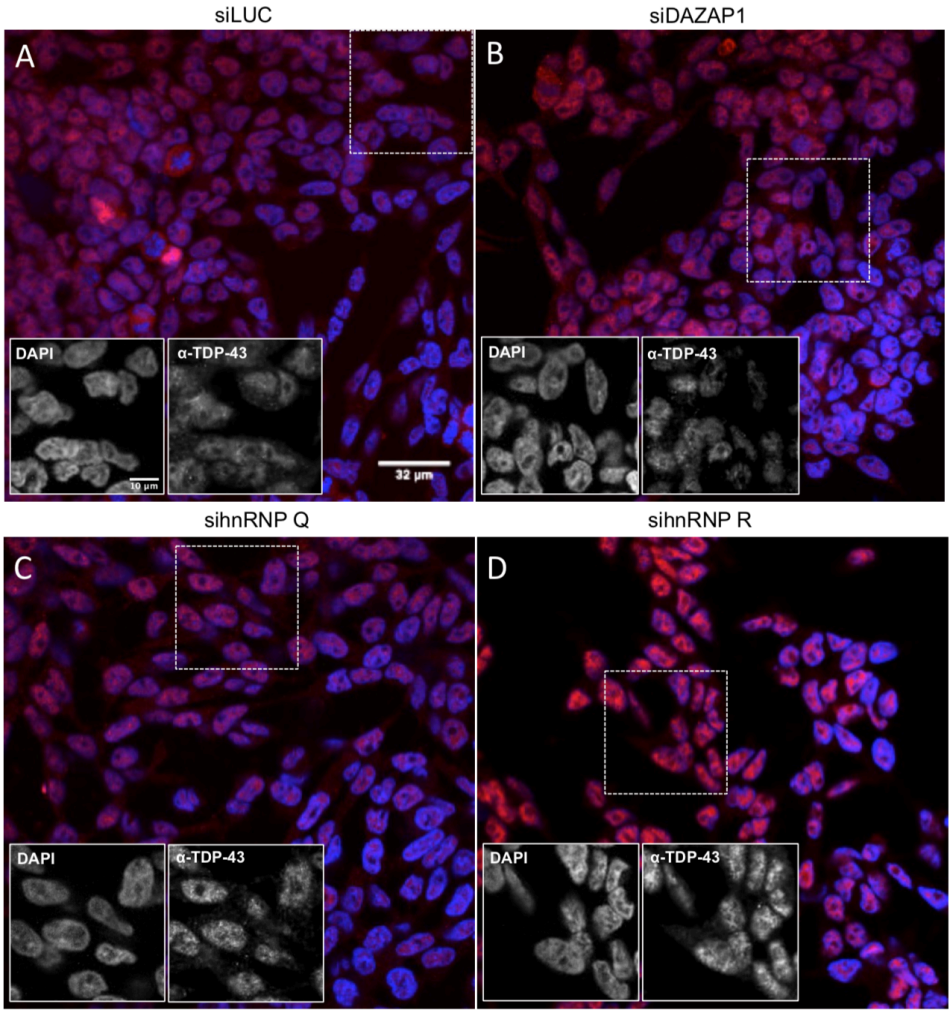

Figure 23. Localization of endogenous TDP-43 in SH-SY5Y cells. Cells were transfected with siRNA against fire-fly Luciferase (control) **(A)**, DAZAP1 **(B)**, hnRNP Q **(C)** and hnRNP R **(D)**. Cell nuclei were

visualized using DAPI staining. Scale bars: 32 μm. For each image, b/w inserts (scale bars: 10 μm) of a selected area (white dashed square) indicating DAPI (on the left) and α-TDP-43 (on the right) staining are also provided.

4.2 Cellular model of TDP-43 pathology

4.2.1 Analysis of siRNA-mediated depletion of DAZAP1, hnRNP Q and hnRNP R using a cellular model of TDP-43 loss-of-function

To examine in depth the effects of siRNA-mediated depletion of DAZAP1, hnRNP Q and hnRNP R in a context more close to the scenario of TDP-43 pathology, we have taken advantage of a cellular model of TDP-43 loss-of-function. This model is already available in our laboratory and enstablished in Flp-In HEK293 cell line. Recently, it has been described a TDP-43 aggregation system, consisting of 12 tandem repeats carrying the 331–369-residue Gln/Asn region of TDP-43 fused to FLAG-tag or green fluorescentprotein (EGFP), reproduces many features of the TDP-43 inclusions observed in patients suffering from ALS and FTLD (Budini et al., 2012, 2014) (Figure 28A). Therefore, in order to evaluate the localization of the endogenous TDP-43 in this cellular model, we used Flp-In HEK293 cells producing FLAG-TDP43-12XQ/N aggregates (upon tetracycline induction) to perform immunofluorescence assays, after DAZAP1, hnRNP Q and hnRNP R knockdown. Despite it is difficult to quantify the amount of TDP-43 aggregation, the results obtained in this experiment show that the endogenous TDP-43 seems to co-localize with the inducible aggregates, and remains mostly nuclear either in the presence or absence of siRNA treatment (Figure 28). Therefore, the depletion of DAZAP1, hnRNP Q and hnRNP R appears not able to affect the aggregation propency of TDP-43, suggesting why, at the present, there is no evidence of the presence of these hnRNPs in the TDP-43 inclusions of ALS and FTLD patients.

Nonetheless, the silencing of both DAZAP1 and hnRNP Q seems to restore *POLDIP3* exon 3 inclusion (Figure 28C, left panel) and *STAG2* exon 30b skipping (Figure 28C, right panel) induced by the formation of the aggregates, as previously observed in the RNA splicing experiments performed in the SH-SY5Y cells.

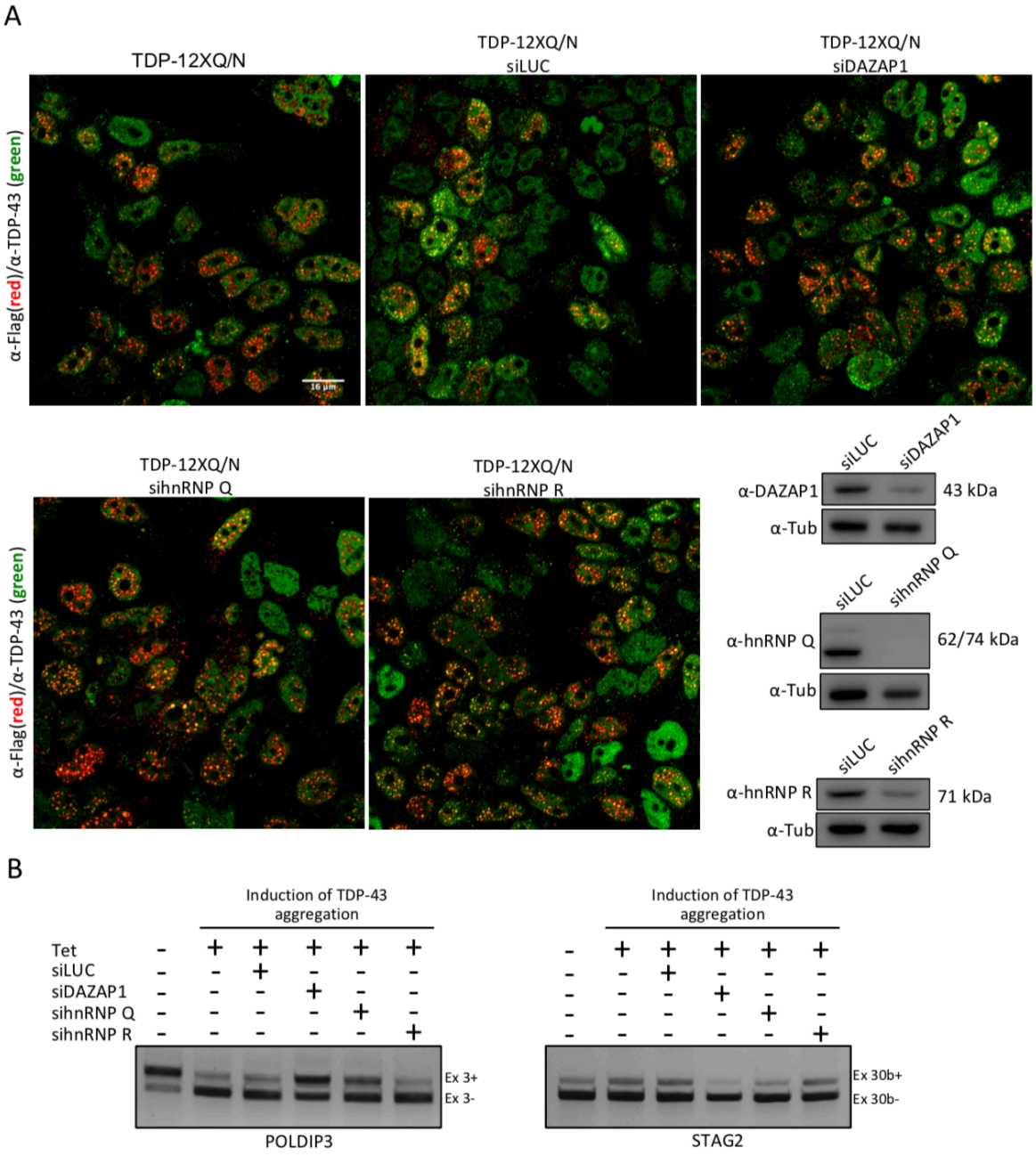

Figure 24. Effects of hnRNP silencing in Flp-In HEK293 cells expressing FLAG-TDP43-12XQ/N aggregates. (A) Schematic representation of TDP-43 12XQ/N. **(B)** Immunofluorescence analysis showing the localization of endogenous (green) and aggregated (red) TDP-43 in the absence of hnRNP silencing (TDP-12XQ/N) and in the presence of siRNA against fire-fly Luciferase (siLUC, control), DAZAP1, hnRNP

Q and hnRNP R. Co-localization of endogenous TDP-43 with 12XQ/N aggregates is observed as yellow dots. Scale bars: 16 μm. Western Blot for checking hnRNP silencing is also reported. **(C)** RT-PCR of *POLDIP3* and *STAG2* genes in the presence of TDP-12XQ/N aggregates (lane 1, Tet) and silencing of siLUC (lane 2, control), siDAZAP1 (lane 3), sihnRNP Q (lane 4) and sinhRNP R (lane 5). Splicing analysis of *POLDIP3* and *STAG2* genes were performed in collaboration with Dr. Fatemeh Mohagheghi.

4.3 Characterization of TDP-43 and DAZAP1 interaction

4.3.1 DAZAP1 does not bind to TDP-43 but can bind in vivo to TDP-43 controlled mRNAs

Another possible connection between TDP-43 and hnRNP proteins able to explain the results obtained until now could be represented by their ability to bind TDP-43 and directly affect its functional properties. To this regard, proteomic studies on TDP-43 have confirmed the presence of hnRNP Q and hnRNP R in complexes that contain TDP-43 (Blokhuis et al., 2016; S. Ling et al., 2010), but no previous studies have uncovered a possible interaction between TDP-43 and DAZAP1. Therefore, we examined this interesting aspect by transfecting HeLa cells with flagged-TDP-43 and testing the presence of DAZAP1 by a co-immunoprecipitation (Co-IP) assay. This experiment shows that TDP-43 and DAZAP1 do not seem to co-IP together (Figure 29A).

Considering that data, we tested if DAZAP1 could be capable of binding to TDP-43 mRNA targets analysed in Figure 23, 24 and 26. To do this, we performed an RNA-immunoprecipitation (RNA-IP) assay by transfecting HeLa cells with flagged-DAZAP1, immunoprecipitating the RNA bound to DAZAP1 and testing by RT-qPCR the binding of DAZAP1 to *BRD8*, *TNIK, STAG2, POLDIP3* and *MADD* transcripts. As shown in Figure 29B, all these transcripts were enriched after RNA-IP analysis, although BRD8 and TNIK in smaller amount. This could be dependent on their lower abundance in HeLa cells and/or

it could be associated with their weaker/ unstabler interaction with TDP-43 than the other tested transcripts. *GAPDH* and *SDHA* were also tested as controls.

Importantly, in both the experiments of immunoprecipitation we decided to take advantage of HeLa cells instead of using SH-SY5Y cells in order to maximize the transfection efficiency with plasmid DNA.

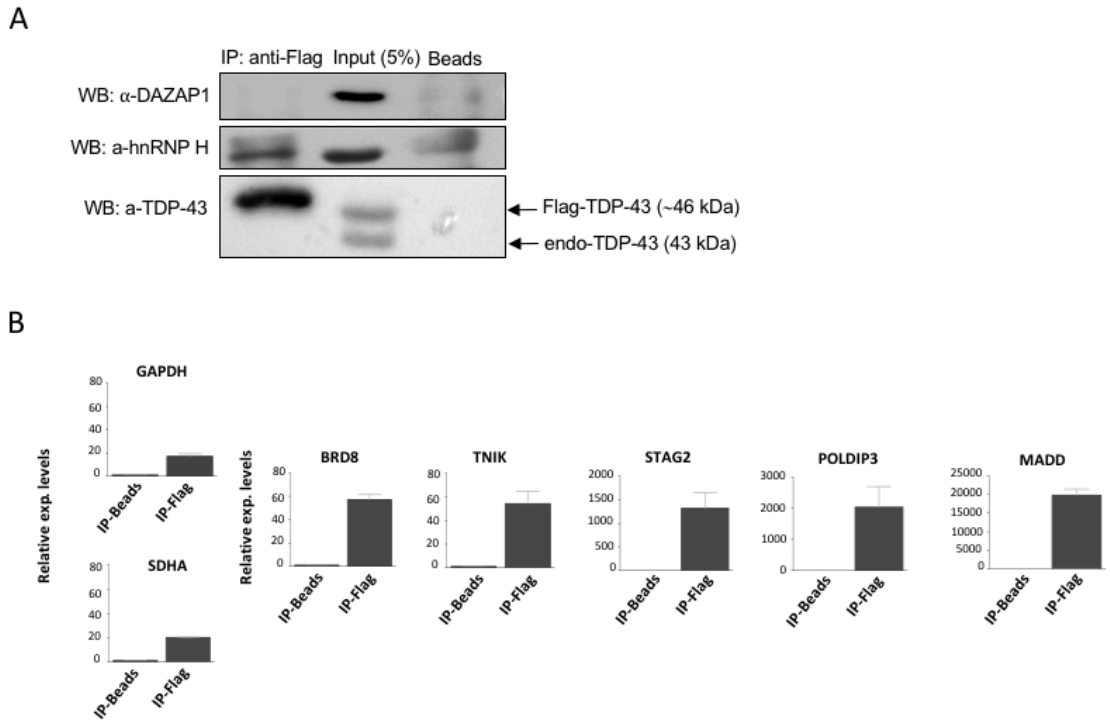

Figure 25. Probing the DAZAP1 - TDP-43 interaction. (A) Co-immunoprecipitation experiment was performed by overexpressing FLAG-TDP-43 in HeLa cells and the immunoprecipitation was checked by Western Blot against DAZAP1 (upper panel). The presence of hnRNP H1 in the immunoprecipitated sample was used as a positive control (middle panel). The lower panel shows the levels of flagged and endogenous TDP-43 in the Input and immunoprecipitated sample. **(B)** RNA immunoprecipitation experiments (n=3) to monitor for DAZAP1 binding to *BRD8, TNIK, STAG2, POLDIP3, MADD* transcripts and also two housekeeping genes, *GAPDH* and *SDHA* (used as controls). RNA immunoprecipitation was performed in collaboration with Dr. Fatemeh Mohagheghi.

4.3.2 TDP-43 and DAZAP1 can alter the expression of neuronal related mRNAs in SH-SY5Y cells

Based on the results obtained from mRNA analysis of TDP-43 targets, in order to determine the wide effects of the hnRNPs of interest, we decided to obtain the whole transcriptome status of SH-SY5Y cells depleted by TDP-43, DAZAP1, hnRNP Q or hnRNP R.

In this regard, because DAZAP1 seems to be the best modifier of the TDP-43 controlled events, we initially focused the attention on the RNA-seq data achieved following silencing of DAZAP1 and TDP-43. Three independent experiments were performed.

Notably, prior to the differential expression analysis, weak expression features with counts-per-million value (CPM) of less than one were excluded from the analysis, resulting in the removal of 47622 of the 64769 features initially generated by RNA-seq analysis. Therefore, a total of 17147 final features underwent to differential expression analysis. The putative differentially expressed genes (DEGs) were identified using a fold change (FC) cut-off of 30% with respect to a control sample treated with siRNA against fire-fly luciferase (siLUC) (upregulation cut-off: >1.3; downregulation cut-off: <0.7-FC).

Among the total 17147 genes analysed, 3533 genes were differentially expressed in siTDP-43 treated cells, in comparison to siLUC treated cells. Of these 3533 genes, 1173 (33%) genes were downregulated and 2360 (67%) genes were upregulated.

In the same way, we analysed the results obtained from cells silenced for DAZAP1 and we found that among the total 17147 genes analysed, 7571 genes resulted to be differentially expressed in siDAZAP1 treated cells in comparison to siLUC treated cells. Of these 7571 genes, 3244 (43%) genes were downregulated and 4327 (57%) genes were upregulated. Interestingly, enough 1924 genes of the differentially expressed genes in siTDP-43 and siDAZAP1 treated cells were commonly regulated (Figure 30A).

To validate the RNA-seq data, we selected 10 genes belonging to the top 100 differentially expressed genes by siTDP-43 and siDAZAP1 treatment, based on their involvement in neuron development and brain inflammation (Figure 30B). The fold changes obtained from RT-qPCR were compared with RNA-seq expression analysis results (Figure 30C). *CUGBP Elav-like Family Member 5* (*CELF5*), *Syntaxin 3* (*STX3*), *Acetylcholinesterase* (*ACHE)*, *Tumor Necrosis Factor* (*TNF*), *Tumor Necrosis Factor Receptor Superfamily, Member 9* (*TNFRSF9*), *Intercellular Adhesion Molecule 1* (*ICAM1*) and *Yippee-like 4* (*YPEL4*), were prominently found to be upregulated both by siDAZAP1 treatment and by siTDP-43 treatment. *ELAV like Neuron-Specific RNA binding protein 3* (*ELAVL3*) and *Neuron-Oncological Ventral Antigen 2* (*NOVA2*) were found to be downregulated in both siTDP-43 and siDAZAP1 treatment, whereas *Reelin* (*RELN*) was found to be downregulated only in siDAZAP1 treated cells and was chosen as a neutral gene (for TDP-43 treated cells) and it was also confirmed by qPCR validation. RNA-seq analysis for both TDP-43 and DAZAP1 was also represented by volcano plot and MAPlot (Figure 31 and 32, respectively), in which $P < 0.05$ was used as a statistical hypothesis test. In both graphs, differentially expressed genes (DEGs) are highlighted in red (downregulated) and in green (upregulated) based on the Pvalue and the cut-off of 30% variation with respect to the control treated cells (siLUC). For both siTDP-43 and siDAZAP1 treated cells in the volcano plot is reported the position of the DEGs validated by using qPCR, whereas the position of *TARDBP* and *DAZAP1* genes is reported in TDP-43-related MAPlot and DAZAP1-related MAPlot, respectively.

Furthermore, we performed a pathway analysis using PANTHER Pathway and DAVID annotations to investigate functional associations of gene expression changes and pathways in which differentially expressed genes were involved and enriched. As shown in Figure 30D 51% of 433 pathways identified in siTDP-43 treated cells and 57% of 889 pathways

identified in siDAZAP1 treated cells were related to brain function and neurodegeneration. Interestingly, the greater amount of common differentially regulated genes is related to inflammation (Figure 33B), suggesting an important role of this pathway in the presence of hnRNP dis-regulation.

Finally, we also looked at the Gene ontology (GO) functional enrichment analysis using the UniProt-KB Retrieve/ID mapping tool (Figure 33A). This analysis showed that siTDP-43 and siDAZAP1-treated cells share a similar amount of differentially expressed genes in the subgroups of "Biological process" and "Molecular function" categories. For both TDP-43 and DAZAP1, the "molecular function" category of GO terms associated with regulated transcripts includes a large percentage of "transcription factor activity, transcription factor binding, nucleic acid binding transcription factor activity, signal transducer activity, transporter activity, molecular function regulator and receptor activity". On the other hand, in the "biological process" category, a similar percentage in genes involved in "cellular process, biological regulation, single-organism process and metabolic processes" groups were notably represented for both siTDP-43 and siDAZAP1.

A

Total genes analyzed	17147	Total genes analyzed	17147
Downregulated (<0.7 vs siLuc):		**Upregulated (>1.3 vs siLuc):**	
siTDP-43	1173	siTDP-43	2360
siDAZAP1	3244	siDAZAP1	4327
siTDP-43/siDAZAP1 common	489	siTDP-43/siDAZAP1 common	1435

B

ENSEMBL	Gene Symbol	Description	RNAseq	
			siTDP-43	siDAZAP1
ENSG00000196361	ELAVL3	ELAV like neuron-specific RNA binding protein 3	0.28	0.93
ENSG00000104967	NOVA2	Neuro-oncological ventral antigen 2	0.38	0.67
ENSG00000189056	RELN	Reelin	1.06	0.47
ENSG00000166900	CELF5	CELF5, CUGBP, Elav-like family member 5	4.59	12.21
ENSG00000087085	STX3	Syntaxin 3	5.49	16.06
ENSG00000232810	ACHE	Acetylcholinesterase	5.63	25.06
ENSG00000049249	TNF	Tumor necrosis factor	20.54	11.18
ENSG00000090339	TNFRSF9	Tumor necrosis factor receptor superfamily, member 9	35.97	10.11
ENSG00000161082	ICAM1	Intercellular adhesion molecule 1	50.03	14.55
ENSG00000166793	YPEL4	YPEL4, yippee-like 4 (Drosophila)	81.11	227.01

C

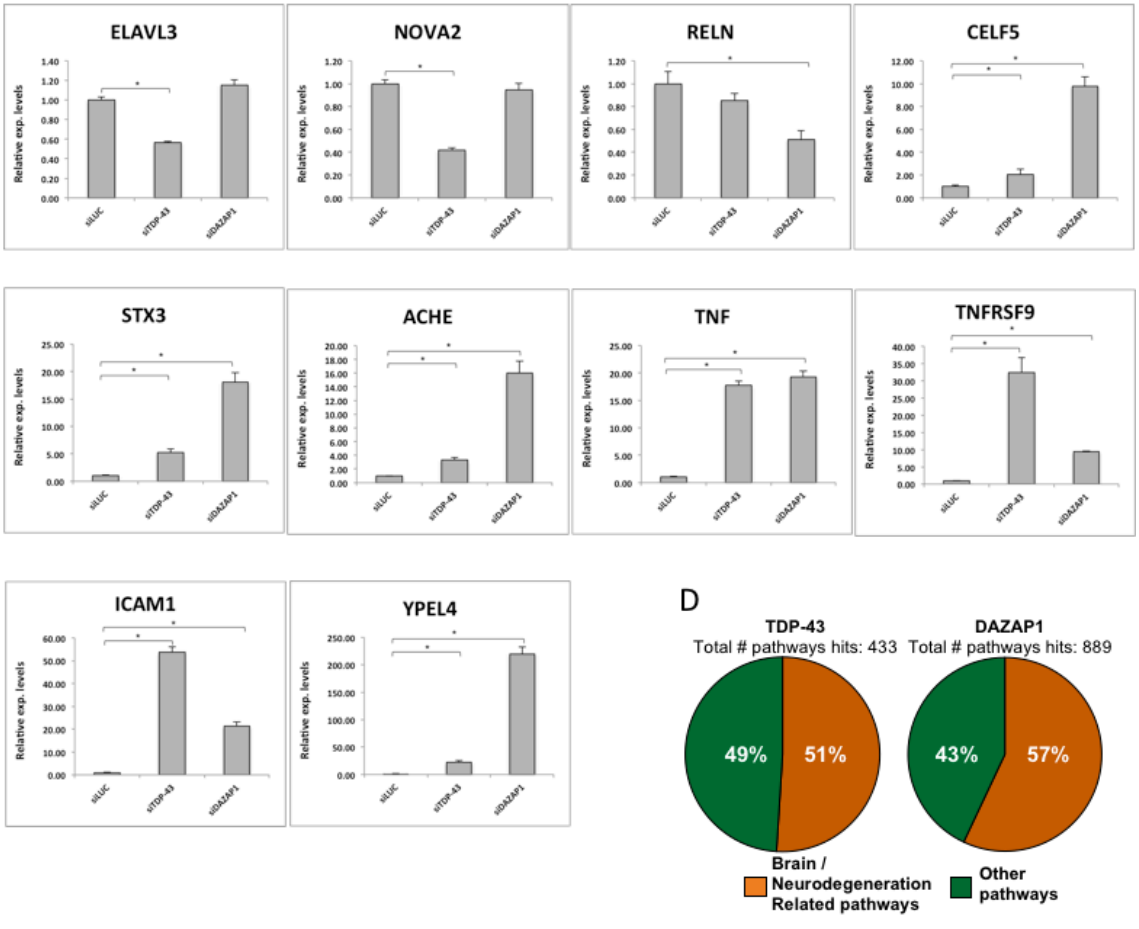

D

Figure 26. Validation of the TDP-43 or DAZAP1 silencing and comparison between RNA-seq and qRT-PCR results. (A) Summary of downregulated (<0.7× versus siLUC) and upregulated (>1.3× versus siLUC) genes after siTDP-43 or siDAZAP1 treatments. The number of common (between siTDP- 43 and siDAZAP1) downregulated and upregulated genes is also shown. **(B)** List of genes associated with brain functions (*ELAV3, NOVA2, RELN, STX3, ACHE, YPEL4, CELF5*) or inflammation (*TNF, TNFRSF9, ICAM1*) selected for validation of the RNA-seq analysis. The expression levels of genes following siTDP-43

or siDAZAP1 treatments versus the control condition (siLUC) is indicated. **(C)** Validation of RNA-seq by real time PCR of the ten selected transcripts. The results are represented as relative expression compared with the control (siLUC). Each bar reports the mean ± standard deviation of three independent experiments. The single asterisks indicate significant differences (P< 0.05) between the indicated measurements. **(D)** Pathways analysis of differentially expressed genes following TDP-43 and DAZAP1 depletion as determined by PANTHER, DAVID and UniProt analyses.

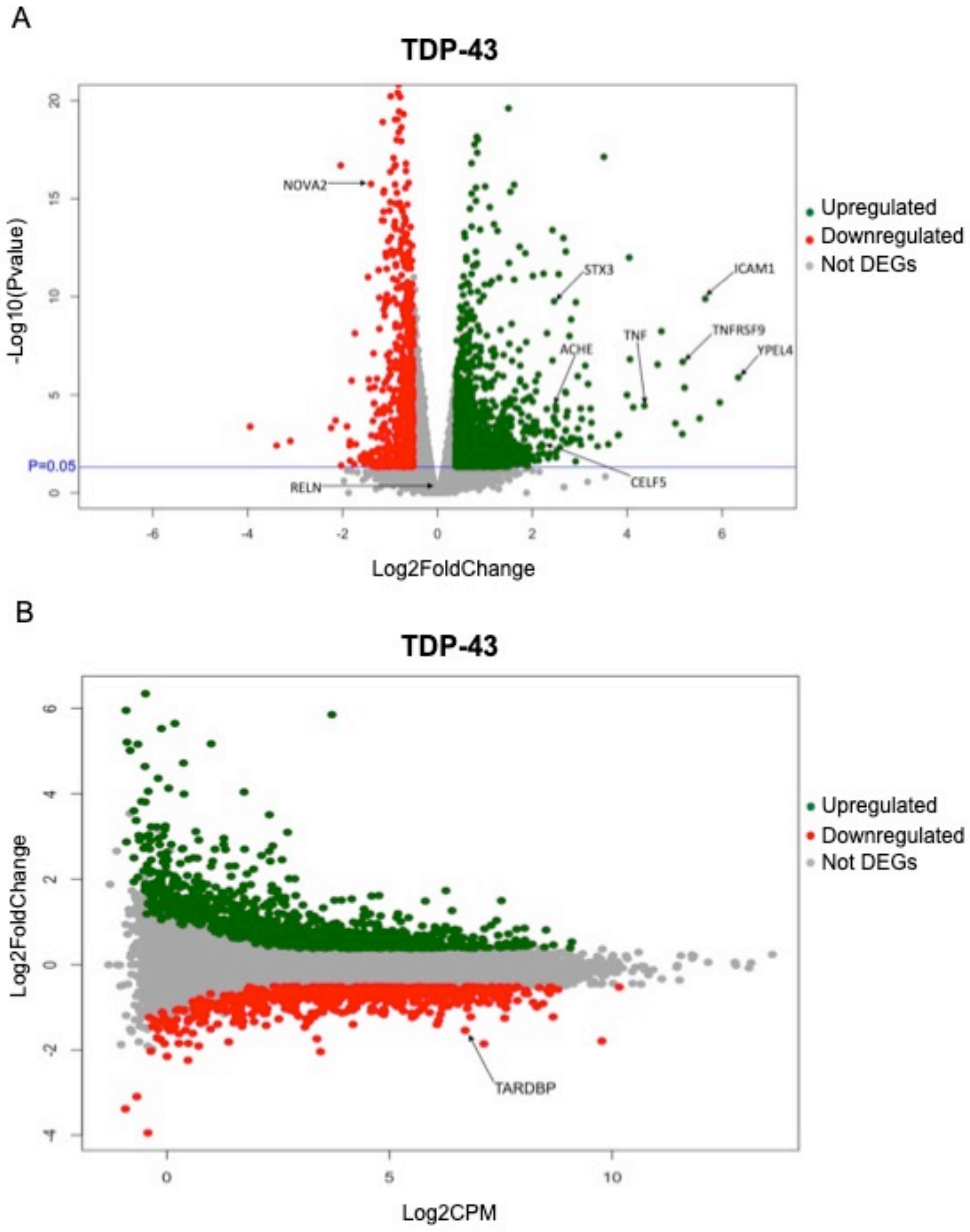

Figure 27. Graphic representation of RNA-seq analysis performed on SH-SY5Y cells depleted for TDP-43. (A) Volcano plot reports in x-axis the magnitude (Log2FoldChange) and in y-axis the significance (–log10(Pvalue)) of siLUC versus siTDP-43 treated cells. Upregulated and downregulated genes are highlighted in green and red, respectively, and validated genes are signalled by arrows. The horizontal blue line signals statistical significance threshold (P= 0.05). **(B)** MAPlot reports in x-axis the normalized library

size (Log2CPM, *counts per million*) and in y-axis the magnitude (Log2FoldChange) of siLUC versus siTDP-43 treated cells. Upregulated and downregulated genes are highlighted in green and red, respectively. The position of *TARDBP* gene (encoding TDP-43 protein) is highlighted by an arrow.

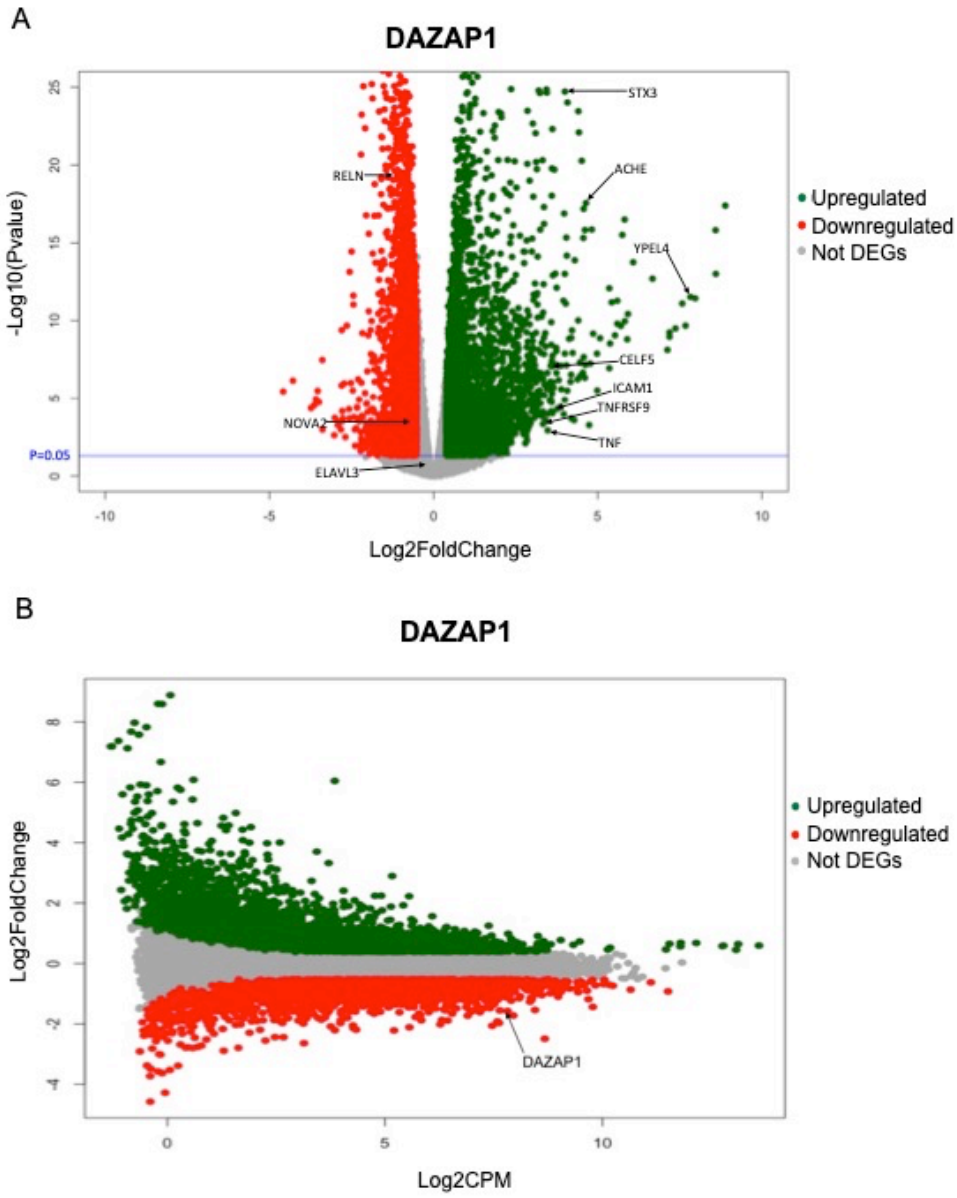

Figure 28. Graphic representation of RNA-seq analysis performed on SH-SY5Y cells depleted for DAZAP1. (A) Volcano plot reports in x-axis the magnitude (Log2FoldChange) and in y-axis the significance (–log10(Pvalue)) of siLUC versus siDAZAP1 treated cells. Upregulated and downregulated genes are highlighted in green and red, respectively, and validated genes are signalled by arrows. The horizontal blue line signals statistical significance threshold (P= 0.05). **(B)** MAPlot reports in x-axis the normalized library size (Log2CPM, *counts per million*) and in y-axis the magnitude (Log2FoldChange) of siLUC versus siDAZAP1 treated cells. Upregulated and downregulated genes are highlighted in green and red, respectively. The position of *DAZAP1* gene (encoding DAZAP1 protein) is highlighted by an arrow.

A

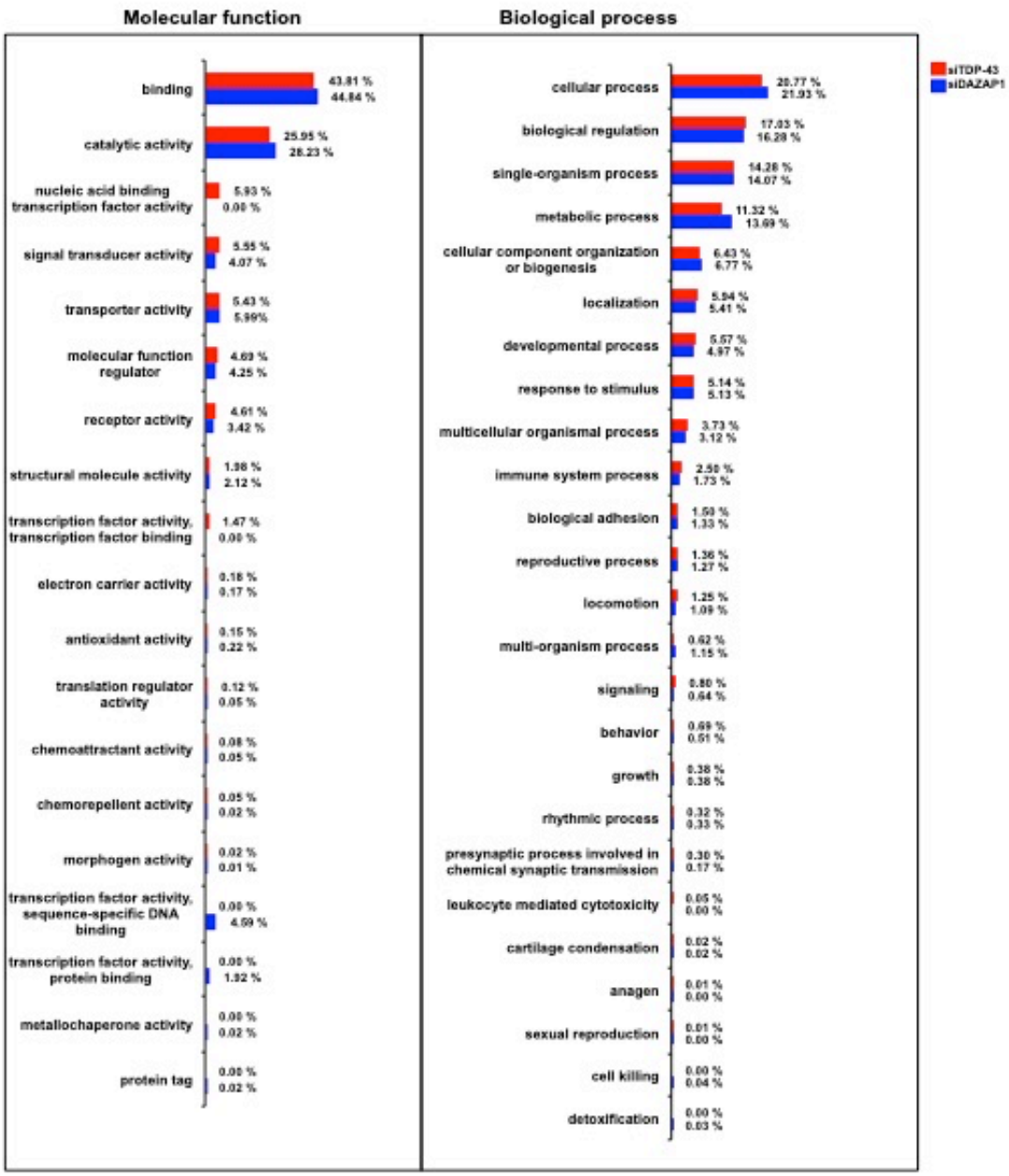

B

Pathway enrichment of common Downregulated genes (<0.7 vs siLuc)

	Total # mapped genes: 309	Total # pathways hits: 165
Genes related with:		%
Inflammation	48	29.1
Neurodegenerative diseases	12	7.3
Nervous system	29	17.6

Pathway enrichment of common Upregulated genes (>1.3 vs siLuc)

	Total # mapped genes: 918	Total # pathways hits: 337
Genes related with:		%
Inflammation	95	28.2
Neurodegenerative diseases	40	11.9
Nervous system	35	10.4

Figure 29. GO functional enrichment analysis of the genes significantly co-regulated by TDP-43 and DAZAP1. (A) For TDP-43, 2269 out of 3535 (1173 downregulated <0.7 and 2360 upregulated >1.3 vs. siLUC) Ensembl identifiers were successfully mapped to 8481 UniProtKB IDs. For DAZAP1, 5137 out of

7571 (3244 downregulated <0.7 and 4327 upregulated>1.3 vs. siLUC) Ensembl identifiers were successfully mapped to 19541 UniProtKB IDs. The clustered columns charts show the percentage of the successfully mapped Ensembl IDs. **(B)** Pathway analysis of the differentially expressed genes common between siTDP-43 and siDAZAP1 depletions, as determined by PANTHER analysis.

4.4 Characterization of hnRNP Q and hnRNP R

4.4.1 Analysis of protein sequence identity and similarity

To further refine the characterization of the hnRNPs in this study, we decided to extend our investigation to hnRNP Q and hnRNP R, in particular because they share similar protein sequence (Zissimos Mourelatos et al., 2001) and because in lower organisms, such as *Drosophila melanogaster* (McDermott et al., 2012) and *Caenorhabditis elegans* (Kabat et al., 2009), they were found in one well conserved ortholog, suggesting the occurrence of a progressive functional divergence during the evolution.

Concerning this aspect, we decided to compare the protein sequence of the major splicing isoforms of each human counterpart with their *D. melanogaster* ortholog (Table 21). To this aim, we used EMBOSS needle (https://www.ebi.ac.uk/Tools/psa/emboss_needle/) and we calculated the percentage of identity and similarity of human hnRNP Q1, hnRNP Q2, hnRNP Q3, hnRNP R1 and hnRNP R2 with respect to the *Drosophila* variant CG17838 (isoform F)/Syp (Figure 34), that we previously used in our TBPH loss- and gain-of-function model and it has been well-described in larvae, pupae, and in all adult tissues (McDermott et al., 2012). The obtained results confirmed the high level of homology of each human splicing variant compared to the *Drosophila* one.

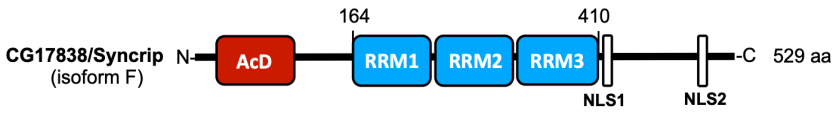

Figure 30. Structure of *Drosophila melanogaster* CG17838 (isoform F)/Syp variant. This variant contains a conserved AcD, three RRMs (RRM1, RRM2 and RRM3) and two NLS. Each domain is highlighted in colored boxes and the relative sequence position and amino acids length is also reported.

Table 21. Percentage of identity and similarity of human hnRNP Q and hnRNP R with respect to *Drosophila* CG17838 (isoform F)/Syp variant.

Isoform	**% identity**	**% similarity**
hnRNP Q1	47.1	59.6
hnRNP Q2	42.9	53.1
hnRNP Q3	45.9	57.1
hnRNP R1	46.0	58.2
hnRNP R2	43.0	53.8

4.4.2 Subcellular localization of hnRNP Q and hnRNP R in SH-SY5Y cells

In order to investigate the reasons underlying a possible functional divergence between hnRNP Q and hnRNP R, we initially decided to look at their subcellular distribution in SH-SY5Y cells through an immunofluorescence analysis. As shown in Figure 35, hnRNP Q was spread amongst cytoplasm and nucleus, while hnRNP R seemed to be mostly nuclear.

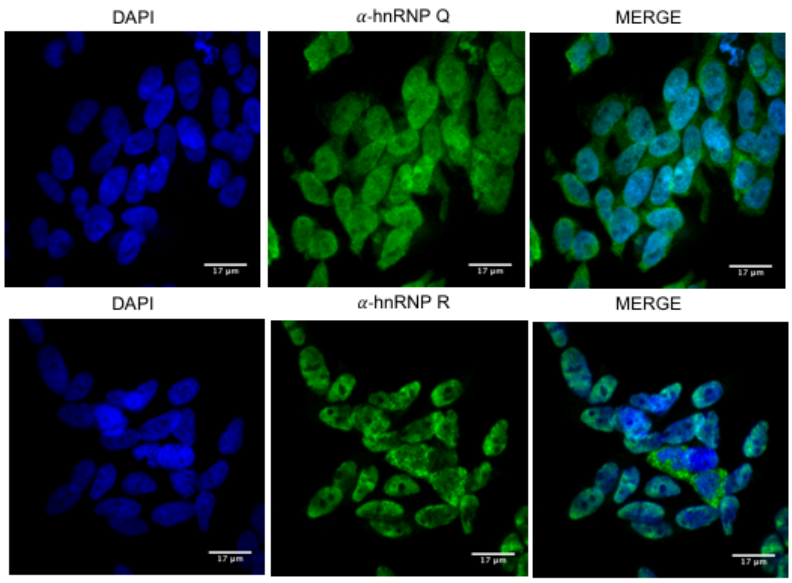

Figure 31. Cellular localization of endogenous hnRNP Q and hnRNP R in SH-SY5Y cells. Immunofluorescence analysis of the endogenous hnRNP Q and hnRNP R (shown in green) in SH-SY5Y cells. Nuclei were visualized using DAPI staining. Scale bars: 17 µm.

These results were also confirmed by nuclear cytoplasmic fractionation, as reported in Figure 36. Regarding hnRNP Q, three major splicing isoforms have been so far previously reported (Mourelatos et al. 2001). These isoforms are characterized by the presence of two NLS in the hnRNP Q3 and hnRNP Q2 variants (with a molecular weight of 70 kDa and 65 kDa, respectively) and one NLS in the hnRNP Q1 (with a molecular weight of 62 kDa). Our experiments detected three immunoreactive bands (~ 58 kDa, ~66 kDa and ~ 75 kDa), differentially distributed between nucleus and cytosol (Figure 36A). The molecular weight of ~ 75 kDa was consistent with that of hnRNP Q2/hnRNP Q3 isoforms and the molecular weight of ~ 66k Da with that of hnRNP Q1 isoform. The lower band (~58 kDa) cannot be associated to any known hnRNP Q isoform and could correspond to a further variant that still remains to be characterized, or non-specific cross-reaction. This observation could be explained by the fact that the latter variant gives a weak signal and is therefore not always

detectable. For this, it was not detected in our previous Western Blot analysis (Figure 22, 28A).

The same analysis was repeated for hnRNP R, confirming its presence predominantly in the nuclear fraction (Figure 36B). The antibody used for staining the membrane (ab30930) detected three bands: ~71 kDa, ~75 kDa and ~80 kDa. In the first set of Western Blot experiments performed using hnRNP R antibody (Figure 22, 28A), we only reported the band corresponding to the predicted molecular size described in the datasheet provided by the company. Due to the fact that the literature regarding different hnRNP R isoforms (and consequently variable size of this protein) is still incomplete, in the second part of the current project, we decided to additionaly consider the other two hnRNP isoforms recognized by the same antibody. These two isoforms were not taken into account in the first part of the experiments, since they were not in agreement with the predicted size reported by the antibody producer.

Therefore, according to the literature, we assigned the higher molecular weight band (~ 80 KDa) to the major hnRNPR isoform, also known as R1 (NP_005817.1. NM_005826.4. [O43390-1]); and the second higher band (~75 kDa) to the more neuronal variant, namely R2 (NP_001284549.1, NM_001297620.1 [O43390-3]). On the other hand, we supposed that the lower band of ~71 kDa was associated with another splicing variant of hnRNP R that still needs to be characterized.

Overall, the different localization of hnRNP Q and hnRNP R suggested that their nuclear-cytoplasmic distribution is differentially regulated and this could result in a differential control of the regulated cellular pathways.

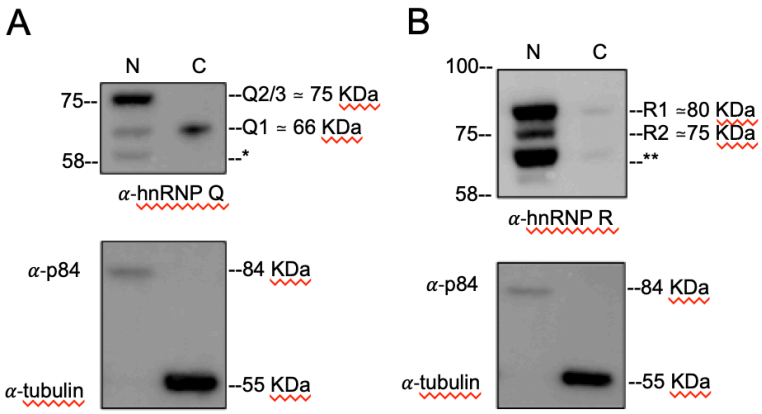

Figure 32. Nuclear and cytoplasmic fractions of endogenous human hnRNP Q and human hnRNP R. **(A)** Western blot analysis of hnRNP Q franctions. The asterisk (*) indicates possible splicing variant of hnRNP Q. **(B)** Western blot analysis of hnRNP R franctions. Double asterisk (**) indicates possible alternative splicing variant of hnRNP R. In both of analysis α-p84 and α-tubulin were used as controls for nuclear and cytoplasmic fractions, respectively.

4.4.3 Subcellular localization of hnRNP Q and hnRNP R is not altered by their reciprocal silencing

Because of the close relationship between these two factors, we decided to investigate if the silencing of hnRNP Q was able to affect the gene expression and cellular localization of hnRNP R and *vice-versa* (Figure 37). We observed no significant differences in the mRNA levels, as well as in the endogenous localization of hnRNP Q after siRNA treatment against hnRNP R and of hnRNP R after siRNA treatment against hnRNP Q.

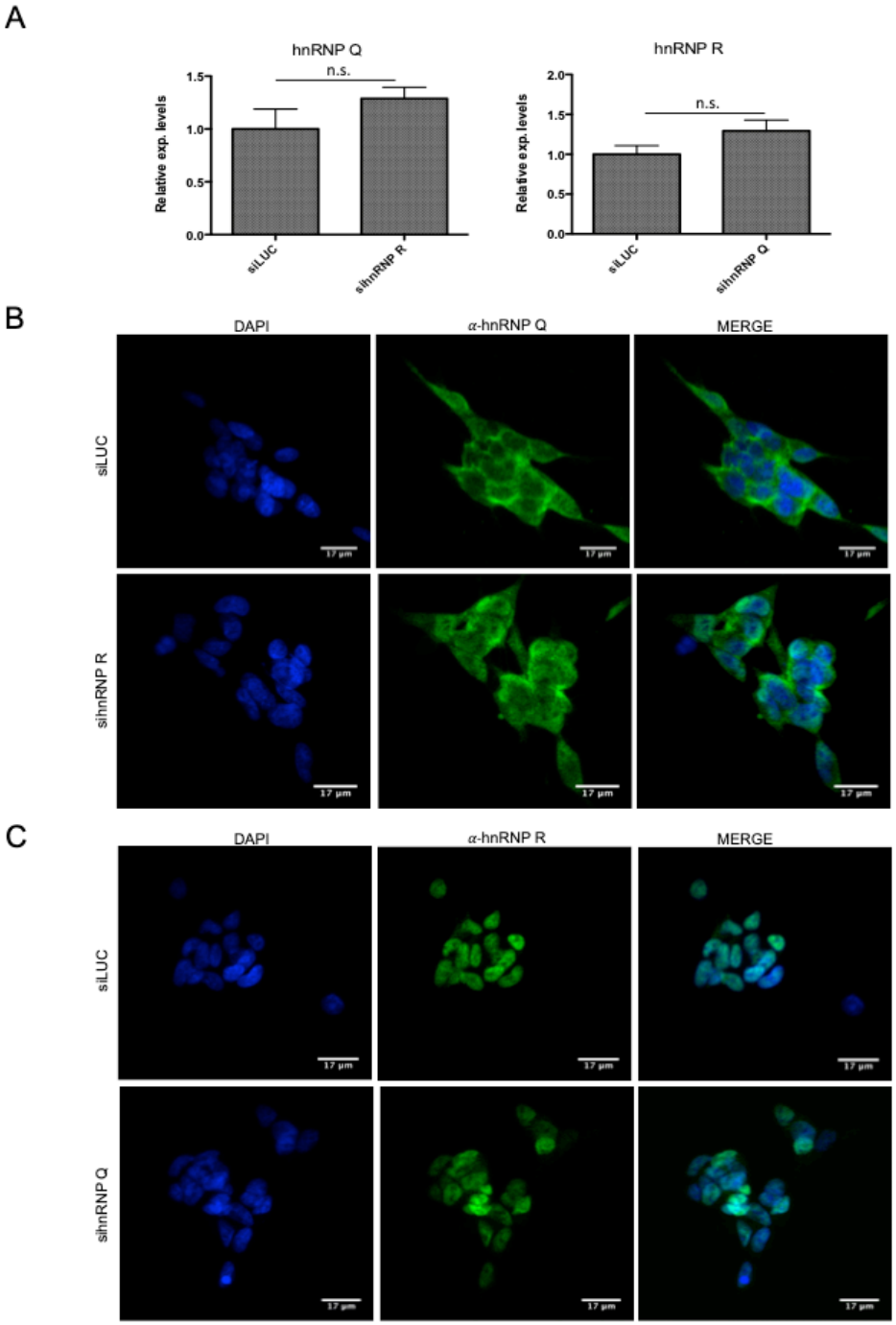

Figure 33. mRNA levels and cellular localization of endogenous hnRNP Q and hnRNP R after siRNA treatment in SH-SY5Y cells. (A) Relative expression of hnRNP Q after siRNA against hnRNP R (sihnRNP R) and *vice-versa.* All the samples were compared to siLUC treated cells. Each bar reports mean ± standard error (n=3). Statistical differences were evaluated using Student's *t*-test (*** P<0.001). **(B)** Immunofluorescence analysis of the endogenous human hnRNP Q and hnRNP R (shown in green) in SH-SY5Y cells after sihnRNP R and sihnRNP Q, respectively. Nuclei were visualized using DAPI staining. Scale bars: 17 μm.

4.4.4 Subcellular localization of hnRNP Q and hnRNP R is not altered by retinoic acid (RA)-induced neuronal differentiation in NSC-34 cells

It is well-known that the activation of specific signaling pathways leading to cellular differentiation can be differently regulated depending on the subcellular localization of specific controlling factors (Robinow and White, 1991). It is also known that both hnRNP Q and hnRNP R can regulate neuronal pathways during development (Chen et al., 2012; McDermott et al., 2012, 2014).

Therefore, we tested if hnRNP Q or hnRNP R might change their cellular localization under neuronal differentiation. To this aim, immunofluorescence experiments were carried out after inducing differentiation up to 5 days with RA at 1 μM (Figure 38A) of the murine motor neuron-like NSC-34 cell line. Considering the high conservation of hnRNP Q and hnRNP R in mouse (more than 99% identity and similarity), we decided to use this cell line due to its ability to differentiate in neuron-like cells better and faster than the SH-SY5Y neuroblastoma cells.

The results indicated that the differentiation did not affect the subcellular distribution of both hnRNP Q and hnRNP R (Figure 38B).

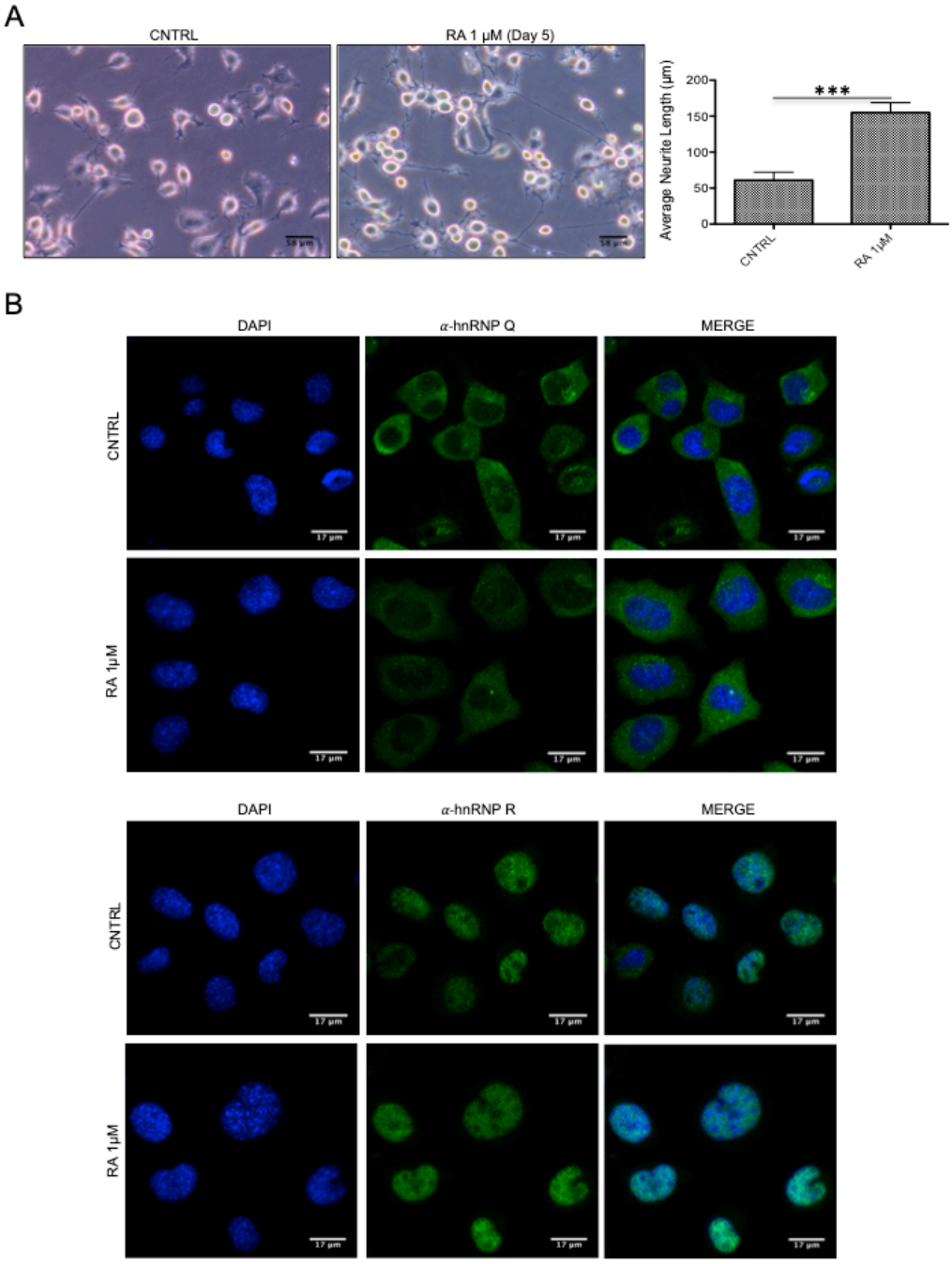

Figure 34. Endogenous localization of hnRNP Q and hnRNP R is not affected by differentiation with 1 µM of RA in NSC-34 cells. (A) Light microscopy images of undifferentiated (CNTRL) and differentiated cells treated up to 5 days with medium containing 1 µM RA. Scale bars: 58 µm, 20X magnification. Neurite length comparison (grey bars) of CNTRL and RA is also reported as mean ± standard error (n=5). Statistical differences were evaluated using Student's *t*-test (* P<0.001). **(B)** Immunofluorescence analysis of the endogenous mouse hnRNP Q and hnRNP R (shown in green) in NSC-34 cells with or without 1 µM RA treatment. Nuclei were visualized using DAPI staining. Scale bars: 17 µm.

4.4.5 Depletion of hnRNP Q and hnRNP R alters neuronal-related genes

To define functional characteristics of human hnRNP Q and hnRNP R within cells, we decided to perform gene expression profiling of SH-SY5Y silenced for these hnRNPs.

First of all, we demonstrated the reduction of mRNA levels of hnRNP Q and hnRNP R using qPCR after their knockdown (Figure 39A-40A).

Then, we performed an RNA-seq analysis by comparing data obtained from sihnRNP Q or sihnRNP R treated cells, relative to siLUC control samples. Three independent experiments were performed.

As described for RNA-seq analysis of DAZAP1 and TDP-43, prior to the differential expression analysis, weak expression features with counts-per-million value (CPM) of less than one were excluded from the analysis, resulting in the removal of 47622 of the 64769 features initially generated by RNA-seq analysis. Therefore, a total of 17147 final features underwent to differential expression analysis. Up- and downregulated genes were identified applying a FC cut-off of 30% with respect to control siLUC samples (upregulation cut-off: >1.3; downregulation cut-off: <0.7-FC) and the P value < 0.05. Regarding sihnRNP Q, the total numer of DEGs was 2819 (out of the 17147 analyzed genes), among which 1380 (49%) genes were upregulated and 1439 (51%) genes were downregulated (Figure 39A). On the other hand, after treatment with siRNA against hnRNP R, the total number of DEGs was 1517 genes (out of the 17147 analyzed genes) among which 957 (63%) genes were upregulated and 560 (37%) genes were downregulated (Figure 40A).

Validation of RNA-seq data was carried out by qPCR expression analysis of 10 genes selected among the top 100 DEGs for their potential involvement in brain functions and neuroinflammation (Figures 39B-40B).

Regarding cells silenced for hnRNP Q, *Tumor Necrosis Factor* (*TNF*), *Intercellular*

Adhesion Molecule 1 (*ICAM1*), Proenkephalin (*PENK*), *Tumor Necrosis Factor Receptor Superfamily, Member 9* (*TNFRSF9*), *Kruppel-like Factor 4 (gut)* (*KLF4*), *Kelch-like Family Member 4* (*KLHL4*) and *Neurogulin 3* (*NRG3*) were found to be upregulated, while *RAB26, Member RAS Oncogene Family* (*RAB26*), *Rho GTPase Activating Protein 36* (*ARHGAP36*) and *Cancer/testis Antigen 55* (*CT55*) were found downregulated (Figure 39C). On the other hand, concerning cells silenced for hnRNP R, *CART prepropeptide* (*CARTPT*), *FBJ Murine Osteosarcoma Viral Oncogene Homolog B* (*FOSB*), *Jagged 1* (*JAG1*), *Intercellular Adhesion Molecule 5*, *Telencephalin* (*ICAM5*), *Dual Oxidase Maturation Factor 1* (*DUOXA1*) and *Heme Oxygenase (decycling 1)* (*HMOX1*) were found to be upregulated, while *Potassium Voltage-gated Channel, Shaker-related Subfamily Beta* (*KCNAB1*), *Acid Phosphatase 5, Tartrate Resistant* (*ACP5*), *Syndecan Binding Protein (Syntenin) 2* (*SDCBP2*) and *EGF containing Fibulin-like Extracellular Matrix Protein 1* (*EFEMP1*) were found to be downregulated (Figure 40C). In conclusion, the results of our qPCR validation are consistent with those obtained with the RNA-seq analysis.

A

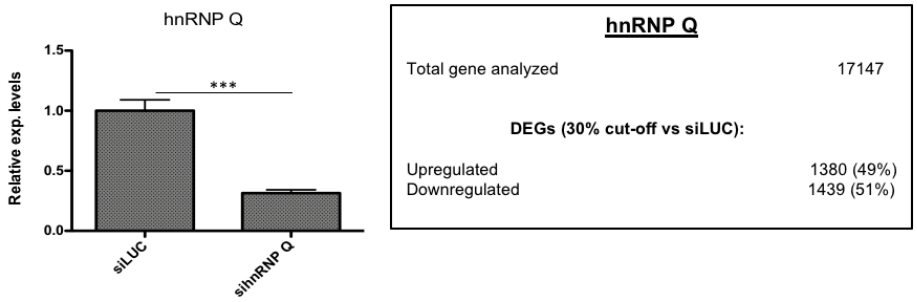

B

ENSEMBL	Gene Symbol	Description	RNAseq
ENSG00000232810	TNF	TNF, tumor necrosis factor	24.52
ENSG00000090339	ICAM1	ICAM1, intercellular adhesion molecule 1	17.45
ENSG00000181195	PENK	PENK, proenkephalin	15.96
ENSG00000049249	TNFRSF9	TNFRSF9, tumor necrosis factor receptor superfamily, member 9	9.87
ENSG00000136826	KLF4	KLF4, Kruppel-like factor 4 (gut)	8.28
ENSG00000102271	KLHL4	KLHL4, kelch-like family member 4	7.95
ENSG00000185737	NRG3	NRG3, neuregulin 3	5.57
ENSG00000167964	RAB26	RAB26, RAB26, member RAS oncogene family	0.18
ENSG00000147256	ARHGAP36	ARHGAP36, Rho GTPase activating protein 36	0.14
ENSG00000169551	CT55	CT55, cancer/testis antigen 55	0.12

C

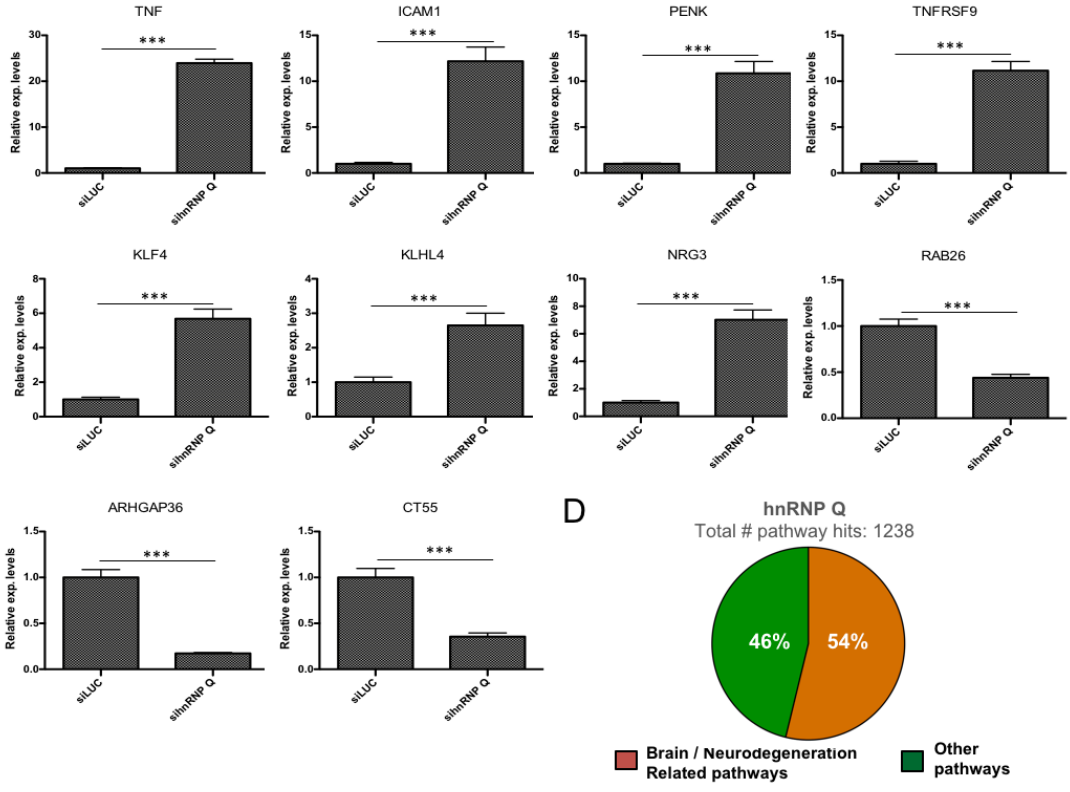

D

Figure 35. Validation of hnRNP Q silencing and comparison between RNA-seq and RT-qPCR results. **(A)** Summary of differentially expressed genes (DEGs) with number of downregulated (<0.7x versus siLUC) and upregulated (>1.3x versus siLUC) genes after sihnRNP Q treatment. Number of DEGs with P <0.05 is also reported. **(B)** List of DEGs validated by RT-qPCR and associated with brain functions/neurodegeneration (*PENK KLF4, KLHL4, NRG3, RAB26* and *ARHGAP36*), inflammation (*TNF, ICAM1, TNFRSF9*) and other functions (*CT55*). **(C)** RT-qPCR validation of ten selected transcripts. Each bar reports mean ± standard error of three independent experiments. Statistical differences were evaluated using

Student's *t*-test (* P<0.05, ** P<0.01, *** P<0.001). **(D)** Pathway analysis of differentially expressed genes following hnRNP Q depletion as determined by PANTHER, DAVID and UniProt analyses.

A

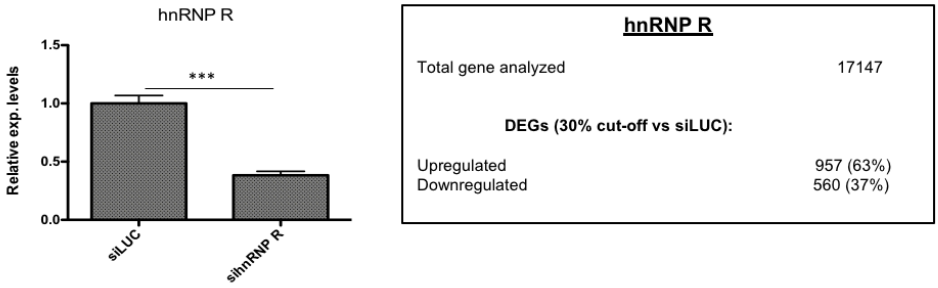

B

ENSEMBL	Gene Symbol	Description	RNAseq
ENSG00000164326	CARTPT	CARTPT, CART prepropeptide	24.59
ENSG00000125740	FOSB	FOSB, FBJ murine osteosarcoma viral oncogene homolog B	10.96
ENSG00000101384	JAG1	JAG1, jagged 1	5.70
ENSG00000105376	ICAM5	ICAM5, intercellular adhesion molecule 5, telencephalin	4.34
ENSG00000140254	DUOXA1	DUOXA1, dual oxidase maturation factor 1	3.91
ENSG00000100292	HMOX1	HMOX1, heme oxygenase (decycling) 1	3.36
ENSG00000169282	KCNAB1	KCNAB1, potassium voltage-gated channel, shaker-related subfamily, beta member 1	0.31
ENSG00000102575	ACP5	ACP5, acid phosphatase 5, tartrate resistant	0.25
ENSG00000125775	SDCBP2	SDCBP2, syndecan binding protein (syntenin) 2	0.18
ENSG00000115380	EFEMP1	EFEMP1, EGF containing fibulin-like extracellular matrix protein 1	0.18

C

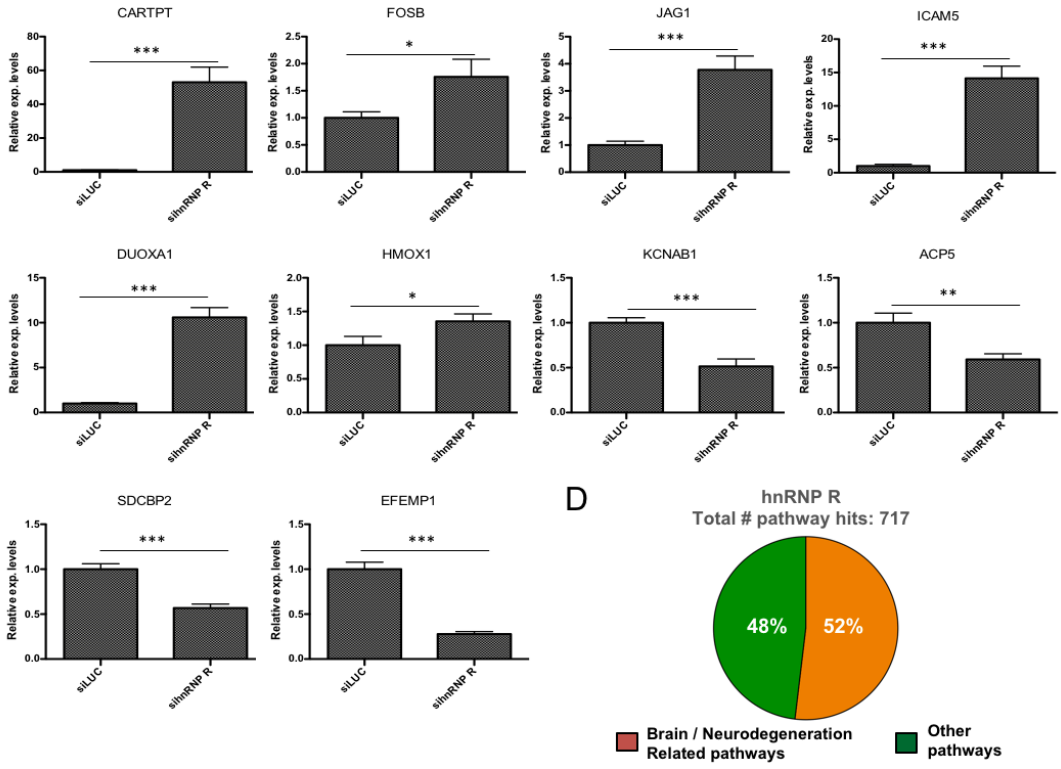

D

Figure 36. Validation of hnRNP R silencing and comparison between RNA-seq and RT-qPCR results. **(A)** Summary of DEGs with number of downregulated (<0.7x versus siLUC) and upregulated (>1.3x versus siLUC) genes after sihnRNP R treatment. Number of DEGs with P<0.05 is also reported. **(B)** List of DEGs validated by RT-qPCR and associated with brain functions/neurodegeneration (*CARTPT, FOSB, JAG1,*

DUOXA1, HMOX1, KCNAB1, SDCBP2, EFEMP1), inflammation (*ICAM5, ACP5*). **(C)** RT-qPCR validation of ten selected transcripts. Each bar reports mean ± standard error of three independent experiments. Statistical differences were evaluated using Student's *t*-test (*P<0.05, ** P<0.01, ***P<0.001). **(D)** Pathway analysis of differentially expressed genes following hnRNP R depletion as determined by PANTHER, DAVID and UniProt analyses.

An overview of these RNA-seq data was also provided by volcano plots (Figure 41) and MAPlots (Figure 42). Upregulated and downregulated genes were highlighted in green and red, respectively. Moreover, in the volcano plot, we reported the position of the DEGs validated in Figure 39C and 40C using qPCR. On the other hand, in the MAPlot, we highlighted the position of *SYNCRIP* (hnRNP Q, Figure 42A) and *HNRNPR* (Figure 42B) gene, respectivelly.

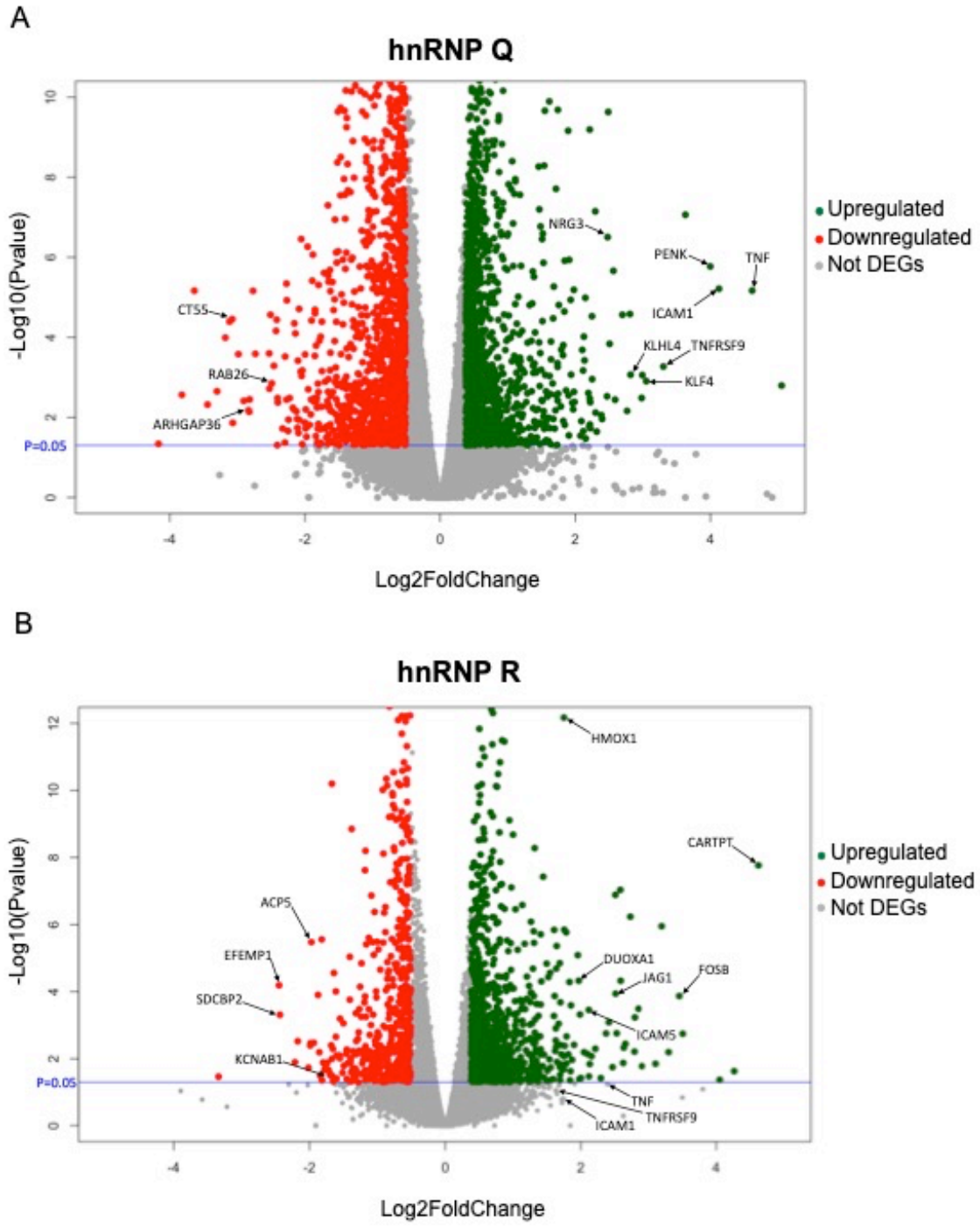

Figure 37. Volcano plot of hnRNP Q and hnRNP R. Schematic representation of RNA-seq data of sihnRNP Q **(A)** and sihnRNP R **(B)** treated cells. Up- and downregulated genes are reported as green and red dots, respectively. Not DEGs are represented as grey dots. Black arrows show qPCR validated genes. The horizontal blue line signals statistical significance threshold (P= 0.05).

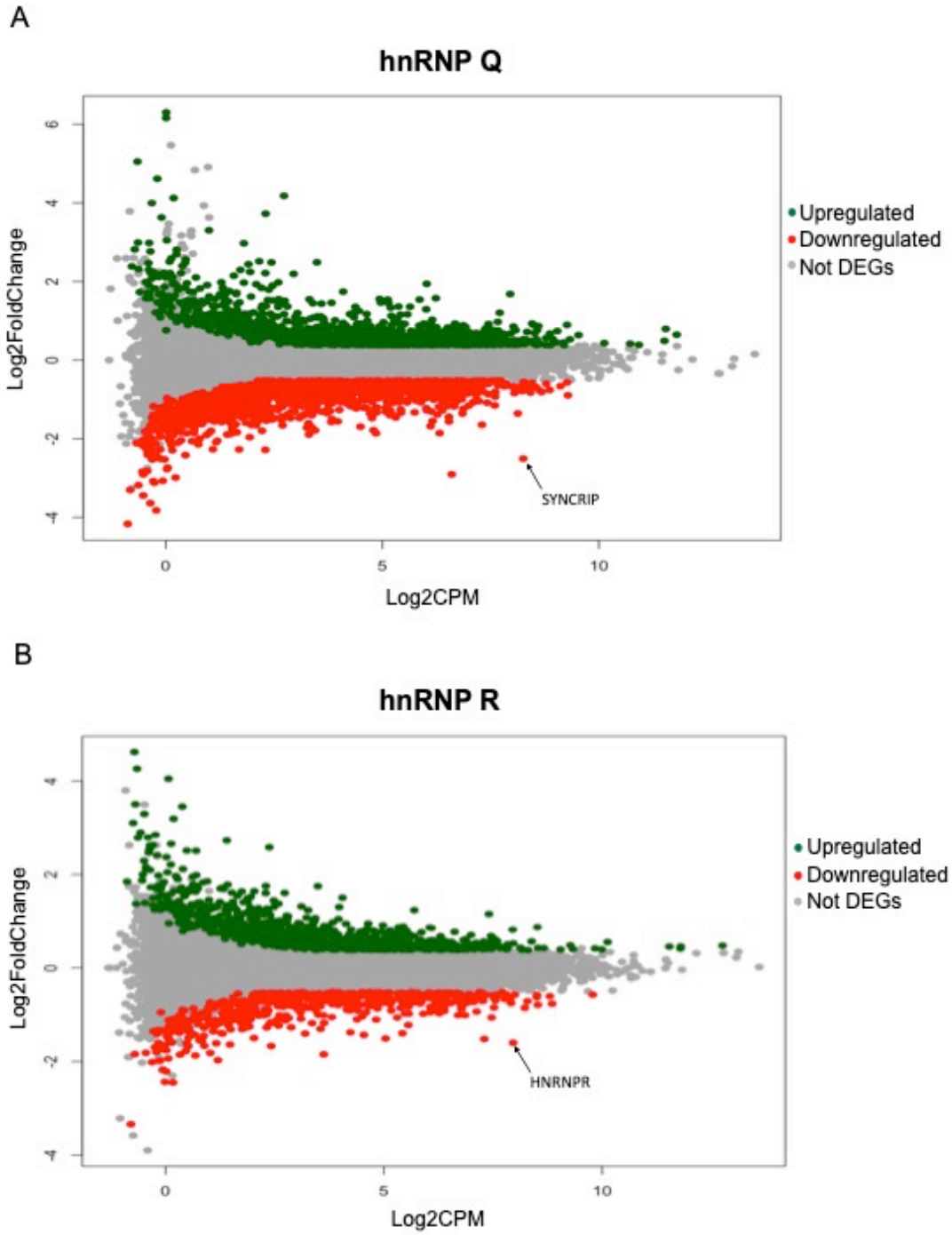

Figure 38. Graphic representation of RNA-seq analysis performed on SH-SY5Y cells depleted for hnRNP Q and hnRNP R. (A) MAPlot reports on the x-axis the normalized library size (Log2CPM, *counts per million*) and on the y-axis the magnitude (Log2FoldChange) of siLUC versus sihnRNP Q treated cells. Upregulated and downregulated genes are highlighted in green and red, respectively. The position of *SYNCRIP* gene (encoding hnRNP Q protein) is highlighted by an arrow. **(B)** MAPlot reports on the x-axis the normalized library size (Log2CPM, *counts per million*) and on the y-axis the magnitude (Log2FoldChange) of siLUC versus sihnRNP R treated cells. Upregulated and downregulated genes are highlighted in green and red, respectively. The position of *HNRNPR* gene (encoding hnRNP R protein) is highlighted by an arrow.

4.4.6 hnRNP Q and hnRNP R show different and common features after GO enrichment and KEGG pathway analysis

GO enrichment was performed to show up functional similarities and differences in DEGs regulated by hnRNP Q and hnRNP R. To this aim, we took advantage of the GOseq R Bioconductor package (Young et al., 2010) and considered for the final analysis only GO term of the "biological process" (BP), "molecular function" (MF), and "cellular component" (CC) categories reaching the P value threshold < 0.05 for significance. In particular, top 15 GO terms of each category were selected to find categories specific for hnRNP Q or hnRNP R and categories commonly present in both two proteins (Figure 43).

In hnRNP Q data set, we found 1152 significantly enriched terms out of 2819 DEGs used as input for GO analysis. The top enriched GO categories were "membrane" (Pvalue = 3.17E-08), "bounding membrane to organelle" Pvalue = 7.29E-07), "cell morphogenesis involved in differentiation" (Pvalue = 1.10E-06), "cell development" (Pvalue = 1.42E-06) and "cell adhesion" (Pvalue = 3.17E-06). On the other hand, in hnRNP R data set, we found 955 significantly enriched terms out of 1517 DEGs used as input for GO analysis. The top enriched GO categories were "system development" (Pvalue = 2.34E-08), "tissue development" (Pvalue = 4.21E-08), "multicellular organism development" (Pvalue = 3.39E-07), "cell differentiation" (Pvalue = 4.28E-07) and "signal transduction" (Pvalue =1.13E-06). Notably, when we looked at GO terms differentially enriched in hnRNP Q and hnRNP R DEGs, we found that "intrinsic component of membrane", "plasma membrane", "cell periphery", "integral component of membrane" and "membrane part" were particularly enriched in hnRNP Q depleted cells, while "signal receptor activity", "transmembrane receptor activity", "transmembrane signalling receptor activity", "receptor activity" and "molecular transducer activity" were more enriched in hnRNP R depleted treated cells.

Regarding KEGG analysis, we found 29 and 16 terms with significant gene enrichment (P < 0.05) for hnRNP Q and hnRNP R, respectively (Figure 44) and the majority of them were inflammation-related pathways. Indeed, “toll-like receptor signalling pathway” (Pvalue = 0.002), “ECM-receptor interaction” (Pvalue = 0.002), “adipocytokine signaling pathway” (Pvalue = 0.003), “toxoplasmosis” (Pvalue = 0.004) and “rheumatoid arthritis” (Pvalue = 0.007) were particularly enriched in DEGs obtained by sihnRNP Q silencing, whereas “cell adhesion molecules (CAMs)” (Pvalue = 4.58E-05), “ECM-receptor interaction” (Pvalue = 0.001), “cytokine-cytokine receptor interaction” (Pvalue = 0.01), “T cell receptor signaling pathway” (Pvalue = 0.02) and “malaria” (Pvalue = 0.02) were particularly enriched in DEGs obtained by sihnRNP R silencing.

In conclusion, this analysis suggested a specific specialization acquired from hnRNP Q and hnRNP R during evolution. In particular, GO terms linked to the organization of lipid layers and in the regulation of cell-cell and cell-extracellular matrix contacts seemed to be influenced by sinhnRNP Q treatment, while, GO terms associated with cell/tissue development and cell signalling was found to be regulated by depletion of hnRNP R.

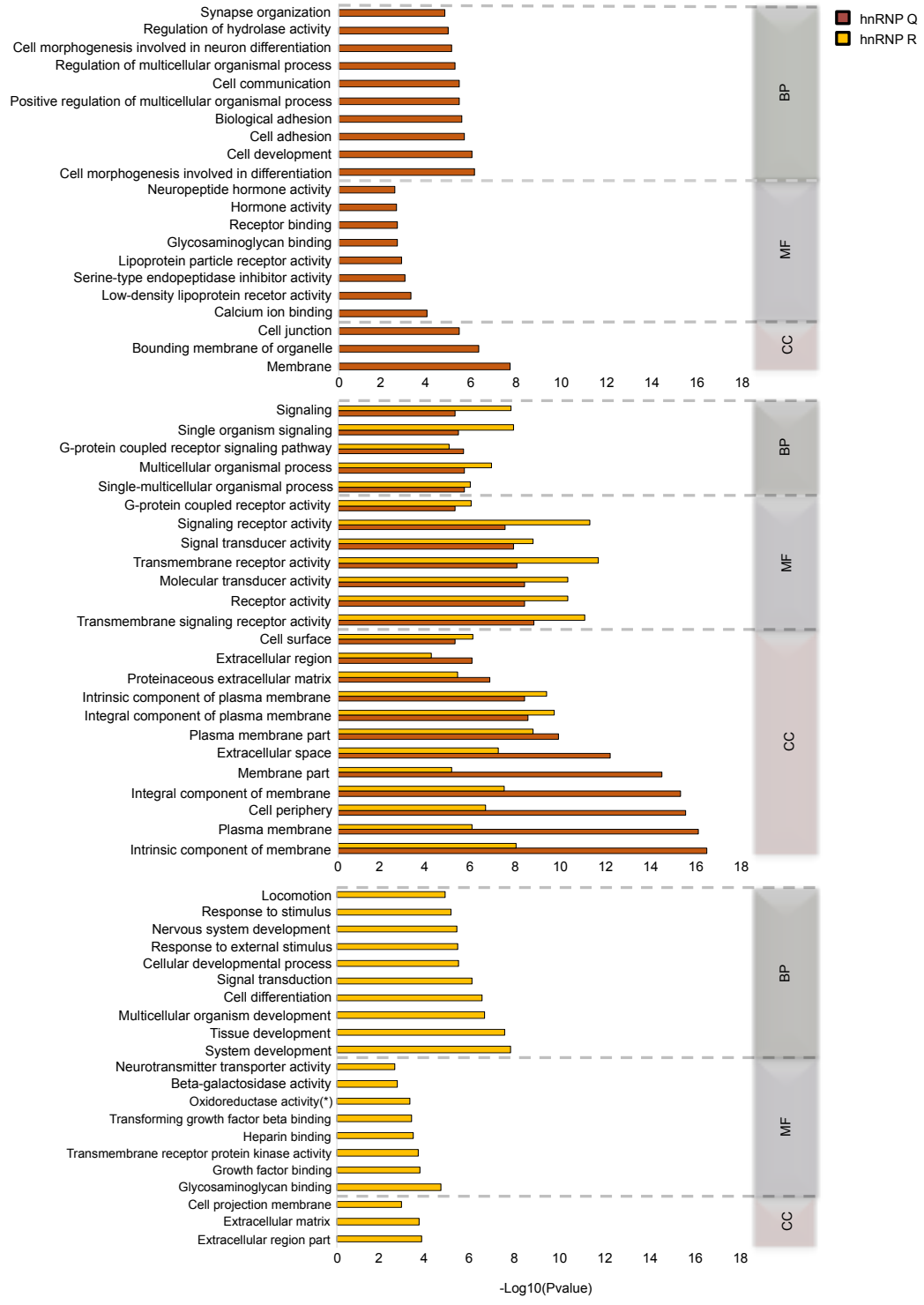

Figure 39. GO enrichment analysis of hnRNP Q and hnRNP R DEGs. Biological process (BP), molecular function (MF) and cellular component (CC) GO categories are represented. Each category reported the first 15 sub-categories (P<0.05) of DEGs for cells treated with siRNA against both hnRNP Q and hnRNP R.

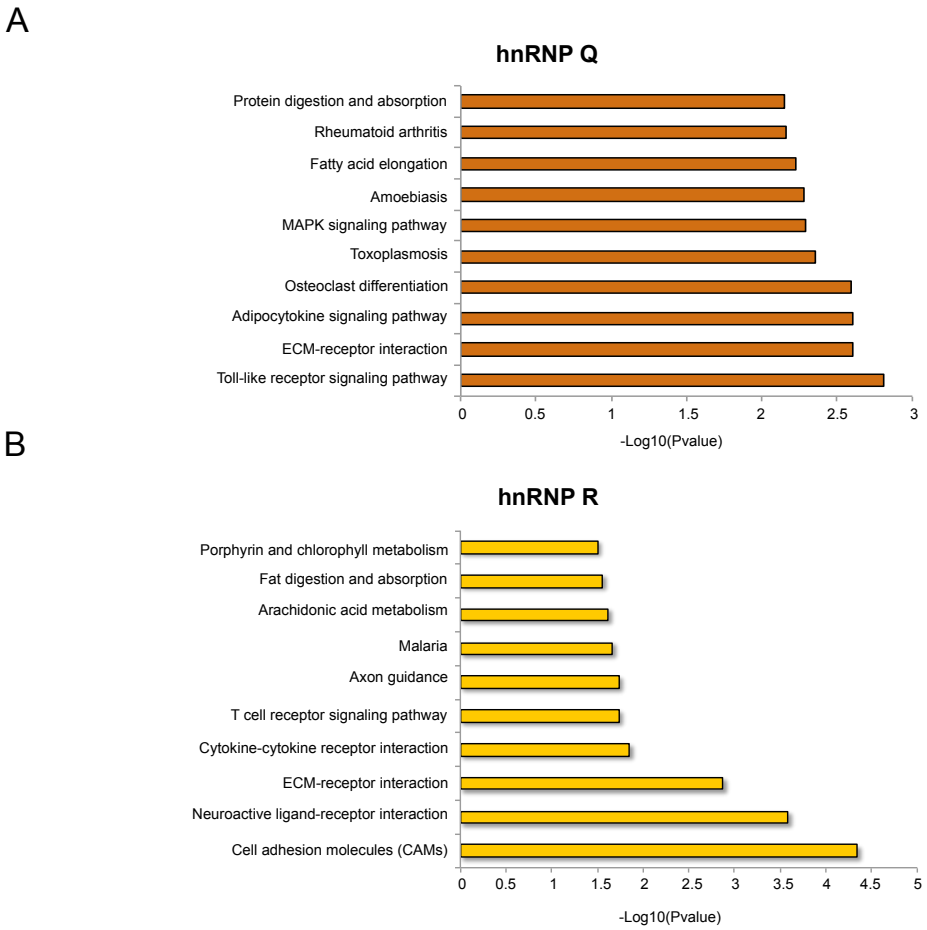

Figure 40. KEGG pathway analysis of hnRNP Q and hnRNP R. **(A)** First 10 pathways identified in DEGs of SH-SY5Y cells treated with siRNA against hnRNP Q ($P<0.05$). **(B)** First 10 pathways identified in DEGs of SH-SY5Y cells treated with siRNA against hnRNP R ($P<0.05$).

4.5 An overview of the entire transcriptome status after silencing of TDP-43, DAZAP1, hnRNP Q and hnRNP R

4.5.1 TDP-43, DAZAP1 and hnRNP Q share common regulated-transcripts associated with ALS pathology

Following the RNA-seq analysis of cells depleted for TDP-43, DAZAP1, hnRNP Q or hnRNP R we decided to combine all the DEGs (FC cut-off of 30% vs siLUC; P <0.05) of each hnRNP silencing in order to find commonly regulated transcripts (Figure 45).

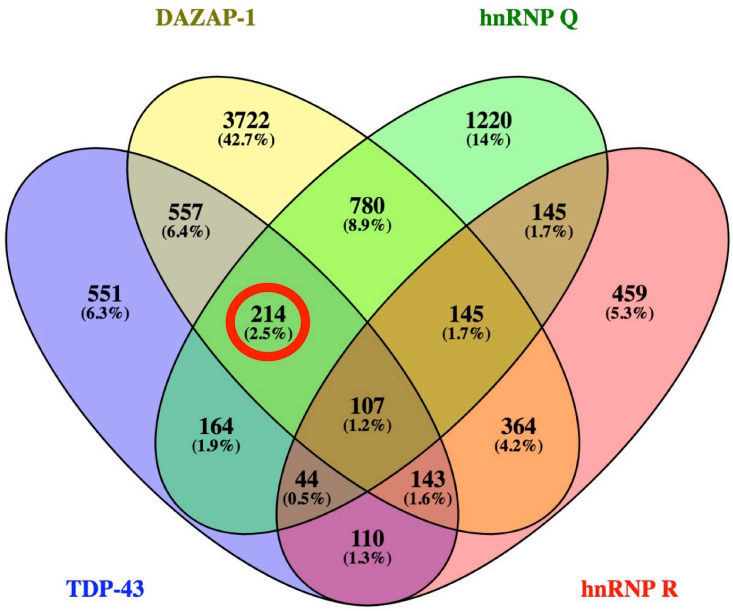

Figure 41. Venn diagramm of RNA-seq data. Comparison of the number of transcripts altered in TDP-43, hnRNP Q and hnRNP R depleted SH-SY5Y cell. Genes co-regulated by TDP-43, DAZAP1 and hnRNP Q but not hnRNP R are highlighted with red circle.

As described previously, our results in SH-SY5Y cells and Flp-In HEK293 expressing TDP-43 12XQ/N demonstrated that DAZAP1 and hnRNP Q were particularly effective in modulating the activity of TDP-43 targets. In this way, we were interested in looking for

all the possible mRNA targets regulated by TDP-43, DAZAP1, hnRNP Q but not hnRNP R and we identified 214 genes reflecting these criteria (Figure 45, Table 22). This list of genes shows that more than 50% of the transcripts affected by TDP-43, DAZAP1, and hnRNP Q play an important role in neuronal maintenance/functions (such as *NOVA2*), immune system and inflammation (*TNF, TNFRSF9, ICAM-1*), and apoptosis (Figure 46). These observations lend further support to recent studies that hypothesize a role of immune system and apoptosis in the ALS pathogenesis. Furthermore, in this list of 214 co-regulated genes there are already several candidates that are extremely promising for the understanding the RNA misregulation occurring during neurodegenerative disorders and that will be discussed in the next chapter.

Table 22. Co-regulated transcripts between TDP-43, DAZAP1 and hnRNP Q

		RNA-seq Fold Change		
ENSEMBL	**Gene Symbol**	**TDP-43**	**DAZAP1**	**hnRNP Q**
ENSG00000181201	*HIST3H2BA*	0.1	3.6	0.1
ENSG00000205625	*RP11-15G8.1*	0.2	0.6	0.7
ENSG00000157703	*SVOPL*	0.3	0.3	0.2
ENSG00000042832	*TG*	0.3	0.4	0.4
ENSG00000100078	*PLA2G3*	0.4	0.3	0.3
ENSG00000258472	*RP11-192H23.4*	0.4	0.2	0.2
ENSG00000104967	*NOVA2*	0.4	0.7	0.7
ENSG00000230138	*RP11-117D22.2*	0.4	0.3	0.2
ENSG00000206838	*SNORA5A*	0.4	0.4	0.5
ENSG00000162188	*GNG3*	0.4	0.4	0.6
ENSG00000154997	*SEPT14*	0.4	2.3	2.2
ENSG00000167244	*IGF2*	0.4	0.2	0.4
ENSG00000130600	*H19*	0.4	0.2	0.6

ENSG00000132141	*CCT6B*	0.5	4.5	0.6
ENSG00000130176	*CNN1*	0.5	0.6	2.2
ENSG00000175785	*PRIMA1*	0.5	0.3	0.6
ENSG00000165424	*ZCCHC24*	0.5	0.4	1.8
ENSG00000265971	*RP11-269G24.6*	0.5	0.4	0.4
ENSG00000179921	*GPBAR1*	0.5	0.2	1.8
ENSG00000167889	*MGAT5B*	0.5	0.5	1.4
ENSG00000142197	*DOPEY2*	0.5	0.5	0.5
ENSG00000163536	*SERPINI1*	0.5	4.3	1.7
ENSG00000115756	*HPCAL1*	0.5	0.5	1.6
ENSG00000173517	*PEAK1*	0.5	2.3	0.6
ENSG00000141753	*IGFBP4*	0.5	0.6	1.4
ENSG00000092929	*UNC13D*	0.5	0.6	0.5
ENSG00000123091	*RNF11*	0.6	0.4	0.7
ENSG00000198570	*RD3*	0.6	0.2	0.5
ENSG00000267980	*AC007292.6*	0.6	0.6	0.6
ENSG00000271155	*RP11-435O5.5*	0.6	2.7	0.6
ENSG00000179242	*CDH4*	0.6	0.5	1.7
ENSG00000185900	*POMK*	0.6	0.5	0.4
ENSG00000100092	*SH3BP1*	0.6	0.6	0.6
ENSG00000135097	*MSI1*	0.6	0.5	0.5
ENSG00000198929	*NOS1AP*	0.6	0.6	0.7
ENSG00000177830	*CHID1*	0.6	1.5	1.3
ENSG00000144677	*CTDSPL*	0.6	0.7	1.5
ENSG00000183044	*ABAT*	0.6	2.1	0.4
ENSG00000270015	*RP11-540B6.6*	0.6	1.3	1.4
ENSG00000069431	*ABCC9*	0.6	0.3	0.6
ENSG00000164125	*FAM198B*	0.6	0.4	1.5
ENSG00000175093	*SPSB4*	0.6	0.6	0.6

ENSG00000084710	*EFR3B*	0.6	0.5	0.5
ENSG00000167524	*SGK494*	0.6	0.5	0.4
ENSG00000101115	*SALL4*	0.6	0.6	1.5
ENSG00000088280	*ASAP3*	0.6	0.7	0.7
ENSG00000171303	*KCNK3*	0.6	0.5	1.4
ENSG00000159873	*CCDC117*	0.6	0.6	1.3
ENSG00000175229	*GAL3ST3*	0.6	0.5	0.6
ENSG00000101986	*ABCD1*	0.6	1.3	0.6
ENSG00000003249	*DBNDD1*	0.6	0.7	0.6
ENSG00000148700	*ADD3*	0.6	0.7	0.5
ENSG00000197122	*SRC*	0.6	0.6	0.6
ENSG00000174672	*BRSK2*	0.6	0.6	0.7
ENSG00000176749	*CDK5R1*	0.6	0.4	0.6
ENSG00000239887	*C1orf226*	0.6	0.5	0.7
ENSG00000146094	*DOK3*	0.7	0.6	0.5
ENSG00000125520	*SLC2A4RG*	0.7	0.3	0.6
ENSG00000149295	*DRD2*	0.7	0.4	1.4
ENSG00000198168	*SVIP*	0.7	0.5	0.6
ENSG00000116981	*NT5C1A*	0.7	0.6	0.6
ENSG00000122254	*HS3ST2*	0.7	0.4	0.7
ENSG00000197586	*ENTPD6*	0.7	0.6	1.3
ENSG00000173621	*LRFN4*	0.7	0.6	0.6
ENSG00000165238	*WNK2*	0.7	0.7	0.7
ENSG00000108433	*GOSR2*	0.7	1.4	1.4
ENSG00000261762	*RP11-650L12.2*	0.7	0.3	0.6
ENSG00000121039	*RDH10*	0.7	1.5	1.4
ENSG00000073670	*ADAM11*	0.7	2.2	0.7
ENSG00000128482	*RNF112*	0.7	0.5	0.6
ENSG00000164742	*ADCY1*	0.7	0.6	0.6

ENSG00000172794	*RAB37*	0.7	0.7	1.4
ENSG00000278619	*MRM1*	0.7	0.5	1.3
ENSG00000149260	*CAPN5*	0.7	0.6	0.7
ENSG00000259291	*RP11-617F23.1*	0.7	0.4	0.5
ENSG00000141750	*STAC2*	0.7	0.3	0.7
ENSG00000100034	*PPM1F*	0.7	0.7	1.3
ENSG00000007402	*CACNA2D2*	0.7	0.7	0.6
ENSG00000133997	*MED6*	0.7	1.6	1.3
ENSG00000139200	*PIANP*	0.7	0.7	0.6
ENSG00000015532	*XYLT2*	0.7	0.5	0.6
ENSG00000171310	*CHST11*	0.7	0.5	0.5
ENSG00000162959	*MEMO1*	0.7	0.6	0.5
ENSG00000130772	*MED18*	1.3	1.5	1.6
ENSG00000171295	*ZNF440*	1.3	1.4	1.5
ENSG00000158373	*HIST1H2BD*	1.3	4.7	1.5
ENSG00000185658	*BRWD1*	1.3	1.8	1.3
ENSG00000171992	*SYNPO*	1.3	0.6	0.6
ENSG00000155729	*KCTD18*	1.3	1.5	0.6
ENSG00000136895	*GARNL3*	1.3	0.7	1.4
ENSG00000177239	*MAN1B1*	1.3	1.6	1.4
ENSG00000158470	*B4GALT5*	1.3	1.3	1.9
ENSG00000112773	*FAM46A*	1.3	1.5	1.9
ENSG00000169981	*ZNF35*	1.3	1.8	1.5
ENSG00000139117	*CPNE8*	1.3	1.5	1.5
ENSG00000152518	*ZFP36L2*	1.3	0.6	1.6
ENSG00000181523	*SGSH*	1.3	1.3	1.7
ENSG00000033100	*CHPF2*	1.3	1.9	1.5
ENSG00000198046	*ZNF667*	1.4	1.6	1.4
ENSG00000090263	*MRPS33*	1.4	1.3	1.4

ENSG00000188042	*ARL4C*	1.4	0.6	1.7
ENSG00000126947	*ARMCX1*	1.4	0.6	1.3
ENSG00000162396	*PARS2*	1.4	2.4	1.6
ENSG00000136167	*LCP1*	1.4	3.7	2.7
ENSG00000138760	*SCARB2*	1.4	1.5	0.6
ENSG00000067113	*PPAP2A*	1.4	1.4	1.5
ENSG00000106617	*PRKAG2*	1.4	1.5	0.7
ENSG00000196437	*ZNF569*	1.4	1.6	0.7
ENSG00000248383	*PCDHAC1*	1.4	2.1	2.2
ENSG00000143469	*SYT14*	1.4	1.4	0.7
ENSG00000273820	*USP27X*	1.4	1.6	1.4
ENSG00000185947	*ZNF267*	1.4	1.6	1.6
ENSG00000250091	*DNAH10OS*	1.4	1.3	0.3
ENSG00000170035	*UBE2E3*	1.4	1.4	1.6
ENSG00000146966	*DENND2A*	1.5	1.5	0.4
ENSG00000272947	*RP11-71H17.9*	1.5	1.5	0.7
ENSG00000116574	*RHOU*	1.5	0.5	0.7
ENSG00000153214	*TMEM87B*	1.5	1.4	2.2
ENSG00000003436	*TFPI*	1.5	1.5	1.9
ENSG00000238105	*GOLGA2P5*	1.5	1.7	0.6
ENSG00000138078	*PREPL*	1.5	1.5	1.4
ENSG00000132824	*SERINC3*	1.5	1.4	1.4
ENSG00000167740	*CYB5D2*	1.5	2.8	1.7
ENSG00000186866	*POFUT2*	1.5	1.7	1.5
ENSG00000031691	*CENPQ*	1.5	1.6	0.7
ENSG00000088727	*KIF9*	1.5	2.1	1.6
ENSG00000210107	*MT-TQ*	1.6	1.8	1.6
ENSG00000106853	*PTGR1*	1.6	1.5	2.0
ENSG00000153363	*LINC00467*	1.6	3.7	1.8

ENSG00000279192	*PWAR5*	1.6	1.9	1.6
ENSG00000108733	*PEX12*	1.6	1.4	1.5
ENSG00000171365	*CLCN5*	1.6	1.5	1.4
ENSG00000157680	*DGKI*	1.6	2.0	1.8
ENSG00000100906	*NFKBIA*	1.6	1.5	1.5
ENSG00000135776	*ABCB10*	1.6	0.4	0.6
ENSG00000105708	*ZNF14*	1.6	2.0	1.8
ENSG00000107165	*TYRP1*	1.6	2.0	1.7
ENSG00000256304	*CCDC150P1*	1.6	0.4	0.6
ENSG00000171451	*DSEL*	1.6	0.5	0.5
ENSG00000177272	*KCNA3*	1.6	2.3	2.9
ENSG00000166192	*SENP8*	1.6	1.5	1.6
ENSG00000128923	*FAM63B*	1.6	1.4	0.4
ENSG00000164305	*CASP3*	1.6	1.3	1.7
ENSG00000114923	*SLC4A3*	1.7	1.5	0.6
ENSG00000134326	*CMPK2*	1.7	2.1	1.8
ENSG00000118976	*OTUD4P1*	1.7	1.5	1.8
ENSG00000280287	*RP13-554M15.7*	1.7	10.7	2.3
ENSG00000253869	*PIGFP1*	1.7	1.7	1.6
ENSG00000085449	*WDFY1*	1.7	1.6	1.5
ENSG00000090612	*ZNF268*	1.7	2.1	1.4
ENSG00000149243	*KLHL35*	1.7	0.3	1.6
ENSG00000087074	*PPP1R15A*	1.7	2.7	1.9
ENSG00000117586	*TNFSF4*	1.7	4.5	2.1
ENSG00000162616	*DNAJB4*	1.7	2.6	1.5
ENSG00000228876	*AC010745.2*	1.7	0.4	1.6
ENSG00000163820	*FYCO1*	1.8	0.4	1.4
ENSG00000128016	*ZFP36*	1.8	3.7	1.5
ENSG00000166432	*ZMAT1*	1.8	6.6	0.4

ENSG00000127561	*SYNGR3*	1.8	2.3	0.6
ENSG00000135318	*NT5E*	1.9	1.9	3.8
ENSG00000223427	*AC016716.1*	1.9	0.5	1.6
ENSG00000107201	*DDX58*	1.9	5.1	2.3
ENSG00000168398	*BDKRB2*	1.9	2.0	2.8
ENSG00000080709	*KCNN2*	1.9	4.0	2.6
ENSG00000135926	*TMBIM1*	1.9	0.4	2.0
ENSG00000168461	*RAB31*	2.0	2.5	1.5
ENSG00000142102	*ATHL1*	2.0	0.6	0.6
ENSG00000254473	*RP11-522I20.3*	2.0	8.8	2.9
ENSG00000142303	*ADAMTS10*	2.0	4.1	0.5
ENSG00000115665	*SLC5A7*	2.0	0.5	2.0
ENSG00000156966	*B3GNT7*	2.1	0.3	2.1
ENSG00000259381	*RP11-192M23.1*	2.2	2.0	2.0
ENSG00000248323	*LUCAT1*	2.2	2.5	0.4
ENSG00000259834	*KCNA3*	2.2	2.3	2.9
ENSG00000166246	*C16orf71*	2.2	4.0	2.5
ENSG00000135048	*TMEM2*	2.2	2.0	1.9
ENSG00000050628	*PTGER3*	2.3	2.0	2.9
ENSG00000248905	*FMN1*	2.3	1.6	1.7
ENSG00000168026	*TTC21A*	2.3	7.3	1.8
ENSG00000276603	*RP11-425M5.7*	2.3	9.0	2.1
ENSG00000166401	*SERPINB8*	2.4	5.4	2.4
ENSG00000168542	*COL3A1*	2.4	2.0	3.1
ENSG00000267682	*CTD-3220F14.2*	2.5	3.2	3.0
ENSG00000183696	*UPP1*	2.5	2.1	1.6
ENSG00000130762	*ARHGEF16*	2.5	1.9	0.5
ENSG00000148180	*GSN*	2.7	1.9	2.1
ENSG00000175592	*FOSL1*	2.8	4.0	4.3

ENSG00000161638	*ITGA5*	2.8	3.8	2.6
ENSG00000146592	*CREB5*	2.8	2.3	1.4
ENSG00000247157	*LINC01252*	2.8	3.6	4.4
ENSG00000136052	*SLC41A2*	2.8	2.9	0.5
ENSG00000224165	*DNAJC27-AS1*	2.9	21.3	3.0
ENSG00000137331	*IER3*	3.1	3.0	1.6
ENSG00000125246	*CLYBL*	3.1	2.4	2.6
ENSG00000063438	*AHRR*	3.1	2.9	3.8
ENSG00000023839	*ABCC2*	3.3	5.3	2.9
ENSG00000140511	*HAPLN3*	3.3	5.2	0.3
ENSG00000114670	*NEK11*	3.3	8.7	2.9
ENSG00000108846	*ABCC3*	3.5	3.1	2.3
ENSG00000266921	*RP11-15A1.7*	3.7	13.4	3.9
ENSG00000163131	*CTSS*	3.9	6.0	4.4
ENSG00000172752	*COL6A5*	4.0	2.7	2.8
ENSG00000159450	*TCHH*	4.2	6.6	5.9
ENSG00000106366	*SERPINE1*	4.4	4.5	7.8
ENSG00000240065	*PSMB9*	4.4	8.0	0.1
ENSG00000106070	*GRB10*	5.4	2.0	2.2
ENSG00000204248	*COL11A2*	5.8	12.2	3.0
ENSG00000134070	*IRAK2*	6.5	4.7	3.3
ENSG00000196664	*TLR7*	7.0	4.0	4.6
ENSG00000187164	*KIAA1598*	7.6	7.6	2.3
ENSG00000122861	*PLAU*	8.7	6.5	2.7
ENSG00000232810	*TNF*	20.5	11.2	24.5
ENSG00000049249	*TNFRSF9*	36.0	10.1	9.9
ENSG00000090339	*ICAM1*	50.0	14.5	17.4

Pathways	TDP-43/DAZAP1/hnRNP Q co-regulated genes
Neurological function	54 (25%)
Immune-related	28 (13%)
Apoptosis-related	23 (11%)
Other pathways	109 (51%)

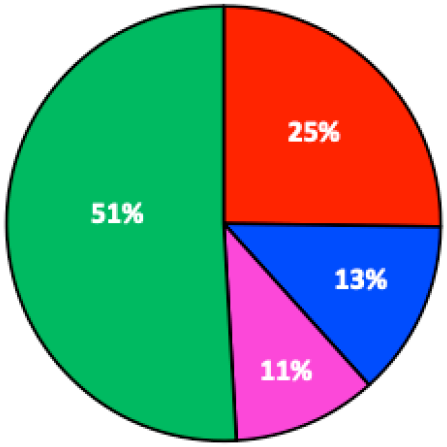

Figure 42. Pathways of genes co-regulated only by TDP-43, DAZAP1 and hnRNP Q. Classification of 214 genes whose expression is co-regulated in TDP-43, DAZAP1, hnRNP Q, but not hnRNP R depleted SH-SY5Y cells according to the GO categorization system.

5. DISCUSSION

5.1 TDP-43 activity is modulated by the interaction with other hnRNP proteins

Since TDP-43 was discovered as a major component of ubiquitinated inclusions in ALS and FTLD patients (Neumann et al., 2006) the interest in better characterizing the pathological role of this protein has considerably increased. In particular, in past years a lot of effort was put into better defining TDP-43 protein-protein interactions and in the identification of all the possible transcripts regulated by TDP-43 that could be altered in pathology. In this context, it has been well-characterized that TDP-43 can interact with other members of the hnRNP family and that this binding can affect the functions of both factors (Buratti and Baralle, 2012). Examples of TDP-43 interacting proteins are several members of hnRNP A/Bs family (D'Ambrogio et al., 2009; Romano et al., 2014), hnRNP H, and FUS/TLS (Freibaum et al., 2010).

In this thesis, I have investigated the relationship between TDP-43 and three hnRNP proteins (DAZAP1, hnRNP Q and hnRNP R) not yet completely characterized, although all these proteins were previously found to be associated with neuronal functions (Bannai et al., 2004; Glinka et al., 2010; Pastor and Pagani, 2011). We had also demonstrated, together with the Neurobiology group, that they represented powerful modifiers of TDP-43/TBPH in *Drosophila melanogaster*.

At the functional level, we first demonstrated that DAZAP1, hnRNP Q and hnRNP R can with different ability modify the splicing pattern or gene expression of well-known TDP-43 targets, such as *POLDIP3, TNIK, STAG2, MADD* and *BRD8*. These genes are involved in several aspects of cell proliferation (*POLDIP3, STAG2*), apoptosis (*MADD, BRD8*) and neuronal functions (*TNIK*). In particular, alteration in the *POLDIP3* (also known as *SKAR*)

pre-mRNA splicing profiles were previously reported to be associated with depletion of TDP-43 in vitro and in motor cortex, spinal cord and spinal motor neurons of patients affected by ALS (Shiga et al., 2012). This previous work observed that knockdown of TDP-43 regulated the production of an alternative splicing isoform, namely variant-2, through the skipping of exon 3 and therefore influenced *POLDIP3* function in mediating cell proliferation and growth (Shiga et al., 2012). In our experiments, we demonstrated that the inclusion of *POLDIP3* exon 3 was also significantly altered in the presence of DAZAP1 and hnRNP Q knockdown (Figure 23A), indicating that splicing regulation is not exclusive for TDP-43 but it can also depend on the participation of other factors. This hypothesis was also corroborated by the fact that the co-silencing of TDP-43 with DAZAP1 was able to recover the *POLDIP3* splicing profile (Figure 24A), indicating that the engagement of DAZAP1 is able to modulate the TDP-43 activity.

Other interesting observations supporting the role of DAZAP1, hnRNP Q and hnRNP R in regulating TDP-43 activity were obtained by studying the pre-mRNA splicing analysis of *TNIK* and *STAG2* genes, as well as investigating changes in mRNA expression levels of *TNIK*.

TNIK is a serine/threonine kinase belonging to the Ste20 family that was originally cloned from a human cDNA library and successively identified in mouse brain (Fu et al., 1999). It was also described as an important factor for synaptic functions and cytoskeleton organization (Traikov et al., 2014; Fu et al., 1999), as well as, as a potential risk factor for several mental disorders (Matigian et al., 2007; Glatt et al., 2005). The association between TDP-43 and TNIK arose from a transcriptomic study in 2015 where the analysis of TDP-43 and FUS depletion led to the identification of several genes related to neuronal pathways and RNA metabolism, whose expression or pre-mRNA splicing profile was modified after siRNA treatment (Colombrita et al., 2015). In our study, we observed that

DAZAP1, hnRNP Q and even hnRNP R were able to alter *TNIK*'s splicing profile (Figure 23B) and, in the case of DAZAP1 and hnRNP Q, also to recover it after TDP-43 depletion (Figure 24B). Furthermore, we showed a decrease of *TNIK* mRNA levels after treatment of cells with an siRNA against hnRNP Q (Figure 26C).

Along the same lines, we looked at the *STAG2* splicing profile. STAG2 is a component of the cohesin complex involved in separation of sister chromatids during cell division (Berkowitz, 2014). In 2015, our laboratory showed that STAG2 was involved in the accumulation of cells in G2/M phase due to upregulation of its exon 30b+ isoform after siTDP-43 treatment (De Conti et al., 2015). In this thesis I show that *STAG2* exon 30b+ inclusion was also affected by DAZAP1 silencing (Figure 23C), and the depletion of both proteins was able to rescue the *STAG2* profile (Figure 24C).

To complete the list of known TDP-43 targets, we further tested our hnRNPs for mediating changes in *MADD* and *BRD8* gene expression regulation. The *MADD* gene is expressed in low levels in all tissues and can act as a pro-apoptotic factor when its phosphorylation is reduced by the Tumour Suppressor Phosphatase and Tensin Homolog (PTEN) (Jayarama et al., 2014). Interestingly, the *MADD* gene was also found to be important for neuronal survival since alteration in its splicing isoforms were found in in neuronal cell lines exposed to high concentrations of oligomeric Aβ peptides (Mo et al., 2012). Tollervey et al. and subsequently De Conti et al. demonstrated that siTDP-43 treatment could affect both the splicing process of this gene, in particular by inducing exon 31 exclusion plus activation of a pseudoexon, but also its mRNA levels (De Conti et al., 2015; Tollervey et al., 2011). Here, we demonstrated that although none of the tested hnRNPs was able to modify the *MADD* splicing profile (Figure 26A), there was significant rescue of its mRNA expression after the contemporary silencing of TDP-43 with DAZAP1 using siRNA (Figure 26D).

Regarding BRD8, little information is available in the literature related to its cellular function. However, this protein is know to be a member of bromodomain (BRD)-containing proteins required for genome maintenance, since its depletion was demonstrated to trigger p53-mediated apoptosis (Lashgari et al., 2018). Interestingly, although *BRD8* was identified as a TDP-43 target gene in HEK293 cells (De Conti et al., 2015), in the neuroblastoma cell line the silencing of TDP-43 was not able to induce an effect on *BRD8* expression levels, suggesting a cell-specific effect for this regulation (Figure 26B). Nevertheless, we could observe a slight and not significant overexpression in siDAZAP1 treated cells (Figure 26B).

Taken together these results suggested a strong correlation between TDP-43 function and hnRNPs, especially with regards to DAZAP1 and to hnRNP Q but not for hnRNP R. These data therefore represented the starting point of my further investigations.

First of all, to complete the analysis of the effects of DAZAP1, hnRNP Q and hnRNP R on TDP-43, we assessed whether these could cause changes in TDP-43 protein levels after treatment with siRNAs against each individual hnRNP and *vice-versa* (Figure 22B-E). This was the first item that had to be tested because it has been shown that appropriate expression of TDP-43 is critical for carrying out its cellular functions. In fact, overexpression of TDP-43 was found to be toxic to neurons (Swarup et al., 2011; Li, Ray, Rao, Shi, Guo, Chen and Woodruff, 2010), and also its complete depletion to be lethal for mouse development (Sephton et al., 2010) and *Drosophila* survival (Feiguin et al., 2009). Similarly, the alteration of DAZAP1, hnRNP Q and hnRNP R expression could be linked to tumorigenesis (Lai et al., 2017; Prima and Hunger, 2007). In my experiments, however, I saw that DAZAP1, hnRNP Q and hnRNP R were not able to change TDP-43 protein levels and the expression of each hnRNPs was not influenced after siRNA depletion of TDP-43.

We also looked at the TDP-43 subcellular localization in SH-SY5Y cells following sihnRNP treatment (Figure 27), since one of the most important features of TDP-43 is the ability to shuttle between nucleus and cytoplasm (Ayala et al., 2008). In fact, although most of the protein is physiologically present in nucleus, approximately 30% of TDP-43 is normally found to be localized in cytosol where it participates in regulating mRNA stability, export and localization of newly transcripts (Lagier-Tourenne et al., 2010). However, modification of TDP-43 homeostasis can lead to re-distribution within cells, as described in neurodegeneration processes in which TDP-43 undergoes cytoplasmic accumulation and consequent aggregation (Neumann et al., 2006). In our experiments, however, TDP-43 localization was not disrupted by depletion of DAZAP1, hnRNP Q and hnRNP R.

Therefore, the results achieved so far indicated that the variations in splicing profile and gene expression levels of TDP-43 targets were not dependent on aberrant modifications of basic TDP-43 features, such as protein expression and subcellular localization. In support of these results, I also examined hnRNP effects using a more realistic scenario of TDP-43 pathology and we analysed the capability of endogenous TDP-43 to aggregate in the presence of FLAG-TDP43-12XQ/N aggregates (Figure 28). In this LOF model, the endogenous TDP-43 can fully interact with these aggregates and undergo sequestration into nuclear and cytoplasmic insoluble aggregates (Budini et al., 2014). Basically, we concluded that in cells treated with siRNA against hnRNPs the aggregation propency of TDP-43 was not affected. Furthermore, we were able to confirm our previous results about the rescue of *MADD* and *STAG2* splicing profile, following siDAZAP1 and sihnRNP Q treatment.

Since DAZAP1 was the most consistent modifier of TDP-43 activity and no previous literature has undercovered a possible connection between these two proteins, our interest

then moved into the characterization of the relationship between TDP-43 and DAZAP1. After ascertaining that DAZAP1 was not directly binding to TDP-43 I saw that it could bind all its mRNA targets (Figure 29). Therefore, we decided to identify all the possible targets commonly regulated by knockdown of both proteins through RNA-seq analysis. We found that the depletion of TDP-43 and DAZAP1 prevalently determined an upregulation of genes with respect to the number of downregulated genes (Figure 30A) and the amount of DEGs grouped in the same categories of GO analysis (Figure 33A) were similar in both conditions, indicating therefore the possibility that both proteins could influence the same cellular pathways with an analogous mechanism.

Moreover, these pathways mostly affected genes related to neuronal and inflammation pathways (Figure 30D and Figure 33B), confirming the importance of hnRNPs in the regulation of RNA metabolism in SH-SY5Y cells. In fact, taking a closer look at the regulated genes chosen for qPCR validation and belonging to the top 100 DEGs, we found nine interesting genes associated to brain functions and inflammatory response: *ACHE, STX3, ELAVL3, NOVA2, CELF5, TNF, TNFRSF9, YPEL4* and *ICAM1* (Figure 30B-C). Notably, these genes were found to be upregulated (*ACHE, STX3, CELF5, TNF, TNFRSF9, ICAM1, YPEL4*) and downregulated (*ELAVL3, NOVA2*) in the same direction in both siTDP-43 and siDAZAP1 treated cells, supporting again the idea of a common mechanism of action of these two hnRNPs (Figure 30B).

In this respect, it is therefore worthwhile to better describe the role of these factors in the nervous system:

ELAVL3 (also known as HuC) is a member of the Elav-like family and one of the mammalian homologous of *Drosophila* Elav (Ogawa et al., 2018). The ELAV-like family is composed of four members: three specifically expressed in neurons known as neuronal ELAVL (nELAVL: ELAVL2, ELAVL3 and ELAVL4) and one ubiquitously expressed

(ELAVL1). nELAVL proteins are RNA-binding proteins involved in RNA metabolism, promoting neuronal differentiation. They are also implicated in neurodegenerative diseases, including Alzheimer's and Parkinson's disease (Ogawa et al., 2018). ELAVL3 has been demonstrated to regulate proteins implicated in amino acid biosynthesis, and it plays a role in mRNA stability and in alternative splicing of genes important for synaptic cytoskeletal dynamics (Ince-Dunn et al., 2012). In particular, ELAVL3 affects the alternative splicing of neuronal pre-mRNAs acting with the same dependence on binding position observed for other RBPs such as TDP-43 (Tollervey et al., 2011), PTB (Llorian et al., 2010) and NOVA (Ule et al., 2006). Moreover, ELAVL3 was found to control glutamate levels, a major neurotransmitter in brain (Ince-Dunn et al., 2012).

NOVA2 is a member of the neuronal RBP collectively known as the NOVA family. The major components of this family are NOVA1 and NOVA2. Compared to NOVA1, which is prevalently expressed in hindbrain and ventral spinal cord, NOVA2 was found in neocortex. The NOVA family was also described to be involved in Paraneoplastic Neurodegeneration (PND). Regarding NOVA2, it has been found to modulate ~ 7% of brain-specific splicing events in neocortex (Ule et al., 2005) and successively it has been demonstrated that it is important in the alternative splicing of genes involved in axon guidance (Leggere et al., 2016; Saito et al., 2016).

Acetylcholinesterase (AChE) is a hydrolase encoded by *ACHE* gene that is required for the regulation of cholinergic signalling (Soreq and Seidman, 2001). In the brain, two isoforms are expressed: a soluble and predominant variant called AChE-S (synaptic AChE) and an inducible variant called AChE-R (read-through) (Soreq and Seidman, 2001). While AChE-S can exist in both soluble and membrane-bound forms, AChE-R was found only in a soluble form (Perrier et al., 2002). However, the expression of both those variants occurs in cholinergic neurons (Johnston et al., 1979), astrocytes (Sáez-Valero et al., 2003) and

cholinoceptive neurons (Aubert et al., 1994). Several studies have reported an aberrant production of AChE during the pathogenesis of AD (Navaratnam et al., 1991; Fishman et al., 1986; Whitehouse et al., 1982). In particular, it has been demonstrated that AChE could promote the formation of amyloid-β (Aβ) fibrils binding Aβ protein (Alvarez et al., 1997) and determining neurotoxicity (Muñoz and Inestrosa, 1999). Indeed, increased levels of AChE were reported to speed up Aβ plaque formation in brains of transgenic mice suffering from neurodegeneration (Rees et al., 2003). Moreover, N-glycosylated AChE was found to be overexpressed in the cerebrospinal fluid of patients with AD (Sáez-Valero et al., 1997). Recently, it has been demonstrated that increased levels of N-glycosylated AChE can disrupt the interaction between O-glycosylated β-neurexins and neuroligin-1 determining loss of glutamatergic synapses and accumulation of post-synaptic proteins (Xiang et al., 2014).

Sintaxin 3 (STX3) is a member of SNARE (Soluble *N*-ethylmaleimide Sensitive Factor Attachment Protein Receptor) machinery that in turn is important for the vesicle trafficking in polarized epithelial cells (Jahn and Scheller, 2006). In particular, STX3 is located to apical plasma membranes (Soo Hoo et al., 2016) where it is involved in fusion post-Golgi vesicles with the membrane (Sharma et al., 2006). In 2006, Darios and colleagues demonstrated that the omega-3 and omega-6 polyunsaturated fatty acids (PUFAs) could change the STX3 structure triggering its binding to the syntaxin partner SNAP25 (Synaptosomal-associated Protein of 25 kDa) and therefore strongly stimulating the neurite outgrowth (Darios and Davletov, 2006). In a previous work, our group established an indirect connection between TDP-43 depletion and STX3. In particular, the downregulation of miRNA Let-b induced by loss of TDP-43 could alter the expression of let-7b targets, including STX3 (Buratti et al., 2010).

CELF5 belongs to the Bruno-like (Brunol) proteins and it is one of the mammalian homologues of *Drosophila* Bruno (Good et al., 2000). Successively, the Bruno-like family were collectively referred as CUGBP, Elav-like family (CELF) because of the first two members identified in humans: CUG binding protein (CUG-BP, now called CELF1) and Elav-type RNA Binding Protein 3 (ETR-3, now called CELF2) (Ladd et al., 2001). Overall, this family is composed of six proteins, namely CELF1, CELF2, CELF3, CELF4, CELF5 and CELF6 that are widely expressed in brain even if CELF1 and CELF2 are found in many tissues (Gallo and Spickett, 2010). To date there is little information regarding the function of CELF proteins. However, they seem to regulate the alternative splicing of transcripts expressed in brain and CELF2, CELF3 and CELF5 could also play a role in neuronal development (Ladd, 2013). Regarding CELF5, it was found expressed all over in the brain, albeit low-expression was detected in medulla oblongata and spinal cord (Ladd, 2013). CELF5 was also linked to Myotonic Dystrophy of Type 1 (DM1), since it was observed to modulate the alternative splicing of Tau exon 6 (Leroy et al., 2006).

YPEL4 belongs to the Yippe-like (YPEL) family and contains a Yippe-like domain that is putatively identified as a zing-finger-like, metal-binding domain (Roxström-Lindquist and Faye, 2001). This protein family takes its name from the *Drosophila* counterpart namely *Yippe*, which shares the 76% of similarity with the human cDNA clone (Roxström-Lindquist and Faye, 2001). In human there are five YPEL proteins: YPEL1, YPEL2, YPEL3, YPEL4 and YPEL5 whose functions still remain to be elucidated (Hosono et al., 2004). However, it is known that YPEL4 is expressed in all human tissues and its functions seem to be connected with ETS Domain-containing Protein Elk-1 (Elk-1) /MAPK signalling pathways (Liang et al., 2010) and cell division (Hosono et al., 2004). Moreover, it was identified as a putative gene involved in Schizophrenia (Schizophrenia Working Group of the Psychiatric Genomics Consortium, 2014).

Finally, we also included in our qPCR validation *TNF, ICAM1* and *TNFRSF9* genes.

TNF-α is encoded by the *TNF* gene and it is a pro-inflammatory cytokine implicated in the regulation of the inflammatory response in body and brain (Neniskyte et al., 2014). In healthy brains, it is expressed at low levels but during injuries or in the presence of ischemia and neurodegenerative disorders the levels of TNF-α increased promoting neuronal inflammation (Neniskyte et al., 2014; Santello and Volterra, 2012).

TNF-α is also important for release of the neurotransmitter norepinephrine (NE) in the central nervous system (Ignatowski et al., 1997), as well as it contributes to the synapse plasticity (Stellwagen and Malenka, 2006).

TNFRSF9 (also known as CD137) is a member of the Tumor Necrosis Factor Receptor (TNFR) Superfamily and is found in wide range of tissues, including brain (Reali et al., 2003). In particular, in central nervous system (CNS) is expressed on plasma membrane and cytoplasm of neurons and astrocytes and its upregulation was described to be mediated by Fibroblastic Growth Factor 2 (FGF2) (Reali et al., 2003) and associated with melanoma brain metastasis (Mittelbronn et al., 2014). The reserve signalling between CD137 and its ligand CD137L was reported to inhibit cell survival in mouse neural stem cells (Yun et al., 2013).

ICAM-1 is an adhesion molecules encoded by *ICAM1* gene and produced by endothelial cells. It is important for mediating the transfer of neutrophil into the brain during brain injuries (Hess et al., 1994). Interestingly, it was described to be upregulated in age-dependent neurodegeneration (Miguel-Hidalgo et al., 2007) and localized in amyloid plaques of Alzheimer's patients (Verbeek et al., 1994).

TNF, ICAM1 and *TNFRSF9* genes are very interesting because they are involved inflammation pathways. Indeed, the activation of the immune system is commonly accepted as one of the central mechanisms underlying neurodegeneration, and capable to

modulate it in a beneficial or detrimental manner. Different events can trigger neurodegenerative pathways, including the deposition of misfolded proteins in CNS, the release of toxic components associated with neurons or synapses destruction and the dysregulation of immune system (Glass et al., 2010; Block and Hong, 2005; Wyss-Coray and Mucke, 2002). For example, in ALS pathology, infiltration of leucocytes (mostly T cells) and deposition of IgG were found in motor neurons subjected to injuries (Holmøy, 2008). T cells inflitration could results in neuronal damage or neuronal protective action. Indeed it has been found that they could lead to cells death through release of cytokine and TNF-α (Neumann et al., 2002), or promote neurogenesis by secretion of Brain Derived Neurotrophic Factor (BDNF) supporting motor neuron survival in mice (Serpe et al., 2005). Moreover, increasing levels of several cytokines were also observed in the cerebrospinal fluid of ALS patients with advanced disease, including Transforming Growth Factor Beta (TGF-β) (McGeer and McGeer, 2002).

Overall, my results have demonstrated the potential impact of not well-characterized hnRNPs, in particular DAZAP1 in brain functions and I have linked this activity to genes affected by TDP-43 misregulation. Moreover, my experiments have strengthened the importance of inflammation during neurodegeneration, since many of the DEGs identified following siTDP-43 and siDAZAP1 are related to inflamatory response.

5.2 hnRNP Q and hnRNP R have evolved to perform different functions within cells

The second part of my PhD thesis was focused on the establishment of a functional diversity between to closely related hnRNPs, namely hnRNP Q and hnRNP R in mammalian cells. As described in the paragraph above, these two proteins were able to modulate in a different manner the splicing profile and mRNA expression of TDP-43

controlled genes. The peculiarity of hnRNP Q and hnRNP R is the extreme similarity in their protein sequences, reflecting the fact that in lower organisms, such as *Drosophila,* they are present as one single protein (McDermott et al., 2012). Here, we demonstrated that in SH-SY5Y cells, hnRNP Q and hnRNP R are expressed in different splicing isoforms and also that they show different cell distribution (Figure 35-36). Regarding this issue, I found that the majority of hnRNP Q protein is located in the cytoplasm (Figure 35) and this was confirmed by the expression of the Q1 counterpart in the cytosol fractions (Figure 36A). On the other hand, I identified hnRNP R as mainly expressed in the nucleus (Figure 35), as also confirmed in the nuclear cytoplasm analysis of SH-SY5Y cells (Figure 36B). Moreover, the cellular localization of both proteins was not altered by the downregulation of each other or after cell differentiation into more neuronal-like cells (Figure 37-38). These findings indicate that in mammals hnRNP Q and hnRNP R have differentiated in two distinctive proteins in order to carry out specific functions within cells. In fact, following an RNA-seq analysis of the whole transcriptome status of cells after siRNA depletion of hnRNP Q and hnRNP R, we were able to observe several common but also many unique features associated with the depletion of both these proteins (Figure 43). Regarding hnRNP Q depleted cells, the most enriched in GO terms were related to membrane architecture, while for hnRNP R depleted cells, the most significant GO terms were connected to tissue and system development, as well as cellular signalling. Taken together these data indicate the functionally diversification of this two proteins during evolution. Interestingly, although the amount of DEGs derived from hnRNP Q silencing was similar between up- and downregulated genes (Figure 39A), in cells silenced with siRNA against hnRNP R we observed a prevalently overexpression of target genes (Figure 40A).

Nonetheless, in both the conditions we identified several genes related to neural and inflammatory pathways (Figure 39-40). In particular, our study on hnRNP Q depletion in SH-SY5Y cells suggests a potential role of this factor in the regulation of three immune-related categories of KEGG pathway analysis namely "Rheumatoid arthritis", "Toxoplasmosis" and "Toll-like receptor signalling pathway" that were enriched after its depletion (Figure 44A). Taking a closer look at these three pathways we found that the infection of the parasite Toxoplasma gondii can affect different neuronal cells, including astrocytes and neurons, and trigger a chronic inflammation due to the contemporary action of host immunity and the evasion of the immune response by the parasite (Carruthers and Suzuki, 2007). Interestingly, an epidemiological study indicated that pharmacological therapy with TNF blocking agents used for the treatment of rheumatoid arthritis could be protective against AD (Chou et al., 2016). Finally, the activation of Toll-like receptor (TLR) signalling has been suggested to contribute to neuronal injury in several neurodegenerative disorders, including ALS (Casula et al., 2011), AD (Reed-Geaghan et al., 2009) and multiple sclerosis (Marta et al., 2008; Prinz et al., 2006).

The same KEGG pathway analysis was repeated for hnRNP R DEGs and the results obtained showed not only its engagement in the regulation of inflammatory response but also the participation in brain functions (Figure 44B). Indeed, three main pathways have been identified by this analysis: "Cell adhesion molecules (CAMs)", "Neuroactive ligand-receptor interaction" and ECM-receptor interaction". Intriguingly, in mature neurons, neural CAMs participates to the control of synaptic formation, structure, plasticity, and release of neurotransmitters (Leshchyns'Ka and Sytnyk, 2016). Furthermore, the expression and function of these molecules was found to be changed in neurodegenerative disorders, such as AD (Leshchyns'Ka and Sytnyk, 2016). Other factors involved in the organization of brain architecture are the extracellular matrix (ECM) molecules (Barros et

al., 2011). In fact, ECM molecules are important for preserving the neural stem cell behavior, for providing a scaffold for neuronal migration and for supporting axonal growth and myelination (Barros et al., 2011). Aberrant protein levels of ECM molecules were also described in Parkinson's disease and ALS (He et al., 2013; Lim et al., 1996).

For both hnRNP Q (Figure 39B-C) and hnRNP R (Figure 40B-C), the qPCR validation of DEGs was carried out through the selection of genes that are ranked in the top 100 of most enriched genes and that correlated with the immune response and brain functions.

Taking a closer look at genes regulated by hnRNP Q depletion, we analysed overexpressed genes, such as *PENK, NRG3, KLF4, KLHL4, TNF, ICAM1* and *TNFRSF9*, as well as downregulated genes, such as *RAB26* and *ARHGAP36*. In particular, proenkephalin A (encoded by *PENK* gene) is the opioid peptide precursor of enkephalin peptides. The proteolytic cleavage of this precursor is able to generate neuropeptides, including peptide F, peptide E, Met-enkephalin, Leu-enkephanlin, BAM20 and BAM22, that seem to be involved in nociception (Lembo et al., 2002; Höllt et al., 1982). Proenkephalin A is expressed in the nervous system and in other tissues such as heart, kidney, intestine and skeletal muscle (Denning et al., 2008) and it can be also released from different immune cells (Plotnikoff et al., 1997). Moreover, it has been found that the expression of proenkephalin A could be altered in patients suffering from dementia or acute neuroinflammatory disorders (Ernst et al., 2010).

Neuregulin 3 (encoded by *NRG3* gene) is the neural-enriched member of the Epidermal Growth Factor (EGF) family proteins and it is structurally related to neuregulin 1 (Zhang et al., 1997). In humans, the interaction between neuregulin 3 and the tyrosine kinase Erb4 was associated with synaptogenesis (Müller et al., 2018) and oligodendrocyte survival (Carteron, 2006). In rat, this interaction was also described to promote the development of adult forebrain through the migration and differentiation of precursor progenitors (Anton et

al., 2004). Interestingly, several polymorphisms in the *NRG3* genes were described to be a risk factor for neuropsychiatric disorders (Chen et al., 2009).

Klf4 (encoded by *KLF4* gene) is a transcription factor containing a zing-finger motif that is involved in several cellular functions, including proliferation and differentiation. In particular, together with Oct4, c-Myc and Sox2 is one of the induced pluripotent stem (iPS) genes able to induce cell pluripotency (Takahashi and Yamanaka, 2006), as well as being important for maintaining self-renewal of embryonic stem cells (ESCs) (Hall et al., 2009). Moreover, Klf4 was reported to be a transcription repressor of axon growth of central nervous system neurons (Moore et al., 2009) and the regulation of its production was demonstrated to be critical for the proper formation of mouse cerebral cortex (Qin and Zhang, 2012).

Rab26 (encoded by *RAB26* gene) is a small GTPase belonging to the Rab family. This large Rab family is implicated in the control of vesicle trafficking from their formation to membrane fusion. Although the function of Rab26 is still not fully elucidated, it was reported to localize with presynaptic membrane vesicles in fly neuromuscular junctions and recruit two components of pre-autophagosomal machinary, namely Atg16L1 and Rab33B (Binotti et al., 2015). This observation is particularly intriguing because it suggests a role of hnRNP Q in the recycling of synapse vesicles via autophagy system, thus providing a further link with TDP-43, since the fly orthologous of TDP-43 was demonstrated to be important for the formation of NMJs. Indeed, the generation of TBPH-null allele flies (Feiguin et al., 2009; Godena et al., 2011; Langellotti et al., 2016; Romano et al., 2018) and hTDP43A315T transgenic mouse (Magrané et al., 2013) dramatically induced morphological modifications at synaptic terminals and a strong reduction of synaptic vesicles in the NMJs, respectively.

Furthermore, neuronal expression was also described for both KLHL4 and ARHGAP36

even if possible neuronal implications, including relationship with neurological disorders, are still unknown (Rack et al., 2014; Braybrook et al., 2001).

On the other hand, looking at DEGs obtained from silencing of hnRNP R we validated six overexpressed genes, including *CARTPT, FOSB, JAG1, DUOXA1, HMOX1* and *ICAM5* and four downregulated genes, such as *KCNAB1, SDCBP2, EFEMP1* and *APC5*. Notably, the *CARTPT* gene is responsible for the production of *CART* mRNA whose expression was found to be increased in the rat brain after stimulation with psychomotor agents (Douglass et al., 1995). The resulting CART neuropeptides was successively described to localize with gamma-aminobutyric acid (GABA) (Smith et al., 1999) and substance P (Hubert and Kuhar, 2005), indicating that these species could act as a neurotransmitter.

The *FOSB* gene encodes both FosB and its alternative splicing variant ΔFosB. Both proteins belong to the Fos family of transcription factors and their production can be promoted especially in the nucleus accumbens and dorsal striatum following administration of many drugs (Nestler et al., 2001). Expression of Fos proteins was also detected in dentate gyrus of hippocampus and cerebral cortex (Ohnishi et al., 2011). The activated form of Fos proteins is achieved by the heterodymerization with Jun proteins resulting in the generation of the Active Activator Protein-1 (AP-1) complex that recognizes AP-1 sites in various promoters (Chinenov and Kerppola, 2001). Fosb expression was also discovered to be linked to neurological disorders, since Fosb-null mice highlighted the adult-onset of spontaneous epilepsy (Yutsudo et al., 2013) and exhibited depression-like behaviors (Ohnishi et al., 2011), as well as to neuroinflammation through the regulation of the receptors of the anaphylatoxin C5a: C5AR1 and/or C5AR2 (Nomaru et al., 2014).

The *DUOXA1* gene encodes the maturation factor of DUOX1 (Dual Oxidase 1) that is a member of the NADPH oxidase family (Bedard and Krause, 2007). It has been reported

that NADPH oxidase provides the major source of reactive oxygen species (ROS) essential for inducing neuronal differentiation, neuronal signalling and neurite formation (Munnamalai and Suter, 2009; Tejada-Simon et al., 2005; Knapp and Klann, 2002). In mouse embryonal carcinoma p19 cells, it has been also demonstrated that their neuronal-like differentiation resulted from the interaction between p53 and DUOXA1 (Ostrakhovitch and Semenikhin, 2011). Moreover, an excessive production of ROS by NADH oxidase can trigger neuroinflammation during CNS pathology, as described for Alzheimer's and Parkinson's disease (Kim et al., 2015).

Jagged1 (encoded by the *JAG1* gene) is one of five ligands that participate to the Notch signalling pathway (Grochowski et al., 2016). In mammals, it is widely expressed during development and it is also present in postnatal brain (Irvin et al., 2004; Stump et al., 2002; Jones et al., 2000). In mouse, Jagged1/Notch signalling was found to control oligodendrocyte differentiation and myelination (Wang et al., 1998). Moreover, Jagged1 is essential for the maintenance of neuronal stem cell niche in adult brain (Nyfeler et al., 2005), as well as being important for synaptic signalling (Alberi et al., 2011). Jagged1/Notch signalling is also involved in spatial memory. Indeed, in hippocampus of patients suffering from Alzheimer's disease their expression was found to be altered (Marathe et al., 2017).

Heme oxigenase 1, also known as HO-1 (encoded by the *HMOX1* gene) is the first of three members belonging to the HO family. The production of HO-1 is regulated by stress stimuli, such as UVA irradiation, sodium arsenite and hydrogen peroxide (Keyse and Tyrrell, 1989). Neuronal protection against glutamate-induced oxidative cell death was observed after overexpression of HO-1 (Chen et al., 2001). Notably, upregulation of the *HMOX1* gene was also found in neurons and astrocytes derived from hippocampus, cerebral cortex, and subcortical white matter of Alzheimer's patients, supporting the role of

chronic oxidative stress in the establishment of neuropathological disorders (Schipper et al., 1995).

KCNAB1 (also known as *Kβv1* gene) encodes the subunit β of the shaker-related voltage-gated potassium channel Kv1 (Leicher et al., 1996). Three different splicing isoforms are present for this gene: *Kβv1.1, Kβv1.2* and *Kβv1.3* (Rettig et al., 1994). *Kβv1.2* and *Kβv1.3* are preferentially transcribed in heart, while *Kβv1.1* is expressed in brain, especially in hippocampus and striatum (Rettig et al., 1994). This particular potassium channel is able to inactivate the subunit α, that is the second subunit that constitutes the Kv1 channel. Potassium channels are extremely important for transducing signals in nervous system (Kuang, 2015) and *Kβv1.1* knockout mice showed normal synaptic plasticity but impairment of learning skills (Giese et al., 1998). Furthermore, a specific mutation in *KCNAB1* gene was also found to be the causative agent of epilepsy and developmental disabilities in a Chinese children (Zhang et al., 2015).

Syntenin-2 (encoded by *SDCBP2*) is a novel PDZ (Postsynaptic density protein, Discs-large, Zona occludens) protein able to bind phosphatidylinositol 4,5-bisphosphate (PIP2) (Geeraerts et al., 2013). This protein is encoded by two alternative splicing isoforms, namely 2α and 2β, and it shares ~70% with the most famous syntenin-1 (Koroll et al., 2001), that is a scaffold protein involved in the regulation of the neural membrane architecture (Hirbec et al., 2005). The available literature has not fully elucidated the cellular function of syntenin-2 in depth. However, syntenin-2 isoform 2α was found to interact with the neural cell-adhesion molecules, namely neurexin-1, suggesting a potential role in brain dynamics (Koroll et al., 2001).

Fibulin-3 (encoded by *EFEMP1*) is a calcium-binding ECM protein belonging to the Fibulin protein family (Timpl et al., 2003) consisting of Fibulin-1, Fibulin-2, Fibulin-3, Fibulin-4 and Fibulin-5. These proteins contain three domains, where the central domain

III contains nine epidermal growth factor (EGF)-like motifs able to bind calcium (Timpl et al., 2003). For most fibulin proteins, the interaction with calcium is essential for binding other ECM proteins and cellular receptors, allowing them to carry out their cellular function in joining supramolecular structures such as basement-membrane networks, elastic fibres, several types of microfibrils and proteoglycan aggregates (Timpl et al., 2003). The function of fibulin-3 is still unknown. However, fibulin-3 expression was strongly detected only in the primary visual cortex (V1C) region of prenatal brain (Ayana et al., 2018) while it was found weakly expressed in adult normal brain but upregulated in gliomas where it promotes cell tumor growth and invasion through the regulation of Notch signalling (Hu et al., 2009, 2012). Moreover, a single mutation in EFEMP1 was described to be associated with age-related macular degeneration (Stone et al., 1999).

Finally, we noticed that the silencing of hnRNP Q could lead to the overexpression of three genes related to inflammatory pathways that we previously illustrated to be upregulated in response to siRNA depletion of both *TDP-43* and *DAZAP1*: *ICAM1*, *TNF* and *TNFRSF9*. This finding corroborated our previous results, regarding the ability of DAZAP1 and hnRNP Q to modulate TDP-43 activity in SH-SY5Y cells.

By contrast, the silencing of hnRNP R led to the overexpression of other two immune-related proteins (ICAM5 and ACP5) without inducing a significant alteration of the same inflammatory genes controlled by TDP-43, DAZAP1 and hnRNP Q.

Overall, this second part of the work allowed a better characterization of the functional diversification of hnRNP Q and hnRNP R, highlighting their importance in controlling genes associated with immune system and neuronal development, differentiation and cell signalling. Most importantly, I was able to relate the majority of them to their aberrant regulation during neurodegenerative diseases.

5.3 TDP-43, DAZAP1 and hnRNP Q potentially regulate same transcripts important for ALS pathogenesis

Over the last decades, perturbations of RBP homeostasis have increasingly acquired significance in the pathogenesis of ALS. Especially TDP-43 was the first hnRNP proteins associated with ALS, since in 2006 it was discovered as a component of ubiquitinated cytoplasmic inclusions in brain of patients (Neumann et al., 2006). Subsequent studies have also identified ALS-causative mutations in the TDP-43 encoding gene, and in other members of hnRNP family, including FUS, hnRNP A1, hnRNP A2/B1, TIA-1 and matrin-3 (Purice and Taylor, 2018).

Therefore, the identification of all possible targets regulated by TDP-43 and other hnRNP proteins acting on the same biological pathway could lead to the understanding of the molecular mechanisms behind the onset and progression of neurodegeneration. Thanks to sequencing technologies it has been possible to characterize gene expression changes or splicing variations associated with RBP misregulation (Buratti et al., 2013).

In this study DAZAP1 and hnRNP Q were found to be the most promising tested hnRNPs able to modulate TDP-43 activity. Interestingly, the combination of RNA-seq results obtained after depletion of TDP-43, DAZAP1 and hnRNP Q have highlighted the presence of brain /ALS-related genes commonly affected by these proteins (Figure 45), contributing to expand the list of genes that can potentially affect neurodegeneration.

Table 23 presents some promising genes and summarizes the knowledge already available in literature regarding their relationship with brain function and/or ALS pathology.

Table 23. Genes commonly regulated by depletion of TDP-43, DAZAP1 and hnRNP Q in SH-SY5Y cells which showed an involvement in brain disorders and/or ALS pathology.

Gene Symbol/(Description)	Brain disorders /ALS pathology	References
IGF2 (Insuline-like Growth Factor 2)	IGF-2 could protect against ALS degeneration of human motor neurons derived from iPSCs through phosphorylation of Akt and glycogen synthase kinase-3β and upregulation of β-catenin.	(Allodi et al., 2016)
SYT14 (Synaptotagmin 14)	SYT14 mutations are causative of autosome-recessive spinocerebellar ataxia-11 (SCAR 11).	(Doi et al., 2011)
	t(1;3)(q32.1;q25.1) leads to disruption of SYT14 and it is associated with developmental abnormalities.	(Quintero-Rivera et al., 2007)
ABAT (4-Aminobutyrate Aminotransferase)	Strong expression in neuronal tissue; responsible for catabolism of GABA (neurotransmitter) into succinic semialdehyde. ABAT plays an essential role in the conversion of dNDPs to dNTPs in the mitochondrial nucleoside salvage pathway and causes a neurometabolic disorder that includes encephalomyopathic MDS.	(Besse et al., 2015)
	Identification of ABAT as putative gene in autism following genotype-based association analysis.	(Barnby et al., 2005)
	ABAT was found to be associated with neurofibrillar tangles (NFTs) following genome-wide analysis of 5-hydroxymethylcytosine regions in AD brain.	(Zhao et al., 2017)

ABCC9 (ATP Binding Cassette Subfamily C Member 9)	*ABCC9/SUR2* gene encoded an ATP-sensitive potassium channel that is strongly implicated in human aged-related neurological disorders, including hippocampal sclerosis of aging (HS-Aging).	(Nelson et al., 2015)
ADCY1 (Adenylate Cyclase 1)	*ADCY1* gene encoded an adenylyl cyclase specifically expressed in brain; it was found to be upregulated in frontal cortex of ALS patients. Notably, in our results it was found downregulated in all tested hnRNPs.	(Andrés-Benito et al., 2017)
ADD3 (Adducin 3)	*ADD3* gene encoded γ-adducin subunit of membrane-skeletal protein, namely Adducin. Mutation of ADD3 was found to inhibit the binding of γ-subunit to α-subunit and determinate cerebral palsy. ADD2-knockout mice showed synaptic plasticity, motor coordination and behavioral deficits accompanied by changes in the expression and phosphorylation levels of the α- (ADD1) and γ-adducin (ADD3) subunits. Adducin is highly phosphorylated in spinal cord tissue derived from ALS patients comparing to individuals without neurological disease. Upregulated upon TDP-43 depletion in adult mouse brain.	(Kruer et al., 2013) (Porro et al., 2010) (Hu et al., 2003) (Polymenidou, Lagier-Tourenne, et al., 2011)
CAPN5 (Calpain 5)	CAPN5 has been shown to be the second most abundantly expressed calpain in the mammalian central nervous system.	(Singh et al., 2014)

CASP3 (Caspase 3)	CASP3 is an important mediator of neuronal programmed cell death. It is also associated with chronic neurodegenerative diseases. In transgenic mice expressing mutant SOD1, inhibition of caspase-3 was found to have a protective role in ALS pathology.	(Troy et al., 2011; Ribe et al., 2008; Ekshyyan, O. and Aw, 2004) (Li et al., 2000)
CDK5R1 (Cyclin Dependent Kinase 5 Regulatory Subunit 1)	*CDK5R1* gene encoded p35, the main activator of Cyclin-dependent kinase 5 (CDK5). It has been associated with AD onset and progression. It was found to be upregulated in frontal cortex of ALS patients. Notably, in our results it was found to be downregulated in all tested hnRNPs.	(Spreafico et al., 2018) (Andrés-Benito et al., 2017)
CTSS (Cathepsin S)	Significant increased expression of Cathepsin S (encoded by *CTSS* gene) was found in the anterior lumbar spinal cord in ALS.	(Berjaoui et al., 2015)
TLR7 (Toll Like Receptor 7)	Significant increased expression of TLR7 was found in the anterior lumbar spinal cord in ALS.	(Berjaoui et al., 2015)
DDX58 (DExD/H-Box Helicase 58)	RNA helicase upregulated in ALS mouse model: TDP-43 (A315T) mice. In particular, TDP-43 bound to its mRNA.	(MacNair et al., 2016)

HS3ST2 (Heparan Sulfate-Glucosamine 3-Sulfotransferase 2)	HS3ST2 is an heparan sulfate biosynthetic enzyme showed greatest decreases in expression in FTLD-U human samples.	(Chen-Plotkin et al., 2008)
RAB31 (RAB31, Member RAS Oncogene Family)	GTP-binding protein upregulated upon TDP-43 depletion in adult mouse brain.	(Polymenidou, Lagier-Tourenne, et al., 2011)
PPP1R15A (Protein Phosphatase 1 Regulatory Subunit 15A)	PPP1R15A is also known as GADD34. Mutant SOD1 mice that are haploinsufficient for GADD34 have a remarkably ameliorated disease.	(Wang et al., 2014)

6. CONCLUSION AND FUTURE DIRECTIONS

In conclusion, my work has provided novel insights on the involvement of the hnRNP family in controlling neuronal and inflammatory pathways, suggesting that differential expression of these proteins could play an essential role in modulating the onset and progression of neurodegenerative disorders, especially those related to TDP-43 pathology.

The future direction of this work could examine the synaptic plasticity/death-signalling pathways after overexpression/depletion of neuronal genes identified by RNA-seq analysis of TDP-43, DAZAP1, hnRNP Q using a cellular model of TDP-43 aggregation and/or using iPSC cells derived from patients carrying TDP-43 mutations. This data will be useful to identify the most promising common neuronal targets identified by RNA-seq analysis of TDP-43, DAZAP1, hnRNP Q that can affect neurodegeneration. This task will also be made easier by performing RNA-seq analysis for other hnRNP proteins that our group has demonstrated can "worsen" TDP-43 gain-of-function toxicity in the *Drosophila* eye, namely CG30122 (hnRNP U), Bl/CG13425 (hnRNP K) and Sqd/CG16901 (hnRNP D). This last aim is currently underway and I am also actively involved in taking forward this part of the work.

7. BIBLIOGRAPHY

- Alberi, L., Liu, S., Wang, Y., Badie, R., Smith-Hicks, C., Wu, J., Pierfelice, T. J., Abazyan, B., Mattson, M. P., Kuhl, D., Pletnikov, M., Worley, P. F. and Gaiano, N. (2011) 'Activity-Induced Notch Signaling in Neurons Requires Arc/Arg3.1 and Is Essential for Synaptic Plasticity in Hippocampal Networks', *Neuron*, Elsevier Inc., vol. 69, no. 3, pp. 437–444 [Online]. DOI: 10.1016/j.neuron.2011.01.004.
- Albert, M. L. and Darnell, R. B. (2004) 'Paraneoplastic neurological degenerations: keys to tumour immunity', *Nature Reviews Cancer*, vol. 4, no. 1, pp. 36–44 [Online]. DOI: 10.1038/nrc1255 (Accessed 24 July 2017).
- Allodi, I., Comley, L., Nichterwitz, S., Nizzardo, M., Simone, C., Benitez, J. A., Cao, M., Corti, S. and Hedlund, E. (2016) 'Differential neuronal vulnerability identifies IGF-2 as a protective factor in ALS', *Scientific Reports*, Nature Publishing Group, vol. 6, no. 1, p. 25960 [Online]. DOI: 10.1038/srep25960 (Accessed 18 May 2018).
- Alvarez, A., Opazo, C., Alarcón, R., Garrido, J. and Inestrosa, N. C. (1997) 'Acetylcholinesterase promotes the aggregation of amyloid-β-peptide fragments by forming a complex with the growing fibrils', *Journal of Molecular Biology*, Academic Press, vol. 272, no. 3, pp. 348–361 [Online]. DOI: 10.1006/JMBI.1997.1245 (Accessed 30 December 2018).
- Anantharaman, V., Koonin, E. V and Aravind, L. (2002) 'Comparative genomics and evolution of proteins involved in RNA metabolism', *Nucleic Acids Research*, vol. 30, no. 7, pp. 1427–1464 [Online]. Available at https://www.ncbi.nlm.nih.gov/pmc/articles/PMC101826/pdf/gkf237.pdf (Accessed 17 July 2017).

- Anderson, P. and Kedersha, N. (2009) 'RNA granules: post-transcriptional and epigenetic modulators of gene expression', *Nature Reviews Molecular Cell Biology*, vol. 10, no. 6, pp. 430–436 [Online]. DOI: 10.1038/nrm2694 (Accessed 27 July 2017).
- Andersson, M. K., Ståhlberg, A., Arvidsson, Y., Olofsson, A., Semb, H., Stenman, G., Nilsson, O. and Aman, P. (2008) 'The multifunctional FUS, EWS and TAF15 proto-oncoproteins show cell type-specific expression patterns and involvement in cell spreading and stress response.', *BMC cell biology*, BioMed Central, vol. 9, p. 37 [Online]. DOI: 10.1186/1471-2121-9-37 (Accessed 25 July 2017).
- Andrés-Benito, P., Moreno, J., Aso, E., Povedano, M. and Ferrer, I. (2017) 'Amyotrophic lateral sclerosis, gene deregulation in the anterior horn of the spinal cord and frontal cortex area 8: implications in frontotemporal lobar degeneration.', *Aging*, Impact Journals, LLC, vol. 9, no. 3, pp. 823–851 [Online]. DOI: 10.18632/aging.101195 (Accessed 18 January 2019).
- Anton, E. S., Ghashghaei, H. T., Weber, J. L., McCann, C., Fischer, T. M., Cheung, I. D., Gassmann, M., Messing, A., Klein, R., Schwab, M. H., Lloyd, K. C. K. and Lai, C. (2004) 'Receptor tyrosine kinase ErbB4 modulates neuroblast migration and placement in the adult forebrain', *Nature Neuroscience*, vol. 7, no. 12, pp. 1319–1328 [Online]. DOI: 10.1038/nn1345.
- Appocher, C., Mohagheghi, F., Cappelli, S., Stuani, C., Romano, M., Feiguin, F. and Buratti, E. (2017) 'Major hnRNP proteins act as general TDP-43 functional modifiers both in Drosophila and human neuronal cells', *Nucleic Acids Research*, Oxford University Press, vol. 45, no. 13, pp. 8026–8045 [Online]. DOI: 10.1093/nar/gkx477.
- Arai, T., Hasegawa, M., Akiyama, H., Ikeda, K., Nonaka, T., Mori, H., Mann, D.,

Tsuchiya, K., Yoshida, M., Hashizume, Y. and Oda, T. (2006) 'TDP-43 is a component of ubiquitin-positive tau-negative inclusions in frontotemporal lobar degeneration and amyotrophic lateral sclerosis.', *Biochemical and biophysical research communications*, vol. 351, no. 3, pp. 602–11 [Online]. DOI: 10.1016/j.bbrc.2006.10.093 (Accessed 20 August 2014).

- Aubert, I., Poirier, J., Gauthier, S. and Quirion, R. (1994) 'Multiple cholinergic markers are unexpectedly not altered in the rat dentate gyrus following entorhinal cortex lesions.', *The Journal of neuroscience : the official journal of the Society for Neuroscience*, Society for Neuroscience, vol. 14, no. 5 Pt 1, pp. 2476–84 [Online]. DOI: 10.1523/JNEUROSCI.14-05-02476.1994 (Accessed 30 December 2018).
- Ayala, Y. M., Misteli, T. and Baralle, F. E. (2008) 'TDP-43 regulates retinoblastoma protein phosphorylation through the repression of cyclin-dependent kinase 6 expression.', *Proceedings of the National Academy of Sciences of the United States of America*, National Academy of Sciences, vol. 105, no. 10, pp. 3785–9 [Online]. DOI: 10.1073/pnas.0800546105 (Accessed 28 July 2017).
- Ayala, Y. M., Pantano, S., D'Ambrogio, A., Buratti, E., Brindisi, A., Marchetti, C., Romano, M. and Baralle, F. E. (2005) 'Human, Drosophila, and C.elegans TDP43: nucleic acid binding properties and splicing regulatory function.', *Journal of molecular biology*, vol. 348, no. 3, pp. 575–88 [Online]. DOI: 10.1016/j.jmb.2005.02.038 (Accessed 29 October 2014).
- Ayala, Y. M., Zago, P., D'Ambrogio, A., Xu, Y.-F., Petrucelli, L., Buratti, E. and Baralle, F. E. (2008) 'Structural determinants of the cellular localization and shuttling of TDP-43.', *Journal of cell science*, vol. 121, no. Pt 22, pp. 3778–85 [Online]. DOI: 10.1242/jcs.038950.
- Ayana, R., Singh, S. and Pati, S. (2018) 'Deconvolution of human Brain cell Type

Transcriptomes Unraveled Microglia-specific Potential Biomarkers', *Frontiers in Neurology*, vol. 9, pp. 1–19 [Online]. DOI: 10.3389/fneur.2018.00266.

- Bajenova, O., Stolper, E., Gapon, S., Sundina, N., Zimmer, R. and Thomas, P. (2003) 'Surface expression of heterogeneous nuclear RNA binding protein M4 on Kupffer cell relates to its function as a carcinoembryonic antigen receptor', *Experimental Cell Research*, vol. 291, no. 1, pp. 228–241 [Online]. DOI: 10.1016/S0014-4827(03)00373-2 (Accessed 25 July 2017).
- Bannai, Hiroko, Fukatsu, K., Mizutani, A., Natsume, T., Iemura, S. I., Ikegami, T., Inoue, T. and Mikoshiba, K. (2004) 'An RNA-interacting protein, SYNCRIP (heterogeneous nuclear ribonuclear protein Q1/NSAP1) is a component of mRNA granule transported with inositol 1,4,5-trisphosphate receptor type 1 mRNA in neuronal dendrites', *Journal of Biological Chemistry*, vol. 279, no. 51, pp. 53427–53434 [Online]. DOI: 10.1074/jbc.M409732200.
- Bannai, H, Fukatsu, K., Mizutani, A., Natsume, T., Iemura, S., Ikegami, T., Inoue, T. and Mikoshiba, K. (2004) 'An RNA-interacting protein, SYNCRIP (heterogeneous nuclear ribonuclear protein Q1/NSAP1) is a component of mRNA granule transported with inositol 1,4,5-trisphosphate receptor type 1 mRNA in neuronal dendrites', *J Biol Chem*, vol. 279, no. 51, pp. 53427–53434 [Online]. DOI: 10.1074/jbc.M409732200.
- Baralle, F. E. and Giudice, J. (2017) 'Alternative splicing as a regulator of development and tissue identity', *Nature Publishing Group*, Nature Publishing Group, vol. 18, no. 7, pp. 437–451 [Online]. DOI: 10.1038/nrm.2017.27.
- Barmada, S. J., Serio, A., Arjun, A., Bilican, B., Daub, A., Ando, D. M., Tsvetkov, A., Pleiss, M., Li, X., Peisach, D., Shaw, C., Chandran, S. and Finkbeiner, S. (2014) 'Autophagy induction enhances TDP43 turnover and survival in neuronal

ALS models', *Nature Chemical Biology*, vol. 10, no. 8, pp. 677–685 [Online]. DOI: 10.1038/nchembio.1563.

- Barnby, G., Abbott, A., Sykes, N., Morris, A., Weeks, D. E., Mott, R., Lamb, J., Bailey, A. J. and Monaco, A. P. (2005) 'Candidate-Gene Screening and Association Analysis at the Autism-Susceptibility Locus on Chromosome 16p: Evidence of Association at GRIN2A and ABAT', *The American Journal of Human Genetics*, Cell Press, vol. 76, no. 6, pp. 950–966 [Online]. DOI: 10.1086/430454 (Accessed 18 January 2019).
- Barros, C. S., Franco, S. J. and Müller, U. (2011) 'Extracellular matrix: functions in the nervous system.', *Cold Spring Harbor perspectives in biology*, Cold Spring Harbor Laboratory Press, vol. 3, no. 1, p. a005108 [Online]. DOI: 10.1101/cshperspect.a005108 (Accessed 1 January 2019).
- Bedard, K. and Krause, K.-H. (2007) 'The NOX Family of ROS-Generating NADPH Oxidases: Physiology and Pathophysiology', *Physiological Reviews*, vol. 87, no. 1, pp. 245–313 [Online]. DOI: 10.1152/physrev.00044.2005 (Accessed 3 January 2019).
- Berjaoui, S., Povedano, M., Garcia-Esparcia, P., Carmona, M., Aso, E. and Ferrer, I. (2015) 'Complex Inflammation mRNA-Related Response in ALS Is Region Dependent.', *Neural plasticity*, Hindawi, vol. 2015, p. 573784 [Online]. DOI: 10.1155/2015/573784 (Accessed 18 January 2019).
- Berkowitz, A. S. B. and K. M. (2014) 'The roles of cohesins in mitosis, meiosis, and human health and disease', *Methods Mol Biol*, vol. 1170, pp. 229–266 [Online]. DOI: doi:10.1007/978-1-4939-0888-2_11.
- Besse, A., Wu, P., Bruni, F., Donti, T., Graham, B. H., Craigen, W. J., McFarland, R., Moretti, P., Lalani, S., Scott, K. L., Taylor, R. W. and Bonnen, P. E. (2015)

'The GABA transaminase, ABAT, is essential for mitochondrial nucleoside metabolism', *Cell Metabolism*, Elsevier Inc., vol. 21, no. 3, pp. 417–427 [Online]. DOI: 10.1016/j.cmet.2015.02.008.

- Beyer, A. L., Christensen, M. E., Walker, B. W. and LeStourgeon, W. M. (1977) 'Identification and characterization of the packaging proteins of core 40S hnRNP particles', *Cell*, vol. 11, no. 1, pp. 127–138 [Online]. DOI: 10.1016/0092-8674(77)90323-3 (Accessed 25 July 2017).
- Biamonti, G. and Riva, S. (1994) 'New insights into the auxiliary domains of eukaryotic RNA binding proteins', *FEBS Letters*, vol. 340, no. 1–2, pp. 1–8 [Online]. DOI: 10.1016/0014-5793(94)80162-2 (Accessed 11 July 2017).
- Binotti, B., Pavlos, N. J., Riedel, D., Wenzel, D., Vorbrüggen, G., Schalk, A. M., Kühnel, K., Boyken, J., Erck, C., Martens, H., Chua, J. J. E. and Jahn, R. (2015) 'The GTPase Rab26 links synaptic vesicles to the autophagy pathway.', *eLife*, eLife Sciences Publications, Ltd, vol. 4, p. e05597 [Online]. DOI: 10.7554/eLife.05597 (Accessed 16 April 2018).
- Blanc, V., Navaratnam, N., Henderson, J. O., Anant, S., Kennedy, S., Jarmuz, A., Scott, J. and Davidson, N. O. (2001) 'Identification of GRY-RBP as an apolipoprotein B RNA-binding protein that interacts with both apobec-1 and apobec-1 complementation factor to modulate C to U editing.', *The Journal of biological chemistry*, American Society for Biochemistry and Molecular Biology, vol. 276, no. 13, pp. 10272–83 [Online]. DOI: 10.1074/jbc.M006435200 (Accessed 8 November 2018).
- Block, M. L. and Hong, J.-S. (2005) 'Microglia and inflammation-mediated neurodegeneration: Multiple triggers with a common mechanism', *Progress in Neurobiology*, Pergamon, vol. 76, no. 2, pp. 77–98 [Online]. DOI:

10.1016/J.PNEUROBIO.2005.06.004 (Accessed 8 May 2018).

- Blokhuis, A. M., Koppers, M., Groen, E. J. N., van den Heuvel, D. M. A., Dini Modigliani, S., Anink, J. J., Fumoto, K., van Diggelen, F., Snelting, A., Sodaar, P., Verheijen, B. M., Demmers, J. A. A., Veldink, J. H., Aronica, E., Bozzoni, I., den Hertog, J., van den Berg, L. H. and Pasterkamp, R. J. (2016) 'Comparative interactomics analysis of different ALS-associated proteins identifies converging molecular pathways.', *Acta neuropathologica*, Springer, vol. 132, no. 2, pp. 175–96 [Online]. DOI: 10.1007/s00401-016-1575-8 (Accessed 28 January 2018).
- Brand, A. H. and Perrimon, N. (1993) 'Targeted gene expression as a means of altering cell fates and generating dominant phenotypes', vol. 415, pp. 401–415.
- Braybrook, C., Warry, G., Howell, G., Arnason, A., Bjornsson, A., Moore, G. E., Ross, M. T. and Stanier, P. (2001) 'Identification and characterization of KLHL4, a novel human homologue of the Drosophila Kelch gene that maps within the X-linked cleft palate and ankyloglossia (CPX) critical region', *Genomics*, vol. 72, no. 2, pp. 128–136 [Online]. DOI: 10.1006/geno.2000.6478.
- Briese, M., Saal-Bauernschubert, L., Ji, C., Moradi, M., Ghanawi, H., Uhl, M., Appenzeller, S., Backofen, R. and Sendtner, M. (2018) 'hnRNP R and its main interactor, the noncoding RNA 7SK, coregulate the axonal transcriptome of motoneurons', *Proceedings of the National Academy of Sciences*, vol. 115, no. 12, pp. E2859–E2868 [Online]. DOI: 10.1073/pnas.1721670115.
- Budini, M., Romano, V., Avendaño-Vázquez, S. E., Bembich, S., Buratti, E. and Baralle, F. E. (2012) 'Role of selected mutations in the Q/N rich region of TDP-43 in EGFP-12xQ/N-induced aggregate formation', *Brain Research*, Elsevier B.V., vol. 1462, pp. 139–150 [Online]. DOI: 10.1016/j.brainres.2012.02.031.
- Budini, M., Romano, V., Quadri, Z., Buratti, E. and Baralle, F. E. (2014) 'TDP-43

loss of cellular function through aggregation requires additional structural determinants beyond its C terminal Q/N prion-like domain', *Human molecular genetics*, vol. 24, no. 1, pp. 1–33 [Online]. DOI: 10.1093/hmg/ddu415.

- Buratti, E. and Baralle, F. E. (2001) 'Characterization and functional implications of the RNA binding properties of nuclear factor TDP-43, a novel splicing regulator of CFTR exon 9.', *The Journal of biological chemistry*, vol. 276, no. 39, pp. 36337–43 [Online]. DOI: 10.1074/jbc.M104236200 (Accessed 29 October 2014).
- Buratti, E. and Baralle, F. E. (2008) 'Multiple roles of TDP-43 in gene expression, splicing regulation, and human disease.', *Frontiers in bioscience : a journal and virtual library*, vol. 13, pp. 867–78 [Online]. Available at http://www.ncbi.nlm.nih.gov/pubmed/17981595 (Accessed 27 July 2017).
- Buratti, E. and Baralle, F. E. (2012) 'TDP-43: Gumming up neurons through protein-protein and protein-RNA interactions', *Trends in Biochemical Sciences*, Elsevier Ltd, vol. 37, pp. 237–247 [Online]. DOI: 10.1016/j.tibs.2012.03.003.
- Buratti, E., Brindisi, A., Giombi, M., Tisminetzky, S., Ayala, Y. M. and Baralle, F. E. (2005) 'TDP-43 Binds Heterogeneous Nuclear Ribonucleoprotein A / B through Its C-terminal Tail AN IMPORTANT REGION FOR THE INHIBITION OF CYSTIC FIBROSIS TRANSMEMBRANE', vol. 280, no. 45, pp. 37572–37584 [Online]. DOI: 10.1074/jbc.M505557200.
- Buratti, E., Conti, L. De, Stuani, C., Romano, M., Baralle, M. and Baralle, F. (2010) 'Nuclear factor TDP-43 can affect selected microRNA levels', vol. 1, pp. 2268–2281 [Online]. DOI: 10.1111/j.1742-4658.2010.07643.x.
- Buratti, E., Do, T., Zuccato, E., Pagani, F., Romano, M. and Baralle, F. E. (2001) 'Nuclear factor TDP-43 and SR proteins promote in vitro and in vivo CFTR exon 9 skipping', vol. 20, no. 7.

- Buratti, E., Romano, M. and Baralle, F. E. (2013) 'TDP-43 high throughput screening analyses in neurodegeneration: Advantages and pitfalls', *Molecular and Cellular Neuroscience*, Elsevier Inc., vol. 56, pp. 465–474 [Online]. DOI: 10.1016/j.mcn.2013.03.001.
- Burd, C. G. and Dreyfuss, G. (1994) 'RNA binding specificity of hnRNP A1: significance of hnRNP A1 high-affinity binding sites in pre-mRNA splicing.', *The EMBO journal*, European Molecular Biology Organization, vol. 13, no. 5, pp. 1197–204.
- Busch, A. and Hertel, K. J. (2012) 'Evolution of SR protein and hnRNP splicing regulatory factors.', *Wiley interdisciplinary reviews. RNA*, NIH Public Access, vol. 3, no. 1, pp. 1–12 [Online]. DOI: 10.1002/wrna.100 (Accessed 26 July 2017).
- Cappelli, S., Romano, M. and Buratti, E. (2018) 'Systematic Analysis of Gene Expression Profiles Controlled by hnRNP Q and hnRNP R , Two Closely Related Human RNA Binding Proteins Implicated in mRNA Processing Mechanisms', vol. 5, no. August, pp. 1–17 [Online]. DOI: 10.3389/fmolb.2018.00079.
- Carruthers, V. B. and Suzuki, Y. (2007) 'Effects of Toxoplasma gondii infection on the brain.', *Schizophrenia bulletin*, Oxford University Press, vol. 33, no. 3, pp. 745–51 [Online]. DOI: 10.1093/schbul/sbm008 (Accessed 23 April 2018).
- Carteron, C. (2006) 'Characterization of a neural-specific splicing form of the human neuregulin 3 gene involved in oligodendrocyte survival', *Journal of Cell Science*, vol. 119, no. 5, pp. 898–909 [Online]. DOI: 10.1242/jcs.02799.
- Casula, M., Iyer, A. M., Spliet, W. G. M., Anink, J. J., Steentjes, K., Sta, M., Troost, D. and Aronica, E. (2011) 'Toll-like receptor signaling in amyotrophic lateral sclerosis spinal cord tissue', *Neuroscience*, Elsevier Inc., vol. 179, pp. 233–243 [Online]. DOI: 10.1016/j.neuroscience.2011.02.001.

- Chen-Plotkin, A. S., Geser, F., Plotkin, J. B., Clark, C. M., Kwong, L. K., Yuan, W., Grossman, M., Van Deerlin, V. M., Trojanowski, J. Q. and Lee, V. M.-Y. (2008) 'Variations in the progranulin gene affect global gene expression in frontotemporal lobar degeneration.', *Human molecular genetics*, Oxford University Press, vol. 17, no. 10, pp. 1349–62 [Online]. DOI: 10.1093/hmg/ddn023 (Accessed 18 January 2019).
- Chen, H.-H., Yu, H.-I., Chiang, W.-C., Lin, Y.-D., Shia, B.-C. and Tarn, W.-Y. (2012) 'hnRNP Q Regulates Cdc42-Mediated Neuronal Morphogenesis', *Molecular and Cellular Biology*, vol. 32, no. 12, pp. 2224–2238 [Online]. DOI: 10.1128/MCB.06550-11 (Accessed 10 April 2018).
- Chen, H.-Y., Yu, Y.-H. and Yen, P. H. (2013) 'DAZAP1 regulates the splicing of Crem, Crisp2 and Pot1a transcripts', *Nucleic Acids Research*, Oxford University Press, vol. 41, no. 21, pp. 9858–9869 [Online]. DOI: 10.1093/nar/gkt746 (Accessed 11 May 2018).
- Chen, H. H., Chang, J. G., Lu, R. M., Peng, T. Y. and Tarn, W. Y. (2008) 'The RNA binding protein hnRNP Q modulates the utilization of exon 7 in the survival motor neuron 2 (SMN2) gene', *Mol Cell Biol*, vol. 28, no. 22, pp. 6929–6938 [Online]. DOI: 10.1128/MCB.01332-08.
- Chen, K., Gunter, K. and Maines, M. D. (2001) 'Neurons Overexpressing Heme Oxygenase-1 Resist Oxidative Stress-Mediated Cell Death', *Journal of Neurochemistry*, John Wiley & Sons, Ltd (10.1111), vol. 75, no. 1, pp. 304–313 [Online]. DOI: 10.1046/j.1471-4159.2000.0750304.x (Accessed 3 January 2019).
- Chen, P.-L., Avramopoulos, D., Lasseter, V. K., McGrath, J. A., Fallin, M. D., Liang, K.-Y., Nestadt, G., Feng, N., Steel, G., Cutting, A. S., Wolyniec, P., Pulver, A. E. and Valle, D. (2009) 'Fine mapping on chromosome 10q22-q23 implicates

Neuregulin 3 in schizophrenia.', *American journal of human genetics*, Elsevier, vol. 84, no. 1, pp. 21–34 [Online]. DOI: 10.1016/j.ajhg.2008.12.005 (Accessed 2 January 2019).

- Chinenov, Y. and Kerppola, T. K. (2001) 'Close encounters of many kinds: Fos-Jun interactions that mediate transcription regulatory specificity', *Oncogene*, vol. 20, no. 19, pp. 2438–2452 [Online]. DOI: 10.1038/sj.onc.1204385 (Accessed 2 January 2019).
- Chou, R. C., Kane, M., Ghimire, S., Gautam, S. and Gui, J. (2016) 'Treatment for Rheumatoid Arthritis and Risk of Alzheimer's Disease: A Nested Case-Control Analysis.', *CNS drugs*, NIH Public Access, vol. 30, no. 11, pp. 1111–1120 [Online]. DOI: 10.1007/s40263-016-0374-z (Accessed 31 December 2018).
- Choudhury, R., Roy, S. G., Tsai, Y. S., Tripathy, A., Graves, L. M. and Wang, Z. (2014) 'The splicing activator DAZAP1 integrates splicing control into MEK/Erk-regulated cell proliferation and migration', *Nature Communications*, Nature Publishing Group, vol. 5, p. 3078 [Online]. DOI: 10.1038/ncomms4078 (Accessed 11 May 2018).
- Chung, C. T., Niemela, S. L. and Miller, R. H. (1989) 'One-step preparation of competent Escherichia coli: transformation and storage of bacterial cells in the same solution.', *Proceedings of the National Academy of Sciences of the United States of America*, National Academy of Sciences, vol. 86, no. 7, pp. 2172–5 [Online]. Available at http://www.ncbi.nlm.nih.gov/pubmed/2648393 (Accessed 3 December 2018).
- Colombrita, C., Onesto, E., Buratti, E., de la Grange, P., Gumina, V., Baralle, F. E., Silani, V. and Ratti, A. (2015) 'From transcriptomic to protein level changes in TDP-43 and FUS loss-of-function cell models', *Biochimica et Biophysica Acta* -

Gene Regulatory Mechanisms, Elsevier B.V., vol. 1849, no. 12, pp. 1398–1410 [Online]. DOI: 10.1016/j.bbagrm.2015.10.015.

- Colombrita, C., Zennaro, E., Fallini, C., Weber, M., Sommacal, A., Buratti, E., Silani, V. and Ratti, A. (2009) 'TDP-43 is recruited to stress granules in conditions of oxidative insult', *Journal of Neurochemistry*, vol. 111, no. 4, pp. 1051–1061 [Online]. DOI: 10.1111/j.1471-4159.2009.06383.x.
- De Conti, L., Baralle, M. and Buratti, E. (2016) 'Neurodegeneration and RNA-binding proteins', *Wiley Interdisciplinary Reviews: RNA*, pp. 1–12 [Online]. DOI: 10.1002/wrna.1394.
- Couthouis, J., Hart, M. P., Shorter, J., DeJesus-Hernandez, M., Erion, R., Oristano, R., Liu, A. X., Ramos, D., Jethava, N., Hosangadi, D., Epstein, J., Chiang, A., Diaz, Z., Nakaya, T., Ibrahim, F., Kim, H.-J., Solski, J. A., Williams, K. L., Mojsilovic-Petrovic, J., Ingre, C., Boylan, K., Graff-Radford, N. R., Dickson, D. W., Clay-Falcone, D., Elman, L., McCluskey, L., Greene, R., Kalb, R. G., Lee, V. M.-Y., Trojanowski, J. Q., Ludolph, A., Robberecht, W., Andersen, P. M., Nicholson, G. A., Blair, I. P., King, O. D., Bonini, N. M., Van Deerlin, V., Rademakers, R., Mourelatos, Z. and Gitler, A. D. (2011) 'A yeast functional screen predicts new candidate ALS disease genes.', *Proceedings of the National Academy of Sciences of the United States of America*, National Academy of Sciences, vol. 108, no. 52, pp. 20881–90 [Online]. DOI: 10.1073/pnas.1109434108 (Accessed 25 July 2017).
- D'Alton, S., Altshuler, M. and Lewis, J. (2015) 'Studies of alternative isoforms provide insight into TDP-43 autoregulation and pathogenesis.', *RNA (New York, N.Y.)*, Cold Spring Harbor Laboratory Press, vol. 21, no. 8, pp. 1419–32 [Online]. DOI: 10.1261/rna.047647.114 (Accessed 26 July 2017).
- D'Ambrogio, A., Buratti, E., Stuani, C., Guarnaccia, C., Romano, M., Ayala,

Y. M. and Baralle, F. E. (2009) 'Functional mapping of the interaction between TDP-43 and hnRNP A2 in vivo', *Nucleic Acids Research*, vol. 37, no. 12, pp. 4116–4126 [Online]. DOI: 10.1093/nar/gkp342.

- Dai, T., Vera, Y., Salido, E. C. and Yen, P. H. (2001) 'Characterization of the mouse Dazap1 gene encoding an RNA-binding protein that interacts with infertility factors DAZ and DAZL', *BMC Genomics*, BioMed Central, vol. 2, no. 1, p. 6 [Online]. DOI: 10.1186/1471-2164-2-6 (Accessed 11 May 2018).
- Dalma-Weiszhausz, D. D., Warrington, J., Tanimoto, E. Y. and Miyada, C. G. (2006) '[1] The Affymetrix GeneChip® Platform: An Overview', in *Methods in enzymology*, vol. 410, pp. 3–28 [Online]. DOI: 10.1016/S0076-6879(06)10001-4 (Accessed 28 July 2017).
- Darios, F. and Davletov, B. (2006) 'Omega-3 and omega-6 fatty acids stimulate cell membrane expansion by acting on syntaxin 3', *Nature*, vol. 440, no. 7085, pp. 813–817 [Online]. DOI: 10.1038/nature04598.
- De Conti, L., Akinyi, M. V., Mendoza-Maldonado, R., Romano, M., Baralle, M. and Buratti, E. (2015) 'TDP-43 affects splicing profiles and isoform production of genes involved in the apoptotic and mitotic cellular pathways', *Nucleic Acids Research*, p. gkv814 [Online]. DOI: 10.1093/nar/gkv814.
- Denning, G. M., Ackermann, L. W., Barna, T. J., Armstrong, J. G., Stoll, L. L., Weintraub, N. L. and Dickson, E. W. (2008) 'Proenkephalin expression and enkephalin release are widely observed in non-neuronal tissues', *Peptides*, Elsevier, vol. 29, no. 1, pp. 83–92 [Online]. DOI: 10.1016/J.PEPTIDES.2007.11.004 (Accessed 2 January 2019).
- Doi, H., Yoshida, K., Yasuda, T., Fukuda, M., Fukuda, Y., Morita, H., Ikeda, S., Kato, R., Tsurusaki, Y., Miyake, N., Saitsu, H., Sakai, H., Miyatake, S., Shiina, M.,

Nukina, N., Koyano, S., Tsuji, S., Kuroiwa, Y. and Matsumoto, N. (2011) 'Exome Sequencing Reveals a Homozygous SYT14 Mutation in Adult-Onset, Autosomal-Recessive Spinocerebellar Ataxia with Psychomotor Retardation', *The American Journal of Human Genetics*, Cell Press, vol. 89, no. 2, pp. 320–327 [Online]. DOI: 10.1016/J.AJHG.2011.07.012 (Accessed 17 January 2019).

- Dombert, B., Sivadasan, R., Simon, C. M., Jablonka, S. and Sendtner, M. (2014) 'Presynaptic localization of SMN and hnRNP R in axon terminals of embryonic and postnatal mouse motoneurons', *PLoS ONE*, vol. 9, no. 10 [Online]. DOI: 10.1371/journal.pone.0110846.
- Douglass, J., McKinzie, A. A. and Couceyro, P. (1995) 'PCR differential display identifies a rat brain mRNA that is transcriptionally regulated by cocaine and amphetamine.', *The Journal of neuroscience : the official journal of the Society for Neuroscience*, vol. 15, no. 3 Pt 2, pp. 2471–81 [Online]. Available at http://www.ncbi.nlm.nih.gov/pubmed/7891182 (Accessed 2 January 2019).
- Dreyfuss, G., Do, Y. and Adam, S. A. (1984) 'Characterization of Heterogeneous Nuclear RNA-Protein Complexes In Vivo with Monoclonal Antibodies', vol. 4, no. 6, pp. 1104–1114.
- Dreyfuss, G., Matunis, M. J., Piiiol-roma, S. and Burd, C. G. (1993) 'hnRNP PROTEINS AND THE BIOGENESIS OF mRNA', pp. 289–321.
- van Eersel, J., Ke, Y. D., Gladbach, A., Bi, M., Götz, J., Kril, J. J. and Ittner, L. M. (2011) 'Cytoplasmic Accumulation and Aggregation of TDP-43 upon Proteasome Inhibition in Cultured Neurons', Iijima, K. M. (ed), *PLoS ONE*, Public Library of Science, vol. 6, no. 7, p. e22850 [Online]. DOI: 10.1371/journal.pone.0022850 (Accessed 27 July 2017).
- Ekshyyan, O. and Aw, T. . Y. (2004) 'Apoptosis in acute and chronic neurological

disorders', *Front Biosci.*, vol. 9, pp. 1567–1576 [Online]. DOI: 10.2741/1357.

- Eréndira Avendaño-Vázquez, S., Dhir, A., Bembich, S., Buratti, E., Proudfoot, N. and Baralle, F. E. (2012) 'Autoregulation of TDP-43 mRNA levels involves interplay between transcription, splicing, and alternative polyA site selection', *Genes and Development*, vol. 26, pp. 1679–1684 [Online]. DOI: 10.1101/gad.194829.112.
- Ernst, A., Buerger, K., Hartmann, O., Dodel, R., Noelker, C., Sommer, N., Schwarz, M., Köhrle, J., Bergmann, A. and Hampel, H. (2010) 'Midregional Proenkephalin A and N-terminal Protachykinin A are decreased in the cerebrospinal fluid of patients with dementia disorders and acute neuroinflammation.', *Journal of neuroimmunology*, Elsevier, vol. 221, no. 1–2, pp. 62–7 [Online]. DOI: 10.1016/j.jneuroim.2010.02.004 (Accessed 16 April 2018).
- Fei, T., Chen, Y., Xiao, T., Li, W., Cato, L., Zhang, P., Cotter, M. B., Bowden, M., Lis, R. T., Zhao, S. G., Wu, Q., Feng, F. Y., Loda, M., He, H. H., Liu, X. S. and Brown, M. (2017) 'Genome-wide CRISPR screen identifies HNRNPL as a prostate cancer dependency regulating RNA splicing', *Proceedings of the National Academy of Sciences*, p. 201617467 [Online]. DOI: 10.1073/pnas.1617467114.
- Feiguin, F., Godena, Vinay K., Romano, G., D'Ambrogio, A., Klima, R. and Baralle, F. E. (2009) 'Depletion of TDP-43 affects Drosophila motoneurons terminal synapsis and locomotive behavior', *FEBS Letters*, Federation of European Biochemical Societies, vol. 583, no. 10, pp. 1586–1592 [Online]. DOI: 10.1016/j.febslet.2009.04.019.
- Feiguin, F., Godena, Vinay K, Romano, G., D'Ambrogio, A., Klima, R. and Baralle, F. E. (2009) 'Depletion of TDP-43 affects Drosophila motoneurons terminal synapsis and locomotive behavior.', *FEBS letters*, Federation of European

Biochemical Societies, vol. 583, no. 10, pp. 1586–92 [Online]. DOI: 10.1016/j.febslet.2009.04.019 (Accessed 29 October 2014).

- Feng, Y., He, D., Yao, Z. and Klionsky, D. J. (2014) 'The machinery of macroautophagy', *Cell Research*, Nature Publishing Group, vol. 24, no. 1, pp. 24–41 [Online]. DOI: 10.1038/cr.2013.168 (Accessed 26 July 2017).
- Fiesel, F. C., Voigt, A., Weber, S. S., Van Den Haute, C., Waldenmaier, A., Görner, K., Walter, M., Marlene, A. L., Kern, J. V., Rasse, T. M., Schmidt, T., Springer, W., Kirchner, R., Bonin, M., Neumann, M., Baekelandt, V., Alunni-Fabbroni, M., Schulz, J. B. and Kahle, P. J. (2010) 'Knockdown of transactive response DNA-binding protein (TDP-43) downregulates histone deacetylase 6', *EMBO Journal*, vol. 29, no. 1, pp. 209–221 [Online]. DOI: 10.1038/emboj.2009.324.
- Fiesel, F. C., Weber, S. S., Supper, J., Zell, A. and Kahle, P. J. (2012) 'TDP-43 regulates global translational yield by splicing of exon junction complex component SKAR', *Nucleic Acids Research*, vol. 40, no. 6, pp. 2668–2682 [Online]. DOI: 10.1093/nar/gkr1082.
- Fishman, E. B., Siek, G. C., MacCallum, R. D., Bird, E. D., Volicer, L. and Marquis, J. K. (1986) 'Distribution of the molecular forms of acetylcholinesterase in human brain: Alterations in dementia of the Alzheimer type', *Annals of Neurology*, John Wiley & Sons, Ltd, vol. 19, no. 3, pp. 246–252 [Online]. DOI: 10.1002/ana.410190305 (Accessed 30 December 2018).
- Freibaum, B. D., Chitta, R. K., High, A. A. and Taylor, J. P. (2010) 'Global analysis of TDP-43 interacting proteins reveals strong association with RNA splicing and translation machinery', *Journal of Proteome Research*, vol. 9, no. 2, pp. 1104–1120 [Online]. DOI: 10.1021/pr901076y.

- Fu, C. A., Shen, M., Huang, B. C. B., Lasaga, J., Payan, D. G. and Luo, Y. (1999) 'TNIK, a novel member of the germinal center kinase family that activates the c-Jun N-terminal kinase pathway and regulates the cytoskeleton', *Journal of Biological Chemistry*, vol. 274, no. 43, pp. 30729–30737 [Online]. DOI: 10.1074/jbc.274.43.30729.
- Fuentealba, R. a, Udan, M., Bell, S., Wegorzewska, I., Shao, J., Diamond, M. I., Weihl, C. C. and Baloh, R. H. (2010) 'Interaction with polyglutamine aggregates reveals a Q/N-rich domain in TDP-43.', *The Journal of biological chemistry*, vol. 285, no. 34, pp. 26304–14 [Online]. DOI: 10.1074/jbc.M110.125039 (Accessed 24 September 2014).
- Furukawa, Y., Kaneko, K. and Nukina, N. (2011) 'Molecular properties of TAR DNA binding protein-43 fragments are dependent upon its cleavage site.', *Biochimica et biophysica acta*, Elsevier B.V., vol. 1812, no. 12, pp. 1577–83 [Online]. DOI: 10.1016/j.bbadis.2011.09.005 (Accessed 29 October 2014).
- Gallo, J.-M. and Spickett, C. (2010) 'The role of CELF proteins in neurological disorders.', *RNA biology*, Taylor & Francis, vol. 7, no. 4, pp. 474–9 [Online]. DOI: 10.4161/RNA.7.4.12345 (Accessed 20 December 2018).
- Gama-Carvalho, M. and Carmo-Fonseca, M. (2001) 'The rules and roles of nucleocytoplasmic shuttling proteins', *FEBS Letters*, vol. 498, no. 2–3, pp. 157–163 [Online]. DOI: 10.1016/S0014-5793(01)02487-5 (Accessed 25 July 2017).
- Geeraerts, A., Hsiu-fang, F., Zimmermann, P. and Engelborghs, Y. (2013) 'The Characterization of the Nuclear Dynamics of Syntenin-2 , a PIP 2 Binding PDZ Protein', *Cytometry Part A*, vol. 83, no. 9, pp. 866–875 [Online]. DOI: 10.1002/cyto.a.22246.
- Gerstberger, S., Hafner, M. and Tuschl, T. (2014) 'A census of human RNA-

binding proteins', *Nature Reviews Genetics*, Nature Publishing Group, vol. 15, no. 12, pp. 829–845 [Online]. DOI: 10.1038/nrg3813.

- Geuens, T., Bouhy, D. and Timmerman, V. (2016) 'The hnRNP family: insights into their role in health and disease', *Human Genetics*, Springer Berlin Heidelberg [Online]. DOI: 10.1007/s00439-016-1683-5.
- Giese, K. P., Storm, J. F., Reuter, D., Fedorov, N. B., Shao, L., Leicher, T., Pongs, O. and Silva, A. J. (n.d.) 'Reduced K + Channel Inactivation , Spike Broadening , and After-Hyperpolarization in Kv ␣ 1 . 1-Deficient Mice with Impaired Learning', pp. 257–273.
- Gitler, A. D. and Shorter, J. (2011) 'RNA-binding proteins with prion-like domains in ALS and FTLD-U.', *Prion*, Taylor & Francis, vol. 5, no. 3, pp. 179–87 [Online]. DOI: 10.4161/pri.5.3.17230 (Accessed 26 July 2017).
- Glass, C. K., Saijo, K., Winner, B., Marchetto, M. C. and Gage, F. H. (2010) 'Mechanisms Underlying Inflammation in Neurodegeneration', *Cell*, Cell Press, vol. 140, no. 6, pp. 918–934 [Online]. DOI: 10.1016/J.CELL.2010.02.016 (Accessed 8 May 2018).
- Glatt, S. J., Everall, I. P., Kremen, W. S., Corbeil, J., a ik, R., Khanlou, N., Han, M., Liew, C.-C. and Tsuang, M. T. (2005) 'Comparative gene expression analysis of blood and brain provides concurrent validation of SELENBP1 up-regulation in schizophrenia', *Proceedings of the National Academy of Sciences*, vol. 102, no. 43, pp. 15533–15538 [Online]. DOI: 10.1073/pnas.0507666102.
- Glickman, M. H. and Ciechanover, A. (2002) 'The Ubiquitin-Proteasome Proteolytic Pathway: Destruction for the Sake of Construction', *Physiological Reviews*, vol. 82, no. 2 [Online]. Available at http://physrev.physiology.org/content/82/2/373?ijkey=63f04b37f6b6460d3cb56ea7

e616fd5eebef7e46&keytype2=tf_ipsecsha (Accessed 27 July 2017).

- Glinka, M., Herrmann, T., Funk, N., Havlicek, S., Rossoll, W., Winkler, C. and Sendtner, M. (2010) 'The heterogeneous nuclear ribonucleoprotein-R is necessary for axonal β-actin mRNA translocation in spinal motor neurons', *Human Molecular Genetics*, Oxford University Press, vol. 19, no. 10, pp. 1951–1966 [Online]. DOI: 10.1093/hmg/ddq073 (Accessed 11 November 2018).
- Glisovic, T., Bachorik, J. L., Yong, J. and Dreyfuss, G. (2008) 'RNA-binding proteins and post-transcriptional gene regulation', *FEBS Letters*, vol. 582, no. 14, pp. 1977–1986 [Online]. DOI: 10.1016/j.febslet.2008.03.004.
- Godena, V. K., Romano, G., Romano, M., Appocher, C., Klima, R., Buratti, E., Baralle, F. E. and Feiguin, F. (2011) 'TDP-43 Regulates Drosophila Neuromuscular Junctions Growth by Modulating Futsch/MAP1B Levels and Synaptic Microtubules Organization', Treisman, J. (ed), *PLoS ONE*, Public Library of Science, vol. 6, no. 3, p. e17808 [Online]. DOI: 10.1371/journal.pone.0017808 (Accessed 8 May 2018).
- Goina, E., Skoko, N. and Pagani, F. (2008) 'Binding of DAZAP1 and hnRNPA1/A2 to an Exonic Splicing Silencer in a Natural BRCA1 Exon 18 Mutant', *Molecular and Cellular Biology*, vol. 28, no. 11, pp. 3850–3860 [Online]. DOI: 10.1128/MCB.02253-07.
- Good, P. J., Chen, Q., Warner, S. J. and Herring, D. C. (2000) 'A family of human RNA-binding proteins related to the Drosophila Bruno translational regulator.', *The Journal of biological chemistry*, American Society for Biochemistry and Molecular Biology, vol. 275, no. 37, pp. 28583–92 [Online]. DOI: 10.1074/jbc.M003083200 (Accessed 20 December 2018).
- Gregory, R. I., Yan, K., Amuthan, G., Chendrimada, T., Doratotaj, B., Cooch, N.

and Shiekhattar, R. (2004) 'The Microprocessor complex mediates the genesis of microRNAs', *Nature*, vol. 432, no. 7014, pp. 235–240 [Online]. DOI: 10.1038/nature03120 (Accessed 27 July 2017).

- Grochowski, C. M., Loomes, K. M. and Spinner, N. B. (2016) 'Jagged1 (JAG1): Structure, expression, and disease associations', *Gene*, vol. 576, no. 1, pp. 381–384 [Online]. DOI: 10.1016/j.gene.2015.10.065 (Accessed 3 January 2019).
- Guil, S., Long, J. C. and Caceres, J. F. (2006) 'hnRNP A1 Relocalization to the Stress Granules Reflects a Role in the Stress Response', *Molecular and Cellular Biology*, vol. 26, no. 15, pp. 5744–5758 [Online]. DOI: 10.1128/MCB.00224-06.
- Hadian, K., Vincendeau, M., Mäusbacher, N., Nagel, D., Hauck, S. M., Ueffing, M., Loyter, A., Werner, T., Wolff, H. and Brack-Werner, R. (2009) 'Identification of a heterogeneous nuclear ribonucleoprotein-recognition region in the HIV rev protein', *Journal of Biological Chemistry*, vol. 284, no. 48, pp. 33384–33391 [Online]. DOI: 10.1074/jbc.M109.021659.
- Hall, J., Guo, G., Wray, J., Eyres, I., Nichols, J., Grotewold, L., Morfopoulou, S., Humphreys, P., Mansfield, W., Walker, R., Tomlinson, S. and Smith, A. (2009) 'Oct4 and LIF/Stat3 Additively Induce Krüppel Factors to Sustain Embryonic Stem Cell Self-Renewal', *Cell Stem Cell*, Elsevier Ltd, vol. 5, no. 6, pp. 597–609 [Online]. DOI: 10.1016/j.stem.2009.11.003.
- Halstead, J. M., Lin, Y. Q., Durraine, L., Hamilton, R. S., Ball, G., Neely, G. G., Bellen, H. J. and Davis, I. (2014) 'Syncrip/hnRNP Q influences synaptic transmission and regulates BMP signaling at the Drosophila neuromuscular synapse', *Biology Open*, vol. 3, no. 9, pp. 839–849 [Online]. DOI: 10.1242/bio.20149027.
- Hammer, N. A., Hansen, T. v O., Byskov, A. G., Rajpert-De Meyts, E., Grøndahl,

M. L., Bredkjaer, H. E., Wewer, U. M., Christiansen, J. and Nielsen, F. C. (2005) 'Expression of IGF-II mRNA-binding proteins (IMPs) in gonads and testicular cancer.', *Reproduction (Cambridge, England)*, Society for Reproduction and Fertility, vol. 130, no. 2, pp. 203–12 [Online]. DOI: 10.1530/rep.1.00664 (Accessed 19 July 2017).

- Han, S. P., Tang, Y. H. and Smith, R. (2010) 'Functional diversity of the hnRNPs: past, present and perspectives.', *The Biochemical journal*, vol. 430, no. 3, pp. 379–392 [Online]. DOI: 10.1042/BJ20100396.
- Hanson, K. A., Kim, S. H., Wassarman, D. A. and Tibbetts, R. S. (2010) 'Ubiquilin Modifies TDP-43 Toxicity in a Drosophila Model of Amyotrophic Lateral Sclerosis (ALS) * □', vol. 285, no. 15, pp. 11068–11072 [Online]. DOI: 10.1074/jbc.C109.078527.
- Harris, C. E., Boden, R. A. and Astell, C. R. (1999) 'A novel heterogeneous nuclear ribonucleoprotein-like protein interacts with NS1 of the minute virus of mice.', *Journal of virology*, American Society for Microbiology (ASM), vol. 73, no. 1, pp. 72–80 [Online]. Available at http://www.ncbi.nlm.nih.gov/pubmed/9847309 (Accessed 17 November 2018).
- Hassfeld, W., Chan, E. K. L., Mathison, D. A., Portman, D., Dreyfuss, G., Steiner, G. and Tan, E. M. (1998) 'Molecular definition of heterogeneous nuclear ribonucleoprotein R (hnRNP R) using autoimmune antibody: Immunological relationship with hnRNP P', *Nucleic Acids Research*, vol. 26, no. 2, pp. 439–445 [Online]. DOI: 10.1093/nar/26.2.439.
- He, F., Krans, A., Freibaum, B. D., Taylor, J. P. and Todd, P. K. (2014) 'TDP-43 suppresses CGG repeat-induced neurotoxicity through interactions with HnRNP A2 / B1', vol. 23, no. 19 [Online]. DOI: 10.1093/hmg/ddu216.

- He, X., Zhang, L., Yao, X., Hu, J., Yu, L., Jia, H., An, R., Liu, Z. and Xu, Y. (2013) 'Association Studies of MMP-9 in Parkinson's Disease and Amyotrophic Lateral Sclerosis', Oreja-Guevara, C. (ed), *PLoS ONE*, Public Library of Science, vol. 8, no. 9, p. e73777 [Online]. DOI: 10.1371/journal.pone.0073777 (Accessed 1 January 2019).
- Hess, D. C., Bhutwala, T., Sheppard, J. C., Zhao, W. and Smith, J. (1994) 'ICAM-1 expression on human brain microvascular endothelial cells', *Neuroscience Letters*, Elsevier, vol. 168, no. 1–2, pp. 201–204 [Online]. DOI: 10.1016/0304-3940(94)90450-2 (Accessed 20 December 2018).
- Hirbec, H., Martin, S. and Henley, J. M. (2005) 'Syntenin is involved in the developmental regulation of neuronal membrane architecture', *Molecular and Cellular Neuroscience*, Academic Press, vol. 28, no. 4, pp. 737–746 [Online]. DOI: 10.1016/J.MCN.2004.12.005 (Accessed 16 April 2018).
- Höllt, V., Cankat Tulunay, F., Woo, S. K., Loh, H. H. and Herz, A. (1982) 'Opioid peptides derived from pro-enkphalin A but not that from pro-enkephalin B are substantial analgesics after administration into brain of mice', *European Journal of Pharmacology*, Elsevier, vol. 85, no. 3–4, pp. 355–356 [Online]. DOI: 10.1016/0014-2999(82)90226-6 (Accessed 2 January 2019).
- Holmøy, T. (2008) 'T cells in amyotrophic lateral sclerosis', *European Journal of Neurology*, vol. 15, no. 4, pp. 360–366 [Online]. DOI: 10.1111/j.1468-1331.2008.02065.x (Accessed 6 January 2019).
- Honda, H., Hamasaki, H., Wakamiya, T., Koyama, S., Suzuki, S. O., Fujii, N. and Iwaki, T. (2015) 'Loss of hnRNPA1 in ALS spinal cord motor neurons with TDP-43-positive inclusions', pp. 37–43 [Online]. DOI: 10.1111/neup.12153.
- Hori, T., Taguchi, Y., Uesugi, S. and Kurihara, Y. (2005) 'The RNA ligands for

mouse proline-rich RNA-binding protein (mouse Prrp) contain two consensus sequences in separate loop structure.', *Nucleic acids research*, Oxford University Press, vol. 33, no. 1, pp. 190–200 [Online]. DOI: 10.1093/nar/gki153.

- Hosono, K., Sasaki, T., Minoshima, S. and Shimizu, N. (2004) 'Identification and characterization of a novel gene family YPEL in a wide spectrum of eukaryotic species', *Gene*, Elsevier, vol. 340, no. 1, pp. 31–43 [Online]. DOI: 10.1016/J.GENE.2004.06.014 (Accessed 30 December 2018).
- Van Der Houven Van Oordt, W., Newton, K., Screaton, G. R. and Cáceres, J. F. (2000) 'Role of SR protein modular domains in alternative splicing specificity in vivo', *Nucleic Acids Research*, vol. 28, no. 24, pp. 4822–4831 [Online]. Available at https://www.ncbi.nlm.nih.gov/pubmed/11121472 (Accessed 24 July 2017).
- Hu, B., Nandhu, M. S., Sim, H., Agudelo-garcia, P. A. and Saldivar, J. C. (2012) 'Fibulin-3 promotes glioma growth and resistance through a novel paracrine regulation of Notch signaling', vol. 72, no. 15, pp. 3873–3885 [Online]. DOI: 10.1158/0008-5472.CAN-12-1060.Fibulin-3.
- Hu, B., Thirtamara-rajamani, K. K., Sim, H. and Viapiano, M. S. (2009) 'Fibulin-3 Is Uniquely Upregulated in Malignant Gliomas and Promotes Tumor Cell Motility and Invasion', *Mol Cancer Res*, vol. 7, no. 11, pp. 1756–1771 [Online]. DOI: 10.1158/1541-7786.MCR-09-0207.
- Hu, J. H., Chernoff, K., Pelech, S. and Krieger, C. (2003) 'Protein kinase and protein phosphatase expression in the central nervous system of G93A mSOD over-expressing mice', *Journal of Neurochemistry*, vol. 85, no. 2, pp. 422–431 [Online]. DOI: 10.1046/j.1471-4159.2003.01669.x.
- Huang, C., Xia, P. Y. and Zhou, H. (2010) 'Sustained expression of TDP-43 and FUS in motor neurons in rodent's lifetime.', *International journal of biological*

sciences, Ivyspring International Publisher, vol. 6, no. 4, pp. 396–406 [Online]. Available at http://www.ncbi.nlm.nih.gov/pubmed/20616880 (Accessed 27 July 2017).

- Huang, J., Chen, X., Wu, K. and Ca, P. X. (2005) 'Cloning and expression of a novel isoform of.pdf', vol. 16, no. 7.
- Hubert, G. W. and Kuhar, M. J. (2005) 'Colocalization of CART with substance P but not enkephalin in the rat nucleus accumbens', *Brain Research*, Elsevier, vol. 1050, no. 1–2, pp. 8–14 [Online]. DOI: 10.1016/J.BRAINRES.2005.05.025 (Accessed 4 May 2018).
- Hüttelmaier, S., Zenklusen, D., Lederer, M., Dictenberg, J., Lorenz, M., Meng, X., Bassell, G. J., Condeelis, J. and Singer, R. H. (2005) 'Spatial regulation of β-actin translation by Src-dependent phosphorylation of ZBP1', *Nature*, vol. 438, no. 7067, pp. 512–515 [Online]. DOI: 10.1038/nature04115 (Accessed 24 July 2017).
- Igaz, L. M., Kwong, L. K., Lee, E. B., Chen-plotkin, A., Swanson, E., Unger, T., Malunda, J., Xu, Y., Winton, M. J., Trojanowski, J. Q. and Lee, V. M. (2011) 'Dysregulation of the ALS-associated gene TDP-43 leads to neuronal death and degeneration in mice', vol. 121, no. 2 [Online]. DOI: 10.1172/JCI44867.726.
- Ignatowski, T. A., Noble, B. K., Wright, J. R., Gorfien, J. L., Heffner, R. R. and Spengler, R. N. (1997) 'Neuronal-associated tumor necrosis factor (TNF alpha): its role in noradrenergic functioning and modification of its expression following antidepressant drug administration.', *Journal of neuroimmunology*, vol. 79, no. 1, pp. 84–90 [Online]. Available at http://www.ncbi.nlm.nih.gov/pubmed/9357451 (Accessed 20 December 2018).
- Imai, T., Tokunaga, A., Yoshida, T., Hashimoto, M., Mikoshiba, K., Weinmaster, G., Nakafuku, M. and Okano, H. (2001) 'The neural RNA-binding protein

Musashi1 translationally regulates mammalian numb gene expression by interacting with its mRNA.', *Molecular and cellular biology*, American Society for Microbiology (ASM), vol. 21, no. 12, pp. 3888–900 [Online]. DOI: 10.1128/MCB.21.12.3888-3900.2001 (Accessed 29 August 2018).

- Ince-Dunn, G., Okano, H. J., Jensen, K. B., Park, W.-Y., Zhong, R., Ule, J., Mele, A., Fak, J. J., Yang, C., Zhang, C., Yoo, J., Herre, M., Okano, H., Noebels, J. L. and Darnell, R. B. (2012) 'Neuronal Elav-like (Hu) Proteins Regulate RNA Splicing and Abundance to Control Glutamate Levels and Neuronal Excitability', *Neuron*, Cell Press, vol. 75, no. 6, pp. 1067–1080 [Online]. DOI: 10.1016/J.NEURON.2012.07.009 (Accessed 19 December 2018).
- Irvin, D. K., Nakano, I., Paucar, A. and Kornblum, H. I. (2004) 'Patterns of Jagged1, Jagged2, Delta-like 1 and Delta-like 3 expression during late embryonic and postnatal brain development suggest multiple functional roles in progenitors and differentiated cells', *Journal of Neuroscience Research*, John Wiley & Sons, Ltd, vol. 75, no. 3, pp. 330–343 [Online]. DOI: 10.1002/jnr.10843 (Accessed 3 January 2019).
- Jahn, R. and Scheller, R. H. (2006) 'SNAREs — engines for membrane fusion', *Nature Reviews Molecular Cell Biology*, Nature Publishing Group, vol. 7, no. 9, pp. 631–643 [Online]. DOI: 10.1038/nrm2002 (Accessed 30 December 2018).
- Janssens, J. and Van Broeckhoven, C. (2013) 'Pathological mechanisms underlying TDP-43 driven neurodegeneration in FTLD-ALS spectrum disorders.', *Human molecular genetics*, Oxford University Press, vol. 22, no. R1, pp. R77-87 [Online]. DOI: 10.1093/hmg/ddt349 (Accessed 27 July 2017).
- Jayarama, S., Li, L.-C., Ganesh, L., Mardi, D., Kanteti, P., Hay, N., Li, P. and Prabhakar, B. S. (2014) 'MADD is a downstream target of PTEN in triggering

apoptosis.', *Journal of cellular biochemistry*, NIH Public Access, vol. 115, no. 2, pp. 261–70 [Online]. DOI: 10.1002/jcb.24657 (Accessed 18 December 2018).

- Johnston, M. V, McKinney, M. and Coyle, J. T. (1979) 'Evidence for a cholinergic projection to neocortex from neurons in basal forebrain.', *Proceedings of the National Academy of Sciences of the United States of America*, National Academy of Sciences, vol. 76, no. 10, pp. 5392–6 [Online]. Available at http://www.ncbi.nlm.nih.gov/pubmed/388436 (Accessed 30 December 2018).
- Jones, E. A., Clement-Jones, M. and Wilson, D. I. (2000) 'JAGGED1 expression in human embryos: correlation with the Alagille syndrome phenotype.', *Journal of medical genetics*, BMJ Publishing Group, vol. 37, no. 9, pp. 658–62 [Online]. DOI: 10.1136/JMG.37.9.658 (Accessed 3 January 2019).
- Kabat, J. L., Barberan-Soler, S. and Zahler, A. M. (2009) 'HRP-2, the Caenorhabditis elegans homolog of mammalian heterogeneous nuclear ribonucleoproteins Q and R, is an alternative splicing factor that binds to UCUAUC splicing regulatory elements', *Journal of Biological Chemistry*, vol. 284, no. 42, pp. 28490–28497 [Online]. DOI: 10.1074/jbc.M109.023101.
- Kajita, Y., Nakayama, J., Aizawa, M. and Ishikawa, F. (1995) 'The UUAG-specific RNA binding protein, heterogeneous nuclear ribonucleoprotein D0. Common modular structure and binding properties of the 2xRBD-Gly family.', *The Journal of biological chemistry*, American Society for Biochemistry and Molecular Biology, vol. 270, no. 38, pp. 22167–75 [Online]. DOI: 10.1074/JBC.270.38.22167.
- Kanai, Y., Dohmae, N. and Hirokawa, N. (2004) 'Kinesin Transports RNA: Isolation and Characterization of an RNA-Transporting Granule', *Neuron*, vol. 43, pp. 513–525 [Online]. https://www.ncbi.nlm.nih.gov/pubmed/15312650 (Accessed

25 July 2017).

- Kechavarzi, B. and Janga, S. C. (n.d.) 'Dissecting the expression landscape of RNA-binding proteins in human cancers', [Online]. DOI: 10.1186/gb-2014-15-1-r14 (Accessed 14 July 2017).
- Keene, J. D. (1999) 'Commentary Why is Hu where? Shuttling of early-response-gene messenger RNA subsets', vol. 96, pp. 5–7 [Online]. Available at https://www.ncbi.nlm.nih.gov/pmc/articles/PMC33538/pdf/pq000005.pdf (Accessed 24 July 2017).
- Keene, J. D. (2001) 'Ribonucleoprotein infrastructure regulating the flow of genetic information between the genome and the proteome.', *Proceedings of the National Academy of Sciences of the United States of America*, National Academy of Sciences, vol. 98, no. 13, pp. 7018–24 [Online]. DOI: 10.1073/pnas.111145598 (Accessed 19 July 2017).
- Keyse, S. M. and Tyrrell, R. M. (1989) 'Heme oxygenase is the major 32-kDa stress protein induced in human skin fibroblasts by UVA radiation, hydrogen peroxide, and sodium arsenite.', *Proceedings of the National Academy of Sciences of the United States of America*, National Academy of Sciences, vol. 86, no. 1, pp. 99–103 [Online]. Available at http://www.ncbi.nlm.nih.gov/pubmed/2911585 (Accessed 3 January 2019).
- Kielkopf, C. L., Lücke, S. and Green, M. R. (2004) 'U2AF homology motifs: protein recognition in the RRM world', *Genes & Development*, vol. 18, no. 13, pp. 1513–1526 [Online]. DOI: 10.1101/gad.1206204 (Accessed 21 February 2019).
- Kim, G. H., Kim, J. E., Rhie, S. J. and Yoon, S. (2015) 'The Role of Oxidative Stress in Neurodegenerative Diseases.', *Experimental neurobiology*, Korean Society for Brain and Neural Science, vol. 24, no. 4, pp. 325–40 [Online]. DOI:

10.5607/en.2015.24.4.325 (Accessed 3 January 2019).

- Knapp, L. T. and Klann, E. (2002) 'Role of reactive oxygen species in hippocampal long-term potentiation: Contributory or inhibitory?', *Journal of Neuroscience Research*, vol. 70, no. 1, pp. 1–7 [Online]. DOI: 10.1002/jnr.10371 (Accessed 3 January 2019).
- Koroll, M., Rathjen, F. and Volkmer, H. (2001) 'The neural cell recognition molecule neurofascin interacts with syntenin-1 but not with syntenin-2, both of which reveal self-associating activity.', *J Biol Chem*, vol. 276, no. 14, pp. 10646–10654.
- Kriegenburg, F., Ellgaard, L. and Hartmann-Petersen, R. (2012) 'Molecular chaperones in targeting misfolded proteins for ubiquitin-dependent degradation.', *The FEBS journal*, vol. 279, no. 4, pp. 532–42 [Online]. DOI: 10.1111/j.1742-4658.2011.08456.x (Accessed 17 June 2014).
- Kruer, M. C., Jepperson, T., Dutta, S., Steiner, R. D., Cottenie, E., Sanford, L., Merkens, M., Russman, B. S., Blasco, P. A., Fan, G., Pollock, J., Green, S., Woltjer, R. L., Mooney, C., Kretzschmar, D., Paisán-Ruiz, C. and Houlden, H. (2013) 'Mutations in γ adducin are associated with inherited cerebral palsy.', *Annals of neurology*, Wiley-Blackwell, vol. 74, no. 6, pp. 805–14 [Online]. DOI: 10.1002/ana.23971 (Accessed 18 January 2019).
- Kuang, Q. (2015) 'Structure of potassium channels', *Cellular and Molecular Life Sciences*, Springer Basel, vol. 72, no. 19, pp. 3677–3693 [Online]. DOI: 10.1007/s00018-015-1948-5.
- Kuo, P., Doudeva, L. G., Wang, Y., Shen, C. J. and Yuan, H. S. (2009) 'Structural insights into TDP-43 in nucleic-acid binding and domain interactions', vol. 37, no. 6, pp. 1799–1808 [Online]. DOI: 10.1093/nar/gkp013.

- Ladd, A. N. (2013) 'CUG-BP, Elav-like family (CELF)-mediated alternative splicing regulation in the brain during health and disease', *Molecular and Cellular Neuroscience*, Elsevier Inc., vol. 56, pp. 456–464 [Online]. DOI: 10.1016/j.mcn.2012.12.003.
- Ladd, A. N., Charlet, N. and Cooper, T. A. (2001) 'The CELF family of RNA binding proteins is implicated in cell-specific and developmentally regulated alternative splicing.', *Molecular and cellular biology*, American Society for Microbiology (ASM), vol. 21, no. 4, pp. 1285–96 [Online]. DOI: 10.1128/MCB.21.4.1285-1296.2001 (Accessed 20 December 2018).
- Lagier-Tourenne, C., Polymenidou, M. and Cleveland, D. W. (2010) 'TDP-43 and FUS/TLS: Emerging roles in RNA processing and neurodegeneration', *Human Molecular Genetics*, vol. 19, no. 1, pp. 46–64 [Online]. DOI: 10.1093/hmg/ddq137.
- Lai, C.-H., Huang, Y.-C., Lee, J.-C., Tseng, J. T.-C., Chang, K.-C., Chen, Y.-J., Ding, N.-J., Huang, P.-H., Chang, W.-C., Lin, B.-W., Chen, R.-Y., Wang, Y.-C., Lai, Y.-C. and Hung, L.-Y. (2017) 'Translational upregulation of Aurora-A by hnRNP Q1 contributes to cell proliferation and tumorigenesis in colorectal cancer', *Cell Death & Disease*, Nature Publishing Group, vol. 8, no. 1, pp. e2555–e2555 [Online]. DOI: 10.1038/cddis.2016.479 (Accessed 11 April 2018).
- Langellotti, S., Romano, V., Romano, G., Klima, R., Feiguin, F., Cragnaz, L., Romano, M. and Baralle, F. E. (2016) 'A novel *Drosophila* model of TDP-43 proteinopathies: N-terminal sequences combined with the Q/N domain induce protein functional loss and locomotion defects', *Disease Models & Mechanisms*, vol. 9, no. 6, pp. 659–669 [Online]. DOI: 10.1242/dmm.023382.
- Lashgari, A., Fauteux, M., Maréchal, A. and Gaudreau, L. (2018) 'Cellular Depletion of BRD8 Causes p53-Dependent Apoptosis and Induces a DNA Damage

Response in Non-Stressed Cells', *Scientific Reports*, Nature Publishing Group, vol. 8, no. 1, p. 14089 [Online]. DOI: 10.1038/s41598-018-32323-3 (Accessed 18 December 2018).

- Lee, E. B., Lee, V. M.-Y. and Trojanowski, J. Q. (2011) 'Gains or losses: molecular mechanisms of TDP-43-mediated neurodegeneration', *Nature reviews. Neuroscience*, vol. 13, no. 1, pp. 38–50 [Online]. DOI: 10.1038/nrn3121.Gains.
- Lee, Y. and Rio, D. C. (2015) 'Mechanisms and Regulation of Alternative Pre-mRNA Splicing.', *Annual review of biochemistry*, no. March, pp. 1–33 [Online]. DOI: 10.1146/annurev-biochem-060614-034316.
- Leggere, J. C., Saito, Y., Darnell, R. B., Tessier-Lavigne, M., Junge, H. J. and Chen, Z. (2016) 'NOVA regulates Dcc alternative splicing during neuronal migration and axon guidance in the spinal cord', *eLife*, vol. 5 [Online]. DOI: 10.7554/eLife.14264 (Accessed 20 December 2018).
- Leicher, T., Roeper, J., Weber, K., Wang, X. and Pongs, O. (1996) 'Structural and Functional Characterizatiofiof Human Potassium Channel Subunit Beta1 (KCNA1B)', *Neuropharmacology*, vol. 35, no. 7, pp. 787–795.
- Lembo, P. M. C., Grazzini, E., Groblewski, T., O'donnell, D., Roy, M. O., Zhang, J., Hoffert, C., Cao, J., Schmidt, R., Pelletier, M., Labarre, M., Gosselin, M., Fortin, Y., Banville, D., Shen, S. H., Ström, P., Payza, K., Dray, A., Walker, P. and Ahmad, S. (2002) 'Proenkephalin A gene products activate a new family of sensory neuron-specific GPCRs', *Nature Neuroscience*, vol. 5, no. 3, pp. 201–209 [Online]. DOI: 10.1038/nn815.
- Leroy, O., Wang, J., Maurage, C.-A., Parent, M., Cooper, T., Buée, L., Sergeant, N., Andreadis, A. and Caillet-Boudin, M.-L. (2006) 'Brain-specific change in alternative splicing of Tau exon 6 in myotonic dystrophy type 1', *Biochimica et*

Biophysica Acta (BBA) - Molecular Basis of Disease, vol. 1762, no. 4, pp. 460–467 [Online]. DOI: 10.1016/j.bbadis.2005.12.003 (Accessed 20 December 2018).

- Leshchyns'Ka, I. and Sytnyk, V. (2016) 'Synaptic Cell Adhesion Molecules in Alzheimer's Disease', *Neural Plasticity*, vol. 2016 [Online]. DOI: 10.1155/2016/6427537.
- Li, M., Ona, V. O., Guégan, C., Chen, M., Jackson-Lewis, V., Andrews, L. J., Olszewski, A. J., Stieg, P. E., Lee, J. P., Przedborski, S. and Friedlander, R. M. (2000) 'Functional role of caspase-1 and caspase-3 in an ALS transgenic mouse model.', *Science (New York, N.Y.)*, vol. 288, no. 5464, pp. 335–9 [Online]. Available at http://www.ncbi.nlm.nih.gov/pubmed/10764647 (Accessed 22 January 2019).
- Li, Y., Ray, P., Rao, E. J., Shi, C., Guo, W., Chen, X. and Woodruff, E. A. (2010) 'A Drosophila model for TDP-43 proteinopathy', vol. 107, no. 7 [Online]. DOI: 10.1073/pnas.0913602107.
- Li, Y., Ray, P., Rao, E. J., Shi, C., Guo, W., Chen, X., Woodruff, E. A., Fushimi, K. and Wu, J. Y. (2010) 'A Drosophila model for TDP-43 proteinopathy.', *Proceedings of the National Academy of Sciences of the United States of America*, National Academy of Sciences, vol. 107, no. 7, pp. 3169–74 [Online]. DOI: 10.1073/pnas.0913602107 (Accessed 31 July 2017).
- Liang, P., Wan, Y., Yan, Y., Wang, Y., Luo, N., Deng, Y., Fan, X., Zhou, J., Li, Y., Wang, Z., Yuan, W., Tang, M., Mo, X. and Wu, X. (2010) 'MVP interacts with YPEL4 and inhibits YPEL4-mediated activities of the ERK signal pathway.', *Biochemistry and cell biology = Biochimie et biologie cellulaire*, vol. 88, no. 3, pp. 445–50 [Online]. DOI: 10.1139/o09-166 (Accessed 30 December 2018).
- Lim, G. P., Backstrom, J. R., Cullen, M. J., Miller, C. A., Atkinson, R. D. and

Tökés, Z. A. (1996) 'Matrix Metalloproteinases in the Neocortex and Spinal Cord of Amyotrophic Lateral Sclerosis Patients', *Journal of Neurochemistry*, John Wiley & Sons, Ltd (10.1111), vol. 67, no. 1, pp. 251–259 [Online]. DOI: 10.1046/j.1471-4159.1996.67010251.x (Accessed 1 January 2019).

- Lim, I., Jung, Y., Kim, D. Y. and Kim, K. T. (2016) 'HnRNP q has a suppressive role in the translation of mouse cryptochrome1', *PLoS ONE*, vol. 11, no. 7, pp. 1–13 [Online]. DOI: 10.1371/journal.pone.0159018.
- Lin, M.-J., Cheng, C.-W. and Shen, C.-K. J. (2011) 'Neuronal Function and Dysfunction of Drosophila dTDP', Marion-Poll, F. (ed), *PLoS ONE*, Public Library of Science, vol. 6, no. 6, p. e20371 [Online]. DOI: 10.1371/journal.pone.0020371 (Accessed 25 October 2018).
- Lin, Y.-T., Wen, W.-C. and Yen, P. H. (2012) 'Transcription-dependent nuclear localization of DAZAP1 requires an N-terminal signal', *Biochemical and Biophysical Research Communications*, Academic Press, vol. 428, no. 3, pp. 422–426 [Online]. DOI: 10.1016/J.BBRC.2012.10.076 (Accessed 11 May 2018).
- Lin, Y.-T. and Yen, P. H. (2006) 'A novel nucleocytoplasmic shuttling sequence of DAZAP1, a testis-abundant RNA-binding protein.', *RNA (New York, N.Y.)*, Cold Spring Harbor Laboratory Press, vol. 12, no. 8, pp. 1486–93 [Online]. DOI: 10.1261/rna.42206 (Accessed 11 May 2018).
- Ling, S.-C., Albuquerque, C. P., Han, J. S., Lagier-Tourenne, C., Tokunaga, S., Zhou, H. and Cleveland, D. W. (2010) 'ALS-associated mutations in TDP-43 increase its stability and promote TDP-43 complexes with FUS/TLS.', *Proceedings of the National Academy of Sciences of the United States of America*, National Academy of Sciences, vol. 107, no. 30, pp. 13318–23 [Online]. DOI: 10.1073/pnas.1008227107 (Accessed 24 April 2018).

- Ling, S., Albuquerque, C. P., Seok, J., Lagier-tourenne, C. and Tokunaga, S. (2010) 'ALS-associated mutations in TDP-43 increase its stability and promote TDP-43 complexes with FUS / TLS', [Online]. DOI: 10.1073/pnas.1008227107/-/DCSupplemental.www.pnas.org/cgi/doi/10.1073/pnas.1008227107.
- Llorian, M., Schwartz, S., Clark, T. A., Hollander, D., Tan, L.-Y., Spellman, R., Gordon, A., Schweitzer, A. C., de la Grange, P., Ast, G. and Smith, C. W. J. (2010) 'Position-dependent alternative splicing activity revealed by global profiling of alternative splicing events regulated by PTB', *Nature Structural & Molecular Biology*, Nature Publishing Group, vol. 17, no. 99, pp. 1114–1123 [Online]. DOI: 10.1038/nsmb.1881 (Accessed 22 January 2019).
- Lu, Y., Ferris, J. and Gao, F.-B. (2009) 'Frontotemporal dementia and amyotrophic lateral sclerosis-associated disease protein TDP-43 promotes dendritic branching.', *Molecular brain*, BioMed Central, vol. 2, p. 30 [Online]. DOI: 10.1186/1756-6606-2-30 (Accessed 31 July 2017).
- Lukong, K. E., Chang, K., Khandjian, E. W. and Richard, S. (2008) 'RNA-binding proteins in human genetic disease.', *Trends in genetics : TIG*, vol. 24, no. 8, pp. 416–425 [Online]. DOI: 10.1016/j.tig.2008.05.004.
- Lunde, B. M., Moore, C. and Varani, G. (2007) '{RNA}-binding proteins: modular design for efficient function', *Nat Rev Mol Cell Biol*, vol. 8, no. 6, pp. 479–490 [Online]. DOI: 10.1038/nrm2178.
- MacNair, L., Xiao, S., Miletic, D., Ghani, M., Julien, J.-P., Keith, J., Zinman, L., Rogaeva, E. and Robertson, J. (2016) 'MTHFSD and DDX58 are novel RNA-binding proteins abnormally regulated in amyotrophic lateral sclerosis', *Brain*, vol. 139, no. 1, pp. 86–100 [Online]. DOI: 10.1093/brain/awv308 (Accessed 18 January 2019).

- Magrané, J., Cortez, C., Gan, W., Manfredi, G. and York, N. (2013) 'Abnormal Mitochondrial Transport and Morphology are Common Pathological Denominators in SOD1 and TDP43 ALS Mouse Models Brain and Mind Research Institute , Weill Medical College of Cornell University , Skirball Institute , Department of Physiology and Neu', vol. 8174, pp. 1–43.
- Makeyev, E. V, Zhang, J., Carrasco, M. A. and Maniatis, T. (n.d.) 'The MicroRNA miR-124 Promotes Neuronal Differentiation by Triggering Brain-Specific Alternative Pre-mRNA Splicing', [Online]. DOI: 10.1016/j.molcel.2007.07.015 (Accessed 24 July 2017).
- Marathe, S., Jaquet, M., Annoni, J.-M. and Alberi, L. (2017) 'Jagged1 Is Altered in Alzheimer's Disease and Regulates Spatial Memory Processing', *Frontiers in Cellular Neuroscience*, Frontiers, vol. 11, p. 220 [Online]. DOI: 10.3389/fncel.2017.00220 (Accessed 16 April 2018).
- Maris, C., Dominguez, C. and Allain, F. H. T. (2005) 'The RNA recognition motif, a plastic RNA-binding platform to regulate post-transcriptional gene expression', *FEBS Journal*, Blackwell Science Ltd, vol. 272, no. 9 [Online]. DOI: 10.1111/j.1742-4658.2005.04653.x (Accessed 18 July 2017).
- Marta, M., Andersson, Å., Isaksson, M., Kämpe, O. and Lobell, A. (2008) 'Unexpected regulatory roles of TLR4 and TLR9 in experimental autoimmune encephalomyelitis', *European Journal of Immunology*, vol. 38, no. 2, pp. 565–575 [Online]. DOI: 10.1002/eji.200737187.
- Masuda, K., Marasa, B., Martindale, J. L., Halushka, M. K. and Gorospe, M. (2009) 'Tissue- and age-dependent expression of RNA-binding proteins that influence mRNA turnover and translation.', *Aging*, vol. 1, no. 8, pp. 681–698 [Online]. DOI: 10.18632/aging.100073 (Accessed 19 July 2017).

- Matigian, N., Windus, L., Smith, H., Filippich, C., Pantelis, C., McGrath, J., Mowry, B. and Hayward, N. (2007) 'Expression profiling in monozygotic twins discordant for bipolar disorder reveals dysregulation of the WNT signalling pathway', *Molecular Psychiatry*, vol. 12, no. 9, pp. 815–825 [Online]. DOI: 10.1038/sj.mp.4001998.
- McDermott, S. M., Meignin, C., Rappsilber, J. and Davis, I. (2012) 'Drosophila Syncrip binds the gurken mRNA localisation signal and regulates localised transcripts during axis specification.', *Biology open*, Company of Biologists, vol. 1, no. 5, pp. 488–97 [Online]. DOI: 10.1242/bio.2012885 (Accessed 4 April 2018).
- McDermott, S. M., Yang, L., Halstead, J. M., Hamilton, R. S., Meignin, C. and Davis, I. (2014) 'Drosophila Syncrip modulates the expression of mRNAs encoding key synaptic proteins required for morphology at the neuromuscular junction.', *RNA (New York, N.Y.)*, Cold Spring Harbor Laboratory Press, vol. 20, no. 10, pp. 1593–606 [Online]. DOI: 10.1261/rna.045849.114 (Accessed 9 November 2018).
- McGeer, P. L. and McGeer, E. G. (2002) 'Inflammatory processes in amyotrophic lateral sclerosis', *Muscle & Nerve*, vol. 26, no. 4, pp. 459–470 [Online]. DOI: 10.1002/mus.10191 (Accessed 6 January 2019).
- Meijering, E., Jacob, M., Sarria, J.-C. F., Steiner, P., Hirling, H. and Unser, M. (2004) 'Design and validation of a tool for neurite tracing and analysis in fluorescence microscopy images', *Cytometry*, vol. 58A, no. 2, pp. 167–176 [Online]. DOI: 10.1002/cyto.a.20022 (Accessed 31 July 2018).
- Meininger, I., Griesbach, R. A., Hu, D., Gehring, T., Seeholzer, T., Bertossi, A., Kranich, J., Oeckinghaus, A., Eitelhuber, A. C., Greczmiel, U., Gewies, A., Schmidt-Supprian, M., Ruland, J., Brocker, T., Heissmeyer, V., Heyd, F. and Krappmann, D. (2016) 'Alternative splicing of MALT1 controls signalling and

activation of CD4+ T cells', *Nature Communications*, Nature Publishing Group, vol. 7, p. 11292 [Online]. DOI: 10.1038/ncomms11292 (Accessed 9 April 2018).

- Mercado, P. A., Ayala, Y. M., Romano, M., Buratti, E. and Baralle, F. E. (2005) 'Depletion of TDP 43 overrides the need for exonic and intronic splicing enhancers in the human apoA-II gene', *Nucleic Acids Research*, vol. 33, no. 18, pp. 6000–6010 [Online]. DOI: 10.1093/nar/gki897.
- Miau, L. H., Chang, C. J., Shen, B. J., Tsai, W. H. and Lee, S. C. (1998) 'Identification of heterogeneous nuclear ribonucleoprotein K (hnRNP K) as a repressor of C/EBPbeta-mediated gene activation.', *The Journal of biological chemistry*, American Society for Biochemistry and Molecular Biology, vol. 273, no. 17, pp. 10784–91 [Online]. DOI: 10.1074/JBC.273.17.10784 (Accessed 25 July 2017).
- Michelotti, E. F., Michelotti, G. A., Aronsohn, A. I. and Levens, D. (1996) 'Heterogeneous nuclear ribonucleoprotein K is a transcription factor.', *Molecular and cellular biology*, American Society for Microbiology (ASM), vol. 16, no. 5, pp. 2350–60 [Online]. Available at http://www.ncbi.nlm.nih.gov/pubmed/8628302 (Accessed 26 March 2019).
- Miguel-Hidalgo, J. J., Nithuairisg, S., Stockmeier, C. and Rajkowska, G. (2007) 'Distribution of ICAM-1 immunoreactivity during aging in the human orbitofrontal cortex.', *Brain, behavior, and immunity*, NIH Public Access, vol. 21, no. 1, pp. 100–11 [Online]. DOI: 10.1016/j.bbi.2006.05.001 (Accessed 23 April 2018).
- Miguel, L., Frébourg, T., Campion, D. and Lecourtois, M. (2011) 'Both cytoplasmic and nuclear accumulations of the protein are neurotoxic in Drosophila models of TDP-43 proteinopathies', *Neurobiology of Disease*, vol. 41, no. 2, pp. 398–406 [Online]. DOI: 10.1016/j.nbd.2010.10.007 (Accessed 31 July 2017).

- Mittelbronn, M., Ronellenfitsch, M., Schwarz, H., Weide, B., Baumgarten, P., Bernatz, S., Beschorner, R., Blank, A.-E., Braczynski, A., Harter, P. and Hattingen, E. (2014) 'Tumor necrosis factor receptor superfamily member 9 is upregulated in the endothelium and tumor cells in melanoma brain metastasis', *Neuroimmunology and Neuroinflammation*, vol. 1, no. 3, p. 135 [Online]. DOI: 10.4103/2347-8659.143670.
- Mizutani, A, Fukuda, M., Ibata, K., Shiraishi, Y. and Mikoshiba, K. (2000) 'SYNCRIP, a cytoplasmic counterpart of heterogeneous nuclear ribonucleoprotein R, interacts with ubiquitous synaptotagmin isoforms.', *The Journal of biological chemistry*, American Society for Biochemistry and Molecular Biology, vol. 275, no. 13, pp. 9823–31 [Online]. DOI: 10.1074/JBC.275.13.9823 (Accessed 25 July 2017).
- Mizutani, Akihiro, Fukuda, M., Ibata, K., Shiraishi, Y. and Mikoshiba, K. (2000) 'SYNCRIP, a cytoplasmic counterpart of heterogeneous nuclear ribonucleoprotein R, interacts with ubiquitous synaptotagmin isoforms', *Journal of Biological Chemistry*, vol. 275, no. 13, pp. 9823–9831 [Online]. DOI: 10.1074/jbc.275.13.9823.
- Mizutani, A., Fukuda, M., Niinobe, M. and Mikoshiba, K. (1997) 'Regulation of AP-2-Synaptotagmin Interaction by Inositol High Polyphosphates', vol. 240, pp. 128–131 [Online]. Available at https://www.ncbi.nlm.nih.gov/pubmed/9367896 (Accessed 9 April 2018).
- Mo, Y., Williams, C. and Miller, C. A. (2012) 'DENN/MADD/IG20 Alternative Splicing Changes and Cell Death in Alzheimer's Disease', *Journal of Molecular Neuroscience*, vol. 48, no. 1, pp. 97–110 [Online]. DOI: 10.1007/s12031-012-9782-9 (Accessed 18 December 2018).

- Mohagheghi, F., Prudencio, M., Stuani, C., Cook, C., Jansen-West, K., Dickson, D. W., Petrucelli, L. and Buratti, E. (2016) 'TDP-43 functions within a network of hnRNP proteins to inhibit the production of a truncated human SORT1 receptor.', *Human Molecular Genetics*, vol. 25, no. 949, pp. 1–38 [Online]. DOI: 10.1093/hmg/ddv491.
- Moore, D. L., Blackmore, M. G., Hu, Y., Kaestner, K. H., Bixby, J. L., Lemmon, V. P. and Goldberg, J. L. (2009) 'KLF family members regulate intrinsic axon regeneration ability.', *Science (New York, N.Y.)*, NIH Public Access, vol. 326, no. 5950, pp. 298–301 [Online]. DOI: 10.1126/science.1175737 (Accessed 2 January 2019).
- Morton, S., Yang, H.-T., Moleleki, N., Campbell, D. G., Cohen, P. and Rousseau, S. (2006) 'Phosphorylation of the ARE-binding protein DAZAP1 by ERK2 induces its dissociation from DAZ.', *The Biochemical journal*, Portland Press Ltd, vol. 399, no. 2, pp. 265–73 [Online]. DOI: 10.1042/BJ20060681 (Accessed 1 June 2018).
- Mourelatos, Z, Abel, L., Yong, J., Kataoka, N. and Dreyfuss, G. (2001) 'SMN interacts with a novel family of hnRNP and spliceosomal proteins.', *The EMBO journal*, EMBO Press, vol. 20, no. 19, pp. 5443–52 [Online]. DOI: 10.1093/emboj/20.19.5443 (Accessed 2 May 2018).
- Mourelatos, Zissimos, Abel, L., Yong, J., Kataoka, N. and Dreyfuss, G. (2001) ' Mourelatos et al., 2001 EMBOJ', vol. 20, no. 19, pp. 5443–5452.
- Müller, T., Braud, S., Jüttner, R., Voigt, B. C., Paulick, K., Sheean, M. E., Klisch, C., Gueneykaya, D., Rathjen, F. G., Geiger, J. R., Poulet, J. F. and Birchmeier, C. (2018) 'Neuregulin 3 promotes excitatory synapse formation on hippocampal interneurons.', *The EMBO journal*, European Molecular Biology Organization, vol. 37, no. 17 [Online]. DOI: 10.15252/embj.201798858 (Accessed 1 January 2019).

- Munnamalai, V. and Suter, D. M. (2009) 'Reactive oxygen species regulate F-actin dynamics in neuronal growth cones and neurite outgrowth.', *Journal of neurochemistry*, vol. 108, no. 3, pp. 644–61 [Online]. DOI: 10.1111/j.1471-4159.2008.05787.x (Accessed 3 January 2019).
- Muñoz, F. J. and Inestrosa, N. C. (1999) 'Neurotoxicity of acetylcholinesterase amyloid β-peptide aggregates is dependent on the type of Aβ peptide and the AChE concentration present in the complexes', *FEBS Letters*, John Wiley & Sons, Ltd, vol. 450, no. 3, pp. 205–209 [Online]. DOI: 10.1016/S0014-5793(99)00468-8 (Accessed 30 December 2018).
- Muqit, M. M. K. and Feany, M. B. (2002) 'Modelling neurodegenerative diseases in', vol. 3, no. March.
- Nakashima-Yasuda, H., Uryu, K., Robinson, J., Xie, S. X., Hurtig, H., Duda, J. E., Arnold, S. E., Siderowf, A., Grossman, M., Leverenz, J. B., Woltjer, R., Lopez, O. L., Hamilton, R., Tsuang, D. W., Galasko, D., Masliah, E., Kaye, J., Clark, C. M., Montine, T. J., Lee, V. M.-Y. and Trojanowski, J. Q. (2007) 'Co-morbidity of TDP-43 proteinopathy in Lewy body related diseases', *Acta Neuropathologica*, vol. 114, no. 3, pp. 221–229 [Online]. DOI: 10.1007/s00401-007-0261-2 (Accessed 26 July 2017).
- Navaratnam, D. S., Priddle, J. D., McDonald, B., Esiri, M. M., Robinson, J. R. and Smith, A. D. (1991) 'Anomalous molecular form of acetylcholinesterase in cerebrospinal fluid in histologically diagnosed Alzheimer's disease.', *Lancet (London, England)*, Elsevier, vol. 337, no. 8739, pp. 447–50 [Online]. DOI: 10.1016/0140-6736(91)93391-L (Accessed 30 December 2018).
- Nehls, J., Koppensteiner, H., Brack-Werner, R., Floss, T. and Schindler, M. (2014) 'HIV-1 Replication in Human Immune Cells Is Independent of TAR DNA Binding

Protein 43 (TDP-43) Expression', Poli, G. (ed), *PLoS ONE*, vol. 9, no. 8, p. e105478 [Online]. DOI: 10.1371/journal.pone.0105478 (Accessed 27 July 2017).

- Nelson, P. T., Jicha, G. A., Wang, W.-X., Ighodaro, E., Artiushin, S., Nichols, C. G. and Fardo, D. W. (2015) 'ABCC9/SUR2 in the brain: Implications for hippocampal sclerosis of aging and a potential therapeutic target', *Ageing Research Reviews*, Elsevier, vol. 24, pp. 111–125 [Online]. DOI: 10.1016/J.ARR.2015.07.007 (Accessed 18 January 2019).
- Neniskyte, U., Vilalta, A. and Brown, G. C. (2014) 'Tumour necrosis factor alpha-induced neuronal loss is mediated by microglial phagocytosis.', *FEBS letters*, Elsevier, vol. 588, no. 17, pp. 2952–6 [Online]. DOI: 10.1016/j.febslet.2014.05.046 (Accessed 20 December 2018).
- Nestler, E. J., Barrot, M. and Self, D. W. (2001) 'DeltaFosB: A sustained molecular switch for addiction', *Proc Natl Acad Sci U S A*, vol. 4, no. 20, pp. 11042–11046.
- Neubauer, G., King, A., Rappsilber, J., Calvio, C., Watson, M., Ajuh, P., Sleeman, J., Lamond, A. and Mann, M. (1998) 'Mass spectrometry and EST-database searching allows characterization of the multi-protein spliceosome complex', *Nature Genetics*, vol. 20, no. 1, pp. 46–50 [Online]. DOI: 10.1038/1700.
- Neumann, H., Medana, I. M., Bauer, J. and Lassmann, H. (2002) 'Cytotoxic T lymphocytes in autoimmune and degenerative CNS diseases.', *Trends in neurosciences*, vol. 25, no. 6, pp. 313–9 [Online]. Available at http://www.ncbi.nlm.nih.gov/pubmed/12086750 (Accessed 6 January 2019).
- Neumann, M., Sampathu, D. M., Kwong, L. K., Truax, A. C., Micsenyi, M. C., Chou, T. T., Bruce, J., Schuck, T., Grossman, M., Clark, C. M., McCluskey, L. F., Miller, B. L., Masliah, E., Mackenzie, I. R., Feldman, H., Feiden, W., Kretzschmar, H. a, Trojanowski, J. Q. and Lee, V. M.-Y. (2006) 'Ubiquitinated TDP-43 in

frontotemporal lobar degeneration and amyotrophic lateral sclerosis.', *Science (New York, N.Y.)*, vol. 314, no. 5796, pp. 130–133 [Online]. DOI: 10.1126/science.1134108.

- Nishida, K., Kuwano, Y., Nishikawa, T. and Masuda, K. (2017) 'RNA Binding Proteins and Genome Integrity', pp. 3–5 [Online]. DOI: 10.3390/ijms18071341.
- Nomaru, H., Sakumi, K., Katogi, A., Ohnishi, Y. N., Kajitani, K., Tsuchimoto, D., Nestler, E. J. and Nakabeppu, Y. (2014) 'Fosb gene products contribute to excitotoxic microglial activation by regulating the expression of complement C5a receptors in microglia.', *Glia*, NIH Public Access, vol. 62, no. 8, pp. 1284–98 [Online]. DOI: 10.1002/glia.22680 (Accessed 23 April 2018).
- Nyfeler, Y., Kirch, R. D., Mantei, N., Leone, D. P., Radtke, F., Suter, U. and Taylor, V. (2005) 'Jagged1 signals in the postnatal subventricular zone are required for neural stem cell self-renewal.', *The EMBO journal*, European Molecular Biology Organization, vol. 24, no. 19, pp. 3504–15 [Online]. DOI: 10.1038/sj.emboj.7600816 (Accessed 3 January 2019).
- Ogawa, Y., Kakumoto, K., Yoshida, T., Kuwako, K., Miyazaki, T., Yamaguchi, J., Konno, A., Hata, J., Uchiyama, Y. and Hirai, H. (2018) 'Elavl3 is essential for the maintenance of Purkinje neuron axons', *Scientific Reports*, Springer US, no. January, pp. 1–13 [Online]. DOI: 10.1038/s41598-018-21130-5.
- Ohnishi, Y. N., Ohnishi, Y. H., Hokama, M., Nomaru, H., Yamazaki, K., Tominaga, Y., Sakumi, K., Nestler, E. J. and Nakabeppu, Y. (2011) 'FosB Is Essential for the Enhancement of Stress Tolerance and Antagonizes Locomotor Sensitization by ΔFosB', *Biological Psychiatry*, vol. 70, no. 5, pp. 487–495 [Online]. DOI: 10.1016/j.biopsych.2011.04.021 (Accessed 2 January 2019).
- Ostrakhovitch, E. A. and Semenikhin, O. A. (2011) 'p53-mediated regulation of

neuronal differentiation via regulation of dual oxidase maturation factor 1', *Neuroscience Letters*, Elsevier, vol. 494, no. 1, pp. 80–85 [Online]. DOI: 10.1016/J.NEULET.2011.02.061 (Accessed 16 April 2018).

- Ou, S. H., Wu, F., Harrich, D., García-Martínez, L. F. and Gaynor, R. B. (1995) 'Cloning and characterization of a novel cellular protein, TDP-43, that binds to human immunodeficiency virus type 1 TAR DNA sequence motifs.', *Journal of virology*, vol. 69, no. 6, pp. 3584–96 [Online]. Available at http://www.ncbi.nlm.nih.gov/pubmed/7745706 (Accessed 26 July 2017).
- Oubridge, C., Ito, N., Evans, P. R., Teo, C. H. and Nagai, K. (1994) 'Crystal structure at 1.92 A resolution of the RNA-binding domain of the U1A spliceosomal protein complexed with an RNA hairpin.', *Nature*, vol. 372, no. 6505, pp. 432–8 [Online]. DOI: 10.1038/372432a0 (Accessed 18 July 2017).
- Pan, H.-A., Lin, Y.-S., Lee, K.-H., Huang, J.-R., Lin, Y.-H. and Kuo, P.-L. (2005) 'Expression patterns of the DAZ-associated protein DAZAP1 in rat and human ovaries', *Fertility and Sterility*, Elsevier, vol. 84, pp. 1089–1094 [Online]. DOI: 10.1016/j.fertnstert.2005.03.075 (Accessed 11 May 2018).
- Passoni, M., Conti, L. De, Baralle, M. and Buratti, E. (2012) 'UG Repeats / TDP-43 Interactions near 5 ′ Splice Sites Exert Unpredictable Effects on Splicing Modulation', *Journal of Molecular Biology*, Elsevier Ltd, vol. 415, no. 1, pp. 46–60 [Online]. DOI: 10.1016/j.jmb.2011.11.003.
- Passos, D. O., Quaresma, A. J. C. and Kobarg, J. (2006) 'The methylation of the C-terminal region of hnRNPQ (NSAP1) is important for its nuclear localization', *Biochemical and Biophysical Research Communications*, vol. 346, no. 2, pp. 517–525 [Online]. DOI: 10.1016/j.bbrc.2006.05.152.
- Pastor, T. and Pagani, F. (2011) 'Interaction of hnRNPA1/A2 and DAZAP1 with

an Alu-Derived Intronic Splicing Enhancer Regulates ATM Aberrant Splicing', Cotterill, S. (ed), *PLoS ONE*, Public Library of Science, vol. 6, no. 8, p. e23349 [Online]. DOI: 10.1371/journal.pone.0023349 (Accessed 11 May 2018).

- Peng, Z.-Y., Huang, J., Lee, S.-C., Shi, Y.-L., Chen, X.-H. and Xu, P. (2009) 'The Expression Pattern of Heterogeneous Nuclear Ribonucleoprotein R in Rat Retina', *Neurochemical Research*, Springer US, vol. 34, no. 6, pp. 1083–1088 [Online]. DOI: 10.1007/s11064-008-9878-3 (Accessed 11 November 2018).
- Perrier, A. L., Massoulié, J. and Krejci, E. (2002) 'PRiMA: the membrane anchor of acetylcholinesterase in the brain.', *Neuron*, Elsevier, vol. 33, no. 2, pp. 275–85 [Online]. DOI: 10.1016/S0896-6273(01)00584-0 (Accessed 30 December 2018).
- Pino, I., Vicent, S. and Rey, N. (2003) 'Altered patterns of expression of members of the heterogeneous nuclear ribonucleoprotein (hnRNP) family in lung cancer', vol. 5002, pp. 131–143 [Online]. DOI: 10.1016/S0169-5002(03)00193-4.
- Piñol-Roma, S., Choi, Y. Do, Matunis, M. J. and Dreyfuss, G. (1988) 'Immunopurification of heterogeneous nuclear ribonucleoprotein particles reveals an assortment of RNA-binding proteins', pp. 215–227.
- Piñol-Roma, S. and Dreyfuss, G. (1992) 'Shuttling of pre-mRNA binding proteins between nucleus and cytoplasm', *Nature*, Nature Publishing Group, vol. 355, no. 6362, pp. 730–732 [Online]. DOI: 10.1038/355730a0 (Accessed 25 July 2017).
- Plotnikoff, N. P., Faith, R. E., Murgo, A. J., Herberman, R. B. and Good, R. A. (1997) 'SHORT ANALYTICAL REVIEW Methionine Enkephalin : A New Cytokine — Human Studies', *Clinical Immunology and Immunopathology*, vol. 82, no. 2, pp. 93–101 [Online]. DOI: 10.1006/clin.1996.4287.
- Polymenidou, M., Lagier-Tourenne, C., Hutt, K. R., Huelga, S. C., Moran, J., Liang, T. Y., Ling, S.-C., Sun, E., Wancewicz, E., Mazur, C., Kordasiewicz, H.,

Sedaghat, Y., Donohue, J. P., Shiue, L., Bennett, C. F., Yeo, G. W. and Cleveland, D. W. (2011) 'Long pre-mRNA depletion and RNA missplicing contribute to neuronal vulnerability from loss of TDP-43.', *Nature neuroscience*, NIH Public Access, vol. 14, no. 4, pp. 459–68 [Online]. DOI: 10.1038/nn.2779 (Accessed 28 July 2017).

– Polymenidou, M., Lagier-tourenne, C., Hutt, K. R., Huelga, S. C., Moran, J., Liang, T. Y., Ling, S., Sun, E., Wancewicz, E., Mazur, C., Kordasiewicz, H., Sedaghat, Y., Donohue, J. P., Shiue, L., Bennett, C. F., Yeo, G. W. and Cleveland, D. W. (2011) 'Long pre-mRNA depletion and RNA missplicing contribute to neuronal vulnerability from loss of', *Nature Publishing Group*, Nature Publishing Group, vol. 14, no. 4, pp. 459–468 [Online]. DOI: 10.1038/nn.2779.

– Porro, F., Rosato-Siri, M., Leone, E., Costessi, L., Iaconcig, A., Tongiorgi, E. and Muro, A. F. (2010) 'β-adducin (Add2) KO mice show synaptic plasticity, motor coordination and behavioral deficits accompanied by changes in the expression and phosphorylation levels of the α- and γ-adducin subunits', *Genes, Brain and Behavior*, John Wiley & Sons, Ltd (10.1111), vol. 9, no. 1, pp. 84–96 [Online]. DOI: 10.1111/j.1601-183X.2009.00537.x (Accessed 18 January 2019).

– Prima, V., Gore, L., Caires, A., Boomer, T., Yoshinari, M., Imaizumi, M., Varella-Garcia, M. and Hunger, S. P. (2005) 'Cloning and functional characterization of MEF2D/DAZAP1 and DAZAP1/MEF2D fusion proteins created by a variant t(1;19)(q23;p13.3) in acute lymphoblastic leukemia', *Leukemia*, Nature Publishing Group, vol. 19, no. 5, pp. 806–813 [Online]. DOI: 10.1038/sj.leu.2403684 (Accessed 11 May 2018).

– Prima, V. and Hunger, S. P. (2007) 'Cooperative transformation by MEF2D/DAZAP1 and DAZAP1/MEF2D fusion proteins generated by the variant

t(1;19) in acute lymphoblastic leukemia', *Leukemia*, Nature Publishing Group, vol. 21, no. 12, pp. 2470–2475 [Online]. DOI: 10.1038/sj.leu.2404962 (Accessed 11 May 2018).

- Prinz, M., Garbe, F., Schmidt, H., Mildner, A., Gutcher, I., Wolter, K., Piesche, M., Schroers, R., Weiss, E., Kirschning, C. J., Rochford, C. D. P., Brück, W. and Becher, B. (2006) 'Innate immunity mediated by TLR9 modulates pathogenicity in an animal model of multiple sclerosis', *Journal of Clinical Investigation*, vol. 116, no. 2, pp. 456–464 [Online]. DOI: 10.1172/JCI26078.
- Purice, M. D. and Taylor, J. P. (2018) 'Linking hnRNP function to ALS and FTD pathology', *Frontiers in Neuroscience*, vol. 12, no. MAY, pp. 1–12 [Online]. DOI: 10.3389/fnins.2018.00326.
- Qin, S. and Zhang, C.-L. (2012) 'Role of Kruppel-like factor 4 in neurogenesis and radial neuronal migration in the developing cerebral cortex.', *Molecular and cellular biology*, American Society for Microbiology, vol. 32, no. 21, pp. 4297–305 [Online]. DOI: 10.1128/MCB.00838-12 (Accessed 8 May 2018).
- Quaresma, A. J. C., Bressan, G. C., Gava, L. M., Lanza, D. C. F., Ramos, C. H. . and Kobarg, J. (2009) 'Human hnRNP Q re-localizes to cytoplasmic granules upon PMA, thapsigargin, arsenite and heat-shock treatments', *Experimental Cell Research*, Academic Press, vol. 315, no. 6, pp. 968–980 [Online]. DOI: 10.1016/J.YEXCR.2009.01.012 (Accessed 6 November 2018).
- Quesnel-Vallières, M., Irimia, M., Cordes, S. P. and Blencowe, B. J. (2015) 'Essential roles for the splicing regulator nSR100/SRRM4 during nervous system development', *Genes & Development*, vol. 29, no. 7, pp. 746–759 [Online]. DOI: 10.1101/gad.256115.114 (Accessed 24 July 2017).
- Quintero-Rivera, F., Chan, A., Donovan, D. J., Gusella, J. F. and Ligon, A. H.

(2007) ‘Disruption of a synaptotagmin (SYT14) associated with neurodevelopmental abnormalities’, *American Journal of Medical Genetics Part A*, John Wiley & Sons, Ltd, vol. 143A, no. 6, pp. 558–563 [Online]. DOI: 10.1002/ajmg.a.31618 (Accessed 17 January 2019).

- R. Suzanne Zukin1 *, Joel D. Richter2 and Claudia Bagni3, 4 (2009) ‘Signals, synapses, and synthesis: how new proteins control plasticity’, *Frontiers in neuronal circuits*, vol. 3:14 [Online]. DOI: 10.3389/neuro.04.014.2009 (Accessed 24 July 2017).
- Rack, P. G., Ni, J., Payumo, A. Y., Nguyen, V., Crapster, J. A., Hovestadt, V., Kool, M., Jones, D. T. W., Mich, J. K., Firestone, A. J., Pfister, S. M., Cho, Y.-J. and Chen, J. K. (2014) ‘Arhgap36-dependent activation of Gli transcription factors.’, *Proceedings of the National Academy of Sciences of the United States of America*, National Academy of Sciences, vol. 111, no. 30, pp. 11061–6 [Online]. DOI: 10.1073/pnas.1322362111 (Accessed 16 April 2018).
- Reali, C., Curto, M., Sogos, V., Scintu, F., Pauly, S., Schwarz, H. and Gremo, F. (2003) ‘Expression of CD137 and its ligand in human neurons, astrocytes, and microglia: Modulation by FGF-2’, *Journal of Neuroscience Research*, John Wiley & Sons, Ltd, vol. 74, no. 1, pp. 67–73 [Online]. DOI: 10.1002/jnr.10727 (Accessed 20 December 2018).
- Reches, A., Nachmani, D., Berhani, O., Duev-Cohen, A., Shreibman, D., Ophir, Y., Seliger, B. and Mandelboim, O. (2016) ‘HNRNPR Regulates the Expression of Classical and Nonclassical MHC Class I Proteins’, *The Journal of Immunology*, vol. 196, no. 12, pp. 4967–4976 [Online]. DOI: 10.4049/jimmunol.1501550.
- Reed-Geaghan, E. G., Savage, J. C., Hise, A. G. and Landreth, G. E. (2009) ‘CD14 and Toll-Like Receptors 2 and 4 Are Required for Fibrillar A -Stimulated

Microglial Activation', *Journal of Neuroscience*, vol. 29, no. 38, pp. 11982–11992 [Online]. DOI: 10.1523/JNEUROSCI.3158-09.2009.

- Rees, T., Hammond, P. ., Soreq, H., Younkin, S. and Brimijoin, S. (2003) 'Acetylcholinesterase promotes beta-amyloid plaques in cerebral cortex', *Neurobiology of Aging*, Elsevier, vol. 24, no. 6, pp. 777–787 [Online]. DOI: 10.1016/S0197-4580(02)00230-0 (Accessed 30 December 2018).
- Rettig, J., Heinemann, S. H., Wunder, F., Lorra, C., Parcej, D. N., Dolly, O. J. and Pongs, O. (1994) 'Inactivation properties of voltage-gated K+ channels altered by presence of beta-subunit', *Nature*, vol. 369, no. 6478, pp. 289–294.
- Reuter, J. A., Spacek, D. V and Snyder, M. P. (2015) 'High-throughput sequencing technologies.', *Molecular cell*, NIH Public Access, vol. 58, no. 4, pp. 586–97 [Online]. DOI: 10.1016/j.molcel.2015.05.004 (Accessed 29 March 2019).
- Reynolds, N. and Cooke, H. J. (2005) 'Role of the DAZ genes in male fertility', *Reproductive BioMedicine Online*, vol. 10, no. 1, pp. 72–80 [Online]. DOI: 10.1016/S1472-6483(10)60806-1 (Accessed 19 July 2017).
- Ribe, E. M., Serrano-Saiz, E., Akpan, N. and Troy, C. M. (2008) 'Mechanisms of neuronal death in disease: defining the models and the players.', *The Biochemical journal*, Portland Press Limited, vol. 415, no. 2, pp. 165–82 [Online]. DOI: 10.1042/BJ20081118 (Accessed 18 January 2019).
- Ritson, G. P., Custer, S. K., Freibaum, B. D., Guinto, J. B., Geffel, D., Moore, J., Tang, W., Winton, M. J., Neumann, M., Trojanowski, J. Q., Lee, V. M.-Y., Forman, M. S. and Taylor, J. P. (2010) 'TDP-43 mediates degeneration in a novel Drosophila model of disease caused by mutations in VCP/p97.', *The Journal of neuroscience : the official journal of the Society for Neuroscience*, Society for Neuroscience, vol. 30, no. 22, pp. 7729–39 [Online]. DOI:

10.1523/JNEUROSCI.5894-09.2010 (Accessed 29 October 2018).

- Robbins, J., Dilwortht, S. M., Laskey, R. A. and Dingwall, C. (1991) 'Two interdependent basic domains in nucleoplasmin nuclear targeting sequence: Identification of a class of bipartite nuclear targeting sequence', *Cell*, vol. 64, no. 3, pp. 615–623 [Online]. DOI: 10.1016/0092-8674(91)90245-T.
- Robinow, S. and White, K. (1991) 'Characterization and spatial distribution of the ELAV protein duringDrosophila melanogaster development', *Journal of Neurobiology*, Wiley Subscription Services, Inc., A Wiley Company, vol. 22, no. 5, pp. 443–461 [Online]. DOI: 10.1002/neu.480220503 (Accessed 24 July 2017).
- Robinson, M. D. and Oshlack, A. (2010) 'A scaling normalization method for differential expression analysis of RNA-seq data',.
- Romano, G., Holodkov, N., Klima, R., Grilli, F., Guarnaccia, C., Nizzardo, M., Rizzo, F., Garcia, R. and Feiguin, F. (2018) 'Downregulation of glutamic acid decarboxylase in Drosophila TDP- 43-null brains provokes paralysis by affecting the organization of the neuromuscular synapses', *Scientific Reports*, vol. 8, no. 1, pp. 1–12 [Online]. DOI: 10.1038/s41598-018-19802-3.
- Romano, M. and Buratti, E. (2013) 'Targeting RNA Binding Proteins Involved in Neurodegeneration', *Journal of Biomolecular Screening*, vol. 18, no. 9, pp. 967–983 [Online]. DOI: 10.1177/1087057113497256.
- Romano, M., Buratti, E., Romano, G., Klima, R., Del, L., Belluz, B., Stuani, C., Baralle, F. and Feiguin, F. (2014) 'Evolutionarily Conserved Heterogeneous Nuclear Ribonucleoprotein (hnRNP) A / B Proteins Functionally Interact with Human and Drosophila TAR DNA-binding Protein 43 (TDP-43) *', vol. 289, no. 10, pp. 7121–7130 [Online]. DOI: 10.1074/jbc.M114.548859.
- Romano, M., Feiguin, F. and Buratti, E. (2012) 'Drosophila Answers to TDP-43

Proteinopathies.', *Journal of amino acids*, vol. 2012, p. 356081 [Online]. DOI: 10.1155/2012/356081.

- Rossoll, W., Kröning, A.-K., Ohndorf, U.-M., Steegborn, C., Jablonka, S. and Sendtner, M. (2002) 'Specific interaction of Smn, the spinal muscular atrophy determining gene product, with hnRNP-R and gry-rbp/hnRNP-Q: a role for Smn in RNA processing in motor axons?', *Human Molecular Genetics*, vol. 11, no. 1, pp. 93–105 [Online]. DOI: 10.1093/hmg/11.1.93.
- Roxström-Lindquist, K. and Faye, I. (2001) 'The Drosophila gene Yippee reveals a novel family of putative zinc binding proteins highly conserved among eukaryotes.', *Insect molecular biology*, vol. 10, no. 1, pp. 77–86 [Online]. Available at http://www.ncbi.nlm.nih.gov/pubmed/11240639 (Accessed 30 December 2018).
- Sáez-Valero, J., Fodero, L. R., White, A. R., Barrow, C. J. and Small, D. H. (2003) 'Acetylcholinesterase is increased in mouse neuronal and astrocyte cultures after treatment with β-amyloid peptides', *Brain Research*, Elsevier, vol. 965, no. 1–2, pp. 283–286 [Online]. DOI: 10.1016/S0006-8993(02)04159-8 (Accessed 30 December 2018).
- Sáez-Valero, J., Sberna, G., McLean, C. A., Masters, C. L. and Small, D. H. (1997) 'Glycosylation of acetylcholinesterase as diagnostic marker for Alzheimer's disease.', *Lancet (London, England)*, Elsevier, vol. 350, no. 9082, p. 929 [Online]. DOI: 10.1016/S0140-6736(97)24039-0 (Accessed 30 December 2018).
- Saito, Y., Miranda-Rottmann, S., Ruggiu, M., Park, C. Y., Fak, J. J., Zhong, R., Duncan, J. S., Fabella, B. A., Junge, H. J., Chen, Z., Araya, R., Fritzsch, B., Hudspeth, A. J. and Darnell, R. B. (2016) 'NOVA2-mediated RNA regulation is required for axonal pathfinding during development', *eLife*, vol. 5 [Online]. DOI:

10.7554/eLife.14371 (Accessed 20 December 2018).

- Santello, M. and Volterra, A. (2012) 'TNFα in synaptic function: Switching gears', *Trends in Neurosciences*, vol. 35, no. 10, pp. 638–647 [Online]. DOI: 10.1016/j.tins.2012.06.001.
- Sasaki, K., Suzuki, A., Kagatsume, S., Ono, M., Matsuzawa, K., Taguchi, Y. and Kurihara, Y. (2012) 'Acetylation of Prrp K150 regulates the subcellular localization', *Gene*, Elsevier B.V., vol. 491, no. 1, pp. 13–19 [Online]. DOI: 10.1016/j.gene.2011.09.022.
- Schipper, H. M., Cissé, S. and Stopa, E. G. (1995) 'Expression of heme oxygenase-1 in the senescent and alzheimer-diseased brain', *Annals of Neurology*, vol. 37, no. 6, pp. 758–768 [Online]. DOI: 10.1002/ana.410370609.
- Schizophrenia Working Group of the Psychiatric Genomics Consortium, S. W. G. of the P. G., Ripke, S., Neale, B. M., Corvin, A., Walters, J. T., Farh, K.-H., Holmans, P. A., Lee, P., Bulik-Sullivan, B., Collier, D. A., Huang, H., Pers, T. H., Agartz, I., Agerbo, E., Albus, M., Alexander, M., Amin, F., Bacanu, S. A., Begemann, M., Belliveau, R. A., Jr, Bene, J., Bergen, S. E., Bevilacqua, E., Bigdeli, T. B., Black, D. W., Bruggeman, R., Buccola, N. G., Buckner, R. L., Byerley, W., Cahn, W., Cai, G., Campion, D., Cantor, R. M., Carr, V. J., Carrera, N., Catts, S. V, Chambert, K. D., Chan, R. C., Chan, R. Y., Chen, E. Y., Cheng, W., Cheung, E. F., Chong, S. A., Cloninger, C. R., Cohen, D., Cohen, N., Cormican, P., Craddock, N., Crowley, J. J., Curtis, D., Davidson, M., Davis, K. L., Degenhardt, F., Favero, J. Del, Demontis, D., Dikeos, D., Dinan, T., Djurovic, S., Donohoe, G., Drapeau, E., Duan, J., Dudbridge, F., Durmishi, N., Eichhammer, P., Eriksson, J., Escott-Price, V., Essioux, L., Fanous, A. H., Farrell, M. S., Frank, J., Franke, L., Freedman, R., Freimer, N. B., Friedl, M., Friedman, J. I., Fromer, M.,

Genovese, G., Georgieva, L., Giegling, I., Giusti-Rodríguez, P., Godard, S., Goldstein, J. I., Golimbet, V., Gopal, S., Gratten, J., Haan, L. de, Hammer, C., Hamshere, M. L., Hansen, M., Hansen, T., Haroutunian, V., Hartmann, A. M., Henskens, F. A., Herms, S., Hirschhorn, J. N., Hoffmann, P., Hofman, A., Hollegaard, M. V, Hougaard, D. M., Ikeda, M., Joa, I., Julià, A., Kahn, R. S., Kalaydjieva, L., Karachanak-Yankova, S., Karjalainen, J., Kavanagh, D., Keller, M. C., Kennedy, J. L., Khrunin, A., Kim, Y., Klovins, J., Knowles, J. A., Konte, B., Kucinskas, V., Kucinskiene, Z. A., Kuzelova-Ptackova, H., Kähler, A. K., Laurent, C., Lee, J., Lee, S. H., Legge, S. E., Lerer, B., Li, M., Li, T., Liang, K.-Y., Lieberman, J., Limborska, S., Loughland, C. M., Lubinski, J., Lönnqvist, J., Macek, M., Magnusson, P. K., Maher, B. S., Maier, W., Mallet, J., Marsal, S., Mattheisen, M., Mattingsdal, M., McCarley, R. W., McDonald, C., McIntosh, A. M., Meier, S., Meijer, C. J., Melegh, B., Melle, I., Mesholam-Gately, R. I., Metspalu, A., Michie, P. T., Milani, L., Milanova, V., Mokrab, Y., Morris, D. W., Mors, O., Murphy, K. C., Murray, R. M., Myin-Germeys, I., Müller-Myhsok, B., Nelis, M., Nenadic, I., Nertney, D. A., Nestadt, G., Nicodemus, K. K., Nikitina-Zake, L., Nisenbaum, L., Nordin, A., O'Callaghan, E., O'Dushlaine, C., O'Neill, F. A., Oh, S.-Y., Olincy, A., Olsen, L., Os, J. Van, Consortium, P. E. I., Pantelis, C., Papadimitriou, G. N., Papiol, S., Parkhomenko, E., Pato, M. T., Paunio, T., Pejovic-Milovancevic, M., Perkins, D. O., Pietiläinen, O., Pimm, J., Pocklington, A. J., Powell, J., Price, A., Pulver, A. E., Purcell, S. M., Quested, D., Rasmussen, H. B., Reichenberg, A., Reimers, M. A., Richards, A. L., Roffman, J. L., Roussos, P., Ruderfer, D. M., Salomaa, V., Sanders, A. R., Schall, U., Schubert, C. R., Schulze, T. G., Schwab, S. G., Scolnick, E. M., Scott, R. J., Seidman, L. J., Shi, J., Sigurdsson, E., Silagadze, T., Silverman, J. M., Sim, K., Slominsky, P., Smoller, J. W., So, H.-C., Spencer, C.

C. A., Stahl, E. A., Stefansson, H., Steinberg, S., Stogmann, E., Straub, R. E., Strengman, E., Strohmaier, J., Stroup, T. S., Subramaniam, M., Suvisaari, J., Svrakic, D. M., Szatkiewicz, J. P., Söderman, E., Thirumalai, S., Toncheva, D., Tosato, S., Veijola, J., Waddington, J., Walsh, D., Wang, D., Wang, Q., Webb, B. T., Weiser, M., Wildenauer, D. B., Williams, N. M., Williams, S., Witt, S. H., Wolen, A. R., Wong, E. H., Wormley, B. K., Xi, H. S., Zai, C. C., Zheng, X., Zimprich, F., Wray, N. R., Stefansson, K., Visscher, P. M., 2, W. T. C.-C. C., Adolfsson, R., Andreassen, O. A., Blackwood, D. H., Bramon, E., Buxbaum, J. D., Børglum, A. D., Cichon, S., Darvasi, A., Domenici, E., Ehrenreich, H., Esko, T., Gejman, P. V, Gill, M., Gurling, H., Hultman, C. M., Iwata, N., Jablensky, A. V, Jönsson, E. G., Kendler, K. S., Kirov, G., Knight, J., Lencz, T., Levinson, D. F., Li, Q. S., Liu, J., Malhotra, A. K., McCarroll, S. A., McQuillin, A., Moran, J. L., Mortensen, P. B., Mowry, B. J., Nöthen, M. M., Ophoff, R. A., Owen, M. J., Palotie, A., Pato, C. N., Petryshen, T. L., Posthuma, D., Rietschel, M., Riley, B. P., Rujescu, D., Sham, P. C., Sklar, P., Clair, D. S., Weinberger, D. R., Wendland, J. R., Werge, T., Daly, M. J., Sullivan, P. F. and O'Donovan, M. C. (2014) 'Biological insights from 108 schizophrenia-associated genetic loci.', *Nature*, Europe PMC Funders, vol. 511, no. 7510, pp. 421–7 [Online]. DOI: 10.1038/nature13595 (Accessed 30 December 2018).

- Scotter, E. L., Chen, H.-J. and Shaw, C. E. (2015) 'TDP-43 Proteinopathy and ALS: Insights into Disease Mechanisms and Therapeutic Targets', *Neurotherapeutics* [Online]. DOI: 10.1007/s13311-015-0338-x.
- Sen, G. L. and Blau, H. M. (2005) 'Argonaute 2/RISC resides in sites of mammalian mRNA decay known as cytoplasmic bodies', *Nature Cell Biology*, Nature Publishing Group, vol. 7, no. 6, pp. 633–636 [Online]. DOI:

10.1038/ncb1265 (Accessed 27 July 2017).

- Sephton, C. F., Cenik, C., Kucukural, A., Dammer, E. B., Cenik, B., Han, Y., Dewey, C. M., Roth, F. P., Herz, J., Peng, J., Moore, M. J. and Yu, G. (2011) 'Identification of neuronal RNA targets of TDP-43-containing ribonucleoprotein complexes', *Journal of Biological Chemistry*, vol. 286, no. 2, pp. 1204–1215 [Online]. DOI: 10.1074/jbc.M110.190884.
- Sephton, C. F., Good, S. K., Atkin, S., Dewey, C. M., Mayer, P., Herz, J. and Yu, G. (2010) 'TDP-43 Is a Developmentally Regulated Protein Essential for Early Embryonic Development', *Journal of Biological Chemistry*, vol. 285, no. 9, pp. 6826–6834 [Online]. DOI: 10.1074/jbc.M109.061846 (Accessed 27 July 2017).
- Serpe, C. J., Byram, S. C., Sanders, V. M. and Jones, K. J. (2005) 'Brain-derived neurotrophic factor supports facial motoneuron survival after facial nerve transection in immunodeficient mice.', *Brain, behavior, and immunity*, vol. 19, no. 2, pp. 173–80 [Online]. DOI: 10.1016/j.bbi.2004.07.005 (Accessed 6 January 2019).
- Sharma, N., Low, S. H., Misra, S., Pallavi, B. and Weimbs, T. (2006) 'Apical targeting of syntaxin 3 is essential for epithelial cell polarity.', *The Journal of cell biology*, Rockefeller University Press, vol. 173, no. 6, pp. 937–48 [Online]. DOI: 10.1083/jcb.200603132 (Accessed 30 December 2018).
- Shen, J. and Hung, M.-C. (2015) 'Signaling-mediated regulation of MicroRNA processing.', *Cancer research*, NIH Public Access, vol. 75, no. 5, pp. 783–91 [Online]. DOI: 10.1158/0008-5472.CAN-14-2568 (Accessed 27 July 2017).
- Shiga, A., Ishihara, T., Miyashita, A., Kuwabara, M. and Kato, T. (2012) 'Alteration of POLDIP3 Splicing Associated with Loss of Function of TDP-43 in Tissues Affected with ALS', vol. 7, no. 8, pp. 1–11 [Online]. DOI:

10.1371/journal.pone.0043120.

– Shiina, Y., Arima, K., Tabunoki, H. and Satoh, J. (2010) 'TDP-43 Dimerizes in Human Cells in Culture', *Cellular and Molecular Neurobiology*, Springer US, vol. 30, no. 4, pp. 641–652 [Online]. DOI: 10.1007/s10571-009-9489-9 (Accessed 27 July 2017).

– Simpson P, Monie T, Szendröi A, Davydova N, Tyzack J, Conte M, Read C, Cary P, Svergun D, Konarev P, Curry S, M. S. (2004) 'Structure and RNA Interactions of the N-Terminal RRM Domains of PTB', *Structure*, vol. 12, pp. 1631–1643 [Online]. DOI: 10.1016/j.str.2004.07.008 (Accessed 19 July 2017).

– Singh, R., Brewer, M. K., Mashburn, C. B., Lou, D., Bondada, V., Graham, B. and Geddes, J. W. (2014) 'Calpain 5 is highly expressed in the central nervous system (CNS), carries dual nuclear localization signals, and is associated with nuclear promyelocytic leukemia protein bodies.', *The Journal of biological chemistry*, American Society for Biochemistry and Molecular Biology, vol. 289, no. 28, pp. 19383–94 [Online]. DOI: 10.1074/jbc.M114.575159 (Accessed 18 January 2019).

– Singh, R. and Valcárcel, J. (2005) 'Building specificity with nonspecific RNA-binding proteins', *Nature Structural & Molecular Biology*, Nature Publishing Group, vol. 12, no. 8, pp. 645–653 [Online]. DOI: 10.1038/nsmb961 (Accessed 25 July 2017).

– Siomi, M. C., Sato, K., Pezic, D. and Aravin, A. A. (2011) 'PIWI-interacting small RNAs: the vanguard of genome defence', *Nature Reviews Molecular Cell Biology*, vol. 12, no. 4, pp. 246–258 [Online]. DOI: 10.1038/nrm3089 (Accessed 19 July 2017).

– Smith, R. W. P., Anderson, R. C., Smith, J. W. S., Brook, M., Richardson, W. A. and Gray, N. K. (2011) 'DAZAP1, an RNA-binding protein required for

development and spermatogenesis, can regulate mRNA translation.', *RNA (New York, N.Y.)*, Cold Spring Harbor Laboratory Press, vol. 17, no. 7, pp. 1282–95 [Online]. DOI: 10.1261/rna.2717711 (Accessed 11 May 2018).

- Smith, Y., Kieval, J., Couceyro, P. R. and Kuhar, M. J. (1999) 'CART peptide-immunoreactive neurones in the nucleus accumbens in monkeys: Ultrastructural analysis, colocalization studies, and synaptic interactions with dopaminergic afferents', *The Journal of Comparative Neurology*, Wiley-Blackwell, vol. 407, no. 4, pp. 491–511 [Online]. DOI: 10.1002/(SICI)1096-9861(19990517)407:4<491::AID-CNE3>3.0.CO;2-0 (Accessed 4 May 2018).
- Soo Hoo, L., Banna, C. D., Radeke, C. M., Sharma, N., Albertolle, M. E., Low, S. H., Weimbs, T. and Vandenberg, C. A. (2016) 'The SNARE Protein Syntaxin 3 Confers Specificity for Polarized Axonal Trafficking in Neurons.', *PloS one*, Public Library of Science, vol. 11, no. 9, p. e0163671 [Online]. DOI: 10.1371/journal.pone.0163671 (Accessed 30 December 2018).
- Soreq, H. and Seidman, S. (2001) 'Acetylcholinesterase — new roles for an old actor', *Nature Reviews Neuroscience*, Nature Publishing Group, vol. 2, no. 4, pp. 294–302 [Online]. DOI: 10.1038/35067589 (Accessed 30 December 2018).
- Spreafico, M., Grillo, B., Rusconi, F., Battaglioli, E. and Venturin, M. (2018) 'Multiple Layers of CDK5R1 Regulation in Alzheimer's Disease Implicate Long Non-Coding RNAs.', *International journal of molecular sciences*, Multidisciplinary Digital Publishing Institute (MDPI), vol. 19, no. 7 [Online]. DOI: 10.3390/ijms19072022 (Accessed 18 January 2019).
- Stains, J. P., Lecanda, F., Towler, D. A. and Civitelli, R. (2005) 'Heterogeneous nuclear ribonucleoprotein K represses transcription from a cytosine/thymidine-rich element in the osteocalcin promoter.', *The Biochemical journal*, Portland Press Ltd,

vol. 385, no. Pt 2, pp. 613–23 [Online]. DOI: 10.1042/BJ20040680 (Accessed 25 July 2017).

- Stefani, M. and Dobson, C. M. (2003) 'Protein aggregation and aggregate toxicity: new insights into protein folding, misfolding diseases and biological evolution.', *Journal of molecular medicine (Berlin, Germany)*, vol. 81, no. 11, pp. 678–99 [Online]. DOI: 10.1007/s00109-003-0464-5 (Accessed 2 June 2014).
- Stellwagen, D. and Malenka, R. C. (2006) 'Synaptic scaling mediated by glial TNF-α', *Nature*, Nature Publishing Group, vol. 440, no. 7087, pp. 1054–1059 [Online]. DOI: 10.1038/nature04671 (Accessed 20 December 2018).
- Stone, E. M., Lotery, A. J., Munier, F. L., Héon, E., Piguet, B., Guymer, R. H., Vandenburgh, K., Cousin, P., Nishimura, D., Swiderski, R. E., Silvestri, G., Mackey, D. A., Hageman, G. S., Bird, A. C., Sheffield, V. C. and Schorderet, D. F. (1999) 'A single EFEMP1 mutation associated with both Malattia Leventineseand Doyne honeycomb retinal dystrophy', *Nature Genetics*, Nature Publishing Group, vol. 22, no. 2, pp. 199–202 [Online]. DOI: 10.1038/9722 (Accessed 4 May 2018).
- Strong, M. J., Volkening, K., Hammond, R., Yang, W., Strong, W., Leystra-Lantz, C. and Shoesmith, C. (2007) 'TDP43 is a human low molecular weight neurofilament (hNFL) mRNA-binding protein', *Molecular and Cellular Neuroscience*, vol. 35, no. 2, pp. 320–327 [Online]. DOI: 10.1016/j.mcn.2007.03.007.
- Stump, G., Durrer, A., Klein, A.-L., Lütolf, S., Suter, U. and Taylor, V. (2002) 'Notch1 and its ligands Delta-like and Jagged are expressed and active in distinct cell populations in the postnatal mouse brain.', *Mechanisms of development*, vol. 114, no. 1–2, pp. 153–9 [Online]. Available at http://www.ncbi.nlm.nih.gov/pubmed/12175503 (Accessed 3 January 2019).

- Svitkin, Y. V., Yanagiya, A., Karetnikov, A. E., Alain, T., Fabian, M. R., Khoutorsky, A., Perreault, S., Topisirovic, I. and Sonenberg, N. (2013) 'Control of Translation and miRNA-Dependent Repression by a Novel Poly(A) Binding Protein, hnRNP-Q', Lykke-Andersen, J. (ed), *PLoS Biology*, Public Library of Science, vol. 11, no. 5, p. e1001564 [Online]. DOI: 10.1371/journal.pbio.1001564 (Accessed 8 November 2018).
- Swarup, V., Phaneuf, D., Bareil, C., Robertson, J., Rouleau, G. A., Kriz, J. and Julien, J.-P. (2011) 'Pathological hallmarks of amyotrophic lateral sclerosis/frontotemporal lobar degeneration in transgenic mice produced with TDP-43 genomic fragments', *Brain*, vol. 134, no. 9, pp. 2610–2626 [Online]. DOI: 10.1093/brain/awr159 (Accessed 19 December 2018).
- Takahama, K., Miyawaki, A., Shitara, T., Mitsuya, K., Morikawa, M., Hagihara, M., Kino, K., Yamamoto, A. and Oyoshi, T. (2015) 'G-Quadruplex DNA- and RNA-Specific-Binding Proteins Engineered from the RGG Domain of TLS/FUS', *ACS Chemical Biology*, American Chemical Society, vol. 10, no. 11, pp. 2564–2569 [Online]. DOI: 10.1021/acschembio.5b00566 (Accessed 25 July 2017).
- Takahashi, K. and Yamanaka, S. (2006) 'Induction of Pluripotent Stem Cells from Mouse Embryonic and Adult Fibroblast Cultures by Defined Factors', *Cell*, vol. 126, no. 4, pp. 663–676 [Online]. DOI: 10.1016/j.cell.2006.07.024.
- Tejada-Simon, M. V, Serrano, F., Villasana, L. E., Kanterewicz, B. I., Wu, G.-Y., Quinn, M. T. and Klann, E. (2005) 'Synaptic localization of a functional NADPH oxidase in the mouse hippocampus.', *Molecular and cellular neurosciences*, vol. 29, no. 1, pp. 97–106 [Online]. DOI: 10.1016/j.mcn.2005.01.007 (Accessed 3 January 2019).
- Thandapani, P., O 'connor, T. R., Bailey, T. L. and Phane Richard, S. (2013)

'Defining the RGG/RG Motif', *Molecular Cell*, vol. 50, pp. 613–623 [Online]. DOI: 10.1016/j.molcel.2013.05.021 (Accessed 23 July 2017).

- Timpl, R., Sasaki, T., Kostka, G., Chu, M., Planck, M. and Martinsried, D.- (2003) 'FIBULINS : A VERSATILE FAMILY OF EXTRACELLULAR MATRIX PROTEINS', *Nat Rev Mol Cell Biol*, vol. 4, no. 6, pp. 479–489 [Online]. DOI: 10.1038/nrm1130.
- Tollervey, J. R., Curk, T., Rogelj, B., Briese, M., Cereda, M., Kayikci, M., König, J., Hortobágyi, T., Nishimura, A. L., Župunski, V., Patani, R., Chandran, S., Rot, G., Zupan, B., Shaw, C. E. and Ule, J. (2011) 'Characterizing the RNA targets and position-dependent splicing regulation by TDP-43', *Nature Neuroscience*, vol. 14, no. 4, pp. 452–458 [Online]. DOI: 10.1038/nn.2778 (Accessed 24 April 2018).
- Tonevitsky, E. A., Trushkin, E. V., Shkurnikov, M. U., Akimov, E. B. and Sakharov, D. A. (2009) 'Changed Profile of Expression of Splicing Regulator Genes in Response to Exercise', *Bulletin of Experimental Biology and Medicine*, Springer US, vol. 147, no. 6, pp. 733–736 [Online]. DOI: 10.1007/s10517-009-0593-0 (Accessed 11 November 2018).
- Le Tonquèze, O., Gschloessl, B., Legagneux, V., Paillard, L. and Audic, Y. (2016) 'Identification of CELF1 RNA targets by CLIP-seq in human HeLa cells', *Genomics Data*, The Authors, vol. 8, pp. 97–103 [Online]. DOI: 10.1016/j.gdata.2016.04.009.
- Traikov, S., Stange, C., Wassmer, T., Paul-Gilloteaux, P., Salamero, J., Raposo, G. and Hoflack, B. (2014) 'Septin6 and septin7 GTP binding proteins regulate AP-3- and ESCRT-dependent multivesicular body biogenesis', *PLoS ONE*, vol. 9, no. 11, pp. 1–12 [Online]. DOI: 10.1371/journal.pone.0109372.
- Troy, C. M., Akpan, N. and Jean, Y. Y. (2011) 'Regulation of Caspases in the

Nervous System: Implications for Functions in Health and Disease', *Progress in Molecular Biology and Translational Science*, Academic Press, vol. 99, pp. 265–305 [Online]. DOI: 10.1016/B978-0-12-385504-6.00007-5 (Accessed 18 January 2019).

- Tsui, S., Dai, T., Roettger, S., Schempp, W., Salido, E. C. and Yen, P. H. (2000) 'Identification of Two Novel Proteins That Interact with Germ-Cell-Specific RNA-Binding Proteins DAZ and DAZL1', *Genomics*, Academic Press, vol. 65, no. 3, pp. 266–273 [Online]. DOI: 10.1006/GENO.2000.6169 (Accessed 2 August 2018).
- Ugras, S. E. and Shorter, J. (2012) 'RNA-Binding Proteins in Amyotrophic Lateral Sclerosis and Neurodegeneration', *Neurology Research International*, Hindawi Publishing Corporation, vol. 5 [Online]. DOI: 10.1155/2012/432780 (Accessed 25 July 2017).
- Ule, J., Stefani, G., Mele, A., Ruggiu, M., Wang, X., Taneri, B., Gaasterland, T., Blencowe, B. J. and Darnell, R. B. (2006) 'An RNA map predicting Nova-dependent splicing regulation', *Nature*, Nature Publishing Group, vol. 444, no. 7119, pp. 580–586 [Online]. DOI: 10.1038/nature05304 (Accessed 22 January 2019).
- Ule, J., Ule, A., Spencer, J., Williams, A., Hu, J.-S., Cline, M., Wang, H., Clark, T., Fraser, C., Ruggiu, M., Zeeberg, B. R., Kane, D., Weinstein, J. N., Blume, J. and Darnell, R. B. (2005) 'Nova regulates brain-specific splicing to shape the synapse', *Nature Genetics*, Nature Publishing Group, vol. 37, no. 8, pp. 844–852 [Online]. DOI: 10.1038/ng1610 (Accessed 11 October 2018).
- Valente, L. and Nishikura, K. (2005) 'ADAR Gene Family and A-to-I RNA Editing: Diverse Roles in Posttranscriptional Gene Regulation', in pp. 299–338 [Online]. DOI: 10.1016/S0079-6603(04)79006-6 (Accessed 23 July 2017).

- Vaquerizas, J. M., Kummerfeld, S. K., Teichmann, S. A. and Luscombe, N. M. (2009) 'A census of human transcription factors: function, expression and evolution', *Nature Reviews Genetics*, vol. 10, no. 4, pp. 252–263 [Online]. DOI: 10.1038/nrg2538 (Accessed 14 July 2017).
- Vassileva, M. T. and Matunis, M. J. (2004) 'SUMO Modification of Heterogeneous Nuclear Ribonucleoproteins', *MOLECULAR AND CELLULAR BIOLOGY*, vol. 24, no. 9, pp. 3623–3632 [Online]. DOI: 10.1128/MCB.24.9.3623–3632.2004.
- VERA, Y., DAI, T., HIKIM, A. P. S., LUE, Y., SALIDO, E. C., SWERDLOFF, R. S. and YEN, P. H. (2002) 'Deleted in Azoospermia Associated Protein 1 Shuttles Between Nucleus and Cytoplasm During Normal Germ Cell Maturation', *Journal of Andrology*, Wiley-Blackwell, vol. 23, no. 5, pp. 622–628 [Online]. DOI: 10.1002/J.1939-4640.2002.TB02303.X (Accessed 11 May 2018).
- Verbeek, M. M., Otte-Höller, I., Westphal, J. R., Wesseling, P., Ruiter, D. J. and de Waal, R. M. (1994) 'Accumulation of intercellular adhesion molecule-1 in senile plaques in brain tissue of patients with Alzheimer's disease.', *The American journal of pathology*, American Society for Investigative Pathology, vol. 144, no. 1, pp. 104–16 [Online]. Available at http://www.ncbi.nlm.nih.gov/pubmed/7904796 (Accessed 20 December 2018).
- Voigt, A., Herholz, D., Fiesel, F. C., Kaur, K., Müller, D., Karsten, P., Weber, S. S., Kahle, P. J., Marquardt, T. and Schulz, J. B. (2010) 'TDP-43-mediated neuron loss In Vivo requires RNA-binding activity', *PLoS ONE*, vol. 5, no. 8 [Online]. DOI: 10.1371/journal.pone.0012247.
- Wang, H.-Y., Wang, I.-F., Bose, J. and Shen, C.-K. J. (2004) 'Structural diversity and functional implications of the eukaryotic TDP gene family', *Genomics*, vol. 83, no. 1, pp. 130–139 [Online]. DOI: 10.1016/S0888-7543(03)00214-3 (Accessed 26

July 2017).

- Wang, I.-F., Wu, L.-S., Chang, H.-Y. and Shen, C.-K. J. (2008) 'TDP-43, the signature protein of FTLD-U, is a neuronal activity-responsive factor', *Journal of Neurochemistry*, Blackwell Publishing Ltd, vol. 105, no. 3, pp. 797–806 [Online]. DOI: 10.1111/j.1471-4159.2007.05190.x (Accessed 27 July 2017).
- Wang, L., Popko, B., Tixier, E. and Roos, R. P. (2014) 'Guanabenz, which enhances the unfolded protein response, ameliorates mutant SOD1-induced amyotrophic lateral sclerosis.', *Neurobiology of disease*, NIH Public Access, vol. 71, pp. 317–24 [Online]. DOI: 10.1016/j.nbd.2014.08.010 (Accessed 18 January 2019).
- Wang, S., Sdrulla, A. D., diSibio, G., Bush, G., Nofziger, D., Hicks, C., Weinmaster, G. and Barres, B. A. (1998) 'Notch receptor activation inhibits oligodendrocyte differentiation.', *Neuron*, Elsevier, vol. 21, no. 1, pp. 63–75 [Online]. DOI: 10.1016/S0896-6273(00)80515-2 (Accessed 3 January 2019).
- Wang, Y., Ma, M., Xiao, X. and Wang, Z. (2012) 'Intronic splicing enhancers, cognate splicing factors and context-dependent regulation rules.', *Nature structural & molecular biology*, NIH Public Access, vol. 19, no. 10, pp. 1044–52 [Online]. DOI: 10.1038/nsmb.2377.
- Wang, Y., Xiao, X., Zhang, J., Choudhury, R., Robertson, A., Li, K., Ma, M., Burge, C. B. and Wang, Z. (2013) 'A complex network of factors with overlapping affinities represses splicing through intronic elements.', *Nature structural & molecular biology*, NIH Public Access, vol. 20, no. 1, pp. 36–45 [Online]. DOI: 10.1038/nsmb.2459 (Accessed 31 August 2018).
- Whitehouse, P., Price, D., Struble, R., Clark, A., Coyle, J. and Delon, M. (1982) 'Alzheimer's disease and senile dementia: loss of neurons in the basal forebrain',

Science, American Association for the Advancement of Science, vol. 215, no. 4537, pp. 1237–1239 [Online]. DOI: 10.1126/science.7058341 (Accessed 30 December 2018).

- Wolozin, B. and Apicco, D. (n.d.) 'RNA binding proteins and the genesis of neurodegenerative diseases', [Online]. DOI: 10.1007/978-3-319-08927-0_3 (Accessed 24 July 2017).
- Wyss-Coray, T. and Mucke, L. (2002) 'Inflammation in Neurodegenerative Disease—A Double-Edged Sword', *Neuron*, Cell Press, vol. 35, no. 3, pp. 419–432 [Online]. DOI: 10.1016/S0896-6273(02)00794-8 (Accessed 8 May 2018).
- Xiang, Y.-Y., Dong, H., Yang, B. B., MacDonald, J. F. and Lu, W.-Y. (2014) 'Interaction of Acetylcholinesterase with Neurexin-1β regulates Glutamatergic Synaptic stability in Hippocampal neurons', *Molecular Brain*, BioMed Central, vol. 7, no. 1, p. 15 [Online]. DOI: 10.1186/1756-6606-7-15 (Accessed 30 December 2018).
- Xu, R.-M., Jokhan, L., Cheng, X., Mayeda, A. and Krainer, A. R. (1997) 'Crystal structure of human UP1, the domain of hnRNP A1 that contains two RNA-recognition motifs', *Structure*, vol. 5, no. 4, pp. 559–570 [Online]. DOI: 10.1016/S0969-2126(97)00211-6 (Accessed 20 July 2017).
- Yang, C.-K. and Yen, P. (2013) 'Differential Translation of Dazap1 Transcripts during Spermatogenesis', Yan, W. (ed), *PLoS ONE*, Public Library of Science, vol. 8, no. 4, p. e60873 [Online]. DOI: 10.1371/journal.pone.0060873 (Accessed 11 May 2018).
- Yang, H., Peggie, M., Cohen, P. and Rousseau, S. (2009) 'Biochemical and Biophysical Research Communications DAZAP1 interacts via its RNA-recognition motifs with the C-termini of other RNA-binding proteins', *Biochemical and*

Biophysical Research Communications, Elsevier Inc., vol. 380, no. 3, pp. 705–709 [Online]. DOI: 10.1016/j.bbrc.2009.01.166.

- Yano, M., Hayakawa-Yano, Y., Mele, A. and Darnell, R. B. (n.d.) 'Nova2 regulates neuronal migration through an RNA switch in disabled-1 signaling', [Online]. DOI: 10.1016/j.neuron.2010.05.007 (Accessed 24 July 2017).
- Yoo, B. C., Hong, S.-H., Ku, J.-L., Kim, Y.-H., Shin, Y.-K., Jang, S.-G., Kim, I.-J., Jeong, S.-Y. and Park, J.-G. (2009) 'Galectin-3 stabilizes heterogeneous nuclear ribonucleoprotein Q to maintain proliferation of human colon cancer cells', *Cellular and Molecular Life Sciences*, Birkhäuser-Verlag, vol. 66, no. 2, pp. 350–364 [Online]. DOI: 10.1007/s00018-009-8562-3 (Accessed 17 November 2018).
- Youhna M. Ayala, Paola Zago, Andrea D'Ambrogio, Ya-Fei Xu, Leonard Petrucelli, E. B. F. E. B. (2008) 'Structural determinants of the cellular localization and shuttling of TDP-43', *Journal of Cell Science*, vol. 121, pp. 2778–3785 [Online]. DOI: 10.1242/jcs.038950 (Accessed 27 July 2017).
- Young, M. D., Wakefield, M. J., Smyth, G. K. and Oshlack, A. (2010) 'Gene ontology analysis for RNA-seq: accounting for selection bias', *Genome Biology*, vol. 11, no. 2 [Online]. DOI: 10.1186/gb-2010-11-2-r14.
- Yun, C. H., Lee, H. M., Lee, S. C., Kim, B. S., Park, J. W. and Lee, B. J. (2013) 'Involvement of CD137 ligand signaling in neural stem cell death', *Molecules and Cells*, Springer Netherlands, vol. 36, no. 3, pp. 245–251 [Online]. DOI: 10.1007/s10059-013-0137-3 (Accessed 20 December 2018).
- Yutsudo, N., Kamada, T., Kajitani, K., Nomaru, H., Katogi, A., Ohnishi, Y. H., Ohnishi, Y. N., Takase, K., Sakumi, K., Shigeto, H. and Nakabeppu, Y. (2013) 'fosB-Null Mice Display Impaired Adult Hippocampal Neurogenesis and Spontaneous Epilepsy with Depressive Behavior', *Neuropsychopharmacology*, vol.

38, no. 5, pp. 895–906 [Online]. DOI: 10.1038/npp.2012.260 (Accessed 2 January 2019).

- Zhang, D., Sliwkowski, M. X., Mark, M., Frantz, G., Akita, R., Sun, Y., Hillan, K., Crowley, C., Brush, J. and Godowski, P. J. (1997) 'Neuregulin-3 (NRG3): a novel neural tissue-enriched protein that binds and activates ErbB4.', *Pnas*, vol. 94, no. 18, pp. 9562–9567 [Online]. DOI: 10.1073/pnas.94.18.9562.
- Zhang, Y., Kong, W., Gao, Y., Liu, X., Gao, K., Xie, H. and Wu, Y. (2015) 'Gene Mutation Analysis in 253 Chinese Children with Unexplained Epilepsy and Intellectual / Developmental Disabilities', pp. 1–13 [Online]. DOI: 10.1371/journal.pone.0141782.
- Zhao, J., Zhu, Y., Yang, J., Li, L., Wu, H., De Jager, P. L., Jin, P. and Bennett, D. A. (2017) 'A genome-wide profiling of brain DNA hydroxymethylation in Alzheimer's disease', *Alzheimer's & Dementia*, Elsevier, vol. 13, no. 6, pp. 674–688 [Online]. DOI: 10.1016/J.JALZ.2016.10.004 (Accessed 18 January 2019).
- Zhao, W. M., Jiang, C., Kroll, T. T. and Huber, P. W. (2001) 'A proline-rich protein binds to the localization element of Xenopus Vg1 mRNA and to ligands involved in actin polymerization.', *The EMBO journal*, European Molecular Biology Organization, vol. 20, no. 9, pp. 2315–25 [Online]. DOI: 10.1093/emboj/20.9.2315 (Accessed 7 August 2018).